Mediators of Inflammation

Immunometabolism: Molecular Mechanisms, Diseases, and Therapies 2018

Lead Guest Editor: José C. Rosa
Guest Editors: Fabio S. Lira, William Festuccia, Barbara Wessner, and Nicolette C. Bishop

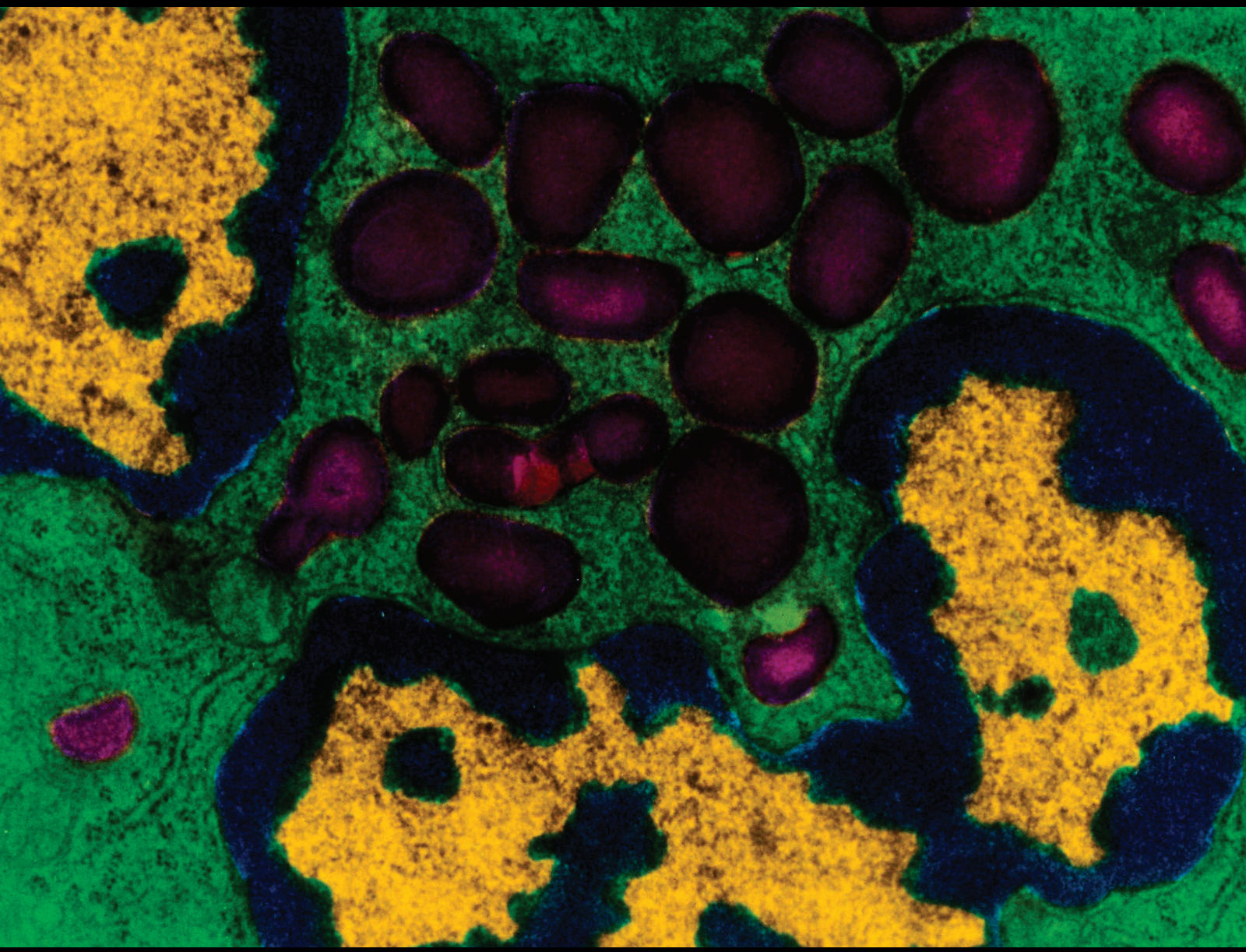

Immunometabolism: Molecular Mechanisms, Diseases, and Therapies 2018

Mediators of Inflammation

Immunometabolism: Molecular Mechanisms, Diseases, and Therapies 2018

Lead Guest Editor: José C. Rosa
Guest Editors: Fabio S. Lira, William Festuccia, Barbara Wessner, and Nicolette C. Bishop

Editorial Board

Contents

Hindawi
Mediators of Inflammation
Volume 2019, Article ID 2340914, 2 pages
https://doi.org/10.1155/2019/2340914

Editorial

Immunometabolism: Molecular Mechanisms, Diseases, and Therapies 2018

José C. Rosa,[1] **Fabio S. Lira**,[2] **William Festuccia**,[3] **Barbara Wessner**,[4] **and Nicolette C. Bishop**[5]

[1]*Department of Cell Biology and Development, Institute of Biomedical Sciences, University of Sao Paulo, Sao Paulo 05508000, Brazil*
[2]*Exercise and Immunometabolism Research Group, Department of Physical Education, Universidade Estadual Paulista (UNESP), Presidente Prudente, SP 19060-900, Brazil*
[3]*Department of Physiology and Biophysics, Institute of Biomedical Sciences, University of Sao Paulo, Sao Paulo 05508000, Brazil*
[4]*Centre for Sport Science and University Sports, Vienna, Austria*
[5]*School of Sports, Exercise and Health Science, Loughborough University, Loughborough, UK*

Correspondence should be addressed to José C. Rosa; josecesar23@hotmail.com

Received 26 December 2018; Accepted 26 December 2018; Published 30 January 2019

This third edition of this special issue focused on the interrelationships between metabolic pathways, metabolites, and the immune system. Chronic low-grade inflammation is a common phenotype found in several diseases including obesity, cancer, type 2 diabetes, and cardiovascular diseases, directly participating in their development, as well as a connecting factor between them. Evidence accumulated over the years has shed light on the important role of dysregulated metabolic pathways caused by nutrient excess, lipid overload, sedentary behaviour, and aging as promoting factors and modulators of inflammation. Immune cells through the secretion of cytokines and other inflammatory mediators, on the other hand, also modulate insulin signalling, glucose, and lipid metabolism.

This special issue received the submission of 20 manuscripts focused on different aspects of the intricate relationship between the immune system and metabolism; among which, 9 were accepted for publication. Three of these articles provide insightful reviews of the literature within the scope of this issue. Yamashita and colleagues, for example, reviewed the molecular mechanisms by which chronic exposure to excessive amounts of the nutrient lipids, glucose, and amino acids regulates inflammatory pathways, with a special emphasis in the role of the nutrient and energy sensors mTOR, AMPK, and PPARs in this context. Belizário and colleagues, on the other hand, reviewed the emerging role of microbiota as a major factor in the development of chronic inflammatory diseases. This timely review article, among other aspects, discussed the role of dysbiosis as the trigger of inflammation in different pathological conditions and the possibility of management of microbiota as a nonpharmacological intervention to counteract disease development. Finally, Brinchmann and colleagues elegantly revisited the role of galectins, β-galcotosid-binding lectin found in the intra- and extracellular compartments, in the regulation of metabolism and inflammation and as possible targets to treat chronic diseases.

In addition to review articles, this special issue also published 6 interesting original studies. Among them, 4 described possible beneficial effects of anti-inflammatory strategies to counteract disease development. Lin et al., for example, demonstrate that shock wave therapy induces mitochondrial delivery to lung parenchyma and, by reducing alveolar macrophage infiltration and fibrosis, protects from acute respiratory distress syndrome. In another original study, Qian et al. robustly showed that osthole, a natural coumarin extract, reduces inflammation and the production of proinflammatory cytokines by macrophages increasing mice survival to septic shock. In the same direction, Samblas and colleagues elegantly demonstrate that folic acid, a naturally

occurring dietary component of the methionine pathway for the synthesis of S-adenosyl methionine (SAM), the universal methyl-donor for DNA methylation, reduces the production and secretion of the proinflammatory cytokines TNF-α and IL-1β induced by LPS in macrophages. Finally, Wang et al. showed that inhibition of the histone deacetylase HDAC2 with CAY10683 protected rats from LPS-induced acute liver failure and endotoxemia by improving the integrity of the intestinal barrier and reducing the activation of the LPS-TLR4-MYD-88 pathway.

Noteworthy, two original studies of this special issue have evaluated the changes in the metabolic profile of immune cells in different conditions. Ahmed and colleagues demonstrate through transcriptional profile dataset that treatment of human and mice macrophages with interferon- (IFN-) α promotes important changes in their metabolic signature characterized by activation of pathways involved in cellular bioenergetics, cellular oxidant status, cAMP/AMP and cGMP/GMP ratios, branched chain amino acid catabolism, cell membrane composition, fatty acid synthesis, and β-oxidation. Finally, Santarsiero and colleagues elegantly showed that patients with Behçet's syndrome (BS), a multisystemic disorder characterized by chronic inflammation and vasculitis, displayed elevated mRNA levels of the mitochondrial citrate carrier (SLC25A1) and ATP-citrate lyase (ACLY) in peripheral blood mononuclear cells (PBMCs) suggesting a dysregulation of citrate metabolism that could participate in the increased proinflammatory response displayed by these cells.

Altogether, the studies published in this special issue bring new insights into the intricate mechanisms driving the inflammatory processes associated with metabolic diseases. We hope that these studies will pave the way for the development of novel efficient strategies to prevent and treat these increasingly common conditions.

Conflicts of Interest

José C. Rosa confirms that the editors of this special issue have no conflicts of interest or private agreements with companies. Nicolette C. Bishop can confirm that she has no conflicts of interest or private agreements with companies. Barbara Wessner confirms that she do not have any conflict of interest or private agreements with companies. William T. Festuccia has no conflicts of interest or private agreements with companies. Fabio S. Lira has no conflicts of interest or private agreements with companies.

José C. Rosa
Fabio S. Lira
William Festuccia
Barbara Wessner
Nicolette C. Bishop

Hindawi
Mediators of Inflammation
Volume 2018, Article ID 2037838, 12 pages
https://doi.org/10.1155/2018/2037838

Review Article

Gut Microbiome Dysbiosis and Immunometabolism: New Frontiers for Treatment of Metabolic Diseases

José E. Belizário,[1] **Joel Faintuch**,[2] **and Miguel Garay-Malpartida**[3]

[1]*Department of Pharmacology, Institute of Biomedical Sciences, University of São Paulo, SP CEP 05508-900, Brazil*
[2]*Department of Gastroenterology of Medical School, University of São Paulo, SP CEP 05403-000, Brazil*
[3]*School of Arts, Sciences and Humanities (EACH), University of São Paulo, São Paulo, SP CEP 03828-000, Brazil*

Correspondence should be addressed to José E. Belizário; jebeliza@usp.br

Received 23 February 2018; Accepted 23 October 2018; Published 9 December 2018

Guest Editor: Fabio S. Lira

Maintenance of healthy human metabolism depends on a symbiotic consortium among bacteria, archaea, viruses, fungi, and host eukaryotic cells throughout the human gastrointestinal tract. Microbial communities provide the enzymatic machinery and the metabolic pathways that contribute to food digestion, xenobiotic metabolism, and production of a variety of bioactive molecules. These include vitamins, amino acids, short-chain fatty acids (SCFAs), and metabolites, which are essential for the interconnected pathways of glycolysis, the tricarboxylic acid/Krebs cycle, oxidative phosphorylation (OXPHOS), and amino acid and fatty acid metabolism. Recent studies have been elucidating how nutrients that fuel the metabolic processes impact on the ways immune cells, in particular, macrophages, respond to different stimuli under physiological and pathological conditions and become activated and acquire a specialized function. The two major inflammatory phenotypes of macrophages are controlled through differential consumption of glucose, glutamine, and oxygen. M1 phenotype is triggered by polarization signal from bacterial lipopolysaccharide (LPS) and Th1 proinflammatory cytokines such as interferon-γ, TNF-α, and IL-1β, or both, whereas M2 phenotype is triggered by Th2 cytokines such as interleukin-4 and interleukin-13 as well as anti-inflammatory cytokines, IL-10 and TGFβ, or glucocorticoids. Glucose utilization and production of chemical mediators including ATP, reactive oxygen species (ROS), nitric oxide (NO), and NADPH support effector activities of M1 macrophages. Dysbiosis is an imbalance of commensal and pathogenic bacteria and the production of microbial antigens and metabolites. It is now known that the gut microbiota-derived products induce low-grade inflammatory activation of tissue-resident macrophages and contribute to metabolic and degenerative diseases, including diabetes, obesity, metabolic syndrome, and cancer. Here, we update the potential interplay of host gut microbiome dysbiosis and metabolic diseases. We also summarize on advances on fecal therapy, probiotics, prebiotics, symbiotics, and nutrients and small molecule inhibitors of metabolic pathway enzymes as prophylactic and therapeutic agents for metabolic diseases.

1. Introduction

Human microbiomes refer to collective genomes of bacteria, archaea, viruses, protozoans, and fungi that coinhabit multiple ecosystems in the human body (Bäckhed et al. [1], Belizario and Napolitano [2]). An adult man of 70 kg might contain up to 3.8×10^{13} bacteria, which is equal to the number of cells of an adult human body (Sender et al. [3]). Bacteria are morphologically and biochemically classified based on various properties including wall type, shape, requirement of oxygen (anaerobic or aerobic), endospore production, motility, and their metabolism. Bacteria are also classified by phylogenetic diversity of variable nucleotide sequences of small subunit ribosomal RNA operons or 16S and 18S rRNA genes [1, 2].

The Human Microbiome Project (HMP) have been defining criteria for high-quality and comprehensive metagenomic analysis of genetic material recovered directly from distinct sites on the human body to determine the microbial relative abundance of multiple strains and species of different phyla at physiological conditions [4–6]. Advances on computational techniques have allowed studies of public

human metagenomes based on the phylogenetic clustering and assembly of bacterial genomes into taxonomic domain, kingdom, phylum, class, order, family, genus, and species [4–8]. The analyses of various human microbiome datasets revealed the immense diversity at both populations and individuals over evolutionary and lifetime [7–9]. The gut microbiota of healthy individuals is composed of permanent and transitory microbial species and subspecies of over 17 candidate bacterial phyla belonging to Firmicutes (>70%), Bacteroidetes (>30%), Proteobacteria (<5%), Actinobacteria (<2%), Fusobacteria and Verrucomicrobia (<1%), and other phyla. The novel bacterial genome assembly and taxonomic profiling based on 1550 metagenome-assembled genomes (MAGs) have revealed nearly 70,000 bacterial and archaeal genomes and new species that are under deep investigation [6–8]. A common set of prevalent microbial species found in normal human stools includes the *Clostridiales* species such as *Coprococcus*, *Ruminococcus*, *Eubacterium*, *Bacteroides dorei* and *fragilis*, and *Alistipes finegoldii* and *onderdonkii* [7, 8]. The fully broad taxonomic distribution, microbial evolution, and metabolism of bacterial species regarding caloric load and nutrient absorption have served to cluster species-level phylotypes into major human enterotypes [9–12]. The prevalent human enterotype type 1 is characterized by high levels of *Bacteroides* and type 2 by few *Bacteroides* but high levels of *Prevotella*. They are, respectively, associated with individuals that ingest either high content of animal protein (type 1) or carbohydrates (type 2).

The gastrointestinal (GI) tract possesses its own nervous system known as the enteric nervous system. This system communicates with the central nervous system through nerves, such as the vagus, neuromodulators, and neurotransmitters of sympathetic and parasympathetic branches of the autonomic nervous system [1]. Bacterial richness and diversity in the GI microbiota occupy a central role in normal metabolic and immunological functions of tissues and organs [1, 2]. Here, we will update on diverse studies exploring the roles of microbiomes, nutrients, and metabolites on immune cell function, etiology of inflammatory, and metabolic diseases, including their wide range of mechanisms. We also describe why and how novel dietary and pharmacological strategies including fecal transplantation, probiotics, prebiotics, and small molecules may help to treat and modulate species-level phyla types and promote the restoration of microbiomes causing metabolic syndromes.

2. Gut Microbiota Controls the Host's Metabolic Physiological States

Microorganisms in the gut perform their functions largely through enzyme pathways, in order to digest complex dietary carbohydrates and proteins [13, 14]. Gut microbiota provides the branched-chain amino acids leucine, isoleucine, and valine, and particularly glycine, which is required for the synthesis of glutathione—the main intracellular antioxidant and detoxifying agent necessary for many biological functions of the host. Bacteria of the gut synthesize a large variety of signaling molecules of low molecular weight that include methane, hydrogen sulfide, and nongaseous metabolites [13, 14]. Those products are able turn on or off both host genes and microbe virulence and metabolism genes. Microorganisms also sense diverse environmental signals, including host hormones and nutrients, and respond to them by differential gene regulation and niche adaptation [13, 14].

The maintenance of a stable, fermentative gut microbiota requires diets rich in whole plant foods, particularly rich in fibers [13, 14]. These substrates are processed by the intestinal microbiota enzymes, such as glycoside hydrolases and polysaccharide lyases to produce polyamines, polyphenols, and vitamins B and K. Under anaerobic conditions, species belonging to the *Bacteroides* genus, and to the *Clostridiaceae* and *Lactobacillaceae* families, in special, *Citrobacter* and *Serratia* strains, produce short-chain fatty acids (SCFAs) which are volatile fat acids able to cross the blood-brain barrier via monocarboxylate transporters. SCFAs produced by intestinal bacteria are acetate (2 carbon atoms), propionate (3 carbon atoms), and butyrate (4 carbon atoms), and their molar ratios vary from 3 : 1 : 1 to 10 : 2 : 1, respectively. Most of SCFAs are metabolized to CO_2. Butyrate acts on colonocytes, goblet cells, and Paneth cells and provides energy for cellular metabolism and regulates apoptosis, cellular differentiation, and chemical modification of nuclear proteins and nucleic acid. Acetate and propionate pass into the bloodstream and are taken up by the liver and peripheral organs, where they can act as substrates for gluconeogenesis and lipogenesis [14, 15]. The G-protein-coupled receptors (GPRs), GPR41 and GPR43, also named free fatty acid receptors 2 and 3 (FFARs 2/3) present in many tissues, including adipose, gut enteroendocrine cells, and inflammatory cells act as major receptors of SCFAs [14, 15]. Under certain physiological conditions, SCFAs can induce the secretion of glucagon-like peptides (GLP-1 and GLP-2) and peptide YY (PYY). GLP1 stimulates β cells of the pancreas to produce insulin, whereas PYY inhibits nutrient absorption in the intestinal lumen as well as control the appetite. The gut microbiota contributes to fat deposition through the regulation of the nuclear farnesoid X receptor (FXR), the bile acid receptor that is responsible for the regulation of bile acid synthesis, and hepatic triglyceride accumulation [16]. Bile acids, for example, deoxycholic acid, have antimicrobial effects on microbes of the gut and also induce the synthesis of antimicrobial peptides by gut epithelial tissue [17]. Moreover, microbiota converts carnitin and choline to trimethylamine and thus regulates directly the bioavailability of choline and indirectly the accumulation of triglycerides in the liver. The gut microbiota also helps the absorption of calcium, magnesium, and iron. High or low productions of SCFAs, tryptophan metabolites, GABA, noradrenaline, dopamine, acetylcholine, and 5-hydroxytryptamine (serotonin) are associated with various inflammatory and metabolic diseases and neuropsychiatric disorders [18]. Some of these factors act as major neurotransmitters and modulators of the brain-gut axis, and serotonin has central roles in sexuality, substance addiction, appetite, emotions, and stress response [18].

Thousands of microbiota-derived metabolites with known and unknown functions have been identified as components of the human metabolome [19–21]. GI microbiota produces

large quantities of epigenetically active metabolites, such as folate and A and B vitamins (including riboflavin (B_2), niacin (B_3), pantothenic acid (B_5), pyridoxine (B_6), folate (B_9), and cobalamin (B_{12})) that regulate the activity of host chromatin-modulating enzymes and genetic responses to environmental signals [22]. Acetyl-CoA produced by a number of metabolic processes is the acetyl donor for histone modification (acetylation and deacetylation) catalyzed by histone acetyltransferases. Glycine, serine, and methionine are substrates for DNA methylation and demethylation enzymes. Therefore, changes in gut microbiota can result in epigenomic changes not only directly in adjacent intestinal cells but also in distant cell lineages, such as hepatocytes and adipocytes [22]. Finally, bacteria can inhibit the growth of their competitors by long distance microbial communication, via release of metabolites and quorum sensing peptides, which are considered a biological strategy for maintenance of density of commensal species, and elimination of pathogenic bacteria [23, 24].

3. Gut Microbiota Drives Host Immunological Functions

A collection of $100\text{-}400 \times 10^{12}$ of bacteria inhabits and lives in mutualistic relationships in the human GI tract [3]. The GI double mucus layer is formed by heavily O-glycosylated mucin proteins encoded by MUC2 gene of the mucin protein family. Most of the bacteria of the colon are tightly attached to the outer mucus layer, and the inner layer forms a physical barrier that limits bacterial contact with the epithelium. Most of microbial species in GI tract are transmitted at early life to babies through mother's milk, which contains predominantly *Bifidobacteria* and *Lactobacillus* species [25, 26]. Along the transition of infancy to adult life, increase in food sources drives the complexity and diversity of bacterial communities of the genera *Bacteroides*, *Parabacteroides* (Bacteroidetes), and *Clostridium* (Firmicutes) [1, 2, 25, 26]. Bacterial density in the jejunum/ileum ($<10^5$) and in the large intestine progressively increases in comparison with the stomach and duodenum, and the highest taxa and cell density are present in the colon, which contains 10^9-10^{12} colony-forming units per ml (99% of total GI population). They are anaerobes such *Bacteroides*, *Porphyromonas*, *Bifidobacterium*, *Lactobacillus*, and *Clostridium*. Anaerobic bacteria and oxygen-sensitive microbes are capable of producing of short-chain fatty acids than facultative aerobic bacteria such as *E. coli*, by a factor of 1000. Disruption of the dynamic interrelation between the host and the microbial communities causes dysbiosis, which is a bacterial imbalance between aerobic and facultative anaerobic bacteria ratios [1, 2]. Hypoxia prevents the growth of pathogenic facultative anaerobes such as *E. coli* and *Salmonella*. The rupture of gut barrier provoked by dysbiosis leads to local and systemic inflammation [1, 2, 27]. A study by Byndloss et al. unequivocally demonstrated that dysbiosis could be caused by high levels of oxygen and nitrates, which are compounds that contribute to the growth of *Escherichia* and *Salmonella species* [28]. Many diseases, including inflammatory bowel diseases (IBDs), irritable bowel syndrome (IBS), diabetes, obesity, and cancer, have been associated with specific bacterial dysbiosis [29–31]. The potential temporary shifts of microbiota species, for example, by the reduction of anti-inflammatory species, such as *Faecalibacterium prausnitzii* and *Akkermansia muciniphila* which predominate in healthy individuals, or by the proliferation of potentially proinflammatory bacteria such as *Bacteroides* and *Ruminococcus gnavus*, can promote the disease progression and chronicity [29–32]. Comparative studies in lean and obese animal models have indicated that low Bacteroidetes/Firmicutes ratio is a hallmark of obesity [33]. Firmicutes rely heavily on dietary carbohydrates, whereas Proteobacteria rely on proteins as carbon source. For instance, *Akkermansia muciniphila* is a mucin-degrading bacterium in the phylum of *Verrucomicrobia* that is present in great abundance in healthy humans, but is present in reduced number in patients with inflammatory and gastrointestinal diseases, obesity, and type 2 diabetes (T2D) [34]. In fact, distinct microbial communities and mechanisms can drive host's susceptibility to diseases and influence on clinical outcomes [35].

The gut microbiota plays a critical role in the immune system by controlling the development and functionality of gut-associated lymphoid tissues (GALT), including Peyer's patches, isolated lymphoid follicles, and mesenteric lymph nodes [30, 31, 36, 37]. Microbes and their products are necessary for the immune system to distinguish self from nonself (invaders) at early life and activation and maintenance of innate hematolymphoid cells (ILC1, 2, and 3), natural killer (NK) cells, and cytotoxic and noncytotoxic and helper lymphoid cells [36–39]. NK cells and ILC1 produce large amounts of IFN-γ, antimicrobial peptides (AMPs), granulysin, defensins, lysozyme, and Reg IIIγ, which together play critical functions on the regulation of microbial ecology and immune surveillance [24, 31, 39, 40]. For instance, polysaccharide A, α-galactosylceramide, and tryptophan metabolites produce by microbial communities stimulate immune cells to produce interleukin-22, Reg3γ, IgA, and interleukin-17 [37]. IgA is one important component of innate response to prevent invasion of the microorganisms into circulation [30]. T helper (Th) 17 cells and regulatory T cells (Treg) are antigen-specific populations that respond to transforming growth factor-β and retinoic acid and control immune tolerance [38, 39]. This control of whole body immune system by gut bacteria appears to be a delicate framework since loss of a specific species can lead to overreaction or suppression of the innate immune response [27, 35, 36].

A variety of membrane and intracellular receptors named "pattern recognition receptors" or PRRs expressed on the epithelial and immune cells act as sensors of bacterial and cellular products, which are named the pathogen-associated molecular patterns (PAMPs) and damaged-associated molecular patterns (DAMPs) [41, 42]. PAMPs and DAMPs such as lipopolysaccharides (LPS), lipid A, peptidoglycans, flagellin, microbial RNA/DNA, as well as host cell constituents, such as uric acid, HMGB1 (high-mobility group box 1 protein), double-stranded DNA, and mitochondrial, are recognized by the members of the Toll-like receptor (TLR) family and nuclear oligomerization domain-like receptor of

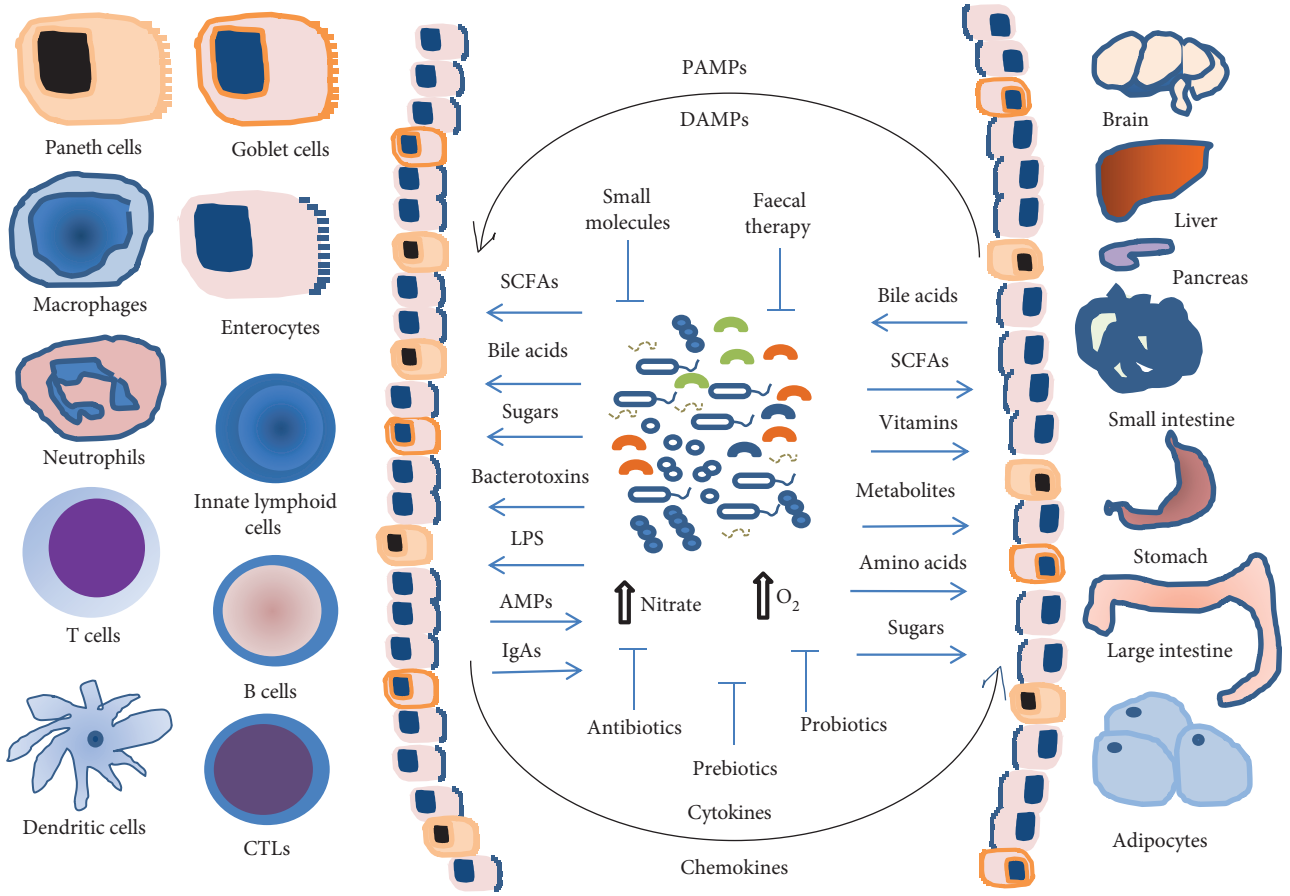

Figure 1: Interplay of gut microbiome-intestinal epithelial cells (enterocytes, goblet cells and paneth cells) and host metabolism and immunity. The commensal, symbiotic, and pathogenic microorganisms provide a great variety of nutrients and metabolites for host metabolism, for energy homeostasis of organs and tissues, and for the innate and adaptive immune cell activation and function. A shift toward dysbiosis results from a decrease in symbiont and/or an increase in pathobiont bacteria in intestinal lumen. Increases in nitrate and oxygen (O_2) allow the growth of facultative anaerobic bacteria. Increase in the gut permeability and release of PAMPs, such as peptidoglycan and LPS, and DAMPs, such as double-stranded RNA, mtDNA, and ATP. Increase in the production of cytokines, chemokines, nitric oxide (NO), and reactive oxygen species (ROS) by dendritic cells and macrophages causes local and systemic inflammation. Chronic, low-grade systemic inflammation leads to impaired insulin action, insulin resistance, obesity, hypertension, and metabolic syndrome. Probiotics, prebiotics, fecal therapy, and small molecules targeting host genes and specific bacterial species or phylum/class may help to reestablish tissue homeostasis and microbiome healthy. SCFAs: short-chain fatty acids; PAMPs: pathogen-associated molecular patterns; DAMPs: damage-associated molecular patterns; LPS: lipopolysaccharide; AMPs: antimicrobial peptides; IgA: immunoglobulin A.

NOD/NLR family [41, 42]. Extracellular and intracellular complexes formed by DAMPs and PAMPs and NOD/NLR receptors constitute the inflammasomes [43]. These cytosolic complexes associate with the adapter protein ASC (apoptosis-associated speck-like protein) and proinflammatory proteases of caspase family caspase 1, caspase 11, caspase 4, and caspase 5 [43]. Following the inflammasome activation occurs the production of interleukins IL-1β and IL-18. These cytokines increase the synthesis of other cytokines such as TNF-α, IL-6, IL-17, IL-22, and IL-23 and several active chemical inflammatory mediators [43].

Various studies using gene-deficient mice models have defined the direct and complex interplay of bacterial dysbiosis and genetic and environmental factors [35, 36, 44]. Many inflammatory diseases are caused by mutations or loss of some innate response genes in lymphoid tissues and smaller Peyer's patches and mesenteric lymph nodes [38, 39]. The components of inflammasomes such as MyD88, TLRs, NODs, NLrp3/6, ASC, and caspase 1 and caspase 11 are known to play a control of the intestinal dysbiosis [29, 38, 39, 45, 46]. For instance, NOD1$^{-/-}$ and NOD2$^{-/-}$ transgenic mice have increased susceptibility not only to inflammatory bowel disease but also to type 1 diabetes and cancer [38, 39, 45, 46]. The animal housing conditions and diet-induced microbiota composition are some examples that may be responsible for strain phenotypic differences in transgenic animals [47, 48]. Germ-free (GF) mice display underdeveloped lymphoid tissues, impairment of T and B cell function, and decreased CD4$^+$ T cells and antibody production. Their Th17 and Treg cells are less efficient in the control of infection. Colonization of GF mice with limited number of bacterial species (gnotobiotic mouse models) can restore immunological functions [47, 48]. The phenotypes observed in these mice models are not always observed in human studies. It is important to mention that 85% of the murine microbiome species have not been detected in human

microbiomes [49, 50]. Furthermore, the humanization of mouse models with human cells or human microbiota cannot adequately display the whole spectrum of relevant human disease phenotypes [47, 48].

Figure 1 displays major classes of molecules, metabolites, and nutrients produced by bacterial species, immune cells, tissues, and organs that regulate the dynamic interplay between host cells and gut microbiome, as well as therapeutic strategies for controlling dysbiosis and diseases.

4. Immunometabolism and Mitochondrion Reprogramming Pathways

Mitochondria serve as the powerhouse of the cell by producing and releasing critical signals to the environment and synthesizing ATP, the body's energy required for metabolic processes [51]. The bioenergetic pathways of glycolysis, the tricarboxylic acid (TCA) cycle (also known as Krebs cycle and the citric acid cycle), and fatty acid and amino acid metabolism are central metabolic processes for complete oxidation of all nutrients in the mitochondria [51, 52]. Cells use aerobic glycolysis to produce glucose-derived pyruvate that is converted into acetyl coenzyme A (acetyl-CoA). Acetyl-CoA molecules derived from glucose, glutamine, or fatty acid metabolism enter in the TCA cycle and are converted into CO_2, NADH, and $FADH_2$ during oxidative phosphorylation (OXPHOS) OXPHOS occurs through passing electrons along a series of carrier molecules, called the electron transport chain, with the help of electron carriers, such as NAD(P)H and $FADH_2$, that serve as substrate to generate adenosine triphosphate (ATP) in the mitochondrial matrix [51, 52]. The electrons are transferred from NADH to O_2 through three protein complexes: NADH dehydrogenase, cytochrome reductase, and cytochrome oxidase. Electron transport between the complexes occurs through other mobile electron carriers, ubiquinone and cytochrome c. The newly synthesized ATP is transported to the cytosol by adenine nucleotide translocase in exchange for ADP. Acetyl-CoA is the precursor for the synthesis of cholesterol and fatty acids, which are incorporated in the cellular plasma membranes.

Immunometabolism comprehends the hub of biochemical activities carry out by immune cells to modulate gene expression profile and switching metabolic pathways and their key enzymes [53]. After a stimulatory signal, various immune cells, in particular, macrophages, DCs, and T cells, exhibit distinct reprogramming metabolic pathways to promote their activation, survival, and lineage generation [53]. This reprogramming in the metabolic pathways is best characterized in macrophages and is illustrated in Figure 2. A seminal study by Newsholme et al. led to the discovery that the consumption rate of glucose, glutamine, and fatty acids and the enzymatic activities of glucose-6-phosphate dehydrogenase, 6-phosphogluconate dehydrogenase, citrate synthase, oxoglutarate dehydrogenase, and glutaminase differ in resting and elicited (inflammatory) macrophages [54]. Their study demonstrated that all glucose utilized by inflammatory macrophages was converted into lactate and very little of it was oxidized [54, 55]. Since then, the shift from oxidative phosphorylation (OXPHOS) toward glycolysis and glutaminolysis has been considered as a metabolic reprogramming pathway of the inflammatory cells. Remarkably, macrophages, T cells, and among other immune cells use glycolysis for rapid production of radical oxygen species (ROS) used for limiting infection. Glycolysis also provides rapid production of ATP and metabolic intermediates for the synthesis of ribose for nucleotides and amino acids for the biosynthesis by RNA and DNA of proteins by macrophages. Glycolysis is a preferential pathway for the activation of dendritic cells, $CD4^+$ T helper 1 (Th1), Th2, and Th17 cells, NK cells, and cytotoxic $CD8^+$ cells [51, 52]. Interesting, this metabolic adaptation to aerobic glycolysis (in the presence of oxygen) was first described as a hallmark of tumor cells by Warburg et al. in a seminal report published 60 years ago [56].

Unstimulated macrophages displaying M0 phenotype and exhibiting the differentiation surface markers $CD68^+$/$CD80/^{low}$/$CD206^{high}$ acquire and display the M1 phenotype ($CD68^+$/$CD80/^{low}$/$CD206^{low}$) or M2 phenotype ($CD68^+$/$CD80^{high}$/$CD206/^{low}$) after switching their metabolism and function in response to stimuli or polarization signals that initiate a pro- or anti-inflammatory response [57]. M1 cells display Th1-oriented proinflammatory effector properties and promote tissue damage and antimicrobial and antitumor resistance, whereas M2 cells exhibit tissue remodeling and repair functions, promote wound healing, angiogenesis, and resistance to parasites, and favor tumor growth. The reprogramming metabolic pathways in M1/M2 macrophages alter their functions, including cytokine production, phagocytosis, and antigen presentation [58–60]. The classical activation pathway or reprogramming pathway in M1 macrophages promotes the accumulation of citrate and high production of NO, ROS, cytokines, and prostaglandins [60, 61]. M1 macrophages release ROS and NO in phagosomes where they promote the killing of pathogens. Th2 cytokines, such as IL-4 and IL-13, regulate macrophage alternative pathway or M2 reprogramming pathway. The major feature of M2 reprograming pathways is that TCA cycle occurs coupled to oxidative phosphorylation, β-oxidation of fatty acids, and mitochondrial biogenesis. In addition, M2 macrophages do not produce NO. It is important to consider that M2 macrophages display various distinct forms (M2a, b, and c) depending on the local tissue environment and exposure to stimuli [57].

The generation of UDP-GlcNAc intermediates promotes the glycosylation of M2-associated receptors, such as the mannose receptor [60]. Thus, both macrophage M1 and M2 phenotypes can be controlled by either oxygen and nutrients or cytokines and damage- and pathogen-associated molecular pattern- (DAMP- and PAMP-) mediated signals [60]. These events are controlled by the signaling and transcriptional pathways induced by canonical regulators of cellular metabolism, such as C-myc transcription factor, coactivator proteins such as PPARγ and PGC-1β (peroxisome proliferative-activated receptor γ, coactivator 1β), and signaling pathways driven by AMPK (5′-adenosine monophosphate-activated protein kinase), mTORC1/2 (mammalian target of rapamycin complexes), and STAT6

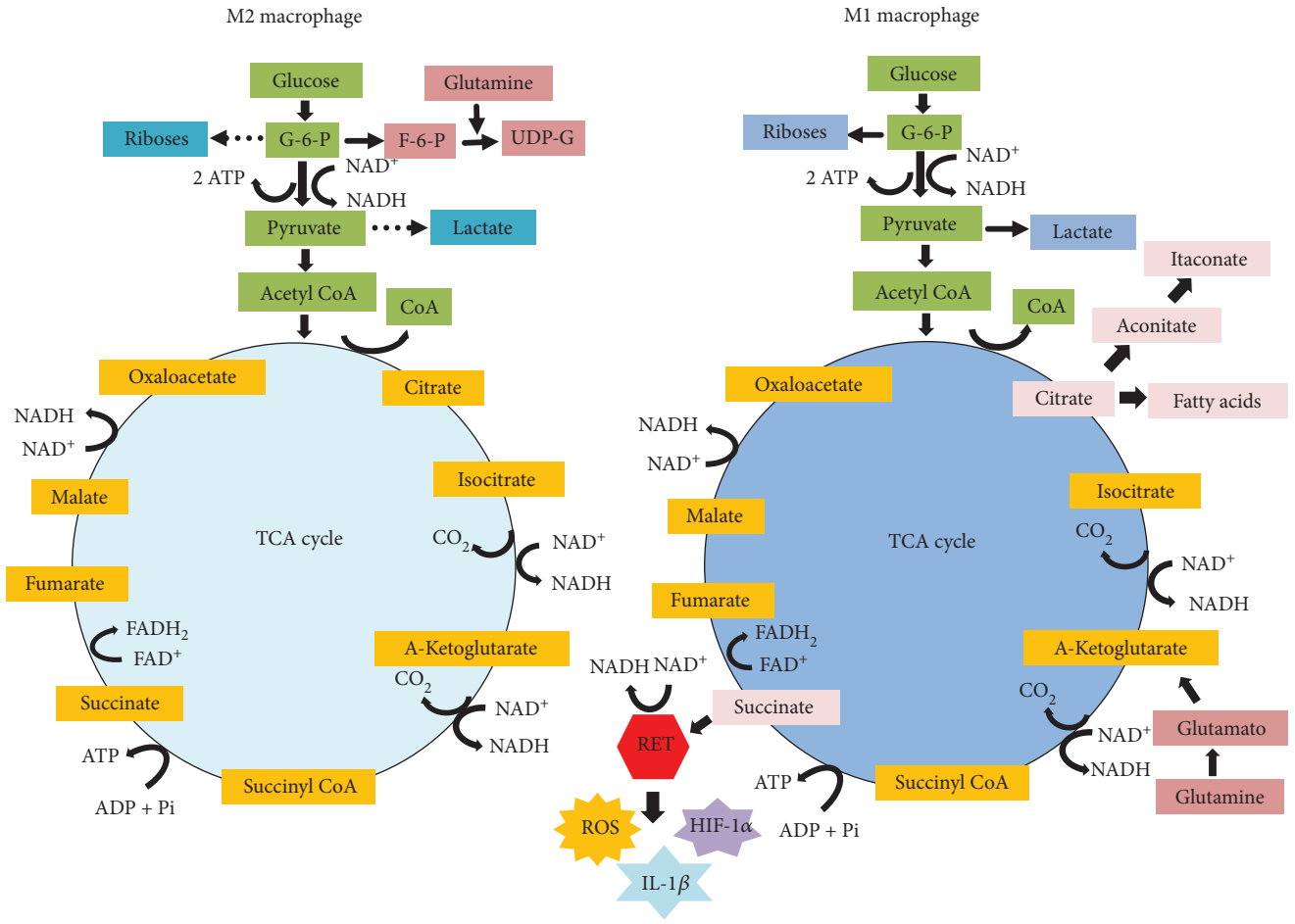

Figure 2: Metabolic pathways supporting macrophage reprogramming in either M2 or M1 phenotype. IL-4-stimulated M2 macrophage utilizes glycolysis, TCA, and mitochondrial oxidative phosphorylation (OXPHOS) to generate NADPH and ATP for energy. G-6-P and glutamine are used for generation of UDP-Glc-Nac required for receptors and protein glycosylation. LPS-stimulated M1 macrophage produces G-6-P that is reduced to pyruvate, in parallel, NAD^+ is reduced to NADPH, and 2 ATP molecules are produced. In hypoxia, pyruvate is reduced to lactate, restoring NAD^+ to glycolysis recycle, and thus, OXPHOX is uncoupled to glycolysis. TCA cycle in LPS-stimulated M1 macrophageis deviated after citrate and after succinate. Citrate is used for the syntheses of NO, ROS, and prostaglandins. Citrate is used by the enzyme immune-responsive gene 1 (IRG1) to generate itaconate that acts as an endogenous SDH inhibitor and also as antimicrobial. Succinate is oxidized by SDH and subsequently used for production of ROS from a complex 1 via reverse electron transport (RET). Succinate activates HIF-1α which in turn increases the transcription of IL-1β. Glutaminolysis provides NADPH for generation of ROS. SDH: succinate dehydrogenase; UDP-Glc-Nac: uridine diphosphate N-acetylglucosamine; NO: nitric oxide; ROS: reactive oxygen species. Arrows indicated the direction of reaction and products.

(signal transducer and activator of transcription) [51, 52]. A deep overview of macrophage metabolic pathways and phenotypic and functional outcomes is described elsewhere [62].

In 2013, Tannahil et al. reported that expression of IL-1β mRNA in M1 macrophages stimulated with LPS leads to activation of the transcription factor hypoxia-induced factor 1α (HIF1α), in a glycolysis-dependent manner [63]. HIF1α interacts with pyruvate kinase isoenzyme M2 (PKM2) and promotes the expression of HIF1α-induced genes required for glycolysis [64]. The activation of the Warburg effect (glycolysis) in LPS-stimulated macrophages causes an accumulation of intermediates of the TCA cycle, in particular, succinate, malate, and fumarate due to a flux deviation or a "break point" of the Krebs cycle pathway (see Figure 2). Succinate exerts multiple immunological functions [52, 53, 63]. Oxidation of succinate by the enzyme succinate dehydrogenase (SHD), which converts succinate to fumarate, drives the production of ROS from complex II in the mitochondrion, a process named reverse electron transport (RET). Macrophages respond to activation of HIF-1α via ROS and increasing the expression of IL-1β [58]. Inhibition of SDH with dimethylmalonate inhibits IL-1β expression, while increasing the production of immunosuppressive cytokine IL-10 [52, 63].

Itaconate is one important metabolite formed in the second flux deviation or "break point' of the Krebs cycle pathway during macrophage transition from inactive to proinflammatory state [65]. Itaconate is an unsaturated dicarboxylic acid produced by extra mitochondrial enzyme cys-aconitate decarboxylase encoded by immune-responsive gene 1 (*Irg1*). This enzyme converts cys-aconitate (derived from citrate) to itaconic acid. One of remarkable effect

observed after itaconate treatment is the reduction of the expression of cytokines IL-1β, IL-6, and iNOS [65]. Studies using murine bone marrow-derived macrophages (BMDMs) and RAW-264.7 cells, stimulated with LPS and cytokines, showed that the absence (knockdown) of *Irg* gene leads to impairment in substrate-level phosphorylation (SLP) of mitochondria [66]. SLP is a metabolic reaction that results in the formation of ATP or GTP by the direct transfer of phosphate group to ADP or GDP from another phosphorylated compound. Administration of itaconate (0.5-2 mM) reverses this reaction [66]. Studies using transgenic mice and immune cells deficient of *Irg* 1 gene demonstrated that itaconate acts as an endogenous succinate dehydrogenase inhibitor and that such inhibition causes the accumulation of succinate [67]. Together, these studies confirmed that itaconate regulates succinate levels, mitochondrial respiration, and inflammatory cytokine production and, therefore, acts as an important regulator of macrophage activation. Furthermore, itaconic acid has antimicrobial activity and kills directly intracellular *Salmonella typhimurium*, *Legionella pneumophila*, and *Mycobacterium tuberculosis*; thus, it protects against infection. The cytotoxic effect is associated with the inhibition of the enzyme isocitrate lyase [68]. Isocitrate lyase regulates a bacterial specific metabolic pathway known as the glyoxylate shunt, in which acetyl-CoA is converted to succinate for the synthesis of carbohydrates. In this pathway, isocitrate is cleaved by the enzyme ICL (encoded by aceA) yielding glyoxylate and succinate, which reenter into TCA cycle following the oxidative decarboxylation steps. Thus, the glyoxylate shunt acts as microbial survival pathway [66–68].

5. Gut Dysbiosis Associated with Metabolic Diseases

Studies on the relationship among gut microbes, obesity, insulin resistance, and metabolic syndrome have shown an intricate interplay between host diet, genetics, and microbiome compositional dynamics [49, 69, 70]. A series of experiments have shown that a chronic inflammatory process through translocation of gut bacterial LPS into the bloodstream initiates a silent metabolic endotoxemia and ultimately obesity-related disorders [71–73]. The hallmarks of clinical manifestations of metabolic syndrome include central obesity, high blood pressure, and high levels of blood sugar and serum triglycerides, which are most significant drifts to the development of insulin resistance, type 2 diabetes, hypertension, and fatty liver disease. Individuals robustly colonized by bacteria and archeae of the genera *Faecalibacterium*, *Bifidobacterium*, *Lactobacillus*, *Coprococcus*, and *Methanobrevibacter* have significantly less tendency to develop metabolic disturbances and inflammation and, in turn, type 2 diabetes and ischemic cardiovascular disorders [49, 73]. These species are higher producers of SCFAs and hydrogen peroxides, which are compounds known to inhibit biofilm formation by pathogenic species, including *Staphylococcus aureus* and *E. coli* [73].

Obesity is associated with behavioral and environmental factors, such as excessive consumption of energy-dense foods and sedentary lifestyle [49, 73–75]. Initial clues for the role of microorganisms in energy homeostasis and obesity appeared from the studies using germ-free animals [76]. Several important questions on the complex interaction between host and microbes in pathophysiology of obesity remain answered [49, 74, 75]. Studies in genetic and diet-induced mouse models of obesity confirmed that the ratio of Firmicutes to Bacteroidetes is increased in obese animals, as compared to nonobese control animals [33, 49, 77]. The higher ratio of Firmicutes to Bacteroidetes was also found in clinical studies that evaluated overweight and obese healthy volunteers [33], in high total amount of fecal SCFAs was detected [78]. Mouse and human models have demonstrated inverse relationships between *A. muciniphila* colonization and inflammatory conditions. In fact, *A. muciniphila* is present in low levels in people suffering from morbid obesity, diabetes, and cardiometabolic diseases supporting their role as antiobesity strain [79].

The contribution of GI hypothalamic-pituitary-adrenal axis for predisposition to obesity is still incompletely understood [18, 70]. Recently, one study described the relationship of high-fat diet and the levels of acetate produced by intestinal microbiota in a rat model [80]. The authors concluded that chronic acetate turnover activates the parasympathetic nervous system, which coordinates the secretion of glucose-stimulated insulin, ghrelin, and hyperphagia. They conclude that together these factors cooperate in the promotion of obesity [80]. High-fat diet-induced obesity leads also to chronic low-grade hypothalamic inflammation and activation of both microglia and astrocytes [81]. A study using mice model suggests that acetate accumulated in the hypothalamus. This compound plays a central role in prevention of weight gain through an anorectic effect [82]. The neuroimmuno-endocrine pathway is crucial for glucose homeostasis and control of adiposity in obese people recovering from bariatric surgery [80]. After bariatric surgery by Roux-en-Y gastric bypass (RYGB) methods, human and animal models change food preference [83, 84]. Normally, a fatty acid derivative named oleoylethanolamide (OEA) is produced after ingesting a fat meal. OEA can directly activate PPAR-α receptors, which are responsible for promoting satiety via vagus nerve and dopamine release in the brain [84]. Dopamine-suppressed obese animals display low levels of OEA in the brain. After RYGB surgery, these animals increase the levels of OEA and dopamine 1 receptor (D1R) expression, which promote a shift in GI-brain axis signaling. This leads to dramatic change in animal feeding behavior which includes the preference for low-fat food [84]. RYGB is also known to profoundly affect the secretion of many gastrointestinal hormones, including ghrelin and GLP-1 [83]. Administration of exogenous GLP-1 or GLP-1 analog promotes weight loss and glucose regulation in T2DM patients. Remarkably, metformin, a drug used to treat T2DM, can increase butyrate-producing bacteria and thereby promote the restoration of the healthy microbiome [85]. Together, these discoveries have opened new perspectives for future therapies to improve health by targeting pivotal host cells, microbes, and microbiome-derived metabolites.

6. Targeting Gut Microbiota Dysbiosis and Metabolic Pathways

6.1. Probiotics and Prebiotics. The immunologist Elie Metchnikoff was the first to defend that the ingestion of fermented milk (i.e., yogurt) prepared with *Bacillus bulgaricus* increases health and prolong life span. He anticipated the rational use of probiotic made of live microorganisms with a health benefit through altering the gut microbiome [86]. *Lactobacillus plantaram* and *Bifidobacterium* are probiotic bacteria capable of modulating negative effects of high-fat diets and even managing immunological reactions mediated by inflammatory diseases [25, 38, 45]. *Bifidobacterium* and *Lactobacillus* are producers of folate in the gut. *Lactobacillus rhamnosus* in combination with *Lactobacillus gasseri* and *Bifidobacterium lactis* may reduce weight gain, in particular, fat tissue mass adiposity, in humans [87]. Studies on the effects of *A. muciniphila* alive or pasteurized, in high-fat diet-fed mice, revealed that a small 30 kDa Amuc_1100 protein activates TLR2, allowing the development of an intestinal health immune response [79].

Dietary prebiotics are known to provide immune and metabolic benefits to the host [14, 86]. The poorly digestible carbohydrates, such as nonstarch polysaccharides, resistant starch, nondigestible oligosaccharides (NDOs), and polyphenols, are source of various sugars including glucose, galactose, rhamnose, and rutinose. The carbohydrate-hydrolyzing enzymes of colonic microbiota promote the fermentation of prebiotics, and these produce hydrogen, methane, carbon dioxide, and SCFAs. When associated, the probiotic and prebiotic can selectively stimulate growth and activity of health-promoting bacteria [14, 86]. In this way, probiotic and prebiotics have potential to modulate metabolic processes involved in T2DM and obesity-related disorders [14, 86]. Ingestion of inulin or oligofructose improves metabolic disorders associated with obesity, including insulin resistance and metabolic endotoxemia [34, 71, 79]. These effects may be associated with restoration of gut barrier integrity and reduction of LPS release from Gram-negative bacteria [25, 88].

6.2. Fecal Microbial Transplant (FMT). The use of antibiotics permanently modifies gut microbial community [89]. High doses and frequency of antibiotics, particularly against anaerobes, such as vancomycin, can disrupt and destabilize normal gut microbiome. Extended spectrum antibiotic causes the overgrowth of *Clostridium difficile* and chronic recurrent colitis [89]. Fecal bacteriotherapy is a clinical procedure, in which a liquid suspension of stool from a human donor (a family member or a disease-free screened donor) is inoculated into gut's patients to restore gut microbiota in refractory cases of *Clostridium difficile* colorectal infection after antibiotic therapy [90, 91]. These fecal preparations may contain from 3.0% to 10% of viable, dead bacteria and colonic cells and other components that impact on transplant outcomes, by enhancing or inhibiting immune function of innate lymphoid cells (ILCs) [92]. Today, more than 150 clinical trials involving FMT are being conducted, mostly in the USA to treat a large array of metabolic, infectious, and immunological diseases and complications, including kidney- and liver-transplanted patients, especially with antibiotic-resistant bacterial colonization or infection (ClinicalTrials.gov).

Studies have shown that around 90% of the patients that received FMT for *Clostridium difficile* infection were cured, as compared to 31% of those receiving only vancomycin (van Nood et al. [93]). *Lactobacillus*, *Enterococcus*, *Bifidobacterium*, and *Bacteroides* are known to exert an inhibitory activity against *C. difficile* growth. For instance, a variety of viruses, archaea, fungi, parasitic species, and metabolites are transferred together with FMT [92]. Thus, further studies are needed to confirm their ability to potentially promote host intestinal immunity while optimizing microbiome diversity.

A series of animal model studies have shown that the gut microbiome plays a crucial role in weight gain and obesity [49, 50, 70]. Studies on lean and genetically obese (ob/ob) mice and rats have revealed great difference in their intestinal absorption and microbiome composition, which are related to 50% reduction in Bacteroidetes and proportional increases in Firmicutes and Archaea species [74, 75]. Transferring the microbiota from fat mice to germ-free mice hosts induces greater weight gain than in those receiving the microbiota from lean donors [49, 50]. High-fat intake increases intestinal permeability and diffusion of LPS associated with obesity. In contrast, the administration of *Bifidobaterium infantis* in mice reduces the production of proinflammatory cytokines while promoting white adipose tissue gain [68, 71]. Results of FMT treatment of people with diverse metabolic disorders have not been conclusive. Transfer of intestinal microbiota from lean donors mildly increased insulin sensitivity in subjects with metabolic syndrome [94]. Short exposure to antibiotics may improve peripheral insulin sensitivity in a small number of obese subjects [94]. Furthermore, in a study with 75 obese and prediabetic volunteers that underwent an 8-day antibiotic treatment (amoxicillin and vancomycin), the antibiotic-driven dysbiosis did not alter gut permeability, as confirmed by variation in LPS levels and expression of lipid metabolic enzymes [95]. Such heterogeneity may reflect complex interactions between genetic, lifestyle, and environmental factors derived from different model systems.

6.3. Small Molecules. Acetate, propionate, and butyrate are the most important SCFAs that eventually are given as oral dietary supplementation. SCFAs acting as signaling molecules produce various physiological effects in humans [96]. They bind to GPR41 and GPR43 receptors (free fatty acid receptors 2 and 3, FFARs 2/3) in intestinal L cells signaling the release of GLP-1 and peptide YY [78]. Notably, injection of GLP-1 peptides stimulates insulin signaling in white adipose tissues, therefore reducing adiposity. SCFAs also increase leptin secretion and adipogenesis while inhibiting lipolysis of adipose tissues. In the liver, propionate acts as a gluconeogenic factor while acetate and butyrate act as lipogenic factors [96]. SCFAs, particularly, propionic and butyric acids, may directly prevent low-grade inflammatory response in obesity by controlling gut microbiota [88]. Butyrate acting on human monocyte, marrow-derived DCs, and

macrophages inhibits IL-12 production, decreases costimulatory molecule expression, and blocks NF-κB translocation [37]. Butyrate and structural analog and ketone body β-hydroxybutyrate (also known as 3-hydroxybutyrate) supplementation can inhibit the activity of histone deacetylases (HDACs). HDACS promote specific histone modifications to regulate transcription and DNA replication and repair. It also exerts anti-inflammatory activity by suppressing NF-κB and STAT1 activation [22–95]. Succinate is a well-known inhibitor of the histone demethylases (DNMTs) and the eleven translocation (TET) methylcytosine dioxygenases, which oxidize 5-methylcytosines to promote DNA demethylation [22].

Several small molecule inhibitors of metabolic pathways such as 2-deoxy-glucose, dichroacetate, BPTES (bis-2-(5-phenylacetamido-1,3,4-thiadiazol-2-yl)ethyl sulfide), dimethylmalonate (DMM), rotenone, and metformin have identified as promise therapeutics [51, 52, 60]. Metformin is a first-line medication for the treatment of T2D that significantly improves metabolic parameters such as body weight, insulin, glucose, leptin, and C-reactive protein plasma levels [96]. By inhibiting complex I in mitochondrial respiration chain, metformin elevates the plasma levels of lactate. Lactic acidosis is a critical problem in clinical practice. Metformin causes a switch from OXPHOS to aerobic glycolysis [97]. Thus, users of metformin have a higher risk of metformin-associated lactic acidosis. Metformin treatment increases significantly the relative abundance of *A. muciniphila* in the fecal microbiota in obese mice [34]. *A. muciniphila* is a producer of acetate and propionate, through mucin degradation, and T2D patients treated with metformin increase their butyrate- and propionate-producing bacteria, which may in turn contribute to the beneficial effect of metformin [85]. It is interesting to ask if metformin effects are also associated with M1/M2 macrophage metabolic reprogramming pathways.

Succinate is a strong proinflammatory mediator [51, 63]. DMM inhibits mitochondrial ROS production through inhibition of succinate dehydrogenase (SDA), which converts succinate to fumarate. This metabolic alteration limits the production IL-1β, while increasing the synthesis of immunosuppressive IL-10 [67]. TEPP-46 and DASA-58, two small molecule inhibitors of PKM2 (pyruvate kinase isozyme 2), inhibit LPS-induced HIF-1α and IL-1β, thereby promoting the reprogramming of M1 macrophages to M2 [63, 98]. Thus, further studies are required to confirm these pharmacological targets and approaches to control metabolic disorders.

7. Conclusions and Perspectives

Over the last decade, the sequencing and analyses of a large number of human microbiomes and assembly of their metabolic pathways have expanded our understanding of how bacterial metabolites participate in the microbe-host interactions in health and diseases. The functional variations of gut microbiomes among individuals have indicated the anabolic and catabolic pathways of essential importance in maintaining core community structures for whole body homeostasis. Emerging new biomarkers are promising specific discrimination of phyla and species to confirm evidences for direct participation of microbes in type II diabetes, obesity, metabolic disorders, inflammatory bowel diseases, and even certain cancers.

There is no doubt that dysbiosis, by altering microbiome metabolism and consequently host metabolism, not only affects inflammatory responses and adaptive immunity but also contributes to metabolic disorders. The use of innovative pharmaceutical and nutraceutical products to manage microbial colonization and development of a healthy gut microbial community at early childhood and adult life may prevent the occurrence of common inflammatory and metabolic pathologies. Finally, the discovery and development of drugs that target enzymes of metabolic pathways, and also drive pro- and anti-inflammatory responses of immune cells, will provide the next frontier medicine for metabolic therapies in near future.

Conflicts of Interest

The authors declare that they have no conflicts of interests.

Authors' Contributions

JEB, JF, and MGM conducted the literature review process and selected articles and wrote the manuscript and prepared figures. The authors read and approved the final manuscript.

Acknowledgments

We thank colleagues of the University of Sao Paulo and Clinical Hospital of Medical School for insights and productive discussions. Financial support from the Coordenação de Aperfeiçoamento de Pessoal de Nível Superior (2011/188-37), the Conselho Nacional de Desenvolvimento Científico e Tecnológico (308794/2014-1 and 312206/2016-0), and the Fundação de Amparo à Pesquisa do Estado de São Paulo (2007/04513-1 and 2015/18647-6) is acknowledged.

References

[1] F. Bäckhed, C. M. Fraser, Y. Ringel et al., "Defining a healthy human gut microbiome: current concepts, future directions, and clinical applications," *Cell Host & Microbe*, vol. 12, no. 5, pp. 611–622, 2012.

[2] J. E. Belizario and M. Napolitano, "Human microbiomes and their roles in dysbiosis, common diseases, and novel therapeutic approaches," *Frontiers in Microbiology*, vol. 6, p. 1050, 2015.

[3] R. Sender, S. Fuchs, and R. Milo, "Revised estimates for the number of human and bacteria cells in the body," *PLoS Biology*, vol. 14, no. 8, article e1002533, 2016.

[4] J. Qin, R. Li, J. Raes et al., "A human gut microbial gene catalogue established by metagenomic sequencing," *Nature*, vol. 464, no. 7285, pp. 59–65, 2010.

[5] J. Li, H. Jia, X. Cai et al., "An integrated catalog of reference genes in the human gut microbiome," *Nature Biotechnology*, vol. 32, no. 8, pp. 834–841, 2014.

[6] J. Lloyd-Price, G. Abu-Ali, and C. Huttenhower, "The healthy human microbiome," *Genome Medicine*, vol. 8, no. 1, p. 51, 2016.

[7] J. Lloyd-Price, A. Mahurkar, G. Rahnavard et al., "Strains, functions and dynamics in the expanded Human Microbiome Project," *Nature*, vol. 550, no. 7674, pp. 61–66, 2017.

[8] D. H. Parks, C. Rinke, M. Chuvochina et al., "Recovery of nearly 8,000 metagenome-assembled genomes substantially expands the tree of life," *Nature Microbiology*, vol. 2, no. 11, pp. 1533–1542, 2017.

[9] M. Arumugam, J. Raes, E. Pelletier et al., "Enterotypes of the human gut microbiome," *Nature*, vol. 473, no. 7346, pp. 174–180, 2011.

[10] O. Koren, D. Knights, A. Gonzalez et al., "A guide to enterotypes across the human body: meta-analysis of microbial community structures in human microbiome datasets," *PLoS Computational Biology*, vol. 9, no. 1, article e1002863, 2013.

[11] E. Le Chatelier, T. Nielsen, J. Qin et al., "Richness of human gut microbiome correlates with metabolic markers," *Nature*, vol. 500, no. 7464, pp. 541–546, 2013.

[12] A. H. Moeller, Y. Li, E. Mpoudi Ngole et al., "Rapid changes in the gut microbiome during human evolution," *Proceedings of the National Academy of Sciences of the United States of America*, vol. 111, no. 46, pp. 16431–16435, 2014.

[13] V. Tremaroli and F. Bäckhed, "Functional interactions between the gut microbiota and host metabolism," *Nature*, vol. 489, no. 7415, pp. 242–249, 2012.

[14] I. Rowland, G. Gibson, A. Heinken et al., "Gut microbiota functions: metabolism of nutrients and other food components," *European Journal of Nutrition*, vol. 57, no. 1, pp. 1–24, 2018.

[15] K. Meijer, P. de Vos, and M. G. Priebe, "Butyrate and other short-chain fatty acids as modulators of immunity: what relevance for health?," *Current Opinion in Clinical Nutrition and Metabolic Care*, vol. 13, no. 6, pp. 715–721, 2010.

[16] F. J. Gonzalez, C. Jiang, C. Xie, and A. D. Patterson, "Intestinal farnesoid X receptor signaling modulates metabolic disease," *Digestive Diseases*, vol. 35, no. 3, pp. 178–184, 2017.

[17] J. M. Ridlon, D. J. Kang, P. B. Hylemon, and J. S. Bajaj, "Bile acids and the gut microbiome," *Current Opinion in Gastroenterology*, vol. 30, no. 3, pp. 332–338, 2014.

[18] S. M. Collins, M. Surette, and P. Bercik, "The interplay between the intestinal microbiota and the brain," *Nature Reviews Microbiology*, vol. 10, no. 11, pp. 735–742, 2012.

[19] W. R. Wikoff, A. T. Anfora, J. Liu et al., "Metabolomics analysis reveals large effects of gut microflora on mammalian blood metabolites," *Proceedings of the National Academy of Sciences of the United States of America*, vol. 106, no. 10, pp. 3698–3703, 2009.

[20] N. Pornputtapong, I. Nookaew, and J. Nielsen, "Human metabolic atlas: an online resource for human metabolism," *Database*, vol. 2015, article bav068, 2015.

[21] S. Abubucker, N. Segata, J. Goll et al., "Metabolic reconstruction for metagenomic data and its application to the human microbiome," *PLoS Computational Biology*, vol. 8, no. 6, article e1002358, 2012.

[22] Y. Qin and P. A. Wade, "Crosstalk between the microbiome and epigenome: messages from bugs," *Journal of Biochemistry*, vol. 163, no. 2, pp. 105–112, 2018.

[23] M. B. Miller and B. L. Bassler, "Quorum sensing in bacteria," *Annual Review of Microbiology*, vol. 55, no. 1, pp. 165–199, 2001.

[24] M. J. Ostaff, E. F. Stange, and J. Wehkamp, "Antimicrobial peptides and gut microbiota in homeostasis and pathology," *EMBO Molecular Medicine*, vol. 5, no. 10, pp. 1465–1483, 2013.

[25] G. Reid, J. A. Younes, H. C. Van der Mei, G. B. Gloor, R. Knight, and H. J. Busscher, "Microbiota restoration: natural and supplemented recovery of human microbial communities," *Nature Reviews Microbiology*, vol. 9, no. 1, pp. 27–38, 2011.

[26] D. J. Palmer, J. Metcalfe, and S. L. Prescott, "Preventing disease in the 21st century: the importance of maternal and early infant diet and nutrition," *Journal of Allergy and Clinical Immunology*, vol. 130, no. 3, pp. 733-734, 2012.

[27] C. R. Webb, I. Koboziev, K. L. Furr, and M. B. Grisham, "Protective and pro-inflammatory roles of intestinal bacteria," *Pathophysiology*, vol. 23, no. 2, pp. 67–80, 2016.

[28] M. X. Byndloss, E. E. Olsan, F. Rivera-Chávez et al., "Microbiota-activated PPAR-γ signaling inhibits dysbiotic Enterobacteriaceae expansion," *Science*, vol. 357, no. 6351, pp. 570–575, 2017.

[29] J. C. Clemente, L. K. Ursell, L. W. Parfrey, and R. Knight, "The impact of the gut microbiota on human health: an integrative view," *Cell*, vol. 148, no. 6, pp. 1258–1270, 2012.

[30] E. M. Brown, M. Sadarangani, and B. B. Finlay, "The role of the immune system in governing host-microbe interactions in the intestine," *Nature Immunology*, vol. 14, no. 7, pp. 660–667, 2013.

[31] C. A. Thaiss, N. Zmora, M. Levy, and E. Elinav, "The microbiome and innate immunity," *Nature*, vol. 535, no. 7610, pp. 65–74, 2016.

[32] A. Swidsinski, V. Loening-Baucke, H. Lochs, and L. P. Hale, "Spatial organization of bacterial flora in normal and inflamed intestine: a fluorescence in situ hybridization study in mice," *World Journal of Gastroenterology*, vol. 11, no. 8, pp. 1131–1140, 2005.

[33] F. J. Verdam, S. Fuentes, C. de Jonge et al., "Human intestinal microbiota composition is associated with local and systemic inflammation in obesity," *Obesity*, vol. 21, no. 12, pp. E607–E615, 2013.

[34] A. Everard, C. Belzer, L. Geurts et al., "Cross-talk between *Akkermansia muciniphila* and intestinal epithelium controls diet-induced obesity," *Proceedings of the National Academy of Sciences of the United States of America*, vol. 110, no. 22, pp. 9066–9071, 2013.

[35] U. Roy, E. J. C. Gálvez, A. Iljazovic et al., "Distinct microbial communities trigger colitis development upon intestinal barrier damage via innate or adaptive immune cells," *Cell Reports*, vol. 21, no. 4, pp. 994–1008, 2017.

[36] J. L. Round and S. K. Mazmanian, "The gut microbiota shapes intestinal immune responses during health and disease," *Nature Reviews Immunology*, vol. 9, no. 5, pp. 313–323, 2009.

[37] A. J. McDermott and G. B. Huffnagle, "The microbiome and regulation of mucosal immunity," *Immunology*, vol. 142, no. 1, pp. 24–31, 2014.

[38] L. V. Hooper, D. R. Littman, and A. J. Macpherson, "Interactions between the microbiota and the immune system," *Science*, vol. 336, no. 6086, pp. 1268–1273, 2012.

[39] K. Honda and D. R. Littman, "The microbiota in adaptive immune homeostasis and disease," *Nature*, vol. 535, no. 7610, pp. 75–84, 2016.

[40] A. Fuchs and M. Colonna, "Natural killer (NK) and NK-like cells at mucosal epithelia: mediators of anti-microbial defense and maintenance of tissue integrity," *European Journal of Microbiology and Immunology*, vol. 1, no. 4, pp. 257–266, 2011.

[41] H. Kono and K. L. Rock, "How dying cells alert the immune system to danger," *Nature Reviews Immunology*, vol. 8, no. 4, pp. 279–289, 2008.

[42] B. Sangiuliano, N. M. Pérez, D. F. Moreira, and J. E. Belizário, "Cell death-associated molecular-pattern molecules: inflammatory signaling and control," *Mediators of Inflammation*, vol. 2014, Article ID 821043, 14 pages, 2014.

[43] V. A. K. Rathinam and K. A. Fitzgerald, "Inflammasome complexes: emerging mechanisms and effector functions," *Cell*, vol. 165, no. 4, pp. 792–800, 2016.

[44] M. Mamantopoulos, F. Ronchi, F. van Hauwermeiren et al., "Nlrp6- and ASC-dependent inflammasomes do not shape the commensal gut microbiota composition," *Immunity*, vol. 47, no. 2, pp. 339–348.e4, 2017.

[45] C. L. Maynard, C. O. Elson, R. D. Hatton, and C. T. Weaver, "Reciprocal interactions of the intestinal microbiota and immune system," *Nature*, vol. 489, no. 7415, pp. 231–241, 2012.

[46] F. R. C. Costa, M. C. S. Françozo, G. G. de Oliveira et al., "Gut microbiota translocation to the pancreatic lymph nodes triggers NOD2 activation and contributes to T1D onset," *Journal of Experimental Medicine*, vol. 213, no. 7, pp. 1223–1239, 2016.

[47] D. Laukens, B. M. Brinkman, J. Raes, M. De Vos, and P. Vandenabeele, "Heterogeneity of the gut microbiome in mice: guidelines for optimizing experimental design," *FEMS Microbiology Review*, vol. 40, no. 1, pp. 117–132, 2016.

[48] J. V. Fritz, M. S. Desai, P. Shah, J. G. Schneider, and P. Wilmes, "From meta-omics to causality: experimental models for human microbiome research," *Microbiome*, vol. 1, no. 1, p. 14, 2013.

[49] R. E. Ley, P. J. Turnbaugh, S. Klein, and J. I. Gordon, "Microbial ecology: human gut microbes associated with obesity," *Nature*, vol. 444, no. 7122, pp. 1022-1023, 2006.

[50] R. E. Ley, M. Hamady, C. Lozupone et al., "Evolution of mammals and their gut microbes," *Science*, vol. 320, no. 5883, pp. 1647–1651, 2008.

[51] E. L. Mills, B. Kelly, and L. A. J. O'Neill, "Mitochondria are the powerhouses of immunity," *Nature Immunology*, vol. 18, no. 5, pp. 488–498, 2017.

[52] K. Ganeshan and A. Chawla, "Metabolic regulation of immune responses," *Annual Review of Immunology*, vol. 32, no. 1, pp. 609–634, 2014.

[53] L. A. J. O'Neill, R. J. Kishton, and J. Rathmell, "A guide to immunometabolism for immunologists," *Nature Reviews Immunology*, vol. 16, no. 9, pp. 553–565, 2016.

[54] P. Newsholme, R. Curi, S. Gordon, and E. A. Newsholme, "Metabolism of glucose, glutamine, long-chain fatty acids and ketone bodies by murine macrophages," *Biochemical Journal*, vol. 239, no. 1, pp. 121–125, 1986.

[55] C. Murphy and P. Newsholme, "Importance of glutamine metabolism in murine macrophages and human monocytes to L-arginine biosynthesis and rates of nitrite or urea production," *Clinical Science*, vol. 95, no. 4, pp. 397–407, 1998.

[56] O. Warburg, K. Gawehn, and A. W. Geissler, "Metabolism of leukocytes," *Zeitschrift für Naturforschung B*, vol. 13B, pp. 515-516, 1958.

[57] A. Sica and A. Mantovani, "Macrophage plasticity and polarization: in vivo veritas," *The Journal of Clinical Investigation*, vol. 122, no. 3, pp. 787–795, 2012.

[58] J. Jantsch, D. Chakravortty, N. Turza et al., "Hypoxia and hypoxia-inducible factor-1α modulate lipopolysaccharide-induced dendritic cell activation and function," *The Journal of Immunology*, vol. 180, no. 7, pp. 4697–4705, 2008.

[59] E. Lachmandas, L. Boutens, J. M. Ratter et al., "Microbial stimulation of different Toll-like receptor signalling pathways induces diverse metabolic programmes in human monocytes," *Nature Microbiology*, vol. 2, no. 3, article 16246, 2017.

[60] L. A. J. O'Neill and E. J. Pearce, "Immunometabolism governs dendritic cell and macrophage function," *Journal of Experimental Medicine*, vol. 213, no. 1, pp. 15–23, 2016.

[61] V. Infantino, P. Convertini, L. Cucci et al., "The mitochondrial citrate carrier: a new player in inflammation," *Biochemical Journal*, vol. 438, no. 3, pp. 433–436, 2011.

[62] R. Curi, R. de Siqueira Mendes, L. A. de Campos Crispin, G. D. Norata, S. C. Sampaio, and P. Newsholme, "A past and present overview of macrophage metabolism and functional outcomes," *Clinical Science*, vol. 131, no. 12, pp. 1329–1342, 2017.

[63] G. M. Tannahill, A. M. Curtis, J. Adamik et al., "Succinate is an inflammatory signal that induces IL-1β through HIF-1α," *Nature*, vol. 496, no. 7444, pp. 238–242, 2013.

[64] E. M. Palsson-McDermott, A. M. Curtis, G. Goel et al., "Pyruvate kinase M2 regulates Hif-1α activity and IL-1β induction and is a critical determinant of the Warburg effect in LPS-activated macrophages," *Cell Metabolism*, vol. 21, no. 1, pp. 65–80, 2015.

[65] V. Lampropoulou, A. Sergushichev, M. Bambouskova et al., "Itaconate links inhibition of succinate dehydrogenase with macrophage metabolic remodeling and regulation of inflammation," *Cell Metabolism*, vol. 24, no. 1, pp. 158–166, 2016.

[66] B. Németh, J. Doczi, D. Csete et al., "Abolition of mitochondrial substrate-level phosphorylation by itaconic acid produced by LPS-induced *Irg1* expression in cells of murine macrophage lineage," *The FASEB Journal*, vol. 30, no. 1, pp. 286–300, 2016.

[67] T. Cordes, M. Wallace, A. Michelucci et al., "Immunoresponsive gene 1 and itaconate inhibit succinate dehydrogenase to modulate intracellular succinate levels," *Journal of Biological Chemistry*, vol. 291, no. 27, pp. 14274–14284, 2016.

[68] A. Michelucci, T. Cordes, J. Ghelfi et al., "Immune-responsive gene 1 protein links metabolism to immunity by catalyzing itaconic acid production," *Proceedings of the National Academy of Sciences of the United States of America*, vol. 110, no. 19, pp. 7820–7825, 2013.

[69] D. Zeevi, T. Korem, N. Zmora et al., "Personalized nutrition by prediction of glycemic responses," *Cell*, vol. 163, no. 5, pp. 1079–1094, 2015.

[70] I. T. W. Harley and C. L. Karp, "Obesity and the gut microbiome: striving for causality," *Molecular Metabolism*, vol. 1, no. 1-2, pp. 21–31, 2012.

[71] P. D. Cani, A. M. Neyrinck, F. Fava et al., "Selective increases of bifidobacteria in gut microflora improve high-fat-diet-induced diabetes in mice through a mechanism associated with endotoxaemia," *Diabetologia*, vol. 50, no. 11, pp. 2374–2383, 2007.

[72] R. S. Kootte, A. Vrieze, F. Holleman et al., "The therapeutic potential of manipulating gut microbiota in obesity and type 2 diabetes mellitus," *Diabetes, Obesity and Metabolism*, vol. 14, no. 2, pp. 112–120, 2012.

[73] T. Arora and F. Backhed, "The gut microbiota and metabolic disease: current understanding and future perspectives," *Journal of Internal Medicine*, vol. 280, no. 4, pp. 339–349, 2016.

[74] P. J. Turnbaugh, R. E. Ley, M. A. Mahowald, V. Magrini, E. R. Mardis, and J. I. Gordon, "An obesity-associated gut microbiome with increased capacity for energy harvest," *Nature*, vol. 444, no. 7122, pp. 1027–1031, 2006.

[75] P. J. Turnbaugh, M. Hamady, T. Yatsunenko et al., "A core gut microbiome in obese and lean twins," *Nature*, vol. 457, no. 7228, pp. 480–484, 2008.

[76] F. Backhed, H. Ding, T. Wang et al., "The gut microbiota as an environmental factor that regulates fat storage," *Proceedings of the National Academy of Sciences of the United States of America*, vol. 101, no. 44, pp. 15718–15723, 2004.

[77] C. De Filippo, D. Cavalieri, M. Di Paola et al., "Impact of diet in shaping gut microbiota revealed by a comparative study in children from Europe and rural Africa," *Proceedings of the National Academy of Sciences of the United States of America*, vol. 107, no. 33, pp. 14691–14696, 2010.

[78] A. Schwiertz, D. Taras, K. Schäfer et al., "Microbiota and SCFA in lean and overweight healthy subjects," *Obesity*, vol. 18, no. 1, pp. 190–195, 2010.

[79] P. D. Cani and W. M. de Vos, "Next-generation beneficial microbes: the case of *Akkermansia muciniphila*," *Frontiers in Microbiology*, vol. 8, p. 1765, 2017.

[80] R. J. Perry, L. Peng, N. A. Barry et al., "Acetate mediates a microbiome-brain-β-cell axis to promote metabolic syndrome," *Nature*, vol. 534, no. 7606, pp. 213–217, 2016.

[81] J. P. Thaler, C. X. Yi, E. A. Schur et al., "Obesity is associated with hypothalamic injury in rodents and humans," *The Journal of Clinical Investigation*, vol. 122, no. 1, pp. 153–162, 2012.

[82] G. Frost, M. L. Sleeth, M. Sahuri-Arisoylu et al., "The short-chain fatty acid acetate reduces appetite via a central homeostatic mechanism," *Nature Communications*, vol. 5, no. 1, p. 3611, 2014.

[83] R. J. Seeley, A. P. Chambers, and D. A. Sandoval, "The role of gut adaptation in the potent effects of multiple bariatric surgeries on obesity and diabetes," *Cell Metabolism*, vol. 21, no. 3, pp. 369–378, 2015.

[84] M. K. Hankir, F. Seyfried, C. A. Hintschich et al., "Gastric bypass surgery recruits a gut PPAR-α-striatal D1R pathway to reduce fat appetite in obese rats," *Cell Metabolism*, vol. 25, no. 2, pp. 335–344, 2017.

[85] K. Forslund, F. Hildebrand, T. Nielsen et al., "Disentangling type 2 diabetes and metformin treatment signatures in the human gut microbiota," *Nature*, vol. 528, no. 7581, pp. 262–266, 2015.

[86] M. Roberfroid, "Prebiotics: the concept revisited," *The Journal of Nutrition*, vol. 137, no. 3, pp. 830S–837S, 2007.

[87] M. C. Mekkes, T. C. Weenen, R. J. Brummer, and E. Claassen, "The development of probiotic treatment in obesity: a review," *Beneficial Microbes*, vol. 5, no. 1, pp. 19–28, 2014.

[88] P. D. Cani and N. M. Delzenne, "The gut microbiome as therapeutic target," *Pharmacology & Therapeutics*, vol. 130, no. 2, pp. 202–212, 2011.

[89] L. Dethlefsen, S. Huse, M. L. Sogin, and D. A. Relman, "The pervasive effects of an antibiotic on the human gut microbiota, as revealed by deep 16S rRNA sequencing," *PLoS Biology*, vol. 6, no. 11, article e280, 2008.

[90] E. Gough, H. Shaikh, and A. R. Manges, "Systematic review of intestinal microbiota transplantation (fecal bacteriotherapy) for recurrent *Clostridium difficile* infection," *Clinical Infectious Diseases*, vol. 53, no. 10, pp. 994–1002, 2011.

[91] M. Rupnik, "Toward a true bacteriotherapy for *clostridium difficile* infection," *The New England Journal of Medicine*, vol. 372, no. 16, pp. 1566–1568, 2015.

[92] D. P. Bojanova and S. R. Bordenstein, "Fecal transplants: what is being transferred?," *PLoS Biology*, vol. 14, no. 7, article e1002503, 2016.

[93] E. van Nood, A. Vrieze, M. Nieuwdorp et al., "Duodenal infusion of donor feces for recurrent *Clostridium difficile*," *The New England Journal of Medicine*, vol. 368, no. 5, pp. 407–415, 2013.

[94] A. Vrieze, C. Out, S. Fuentes et al., "Impact of oral vancomycin on gut microbiota, bile acid metabolism, and insulin sensitivity," *Journal of Hepatology*, vol. 60, no. 4, pp. 824–831, 2014.

[95] D. Reijnders, G. H. Goossens, G. D. A. Hermes et al., "Effects of gut microbiota manipulation by antibiotics on host metabolism in obese humans: a randomized double-blind placebo-controlled trial," *Cell Metabolism*, vol. 24, no. 1, pp. 63–74, 2016.

[96] D. J. Morrison and T. Preston, "Formation of short chain fatty acids by the gut microbiota and their impact on human metabolism," *Gut Microbes*, vol. 7, no. 3, pp. 189–200, 2016.

[97] R. DeFronzo, G. A. Fleming, K. Chen, and T. A. Bicsak, "Metformin-associated lactic acidosis: current perspectives on causes and risk," *Metabolism*, vol. 65, no. 2, pp. 20–29, 2016.

[98] J. C. Alves-Filho and E. M. Pålsson-McDermott, "Pyruvate kinase M2: a potential target for regulating inflammation," *Frontiers in Immunology*, vol. 7, p. 145, 2016.

Hindawi
Mediators of Inflammation
Volume 2018, Article ID 5425346, 16 pages
https://doi.org/10.1155/2018/5425346

Research Article

Shock Wave Therapy Enhances Mitochondrial Delivery into Target Cells and Protects against Acute Respiratory Distress Syndrome

Kun-Chen Lin,[1] Christopher Glenn Wallace,[2] Tsung-Cheng Yin,[3,4] Pei-Hsun Sung,[4,5] Kuan-Hung Chen,[1] Hung-I Lu,[6] Han-Tan Chai,[5] Chih-Hung Chen,[7] Yi-Ling Chen,[5,8] Yi-Chen Li,[5] Pei-Lin Shao,[9] Mel S. Lee,[3] Jiunn-Jye Sheu,[6,8] and Hon-Kan Yip[4,5,8,9,10]

[1]*Department of Anesthesiology, Kaohsiung Chang Gung Memorial Hospital and Chang Gung University College of Medicine, Kaohsiung 83301, Taiwan*
[2]*Department of Plastic Surgery, University Hospital of South Manchester, Manchester, UK*
[3]*Department of Orthopaedic Surgery, Kaohsiung Chang Gung Memorial Hospital and Chang Gung University College of Medicine, Kaohsiung 83301, Taiwan*
[4]*Center for Shockwave Medicine and Tissue Engineering, Kaohsiung Chang Gung Memorial Hospital, Kaohsiung 83301, Taiwan*
[5]*Division of Cardiology, Department of Internal Medicine, Kaohsiung Chang Gung Memorial Hospital and Chang Gung University College of Medicine, Kaohsiung 83301, Taiwan*
[6]*Division of Thoracic and Cardiovascular Surgery, Department of Surgery, Kaohsiung Chang Gung Memorial Hospital and Chang Gung University College of Medicine, Kaohsiung 83301, Taiwan*
[7]*Divisions of General Medicine, Department of Internal Medicine, Kaohsiung Chang Gung Memorial Hospital and Chang Gung University College of Medicine, Kaohsiung 83301, Taiwan*
[8]*Institute for Translational Research in Biomedicine, Kaohsiung Chang Gung Memorial Hospital, Kaohsiung 83301, Taiwan*
[9]*Department of Nursing, Asia University, 500 Lioufeng Rd., Wufeng, Taichung 41354, Taiwan*
[10]*Department of Medical Research, China Medical University Hospital, China Medical University, Taichung 40402, Taiwan*

Correspondence should be addressed to Jiunn-Jye Sheu; cvsjjs@gmail.com and Hon-Kan Yip; han.gung@msa.hinet.net

Received 19 March 2018; Accepted 5 August 2018; Published 21 October 2018

Academic Editor: Fabio S Lira

This study tested the hypothesis that shock wave therapy (SW) enhances mitochondrial uptake into the lung epithelial and parenchymal cells to attenuate lung injury from acute respiratory distress syndrome (ARDS). ARDS was induced in rats through continuous inhalation of 100% oxygen for 48 h, while SW entailed application 0.15 mJ/mm^2 for 200 impulses at 6 Hz per left/right lung field. In vitro and ex vivo studies showed that SW enhances mitochondrial uptake into lung epithelial and parenchyma cells (all $p < 0.001$). Flow cytometry demonstrated that albumin levels and numbers of inflammatory cells (Ly6G+/CD14+/CD68+/CD11$^{b/c}$+) in bronchoalveolar lavage fluid were the highest in untreated ARDS, were progressively reduced across SW, Mito, and SW + Mito (all $p < 0.0001$), and were the lowest in sham controls. The same profile was also seen for fibrosis/collagen deposition, levels of biomarkers of oxidative stress (NOX-1/NOX-2/oxidized protein), inflammation (MMP-9/TNF-α/NF-κB/IL-1β/ICAM-1), apoptosis (cleaved caspase 3/PARP), fibrosis (Smad3/TGF-β), mitochondrial damage (cytosolic cytochrome c) (all $p < 0.0001$), and DNA damage (γ-H2AX+), and numbers of parenchymal inflammatory cells (CD11+/CD14+/CD40L+/F4/80+) ($p < 0.0001$). These results suggest that SW-assisted Mito therapy effectively protects the lung parenchyma from ARDS-induced injury.

1. Introduction

The respiratory system (i.e., oral-nasal-laryngeal tract, bronchus, trachea, and alveolar sacs in the lungs) is critical for maintenance of an adequate oxygen supply and excretion of carbon dioxide (CO_2). For this purpose, the lung parenchyma has a dense capillary network mediating gaseous exchange. The lung is vulnerable to damage from a variety of causes, including viruses, bacteria, toxic chemicals/smoke, food aspiration, septic or cardiogenic shock, resuscitation after circulatory arrest, alveolar-type pulmonary edema, massive blood transfusion, and ischemia-reperfusion injury after bypass surgery or organ transplantation [1–9]. Moreover, sustained insults may ultimately develop into clinical acute respiratory distress syndrome (ARDS) [9–11]. Despite pharmacologic advances and continuous renewal of management strategies [12–16], in-hospital mortality from ARDS remains unacceptably high [9, 10, 17–19]. Consequently, there is an urgent need for a safe and efficacious alternative treatment for this high-risk group of patients.

The mechanisms underlying acute lung injury/ARDS are multifactorial and include inflammation, alveolar leukocytosis, protein leakage, mitochondrial-free radical production, mitochondrial damage/loss, generation of reactive oxygen species (ROS) and resultant lung oxidant stress, and apoptosis [4, 9, 20–24]. Within this context, we hypothesize that a treatment that could reverse mitochondrial loss may, in turn, inhibit ROS-free radical generation and improve ARDS parameters. Previous studies by others [25–27] and ourselves [28–30] have shown that mitochondrial transfusion effectively protects against acute organ damage, including sepsis-induced acute lung injury [13, 25], acute ischemia-reperfusion injury of the heart [27], liver [26, 28], and lung [30], and monocrotaline-induced pulmonary arterial hypertension [29]. Additionally, shock wave (SW) therapy entailing delivery of a series of transient pressure waves characterized by a high peak pressure (100 MPa), fast pressure rise (<10 ns), rapid propagation, and short life cycle (10 μs) produced by an appropriate generator reportedly reverses ischemia-related organ dysfunction, mainly by enhancing angiogenesis, recruiting endothelial progenitor cells, and suppressing inflammation and oxidative stress [31–33]. In the present study, therefore, we used a rat model to test the hypothesis that SW-assisted mitochondrial therapy would be superior to either therapy alone for protection of the lung against ARDS injury.

2. Materials and Methods

2.1. Ethics. All animal experimental procedures were approved by the Institute of Animal Care and Use Committee at Kaohsiung Chang Gung Memorial Hospital (Affidavit of Approval of Animal Use Protocol number 2016032205) and performed in accordance with the Guide for the Care and Use of Laboratory Animals (The Eighth Edition of the Guide for the Care and Use of Laboratory Animals (NRC 2011)).

Animals were housed in an Association for Assessment and Accreditation of Laboratory Animal Care International-(AAALAC-) approved animal facility in our hospital with controlled temperature and light cycle (24°C and 12/12 light cycle).

2.2. Inducing ARDS in SD Rats. The ARDS model used in this study has been described in our recent studies [30, 34], wherein pure oxygen (i.e., 100% O_2) was continuously administered to the rat for 48 h. In detail, a close system of glass (i.e., for monitoring the safety of each animal) square box was created. Inside the close system, the adequate food and water were provided for the animals. At least five animals were accommodated for each time in the glass box. Oxygen cannulation was firmly connected to the glass box with an oxygen meter to monitor the oxygen gas supply in the box to achieve each animal exposure to 100% oxygen for 48 hours.

2.3. Animal Grouping and Application of SW. Pathogen-free, adult male Sprague-Dawley (SD) rats ($n = 30$) weighing 325–350 g (Charles River Technology, BioLASCO, Taiwan Co. Ltd., Taiwan) were randomized into five groups ($n = 6$ in each group): group 1, sham controls (intravenous injection of 0.5 ml of normal saline); group 2, ARDS; group 3, ARDS + SW (0.15 mJ/mm^2 for 200 impulses at 6 Hz per left/right lung field applied once 3 h after completing 48 h of oxygen inhalation); group 4, ARDS + mitochondria (Mito) (2000 μg/rat administered intravenously with a time interval identical to SW therapy); and group 5, ARDS + SW + Mito. Animals were sacrificed on day 5 after ARDS induction.

All animals were anesthetized (inhaled 2.0% isoflurane) in a supine position on a warming pad at 37°C during the application of SW to the left and then right lungs. To avoid affecting the heart during SW, the focus type of SW (Storz Duolith SD1, STORZ MEDICAL AG, Switzerland) was utilized. In addition, mitochondrial oxygen consumption rates were determined using a Mito stress test kit (i.e., Seahorse Bioscience, Billerica, MA) and the XF24 Analyzer.

2.4. Mitochondrial Isolation from Donors and MitoTracker Staining for Mitochondria. Liver mitochondria were isolated from donor SD rats as previously described [35]. The rats were fasted overnight prior to the mitochondrial isolation procedure, then sacrificed, and their gallbladders and livers were carefully removed. Immediately, the liver (3 g) was immersed in 50 ml of ice-cold IBc (10 mM Tris-MOPS, 5 mM EGTA/Tris, 200 mM sucrose, and pH 7.4.) in a beaker, followed by rinsing the liver free of blood with ice-cold IBc. The liver was then minced with scissors in a beaker surrounded by ice. IBc was discarded during mincing and replaced with 18 ml of ice-cold fresh IBc. The liver was then homogenized with a Teflon pestle. The homogenates were transferred to a 50 ml polypropylene Falcon tube and centrifuged at 600g for 10 minutes at 4°C. The supernatants were transferred to fresh tubes for centrifugation at 7000g for 10 minutes at 4°C. The supernatants were discarded, and the pellets were washed with 5 ml ice-cold IBc. Again, the supernatants from the pellets were centrifuged at 7000g for 10 minutes at 4°C. The supernatants were discarded, and the pellets containing the mitochondria were resuspended. The concentration of the mitochondrial suspensions was

measured using the Biuret method. Each 10 mg of isolated mitochondria was labeled with 1 M of MitoTracker Red CMXRos (Invitrogen, Carlsbad, CA) through incubation at 37°C for 30 minutes. Mitochondrial transfusion was performed for the study animals immediately after labeling (i.e., <3 hrs after the isolation procedure).

2.5. Procedure and Protocol for Quantification of Oxygen Consumption Rate (OCR) of Isolated Mitochondria (Seahorse Method) (Figure 1). The procedure and protocol have also been described in our recent report [30]. In detail, functional activity of isolated mitochondria from rat liver was determined with an Extracellular Flux Analyzer (XF^{e}24, Seahorse Bioscience, MA, USA) by assessing the degree of coupling between the electron transport chain (ETC) and the oxidative phosphorylation machinery (OXPHOS). Bioenergetics of mitochondria as reflected in the integrity of electron transport chain and capacity of oxidative phosphorylation were evaluated by measuring the mitochondrial oxygen consumption rate (OCR). In this study, isolated mitochondria (10 μg/well) from rat liver were diluted in cold 1X mitochondrial assay solution (MAS) (70 mM sucrose, 220 mM mannitol, 10 mM KH_2PO_4, 5 mM $MgCl_2$, 2 mM HEPES, 1.0 mM EGTA, and pH 7.2), followed by spinning down at 3000g for 30 minutes. After attachment of mitochondria to XF24 plate, coupling reaction was initiated with the administration of substrate (10.0 mM succinate). State 3 was initiated with ADP (0.5 mM), while state 4 was induced with the addition of oligomycin (2 μM). Maximal uncoupler-stimulated respiration was elicited with FCCP (4 μM), whereas complex III repression was induced by antimycin A (4 μM). OCR of mitochondria in reactions mentioned above was sequentially measured.

2.6. In Vitro Study for Determining the Impact of SW on Enhancing Mitochondrial Transfusion in the Rat Lung Epithelial Cells (LEC). To elucidate whether SW therapy could enhance mitochondrial transfusion into the rat lung epithelial cells (LEC), the LECs were cultured in F-12K medium (i.e., 10% FBS + 1% Penicillin-Streptomycin (Gibco) in 1×10^6 cells) in T25 flask for 24 h, followed by with and without SW treatment (0.2 mJ/mm^2 for 100 shots). The cells (3×10^4) were then cultured in EZ slide. 24 h after the cell culturing, 50 μg of exogenous mitochondria was transfused into the cultured cells (3×10^4). 90 minutes later after transfusion, the endogenous mitochondria in these cells were stained by MitoTracker Green (Invitrogen M7514, 1 : 100 nM). Additionally, these cells were also stained by MitoTracker Orange (Invitrogen M7510, 1 : 500 nM).

2.7. Pathological Assessment of Lung Injury. The procedure and protocol have been described in our previous reports [23, 24, 30, 35]. In detail, lung specimens were sectioned at 5 μm for light microscopy and H&E staining was performed to investigate the number of alveolar sacs in a blinded fashion [23, 24, 30, 35]. Three lung sections from each rat were analyzed, and three randomly selected high-power fields (HPFs; 200x) were examined in each section. The mean number per HPF for each animal was then determined by a summation of all numbers divided by 9. The extent of crowded area, which was defined as the region of thickened septa in lung parenchyma associated with partial or complete collapse of alveoli on H&E-stained sections, was also performed in a blinded fashion. The following scoring system [23, 24] was adopted: 0 = no detectable crowded area; 1 = <15% of crowded area; 2 = 15–25% of crowded area; 3 = 25–50% of crowded area; 4 = 50–75% of crowded area; 5 = >75%–100% of crowded area/HPF.

2.8. Bronchoalveolar Lavage and Lung Specimen Preparation. To elucidate the impact of SW mitochondrial treatment on protecting the lung from ARDS injury, bronchoalveolar lavage (BAL) was performed and the BAL fluid was collected for study in six additional rats from each group.

2.9. Immunofluorescent (IF) Studies. The procedures and protocols for IF examination were also based on our recent study [23, 24, 30, 35]. Briefly, for IF staining, rehydrated paraffin sections were first treated with 3% H_2O_2 for 30 minutes and incubated with Immuno-Block reagent (BioSB, Santa Barbara, CA, USA) for 30 minutes at room temperature. Sections were then incubated with primary antibodies specifically against CD14 (1 : 50, Santa Cruz), CD11 (1 : 500, Abcam), F4/80 (1 : 100, Santa Cruz), CD40L (1 : 100, Abcam), and γ-H2AX (1 : 1000, Abcam) while sections incubated with irrelevant antibodies served as controls. Three kidney sections from each rat were analyzed. For quantification, three randomly selected HPFs (400x for IF) were analyzed in each section. The mean number of positively stained cells per HPF for each animal was then determined by the summation of all numbers divided by 9.

2.10. Western Blot Analysis. The procedure and protocol for Western blot analysis have been described in our previous reports [23, 24, 30, 35]. Briefly, equal amounts (50 μg) of protein extract were loaded and separated by SDS-PAGE using acrylamide gradients. After electrophoresis, the separated proteins were transferred electrophoretically to a polyvinylidene difluoride (PVDF) membrane (Amersham Biosciences, Amersham, UK). Nonspecific sites were blocked by incubation of the membrane in blocking buffer (5% nonfat dry milk in T-TBS (TBS containing 0.05% Tween 20)) overnight. The membranes were incubated with the indicated primary antibodies (matrix metalloproteinase- (MMP-) 9 (1 : 3000, Abcam, ab76003, Cambridge, MA, USA), tumor necrosis factor- (TNF-) α (1 : 1000, Cell Signaling, number 3707, Danvers, MA, USA), nuclear factor- (NF-) κB p65 (1 : 600, Abcam, ab16502, Cambridge, MA, USA), NADPH oxidase- (NOX-) 1 (1 : 1500, Sigma, SAB4200097, St. Louis, Mo, USA), NOX-2 (1 : 750, Sigma, SAB4200118, St. Louis, Mo, USA), interleukin- (IL-) 1β (1 : 1000, Cell Signaling, number 12426, Danvers, MA, USA), intercellular adhesion molecule- (ICAM-) 1 (1 : 1000, Abcam, ab2213, Cambridge, MA, USA), caspase 3 (1 : 1000, Cell Signaling, number 9665, Danvers, MA, USA), cleaved poly (ADP-ribose) polymerase (c-PARP) (1 : 1000, Cell Signaling, number 9542), transforming growth factor- (TGF-) β (1 : 500, Abcam, ab64715), phosphorylated- (p-) Smad3 (1 : 1000, Cell Signaling, number 9520), cytosolic

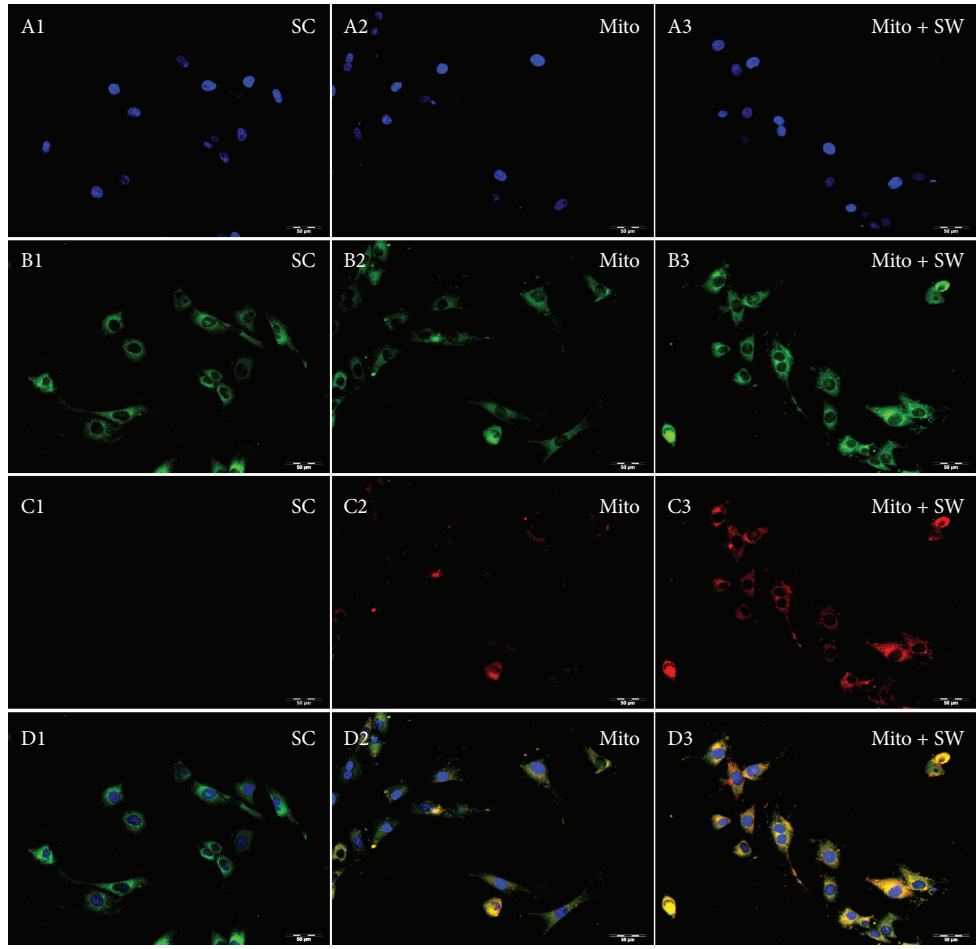

(a)

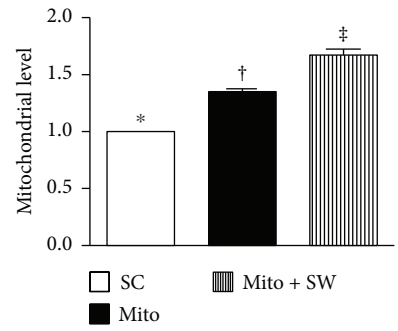

(b)

Figure 1: In vitro study showed SW therapy enhanced mitochondrial transfusion into the rat lung epithelial cells. (A1 to A3) Illustrating the DAPI stain (400x) for identification of rat lung epithelial cells in three groups (i.e., SC, Mito, and Mito + SW). (B1 to B3) Showing MitoTracker stain (400x) for identification of endogenous mitochondria (green color) among three groups. (C1 to C3) Indicating the MitoTracker stain (400x) for identification of exogenous mitochondria to be transfused into the epithelial cells (red color). (D1 to D3) Indicating the merged pictures of B1–B3 and C1–C3. Pink-yellow color indicated that the endogenous and exogenous mitochondria colocalized together. An abundant number of mitochondria were found in the Mito + SW group. (b) Analytic result of mitochondrial level in the cells, * versus other groups with different symbols (†, ‡), $p < 0.001$. All statistical analyses were performed by one-way ANOVA, followed by Bonferroni multiple comparison post hoc test ($n = 6$ for each group). Symbols (*, †, ‡) indicate significance (at 0.05 level). SC = sham control; Mito = mitochondria; SW = shock wave.

cytochrome c (1 : 1000, BD, 556433, Franklin, NJ, USA), mitochondrial cytochrome c (1 : 1000, BD, 556433, Franklin, NJ, USA), and actin (1 : 10000, Millipore, number MAB1501, Billerica, MA, USA)) for 1 hour at room temperature. Horseradish peroxidase-conjugated anti-rabbit immunoglobulin IgG (1 : 2000, Cell Signaling, number 7074, Danvers, MA,

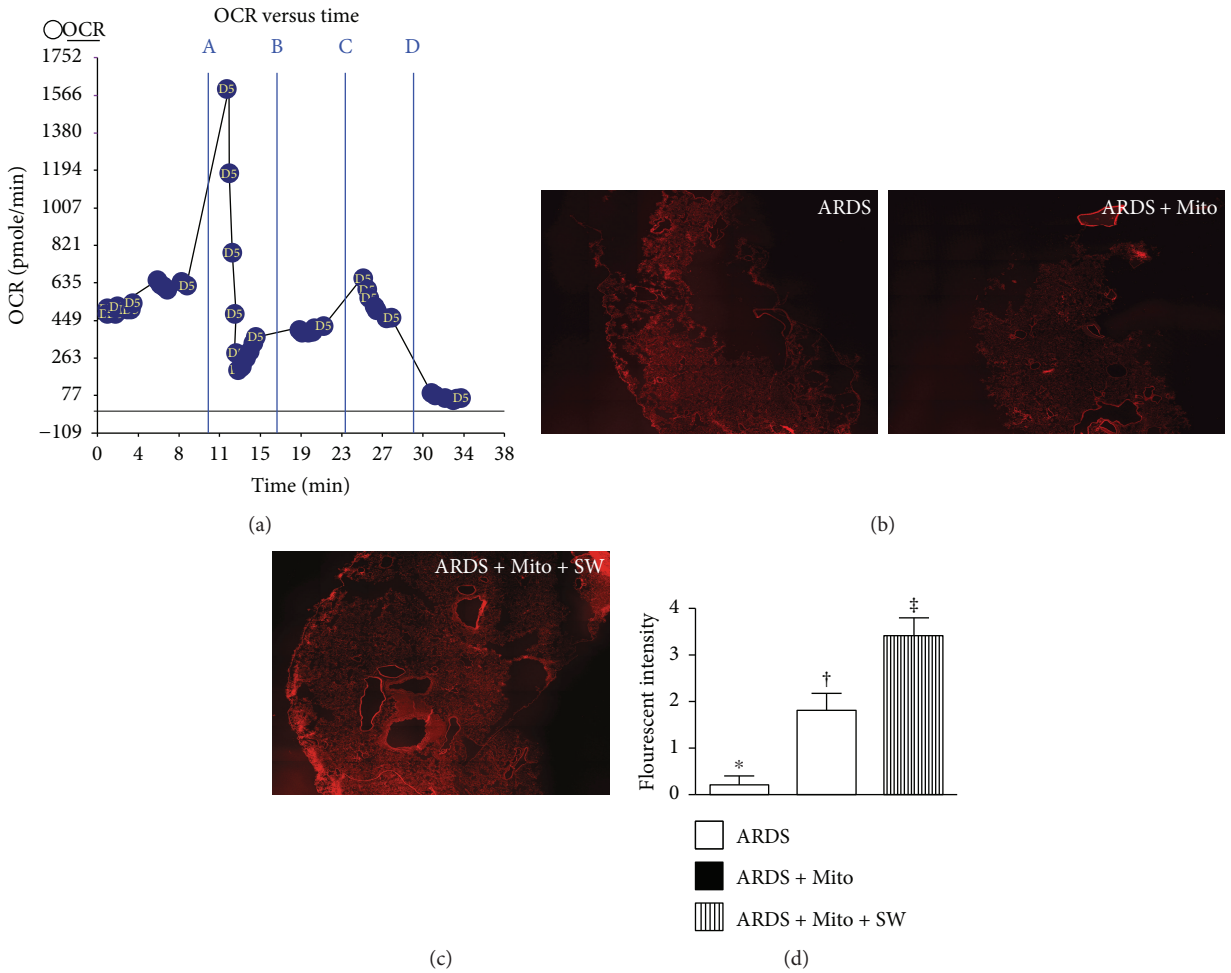

Figure 2: Mitochondrial functional assay and in vivo showed SW therapy enhanced mitochondrial transfusion into the cells. (a) Mitochondrial functional assay showed a satisfactory activity (i.e., high oxygen consumption rate) of isolated mitochondria (determined by the Mito stress test kit and the XF^{e}24 Analyzer) ($n = 4$). (b, c) Illustrating the confocal findings (400x) of lung specimen at a time interval of 24 h after intravenously mitochondrial transfusion. (d) Analytical results of fluorescent intensity, * versus other groups with different symbols (†, ‡), $p < 0.001$. All statistical analyses were performed by one-way ANOVA, followed by Bonferroni multiple comparison post hoc test ($n = 6$ for each group). Symbols (*, †, ‡) indicate significance (at 0.05 level). OCR = oxygen consumption rate. ARDS = acute respiratory distress syndrome; Mito = mitochondria; SW = shock wave.

USA) was used as a secondary antibody for a one-hour incubation at room temperature. The washing procedure was repeated eight times within one hour. Immunoreactive bands were visualized by enhanced chemiluminescence (ECL; Amersham Biosciences, Amersham, UK) and exposed to Biomax L film (Kodak, Rochester, NY, USA). For quantification, ECL signals were digitized using Labwork software (UVP, Waltham, MA, USA).

2.11. Assessment of Oxidative Stress. The procedure and protocol for assessing the protein expression of oxidative stress have been detailed in our previous reports [23, 24, 30, 35]. The Oxyblot Oxidized Protein Detection Kit was purchased from Chemicon, Billerica, MA, USA (S7150). DNPH derivatization was carried out on 6 μg of protein for 15 minutes according to the manufacturer's instructions. One-dimensional electrophoresis was carried out on 12% SDS-polyacrylamide gel after DNPH derivatization. Proteins were transferred to nitrocellulose membranes which were then incubated in the primary antibody solution (anti-DNP 1 : 150) for 2 hours, followed by incubation in secondary antibody solution (1 : 300) for 1 hour at room temperature. The washing procedure was repeated eight times within 40 minutes. Immunoreactive bands were visualized by enhanced chemiluminescence (ECL; Amersham Biosciences, Amersham, UK) which was then exposed to Biomax L film (Kodak, Rochester, NY, USA). For quantification, ECL signals were digitized using Labwork software (UVP, Waltham, MA, USA). For Oxyblot protein analysis, a standard control was loaded on each gel.

2.12. Histopathological Assessment in Lung Parenchyma. To analyze the integrity of collagen synthesis and deposition, three lung paraffin sections (4 μm) were stained with Picrosirius red (1% Sirius red in saturated picric acid solution) for one hour at room temperature using standard methods.

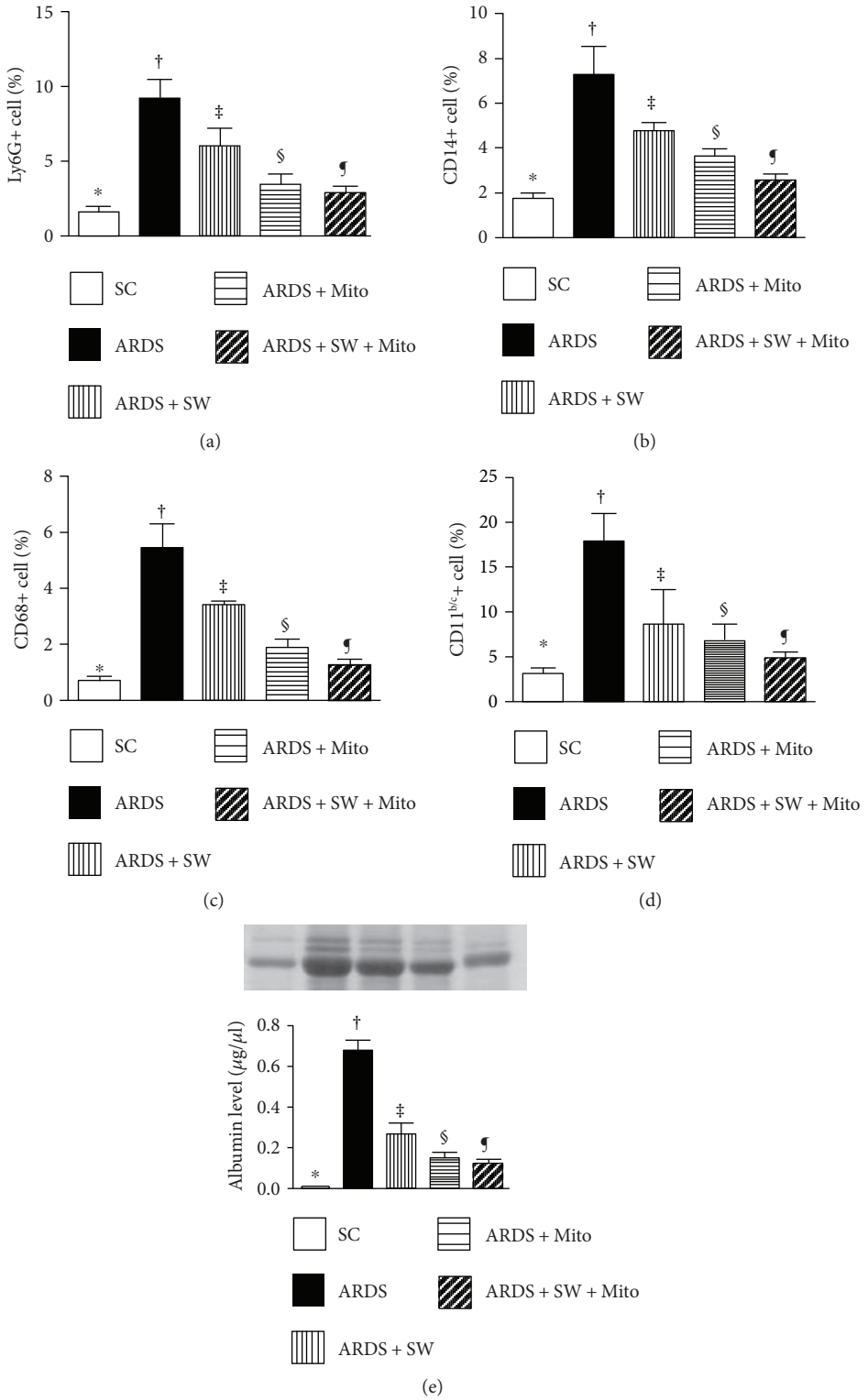

Figure 3: Inflammatory mediators and leakage of albumin in bronchoalveolar lavage (BAL) fluid by day 5 after ARDS induction. (a) Flow cytometric analysis of numbers of Ly6G+ cells in BAL, *versus other groups with different symbols (†, ‡, §, ¶), $p < 0.0001$. (b) Flow cytometric analysis of numbers of CD14+ cells in BAL, *versus other groups with different symbols (†, ‡, §, ¶), $p < 0.0001$. (c) Flow cytometric analysis of numbers of CD68+ cells in BAL, *versus other groups with different symbols (†, ‡, §, ¶), $p < 0.0001$. (d) Flow cytometric analysis of numbers of $CD11^{b/c}$+ cells in BAL, *versus other groups with different symbols (†, ‡, §, ¶), $p < 0.0001$. (e) Protein expression of albumin level in BAL, *versus other groups with different symbols (†, ‡, §, ¶), $p < 0.0001$. All statistical analyses were performed by one-way ANOVA, followed by Bonferroni multiple comparison post hoc test ($n = 6$ for each group). Symbols (*, †, ‡, §, ¶) indicate significance (at 0.05 level). SC = sham control; ARDS = acute respiratory distress syndrome; Mito = mitochondria; SW = shock wave.

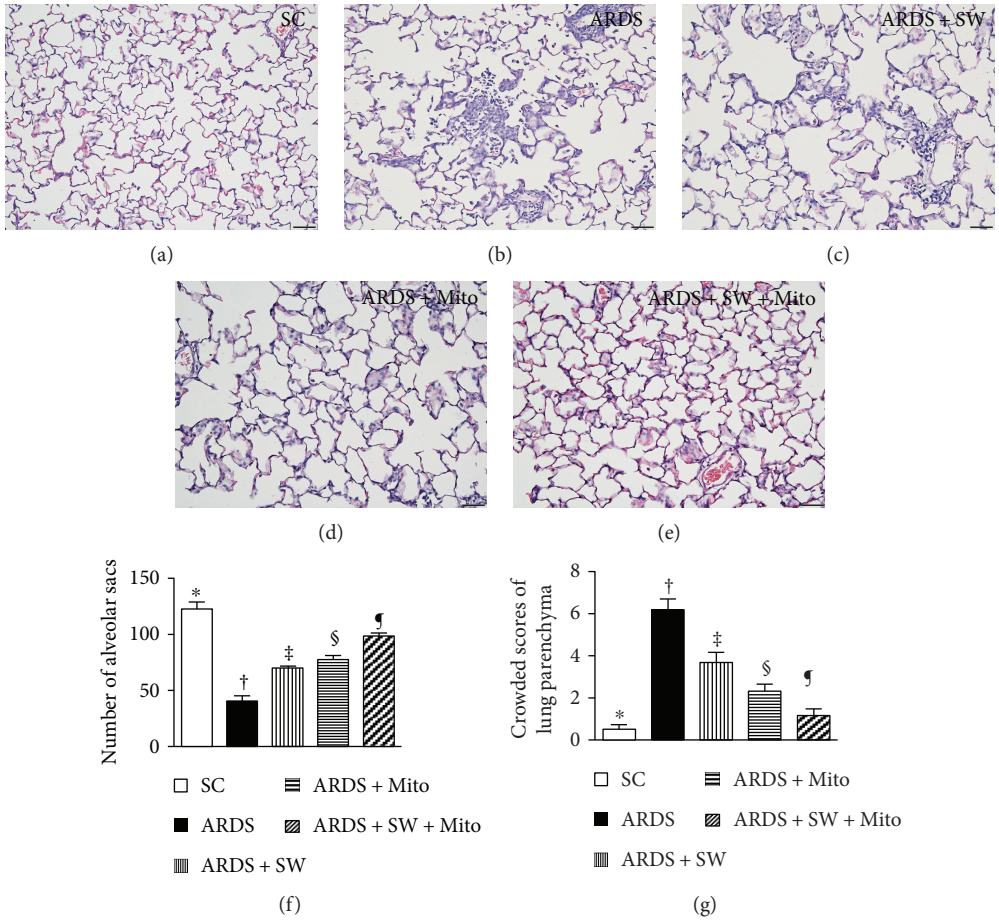

FIGURE 4: Pathological findings of lung parenchyma by day 5 after ARDS induction. (a to e) Pathological findings (i.e., H&E staining) of lung parenchyma under microscopy (200x) among the five groups. The scale bars in the right lower corner represent 50 μm. (f) The number of alveolar sacs among five groups. * versus other groups with different symbols (†, ‡, §, ¶), $p < 0.0001$. (g) Crowded scores of lung parenchyma. * versus other groups with different symbols (†, ‡, §, ¶), $p < 0.0001$. All statistical analyses were performed by one-way ANOVA, followed by Bonferroni multiple comparison post hoc test. Symbols (*, †, ‡, §, ¶) indicate significance (at 0.05 level). SC = sham control; ARDS = acute respiratory distress syndrome; Mito = mitochondria; SW = shock wave.

The sections were then washed twice with 0.5% acetic acid. The water was physically removed from the slides by vigorous shaking. After dehydration in 100% ethanol thrice, the sections were cleaned with xylene and mounted in a resinous medium. Ten low-power fields (10x) of each section were used to identify Sirius red-positive area on each section. The integrated area (μm^2) of condensed collagen deposition in each section was calculated using Image Tool 3 (IT3) image analysis software (University of Texas, Health Science Center, San Antonio (UTHSCSA); Image Tool for Windows, Version 3.0, USA). Three selected sections were quantified for each animal. Three randomly selected HPFs (100x) were analyzed in each section. After determining the number of pixels in each collagen deposition area per HPF, the numbers of pixels obtained from the three HPFs were summed. The procedure was repeated in two other sections for each animal. The mean pixel number per HPF for each animal was then determined by summing all pixel numbers and divided by 9. The mean integrated area (μm^2) of collagen deposition area in lung parenchyma per HPF was obtained using a conversion factor of 19.24 (1 μm^2 corresponded to 19.24 pixels).

To elucidate the fibrosis of lung parenchyma, Masson's trichrome stain was performed according to the manufacturer's instruction. The analytical method for identification of fibrotic area was identical to the method for analysis of condensed collagen deposition area.

2.13. Statistical Analysis. Quantitative data are expressed as means ± SD. Statistical analysis was adequately performed by ANOVA followed by Bonferroni multiple comparison post hoc test. Statistical analysis was performed using SPSS statistical software for Windows version 22 (SPSS for Windows, version 22; SPSS, IL, USA). A value of $p < 0.05$ was considered as statistically significant.

3. Results

3.1. SW Therapy Enhances Exogenous Mitochondrial Transfusion into Lung Epithelial Cells. In vitro observations revealed that SW therapy significantly enhanced transfusion of exogenous mitochondria into rat lung epithelial cells as compared to transfusion alone (Figure 1). In vivo, numbers

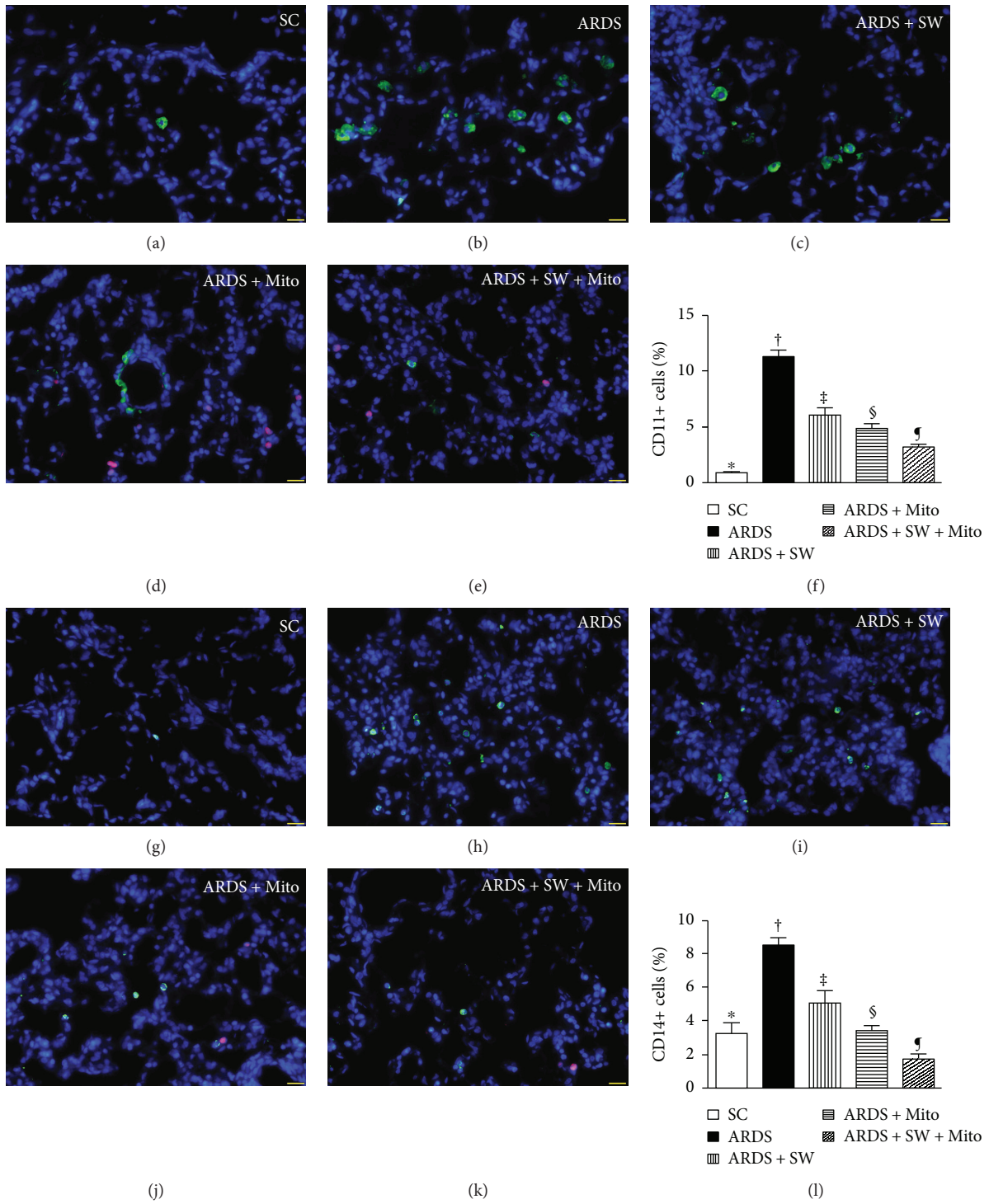

Figure 5: CD11+ and CD14+ cell infiltration in lung parenchyma by day 5 after ARDS induction. (a to e) Immunofluorescent (IF) microscopic finding (400x) for identification of CD11+ cells (green color) in lung parenchyma. Red color indicated exogenous mitochondria. (f) Analytical result of number of CD11+ cells, * versus other groups with different symbols (†, ‡, §, ¶), $p < 0.0001$. (g to k) IF microscopic finding (400x) for identification of CD14+ cells (green color) in lung parenchyma. Red color indicated exogenous mitochondria. Analytical result of number of CD14+ cells, * versus other groups with different symbols (†, ‡, §, ¶), $p < 0.0001$. The scale bars in the right lower corner represent 20 μm. All statistical analyses were performed by one-way ANOVA, followed by Bonferroni multiple comparison post hoc test. Symbols (*, †, ‡, §, ¶) indicate significance (at 0.05 level). SC = sham control; ARDS = acute respiratory distress syndrome; Mito = mitochondria; SW = shock wave.

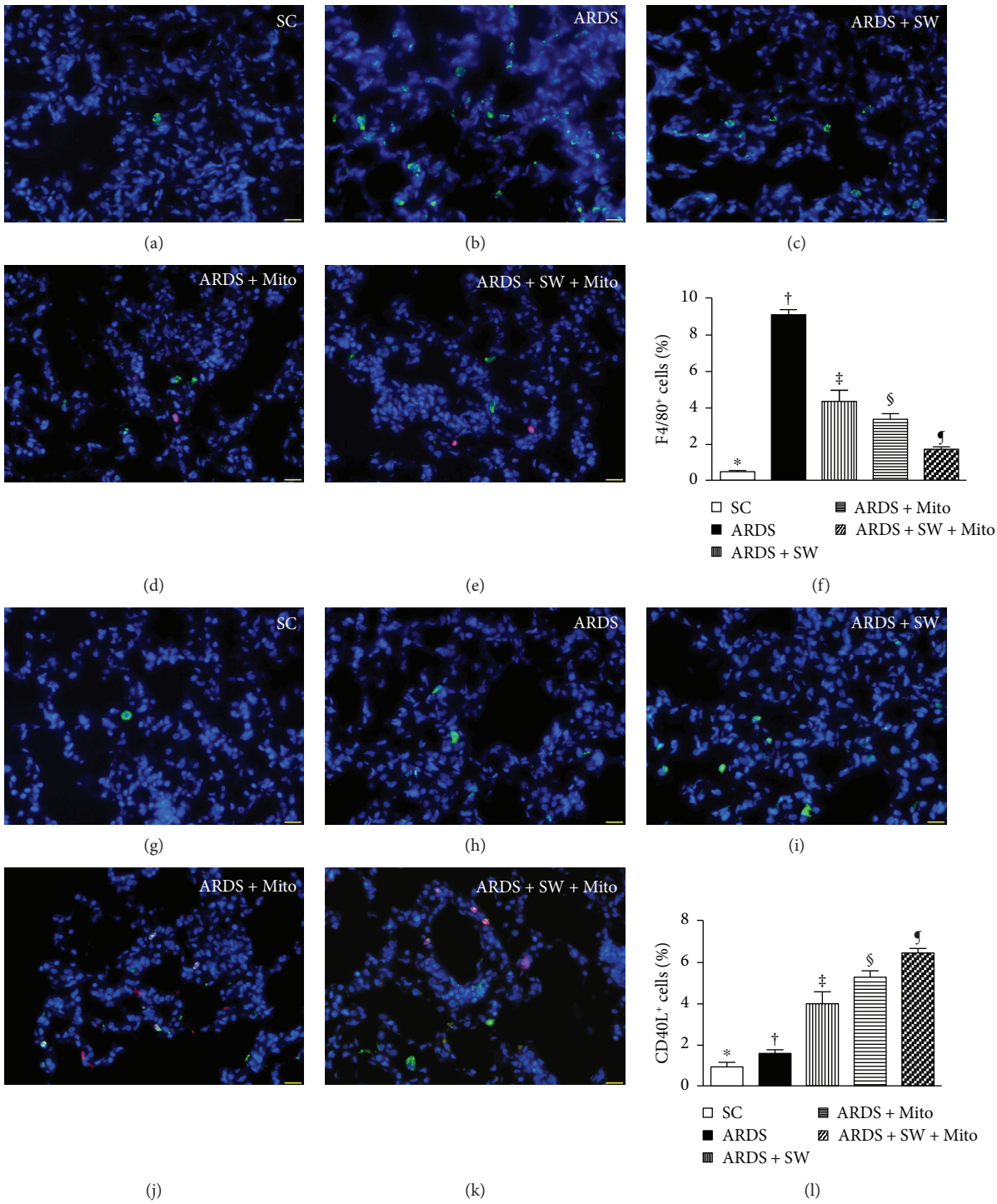

Figure 6: F4/80+ and CD40L+ cell infiltration in lung parenchyma by day 5 after ARDS induction. (a to e) Immunofluorescent (IF) microscopic finding (400x) for identification of F4/80+ cells (green color) in lung parenchyma. Red color indicated exogenous mitochondria. (f) Analytical result of number of F4/80+ cells, * versus other groups with different symbols (†, ‡, §, ¶), $p < 0.0001$. (g to k) IF microscopic finding (400x) for identification of CD40L+ cells (green color) in lung parenchyma. Red color indicated exogenous mitochondria. (l) Analytical result of number of CD40L+ cells, * versus other groups with different symbols (†, ‡, §, ¶), $p < 0.0001$. The scale bars in the right lower corner represent 20 μm. All statistical analyses were performed by one-way ANOVA, followed by Bonferroni multiple comparison post hoc test. Symbols (*, †, ‡, §, ¶) indicate significance (at 0.05 level). SC = sham control; ARDS = acute respiratory distress syndrome; Mito = mitochondria; SW = shock wave.

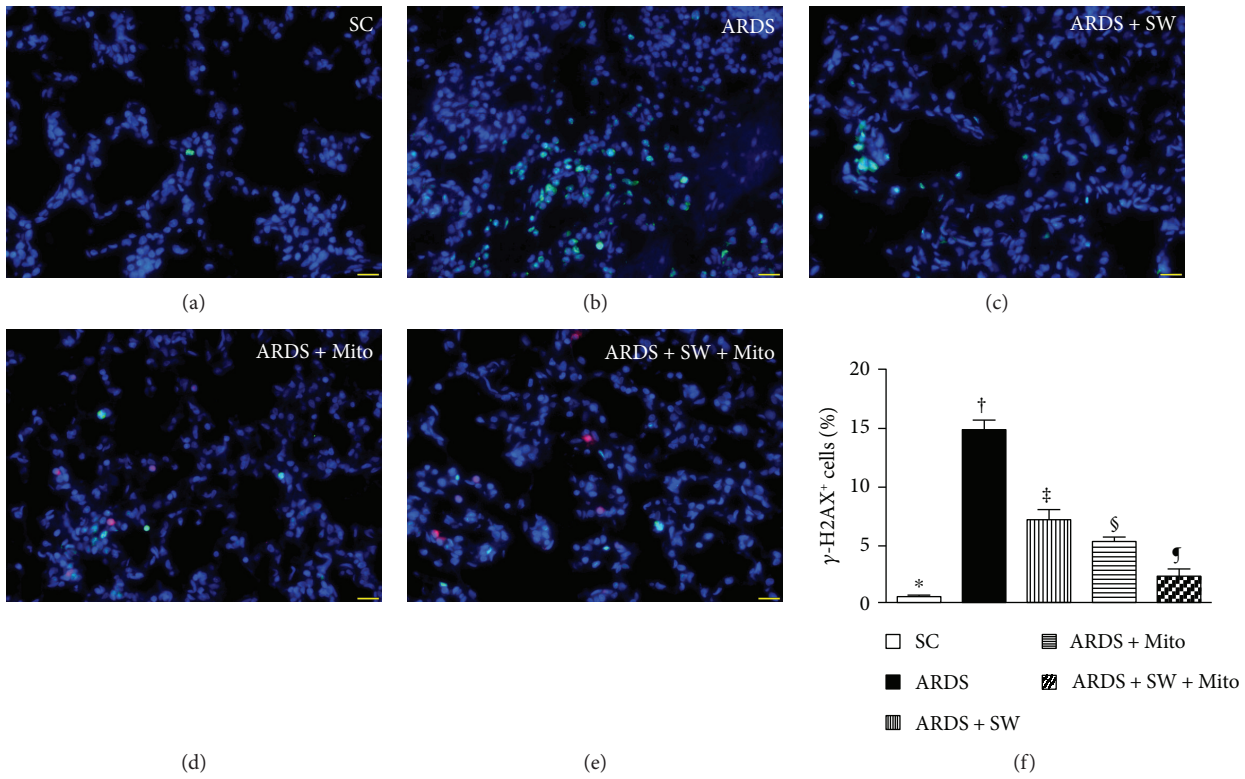

Figure 7: DNA damage marker in lung parenchyma by day 5 after ARDS induction. (a to e) Immunofluorescent (IF) microscopic finding (400x) for identification of γ-H2AX+ cells (green color) in lung parenchyma. Red color indicated exogenous mitochondria. (f) Analytical result of number of γ-H2AX+ cells, * versus other groups with different symbols (†, ‡, §, ¶), $p < 0.0001$. The scale bars in the right lower corner represent 20 μm. Symbols (*, †, ‡, §, ¶) indicate significance (at 0.05 level). SC = sham control; ARDS = acute respiratory distress syndrome; Mito = mitochondria; SW = shock wave.

of mitochondria in the lung parenchyma of ARDS rats treated with SW plus mitochondrial transfusion (SW + Mito) were significantly higher than those in the lungs of untreated ARDS animals or ARDS animals treated with Mito alone (Figure 2). Measurement of the mitochondrial oxygen consumption rate showed that mitochondrial activity was satisfactory for purposes of the present study (Figure 2).

3.2. Flow Cytometric Analysis of Inflammatory Mediators and Albumin Leakage in Bronchoalveolar Lavage (BAL) Fluid. Flow cytometric analysis demonstrated that the numbers of Ly6G+, CD14+, CD68+, and $CD11^{b/c}$+ inflammatory cells were highest in BAL fluid from untreated ARDS rats, were significantly and progressively lower across the ARDS + SW, ARDS + Mito, and ARDS + SW + Mito groups, and were the lowest in the sham control (SC) group (Figure 3). In addition, Western blot analysis showed that the profile of albumin levels in BAL fluid, an indicator of increased lung permeability and exudate leakage related to lung parenchymal damage in ARDS, exhibited the same pattern as the inflammatory cells among the five groups.

3.3. Pathological Findings after ARDS Induction. Hematoxylin and eosin staining revealed that 5 days after ARDS induction, numbers of alveolar sacs, an index of lung parenchyma integrity, was the lowest in untreated ARDS, increased progressively and significantly across the ARDS + SW, ARDS + Mito, and ARDS + SW + Mito groups, and was the highest in the SC group. Conversely, scoring of lung parenchymal crowding, an index of lung parenchymal damage, showed the opposite pattern in the five groups (Figure 4).

3.4. Inflammatory Cell Infiltration of Lung Parenchyma and DNA Damage after ARDS Induction. Immunofluorescence microscopy showed that 5 days after ARDS induction, infiltration of the lung parenchyma by CD11+, CD14+, F4/80+, and CD40L+ inflammatory cells was the highest in untreated ARDS rats, was significantly and progressively lower across the ARDS + SW, ARDS + Mito, and ARDS + SW + Mito groups, and was the lowest in SC rats (Figures 5 and 6). Immunofluorescence microscopy also revealed that the number of positively stained γ-H2AX cells, an indicator of DNA damage, exhibited a pattern identical to that of inflammatory cells among the five groups (Figure 7).

3.5. Histopathological Findings after ARDS Induction. Five days after ARDS induction, sections stained with Sirius oil red exhibited areas of condensed collagen deposition indicative of lung parenchymal damage with activation of fibroblasts and deposition of collagen fibers (Figure 8). Staining was the highest in specimens from untreated ARDS rats, the lowest in SC, significantly higher in the ARDS + SW and ARDS + Mito groups than in the ARDS + SW + Mito group, and significantly higher in the ARDS + SW than in

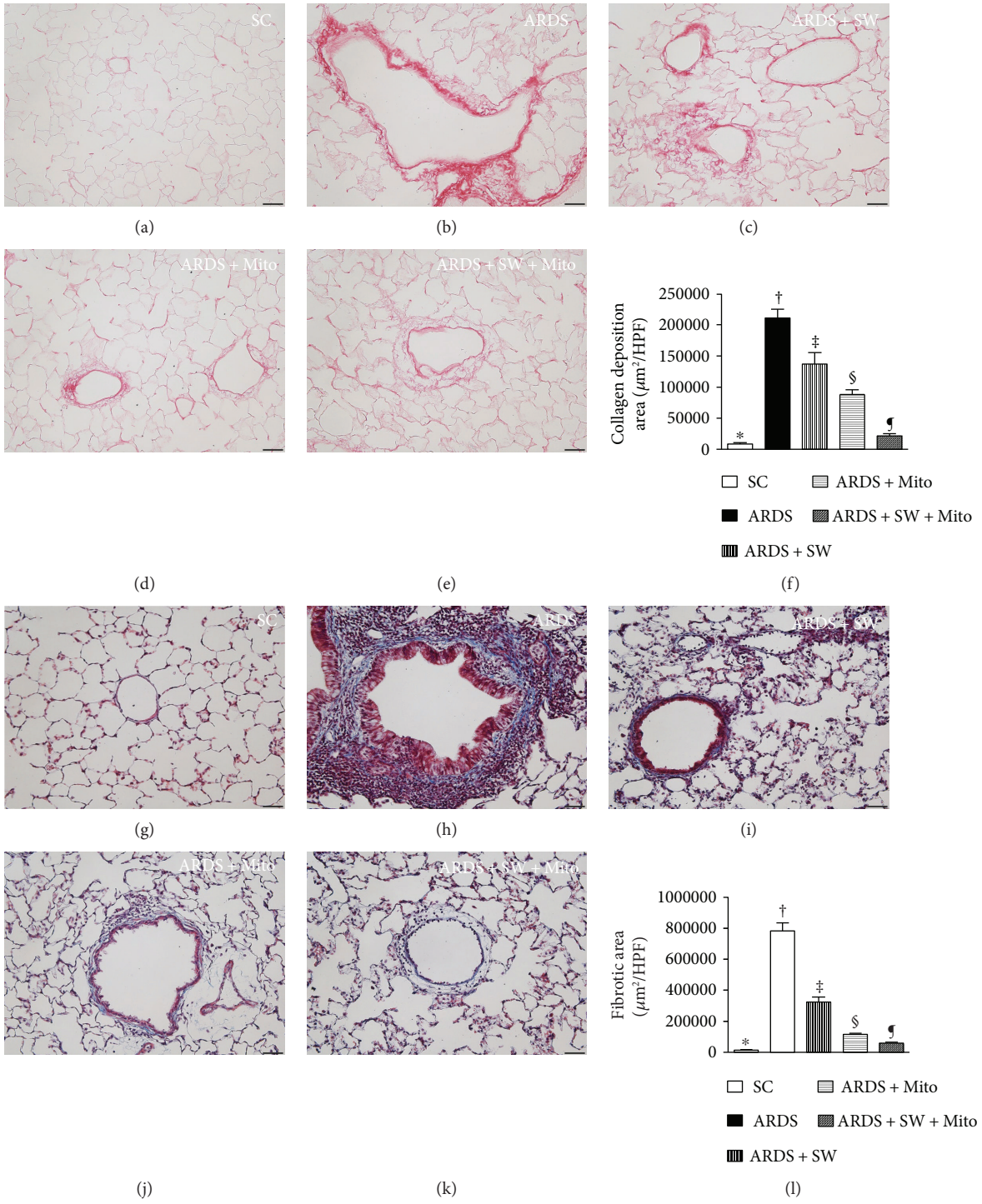

Figure 8: Histopathological findings of lung parenchyma by day 5 after ARDS induction. (a to e) Illustrating the microscopic finding (200x) of Sirius red stain for identification of condensed collagen deposition in lung parenchyma. (f) Analytical result of condensed collagen deposition area, * versus other groups with different symbols (†, ‡, §, ¶), $p < 0.0001$. (g to k) Illustrating the microscopic finding (200x) of Masson's trichrome stain for identification of fibrosis in lung parenchyma. (l) Analytical result of fibrotic area, * versus other groups with different symbols (†, ‡, §, ¶), $p < 0.0001$. The scale bars in the right lower corner represent 50 μm. All statistical analyses were performed by one-way ANOVA, followed by Bonferroni multiple comparison post hoc test. Symbols (*, †, ‡, §, ¶) indicate significance (at 0.05 level). SC = sham control; ARDS = acute respiratory distress syndrome; Mito = mitochondria; SW = shock wave.

the ARDS + Mito group. Additionally, Masson's trichrome staining revealed that in all five groups, the fibrotic areas displayed identical patterns of collagen deposition.

3.6. Oxidative Stress in Lung Parenchyma after ARDS Induction. Five days after ARDS induction, levels of NADPH oxidase- (NOX-) 1, NOX-2, and oxidized protein, three

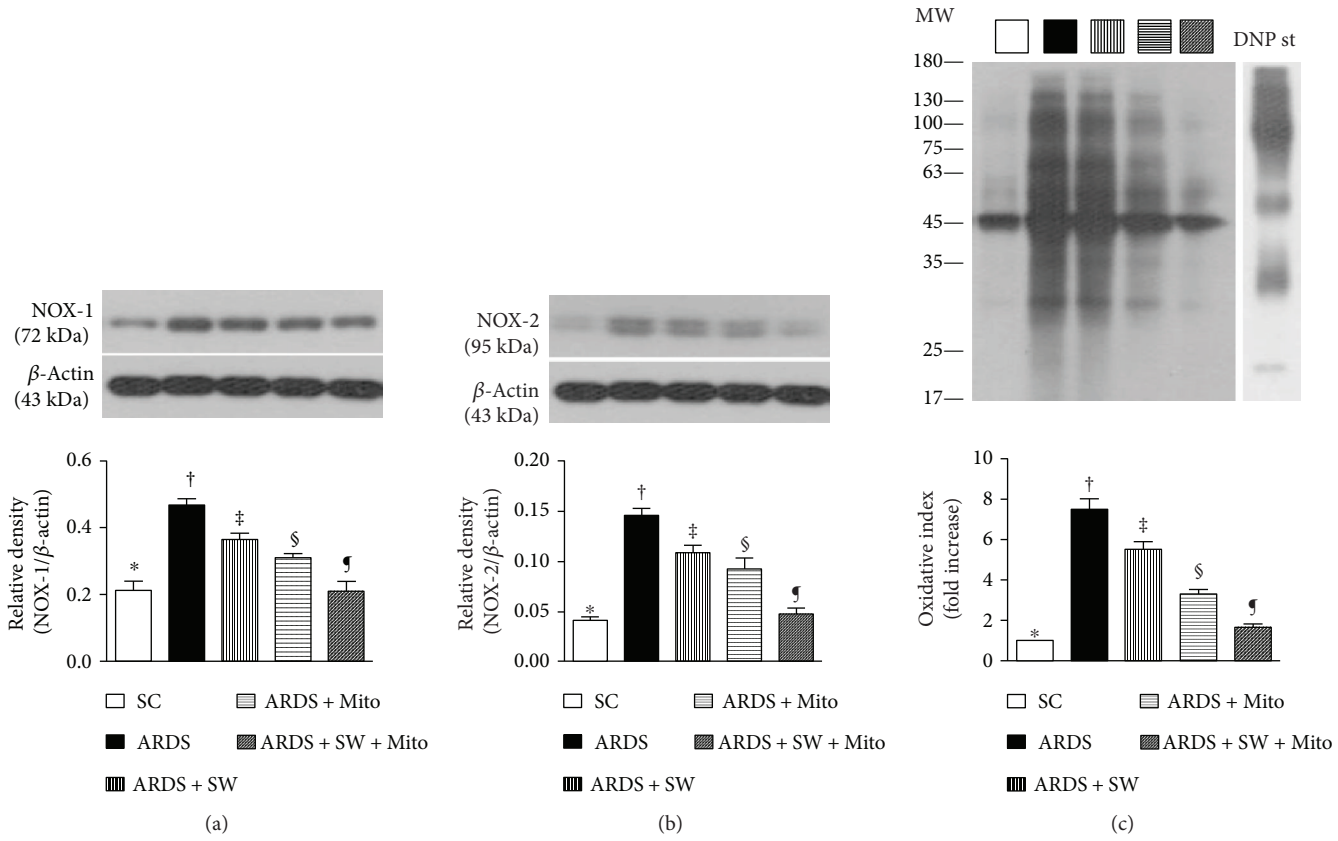

Figure 9: Protein expressions of oxidative stress in lung parenchyma by day 5 after ARDS induction. (a) Protein expressions of NOX-1, * versus other groups with different symbols (†, ‡, §, ¶), $p < 0.0001$. (b) Protein expression of NOX-2, * versus other groups with different symbols (†, ‡, §, ¶), $p < 0.0001$. (c) Expressions of oxidized protein, * versus other groups with different symbols (†, ‡, §, ¶), $p < 0.001$. MW = molecular weight; DNP = 1,3-dinitrophenylhydrazone. All statistical analyses were performed by one-way ANOVA, followed by Bonferroni multiple comparison post hoc test. Symbols (*, †, ‡, §, ¶) indicate significance (at 0.05 level). SC = sham control; ARDS = acute respiratory distress syndrome; Mito = mitochondria; SW = shock wave.

indicators of oxidative stress, were the highest in untreated ARDS rats, were significantly and progressively reduced across the ARDS + SW, ARDS + Mito, and ARDS + SW + Mito groups, and the lowest in the SC group (Figure 9).

3.7. Biomarkers of Inflammation in Lung Parenchyma after ARDS Induction. Five days after ARDS induction, levels of matrix metalloproteinase- (MMP-) 9, tumor necrosis factor- (TNF-) α, nuclear factor- (NF-) κB, interleukin- (IL-) 1β, and intercellular adhesion molecule- (ICAM-) 1, five indices of inflammation, were the highest in untreated ARDS rats, were significantly and progressively reduced across the ARDS + SW, ARDS + Mito, and ARDS + SW + Mito groups, and the lowest in the SC group (Figure 10).

3.8. Biomarkers of Apoptosis, Fibrosis, and Mitochondrial Damage in Lung Parenchyma after ARDS Induction. Levels of cleaved caspase 3 and cleaved poly (ADP-ribose) polymerase (PARP), two indicators of apoptosis, were the highest in untreated ARDS, significantly and progressively reduced across the ARDS + SW, ARDS + Mito, and ARDS + SW + Mito groups, and the lowest in the SC groups. The same pattern was exhibited by Smad3 and transforming growth factor- (TGF-) β, two mediators of fibrosis, as well as cytosolic cytochrome c, an indicator of mitochondrial damage. Conversely, the opposite pattern was exhibited by mitochondrial cytochrome c, an indicator of mitochondrial integrity (Figure 11).

4. Discussion

In this study, we investigated the ability of SW plus mitochondrial therapy to protect the lung parenchyma from ARDS injury. Our main findings are that (1) transfused mitochondria are taken up into rat lung epithelial and parenchymal cells, (2) this effect is enhanced by SW therapy, and (3) SW plus mitochondrial therapy alleviates inflammation and ARDS damage within the lung parenchyma. Our finding that transfused, liver-derived mitochondria are taken up into lung parenchymal cells in ARDS rats is consistent our previous study [30]. Moreover, to our knowledge, this is the first report that SW therapy enhances that effect.

Mitochondrial therapy also appears to mitigate ischemia-reperfusion injury in rat liver [26, 28]. Furthermore, we previously showed that SW therapy ameliorates ischemia-

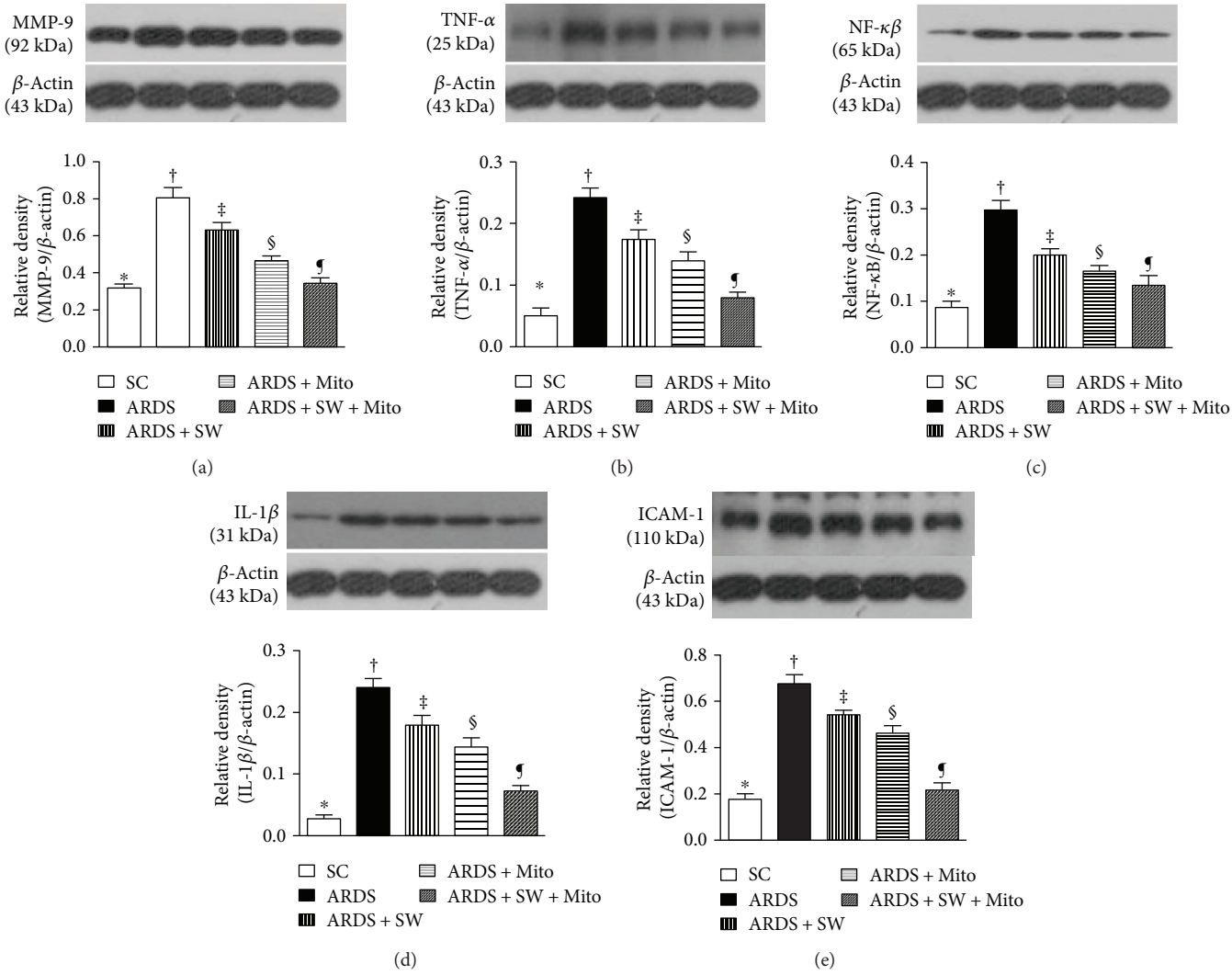

Figure 10: Protein expressions of inflammation in lung parenchyma by day 5 after ARDS induction. (a) Protein expression of matrix metalloproteinase- (MMP-) 9, * versus other groups with different symbols (†, ‡, §, ¶), $p < 0.0001$. (b) Protein expression of tumor necrosis factor- (TNF-) α, * versus other groups with different symbols (†, ‡, §, ¶), $p < 0.0001$. (c) Protein expression of nuclear factor- (NF-) κB, * versus other groups with different symbols (†, ‡, §, ¶), $p < 0.0001$. (d) Protein expression of interleukin- (IL-) 1β, * versus other groups with different symbols (†, ‡, §, ¶), $p < 0.0001$. (e) Protein expression of intercellular adhesion molecule- (ICAM-) 1, * versus other groups with different symbols (†, ‡, §, ¶), $p < 0.0001$. All statistical analyses were performed by one-way ANOVA, followed by Bonferroni multiple comparison post hoc test. Symbols (*, †, ‡, §, ¶) indicate significance (at 0.05 level). SC = sham control; ARDS = acute respiratory distress syndrome; Mito = mitochondria; SW = shock wave.

related tissue fibrosis/ischemia-related organ damage and reduces ischemia-related organ dysfunction [34, 36, 37]. Interestingly, our histopathological findings show that ARDS-related lung fibrosis and condensed collagen deposition are greatly attenuated by SW therapy and that those beneficial effects are enhanced by mitochondrial therapy. We also observed that biomarkers of inflammation, DNA/mitochondrial damage, apoptosis, and fibrosis are all markedly elevated in ARDS animals, which is consistent with our earlier studies [30, 35]. Importantly, these parameters are all reduced by SW or mitochondrial therapy and further ameliorated by the combination of the two therapies. This extends our earlier findings [26, 28–30, 34, 36, 37] and may explain why lung injury scores (i.e., increased septal thickness and decreased number of alveolar sacs) and exudate leakage from lung parenchyma are reduced in ARDS animals treated with SW plus mitochondrial therapy.

SW therapy is widely accepted for clinical application for treatment of lithotripsy [38] as well as skeletal diseases [39, 40], ischemic heart disease [41, 42], and peripheral artery disease [43, 44]. The mechanisms underlying the beneficial effects of SW therapy are thought to be related to its anti-inflammatory [32–34, 45] and angiogenic effects [32–34, 46], which enhance the healing process [47]. On the other hand, the mechanism by which SW therapy enhances transport of mitochondria into cells remains unclear. Perhaps, it induces a transient increase in cell membrane permeability, leading to increased mitochondrial uptake into the

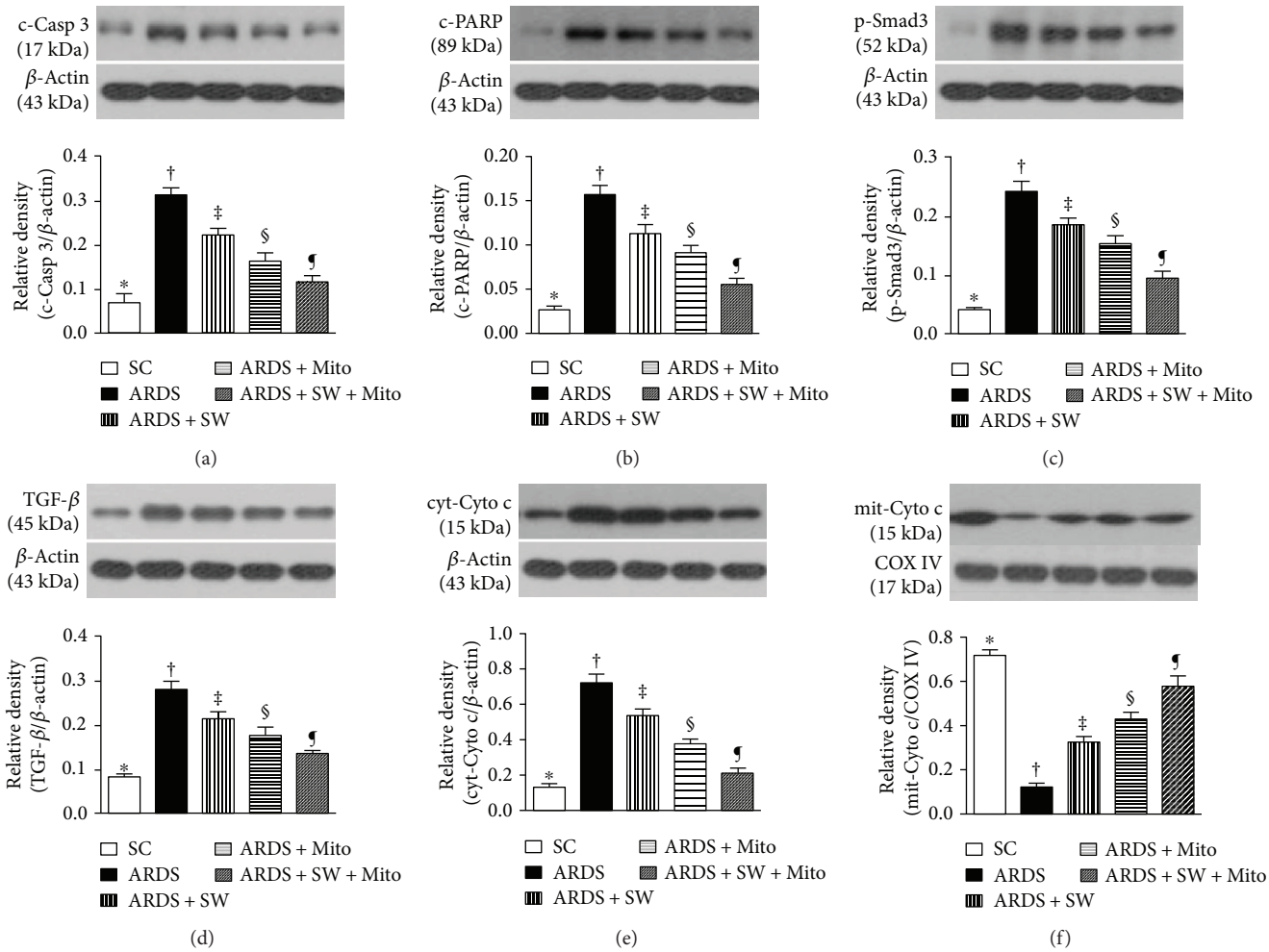

Figure 11: Protein expressions of apoptotic, fibrotic, and mitochondrial damage biomarkers in lung parenchyma by day 5 after ARDS induction. (a) Protein expression of cleaved caspase 3 (c-Casp 3), * versus other groups with different symbols (†, ‡, §, ¶), $p < 0.0001$. (b) Protein expression of cleaved poly(ADP-ribose) polymerase (c-PARP), * versus other groups with different symbols (†, ‡, §, ¶), $p < 0.0001$. (c) Protein expression of phosphorylated- (p-) Smad3, * versus other groups with different symbols (†, ‡, §, ¶), $p < 0.0001$. (d) Protein expression of transforming growth factor- (TGF-) β, * versus other groups with different symbols (†, ‡, §, ¶), $p < 0.0001$. (e) Protein expression of cytosolic cytochrome c (cyt-Cyto c), * versus other groups with different symbols (†, ‡, §, ¶), $p < 0.0001$. (f) Protein expression of mitochondrial cytochrome c (mit-Cyto c), * versus other groups with different symbols (†, ‡, §, ¶), $p < 0.0001$. All statistical analyses were performed by one-way ANOVA, followed by Bonferroni multiple comparison post hoc test. Symbols (*, †, ‡, §, ¶) indicate significance (at 0.05 level). SC = sham control; ARDS = acute respiratory distress syndrome; Mito = mitochondria; SW = shock wave.

cells. Consistent with that idea, previous studies showed that SW therapy increased cellular permeability, thereby facilitating delivery of genes and other molecules into cells [48, 49]. In addition, when exogenous mitochondria are taken up into cells, they often fuse and function with endogenous mitochondria (refer Figure 1). This could, at least in part, explain why SW plus mitochondrial therapy is superior to SW or mitochondrial therapy alone for protecting the lung against ARDS-induced damage.

This study has limitations. First, although the short-term outcome was promising, the long-term outcome of SW plus mitochondrial therapy for ARDS is unclear. Second, without assessment of the optimal doses of SW and mitochondrial therapy for ARDS, the relative efficacies of SW and mitochondrial therapy are uncertain.

5. Conclusions

In summary, the present study shows that SW therapy enhances uptake of mitochondria into lung epithelial and parenchymal cells and that SW-assisted mitochondrial therapy offers additional protection to the lung architecture against ARDS-induced injury.

Abbreviations

ARDS: Acute respiratory distress syndrome
BAL: Bronchoalveolar lavage
c-Casp 3: Cleaved caspase 3
c-PARP: Cleaved poly(ADP-ribose) polymerase
cyt-Cyto c: Cytosolic cytochrome c

ETC: Electron transport chain
IF: Immunofluorescent
ICAM: Intercellular adhesion molecule
IL: Interleukin
LEC: Lung epithelial cells
MMP: Matrix metalloproteinase
Mito: Mitochondria
mit-Cyto c: Mitochondrial cytochrome c
NOX: NADPH oxidase; mitochondria
NF-κB: Nuclear factor-κB
OXPHOS: Oxidative phosphorylation machinery
OCR: Oxygen consumption rate
ROS: Reactive oxygen species
SC: Sham control
SW: Shock wave therapy
TGF: Transforming growth factor.

Data Availability

The data used to support the findings of this study are available from the corresponding author upon request.

Conflicts of Interest

The authors declare that they have no conflicts of interest.

Acknowledgments

This study was supported by a program grant from Chang Gung Memorial Hospital, Chang Gung University (Grant no. CMRPG8F0611).

References

[1] G. Ailawadi, C. L. Lau, P. W. Smith et al., "Does reperfusion injury still cause significant mortality after lung transplantation?," *The Journal of Thoracic and Cardiovascular Surgery*, vol. 137, no. 3, pp. 688–694, 2009.

[2] C. Brun-Buisson, C. Minelli, G. Bertolini et al., "Epidemiology and outcome of acute lung injury in European intensive care units. Results from the ALIVE study," *Intensive Care Medicine*, vol. 30, no. 1, pp. 51–61, 2004.

[3] D. J. Ciesla, E. E. Moore, J. L. Johnson, J. M. Burch, C. C. Cothren, and A. Sauaia, "The role of the lung in postinjury multiple organ failure," *Surgery*, vol. 138, no. 4, pp. 749–758, 2005.

[4] W. A. den Hengst, J. F. Gielis, J. Y. Lin, P. E. Van Schil, L. J. De Windt, and A. L. Moens, "Lung ischemia-reperfusion injury: a molecular and clinical view on a complex pathophysiological process," *American Journal of Physiology-Heart and Circulatory Physiology*, vol. 299, no. 5, pp. H1283–H1299, 2010.

[5] S. M. Fiser, C. G. Tribble, S. M. Long et al., "Ischemia-reperfusion injury after lung transplantation increases risk of late bronchiolitis obliterans syndrome," *The Annals of Thoracic Surgery*, vol. 73, no. 4, pp. 1041–1048, 2002.

[6] M. A. Matthay and G. A. Zimmerman, "Acute lung injury and the acute respiratory distress syndrome: four decades of inquiry into pathogenesis and rational management," *American Journal of Respiratory Cell and Molecular Biology*, vol. 33, no. 4, pp. 319–327, 2005.

[7] J. Phua, J. R. Badia, N. K. J. Adhikari et al., "Has mortality from acute respiratory distress syndrome decreased over time? A systematic review," *American Journal of Respiratory and Critical Care Medicine*, vol. 179, no. 3, pp. 220–227, 2009.

[8] G. D. Rubenfeld, E. Caldwell, E. Peabody et al., "Incidence and outcomes of acute lung injury," *The New England Journal of Medicine*, vol. 353, no. 16, pp. 1685–1693, 2005.

[9] L. B. Ware and M. A. Matthay, "The acute respiratory distress syndrome," *The New England Journal of Medicine*, vol. 342, no. 18, pp. 1334–1349, 2000.

[10] W.-I. Choi, E. Shehu, S. Y. Lim et al., "Markers of poor outcome in patients with acute hypoxemic respiratory failure," *Journal of Critical Care*, vol. 29, no. 5, pp. 797–802, 2014.

[11] B. T. Thompson, R. C. Chambers, and K. D. Liu, "Acute respiratory distress syndrome," *The New England Journal of Medicine*, vol. 377, no. 6, pp. 562–572, 2017.

[12] G. Bernard, "Acute lung failure — our evolving understanding of ARDS," *The New England Journal of Medicine*, vol. 377, no. 6, pp. 507–509, 2017.

[13] P.-C. Li, A. Thorat, S.-C. Hsu et al., "Extracorporeal membrane oxygenation support for rituximab-induced acute respiratory distress syndrome in an ABO-incompatible living donor liver transplant recipient: successful management of a rare complication and a review of the literature," *Annals of Transplantation*, vol. 22, pp. 463–467, 2017.

[14] J. J. Marini, "Advances in the support of respiratory failure: putting all the evidence together," *Critical Care*, vol. 19, article S4, Supplement 3, 2015.

[15] A. S. Neto, F. D. Simonis, and M. J. Schultz, "How to ventilate patients without acute respiratory distress syndrome?," *Current Opinion in Critical Care*, vol. 21, no. 1, pp. 65–73, 2015.

[16] M. W. Sjoding, T. P. Hofer, I. Co, A. Courey, C. R. Cooke, and T. J. Iwashyna, "Interobserver reliability of the Berlin ARDS definition and strategies to improve the reliability of ARDS diagnosis," *Chest*, vol. 153, no. 2, pp. 361–367, 2018.

[17] G. Bellani, J. G. Laffey, T. Pham et al., "Epidemiology, patterns of care, and mortality for patients with acute respiratory distress syndrome in intensive care units in 50 countries," *JAMA*, vol. 315, no. 8, pp. 788–800, 2016.

[18] M. Fahr, G. Jones, H. O'Neal, J. Duchesne, and D. Tatum, "Acute respiratory distress syndrome incidence, but not mortality, has decreased nationwide: a National Trauma Data Bank study," *The American Surgeon*, vol. 83, no. 4, pp. 323–331, 2017.

[19] J. Villar, D. Sulemanji, and R. M. Kacmarek, "The acute respiratory distress syndrome: incidence and mortality, has it changed?," *Current Opinion in Critical Care*, vol. 20, no. 1, pp. 3–9, 2014.

[20] M. Bhargava and C. H. Wendt, "Biomarkers in acute lung injury," *Translational Research*, vol. 159, no. 4, pp. 205–217, 2012.

[21] G. R. S. Budinger, G. M. Mutlu, D. Urich et al., "Epithelial cell death is an important contributor to oxidant-mediated acute lung injury," *American Journal of Respiratory and Critical Care Medicine*, vol. 183, no. 8, pp. 1043–1054, 2011.

[22] T. Dolinay, Y. S. Kim, J. Howrylak et al., "Inflammasome-regulated cytokines are critical mediators of acute lung injury," *American Journal of Respiratory and Critical Care Medicine*, vol. 185, no. 11, pp. 1225–1234, 2012.

[23] C.-K. Sun, C. H. Yen, Y. C. Lin et al., "Autologous transplantation of adipose-derived mesenchymal stem cells markedly

reduced acute ischemia-reperfusion lung injury in a rodent model," *Journal of Translational Medicine*, vol. 9, no. 1, p. 118, 2011.

[24] H. K. Yip, Y. C. Chang, C. G. Wallace et al., "Melatonin treatment improves adipose-derived mesenchymal stem cell therapy for acute lung ischemia–reperfusion injury," *Journal of Pineal Research*, vol. 54, no. 2, pp. 207–221, 2013.

[25] M. N. Islam, S. R. Das, M. T. Emin et al., "Mitochondrial transfer from bone-marrow–derived stromal cells to pulmonary alveoli protects against acute lung injury," *Nature Medicine*, vol. 18, no. 5, pp. 759–765, 2012.

[26] H.-C. Lin, S.-Y. Liu, H.-S. Lai, and I.-R. Lai, "Isolated mitochondria infusion mitigates ischemia-reperfusion injury of the liver in rats," *Shock*, vol. 39, no. 3, pp. 304–310, 2013.

[27] A. Masuzawa, K. M. Black, C. A. Pacak et al., "Transplantation of autologously derived mitochondria protects the heart from ischemia-reperfusion injury," *American Journal of Physiology-Heart and Circulatory Physiology*, vol. 304, no. 7, pp. H966–H982, 2013.

[28] H. H. Chen, Y. T. Chen, C. C. Yang et al., "Melatonin pretreatment enhances the therapeutic effects of exogenous mitochondria against hepatic ischemia–reperfusion injury in rats through suppression of mitochondrial permeability transition," *Journal of Pineal Research*, vol. 61, no. 1, pp. 52–68, 2016.

[29] T. H. Huang, S. Y. Chung, S. Chua et al., "Effect of early administration of lower dose versus high dose of fresh mitochondria on reducing monocrotaline-induced pulmonary artery hypertension in rat," *American Journal of Translational Research*, vol. 8, no. 12, pp. 5151–5168, 2016.

[30] C. K. Sun, F. Y. Lee, Y. H. Kao et al., "Systemic combined melatonin–mitochondria treatment improves acute respiratory distress syndrome in the rat," *Journal of Pineal Research*, vol. 58, no. 2, pp. 137–150, 2015.

[31] A. Aicher, C. Heeschen, K. I. Sasaki, C. Urbich, A. M. Zeiher, and S. Dimmeler, "Low-energy shock wave for enhancing recruitment of endothelial progenitor cells: a new modality to increase efficacy of cell therapy in chronic hind limb ischemia," *Circulation*, vol. 114, no. 25, pp. 2823–2830, 2006.

[32] M. Fu, C. K. Sun, Y. C. Lin et al., "Extracorporeal shock wave therapy reverses ischemia-related left ventricular dysfunction and remodeling: molecular-cellular and functional assessment," *PLoS One*, vol. 6, no. 9, article e24342, 2011.

[33] K.-H. Yeh, J. J. Sheu, Y. C. Lin et al., "Benefit of combined extracorporeal shock wave and bone marrow-derived endothelial progenitor cells in protection against critical limb ischemia in rats," *Critical Care Medicine*, vol. 40, no. 1, pp. 169–177, 2012.

[34] J.-J. Sheu, H. E. E. Ali, B. C. Cheng et al., "Extracorporeal shock wave treatment attenuated left ventricular dysfunction and remodeling in mini-pig with cardiorenal syndrome," *Oncotarget*, vol. 8, no. 33, pp. 54747–54763, 2017.

[35] F.-Y. Lee, K. H. Chen, C. G. Wallace et al., "Xenogeneic human umbilical cord-derived mesenchymal stem cells reduce mortality in rats with acute respiratory distress syndrome complicated by sepsis," *Oncotarget*, vol. 8, no. 28, pp. 45626–45642, 2017.

[36] Y. L. Chen, K. H. Chen, T. C. Yin et al., "Extracorporeal shock wave therapy effectively prevented diabetic neuropathy," *American Journal of Translational Research*, vol. 7, no. 12, pp. 2543–2560, 2015.

[37] C. M. Yuen, S. Y. Chung, T. H. Tsai et al., "Extracorporeal shock wave effectively attenuates brain infarct volume and improves neurological function in rat after acute ischemic stroke," *American Journal of Translational Research*, vol. 7, no. 6, pp. 976–994, 2015.

[38] J. J. Rassweiler, C. Renner, C. Chaussy, and S. Thüroff, "Treatment of renal stones by extracorporeal shockwave lithotripsy: an update," *European Urology*, vol. 39, no. 2, pp. 187–199, 2001.

[39] J. D. Rompe, J. Decking, C. Schoellner, and B. Nafe, "Shock wave application for chronic plantar fasciitis in running athletes: a prospective, randomized, placebo-controlled trial," *The American Journal of Sports Medicine*, vol. 31, no. 2, pp. 268–275, 2003.

[40] L. Wang, L. Qin, H. B. Lu et al., "Extracorporeal shock wave therapy in treatment of delayed bone-tendon healing," *The American Journal of Sports Medicine*, vol. 36, no. 2, pp. 340–347, 2008.

[41] B. Assmus, D. H. Walter, F. H. Seeger et al., "Effect of shock wave–facilitated intracoronary cell therapy on LVEF in patients with chronic heart failure: the CELLWAVE randomized clinical trial," *JAMA*, vol. 309, no. 15, pp. 1622–1631, 2013.

[42] G. Zuoziene, A. Laucevicius, and D. Leibowitz, "Extracorporeal shockwave myocardial revascularization improves clinical symptoms and left ventricular function in patients with refractory angina," *Coronary Artery Disease*, vol. 23, no. 1, pp. 62–67, 2012.

[43] G. Belcaro, M. R. Cesarone, M. Dugall et al., "Effects of shock waves on microcirculation, perfusion, and pain management in critical limb ischemia," *Angiology*, vol. 56, no. 4, pp. 403–407, 2005.

[44] F. Serizawa, K. Ito, K. Kawamura et al., "Extracorporeal shock wave therapy improves the walking ability of patients with peripheral artery disease and intermittent claudication," *Circulation Journal*, vol. 76, no. 6, pp. 1486–1493, 2012.

[45] C. J. Wang, K. D. Yang, F. S. Wang, H. H. Chen, and J. W. Wang, "Shock wave therapy for calcific tendinitis of the shoulder: a prospective clinical study with two-year follow-up," *The American Journal of Sports Medicine*, vol. 31, no. 3, pp. 425–430, 2003.

[46] T. H. Huang, C. K. Sun, Y. L. Chen et al., "Shock wave therapy enhances angiogenesis through VEGFR2 activation and recycling," *Molecular Medicine*, vol. 22, no. 1, 2016.

[47] C. J. Wang, H. S. Chen, C. E. Chen, and K. D. Yang, "Treatment of nonunions of long bone fractures with shock waves," *Clinical Orthopaedics and Related Research*, vol. 387, pp. 95–101, 2001.

[48] U. Lauer, E. Bürgelt, Z. Squire et al., "Shock wave permeabilization as a new gene transfer method," *Gene Therapy*, vol. 4, no. 7, pp. 710–715, 1997.

[49] T. Kodama, A. G. Doukas, and M. R. Hamblin, "Shock wave-mediated molecular delivery into cells," *Biochimica et Biophysica Acta (BBA) - Molecular Cell Research*, vol. 1542, no. 1–3, pp. 186–194, 2002.

Hindawi
Mediators of Inflammation
Volume 2018, Article ID 5906819, 15 pages
https://doi.org/10.1155/2018/5906819

Research Article

Transcriptional Profiling Suggests Extensive Metabolic Rewiring of Human and Mouse Macrophages during Early Interferon Alpha Responses

Duale Ahmed,[1] Allison Jaworski,[2] David Roy,[2] William Willmore,[3] Ashkan Golshani,[1] and Edana Cassol[2]

[1]*Department of Biology, Carleton University, Ottawa, ON, Canada*
[2]*Department of Health Sciences, Carleton University, Ottawa, ON, Canada*
[3]*Institute of Biochemistry, Carleton University, Ottawa, ON, Canada*

Correspondence should be addressed to Edana Cassol; edana.cassol@carleton.ca

Received 21 February 2018; Accepted 24 May 2018; Published 25 July 2018

Academic Editor: José C. Rosa

Emerging evidence suggests that cellular metabolism plays a critical role in regulating immune activation. Alterations in energy and lipid and amino acid metabolism have been shown to contribute to type I interferon (IFN) responses in macrophages, but the relationship between metabolic reprogramming and the establishment of early antiviral function remains poorly defined. Here, we used transcriptional profiling datasets to develop global metabolic signatures associated with early IFN-α responses in two primary macrophage model systems: mouse bone marrow-derived macrophages (BMM) and human monocyte-derived macrophages (MDM). Short-term stimulation with IFN-α (<4 hours) was associated with significant metabolic rewiring, with >500 metabolic genes altered in mouse and human macrophage models. Pathway and network analysis identified alterations in genes associated with cellular bioenergetics, cellular oxidant status, cAMP/AMP and cGMP/GMP ratios, branched chain amino acid catabolism, cell membrane composition, fatty acid synthesis, and β-oxidation as key features of early IFN-α responses. These changes may have important implications for initial establishment of antiviral function in these cells.

1. Introduction

Type I interferons (IFN) (IFN-α and IFN-β) play a seminal role in antiviral, antibacterial, and antitumour responses and act as critical regulators of the innate and adaptive immune system [1–5]. These pleiotropic cytokines are produced following engagement of pattern recognition receptors and signal through the ubiquitously expressed transmembrane IFN-α receptor (IFNAR), composed of IFNAR1 and IFNAR2 subunits [5–7]. Cellular responses to type I IFN are cell type- and context-dependent and vary during the course of an immune response [8–11]. The variability in these responses are due, in part, to the cumulative effects of JAK-STAT, the p38 MAP kinase (MAPK), the MAP kinase kinase/ERK/MAPK signal-interacting kinase, and the phosphatidylinositol 3-kinase (PI3K)/AKT/mammalian target of rapamycin (mTOR) signaling pathways [11–13].

Emerging evidence suggests that cellular metabolism plays a critical role in regulating and fine tuning immune function [14–16]. Alterations in cellular bioenergetics, amino acid metabolism, and lipid metabolism have been shown to affect cytokine production, signaling protein activity, and cell differentiation [17–19]. In macrophages, stimulation with type I IFNs has been shown to increase glycolytic flux, inhibit sterol biosynthesis, shift lipid metabolism from de novo synthesis to lipid import, and increase tryptophan catabolism [20–25]. This metabolic reprogramming is required to mount functional antiviral responses and has been shown to regulate antigen presentation, inflammatory mediator production, phagocytosis efficiency, and intracellular killing [26, 27].

Recent studies suggest metabolic adaptations in macrophages occur at the molecular level (i.e., gene expression) very early during the process activation and functional

polarization [28–30]. In lipopolysaccharide- (LPS-) stimulated macrophages, cellular activation has been shown to undergo stages of time-resolved metabolic reprogramming into initiation, early, and amplification phases [28]. To date, there has been no systematic characterization of metabolic reprogramming associated with type I IFN responses, particularly when examined as a function of time. In the current study, we used transcriptional profiling to evaluate global changes in metabolic gene expression following short-term IFN-α stimulation (<4 hours) in two well-characterized primary macrophage model systems: mouse bone marrow-derived macrophages (BMM) and human monocyte-derived macrophages (MDM). Our findings provide a systematic understanding of altered metabolic genes associated with early IFN-α responses in BMM and MDM and identify potential metabolic mechanisms that may contribute to initial establishment of antiviral immune responses.

2. Materials and Methods

2.1. Microarray Normalization and Processing. Microarray datasets were extracted from the Gene Expression Omnibus (GEO) repository from the National Center for Biotechnology Information (NCBI). Datasets were identified using the search terms "Macrophage Interferon" and "Type I Interferon" [31]. A total of 10 datasets were identified using these search criteria. Two studies were identified that assessed short-term stimulation (<4 hours) in either mouse bone marrow-derived macrophages (BMM) or human monocyte-derived macrophages (MDM). The selected BMM dataset [32] differentiated bone marrow cells in DMEM media with 10 ng/mL of macrophage colony-stimulating factor (M-CSF), 10% FBS, and 1% penicillin/streptomycin for seven days before replacing the media on day six. BMM were stimulated with 62 U/mL IFN-α (approximately 1 ng/mL) for 2.5 hours prior to cell lysis and RNA extraction (Supplementary Figure S1). The selected MDM dataset [33] isolated monocytes *via* adherence (4 hours) and differentiated cells in DMEM media with 2 mM L-glutamine, 100 U/mL penicillin, 100 μg/mL streptomycin, and 10% FCS for 7 days. After differentiation, MDM were treated with 10 ng/mL IFN-α for 4 hours prior to cell lysis and RNA extraction (Supplementary Figure S1). Raw gene expression data was normalized by median centering, and preprocessing was performed in dChip [34]. Probes were excluded from the analysis when present calls ($p < 0.05$) were identified in less than 20% of samples.

2.2. Identification of Significant Metabolic Genes in IFN-Stimulated Macrophages. Metabolic genes were identified using the MetScape plugin in Cytoscape [35–37]. These genes were identified by mapping Entrez Gene IDs to metabolic pathways found in the Kyoto Encyclopedia of Genes and Genomes (KEGG) and Edinburgh Human Metabolic Network (EHMN) databases. Manual curation was performed to identify metabolic genes that did not map to KEGG or EHMN pathways. Fold change (FC) analyses, p values, and false discovery rates (FDR) were calculated in R. Differentially expressed genes were defined as a $-1.2 \leq \text{FC} \geq 1.2$, p value ≤ 0.05, and FDR ≤ 0.1. This fold change cutoff was selected to be inclusive of small differences in gene expression. Biologically relevant alterations in metabolic gene expression were identified by combining FC with pathway and network analyses. Classification analyses including principal component analysis (PCA), partial least squares-discriminant analysis (PLS-DA), random forest (RF), and unsupervised hierarchical clustering were performed in MetaboAnalyst [38]. Gene Set Enrichment Analysis (GSEA) [39] was performed using the hallmark gene sets (H; $n = 50$), the curated gene sets (C2; $n = 4731$), and the GO gene sets (C5; $n = 5917$) from Molecular Signatures Database (MSigDB) version 6.0. Significant enrichment was defined as a $p \leq 0.05$ and FDR < 0.25. Metabolic pathway enrichment and topology analysis were performed in MetaboAnalyst. Significant enrichment of metabolic datasets was defined as $p \leq 0.05$. Metabolic network annotation and analysis were performed in Cytoscape and the Database for Annotation, Visualization and Integrated Discovery (DAVID) [40, 41]. The work flow is shown in Figure 1(a).

3. Results

3.1. Type I IFN Stimulation of Mouse BMM and Human MDM Is Associated with Enrichment of Metabolic Gene Sets. Of the >45,000 unique probe sets analyzed across the two datasets, 28,903 and 29,479 probes were identified as present in the BMM and MDM datasets, respectively. In total, 7338 genes were differentially expressed in IFN-α-stimulated BMM compared to unstimulated controls (Supplementary Table S1). Conversely, 3804 genes were differentially expressed in IFN-α stimulated MDM compared to controls (Supplementary Table S2). GSEA identified significantly enriched gene sets within each dataset. Two hundred and eighty-five gene sets were enriched in BMM distributed across three main functional categories including immune signaling and function ($n = 151$), cellular metabolism ($n = 40$), and other biological states and processes ($n = 94$). Enriched metabolic processes in BMM included glycolysis and gluconeogenesis, the regulation of nitric oxide biosynthetic process, and tryptophan, arginine, and proline metabolism (Supplementary Table S3). In MDM, GSEA identified 948 enriched gene sets (immune signaling and function: $n = 360$, cellular metabolism: $n = 107$, and other biological states and processes: $n = 481$). Enriched metabolic processes included reactive oxygen species (ROS) metabolism and biosynthesis, tryptophan metabolism, regulation of steroid biosynthetic process, and regulation of oxidoreductase activity (Supplementary Table S4).

3.2. Metabolic Genes Represent Important Classifiers of Early Type I IFN Responses in BMM and MDM. Given the significant enrichment of metabolic gene sets in GSEA analysis, we used MetScape to identify all metabolic genes detected across datasets. Of the >1600 metabolic genes identified, 517 and 354 were altered following short-term IFN-α stimulation of BMM and MDM, respectively ($-1.2 \leq \text{FC} \geq 1.2$, p value ≤ 0.05, FDR ≤ 0.1). Ninety-four genes were altered in both datasets with the same directionality (either

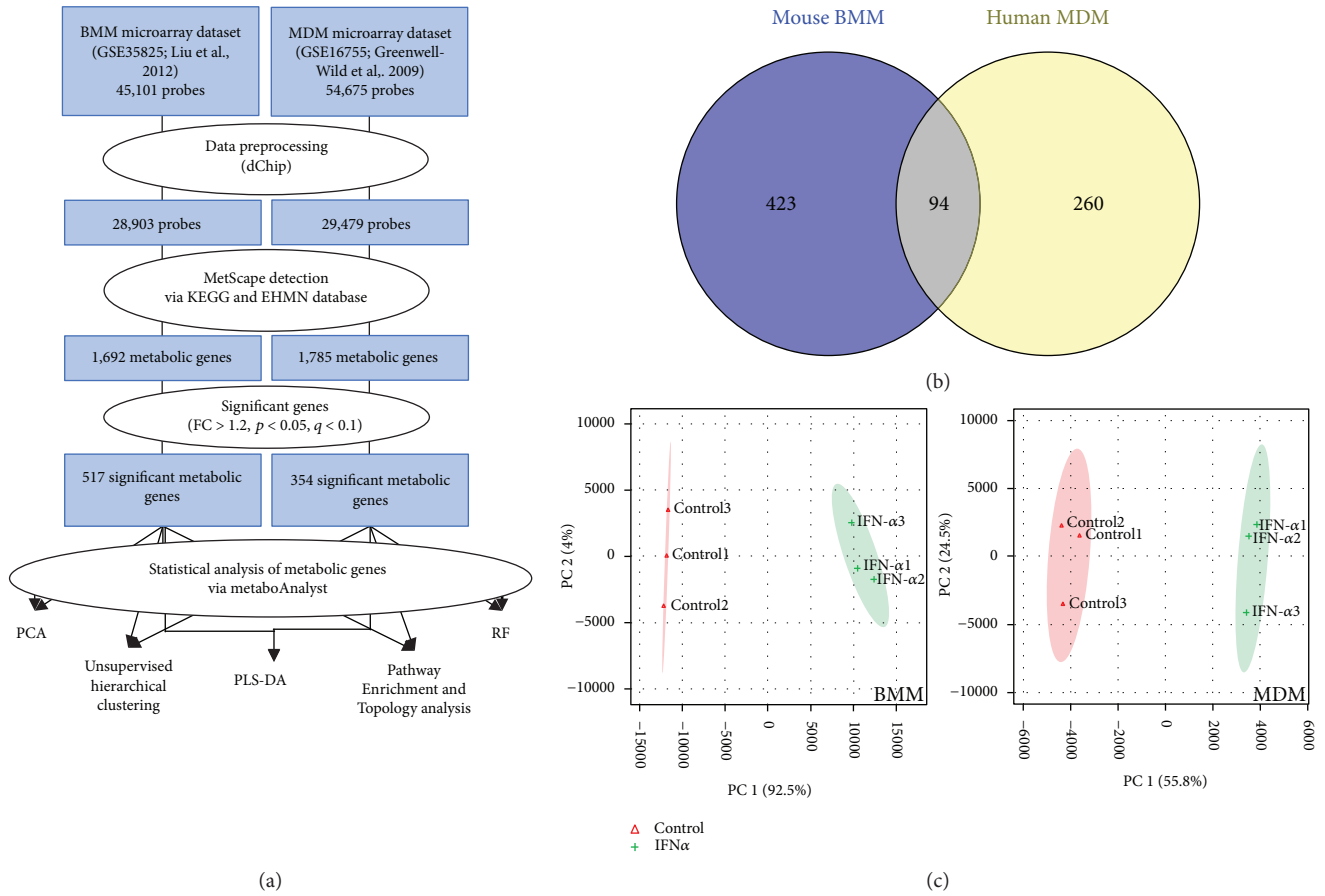

Figure 1: Short term IFN-α stimulation is associated with altered expression of metabolic genes in human monocyte-derived macrophages (MDM) and mouse bone marrow-derived macrophages (BMM). (a) Workflow used to identify differentially expressed metabolic genes in IFN-α-stimulated mouse BMM (2.5 hours) and human MDM (4 hours). Metabolic genes were identified in MetScape using the Kyoto Encyclopedia of Genes and Genomes (KEGG) and the Edinburgh Human Metabolic Network (EHMN) databases. (b) Venn diagram showing the number of metabolic genes common to the BMM (yellow) and MDM (blue) datasets (FC > 1.2, $p < 0.05$, FDR < 0.10). (c) Principal component analysis (PCA) of metabolic gene sets from BMM (left) and MDM (right) following IFN-α stimulation ($n = 517$ and 354 metabolic genes in the BMM and MDM datasets, resp.).

upregulated or downregulated) (Figure 1(b)) including genes associated with cellular bioenergetics (*PFKFB3*, *PDP*), tryptophan metabolism (*KMO*, *WARS*), nucleotide metabolism (*NT5C3*, *CNP*), and lipid metabolism (*SPTLC2*, *AGPAT5*, *SQLE*, and *SOAT1*). PCA showed a clear separation between the control and IFN-α-treated samples in both BMM and MDM based on the metabolic gene subset (Figure 1(c)). Similarly, random forest analysis classified control and IFN-α-stimulated cells with 100% predictive accuracy using metabolic genes. Variable importance in projection (VIP) analysis identified genes involved in nucleotide degradation (*PNP*, *AMPD3*) and lipid metabolism (*ETNK1*, *HMGCS1*) as top classifiers in IFN-α stimulation in BMM. Top classifiers in MDM included genes associated with glycolysis (*PFKFB3*), tryptophan catabolism (*KYNU*), and reactive oxygen species production (*GCH1*, *SOD2*) (Figures 2(c) and 2(d)). Only *EIF2AK2*, *NAMPT*, and *NT5C3* and the ubiquitin-related gene *USP18* overlapped as top classifiers across datasets. EIF2AK2 is involved in mRNA translation and inflammasome activation [42], NAMPT is a key NAD^+producing gene [43], and NT5C3 is an antiviral pyrimidine nucleotidase [44].

Pathway enrichment and topology analysis identified enrichment in purine, pyrimidine, inositol phosphate, and branched-chain amino acid metabolism in addition to lysine degradation in both BMM and MDM. Metabolic pathways uniquely enriched in BMM included arginine and proline metabolism, steroid biosynthesis, sphingolipid and glycerophospholipid metabolism (Figure 2(a), Supplementary Figure S2). Metabolic pathways uniquely enriched in MDM included amino sugar and nucleotide sugar metabolism, nicotinate and nicotinamide metabolism, galactose metabolism, and fatty acid (FA) metabolism (Figure 2(b), Supplementary Figure S2).

3.3. Short Term IFN-α Stimulation Alters Genes Associated with Energy Metabolism in BMM and MDM. To better functionally characterize differential gene expression in IFN-α-stimulated BMM and MDM, altered genes ($-1.2 \leq FC \geq 1.2$, p value ≤ 0.05, FDR ≤ 0.1) were mapped to metabolic

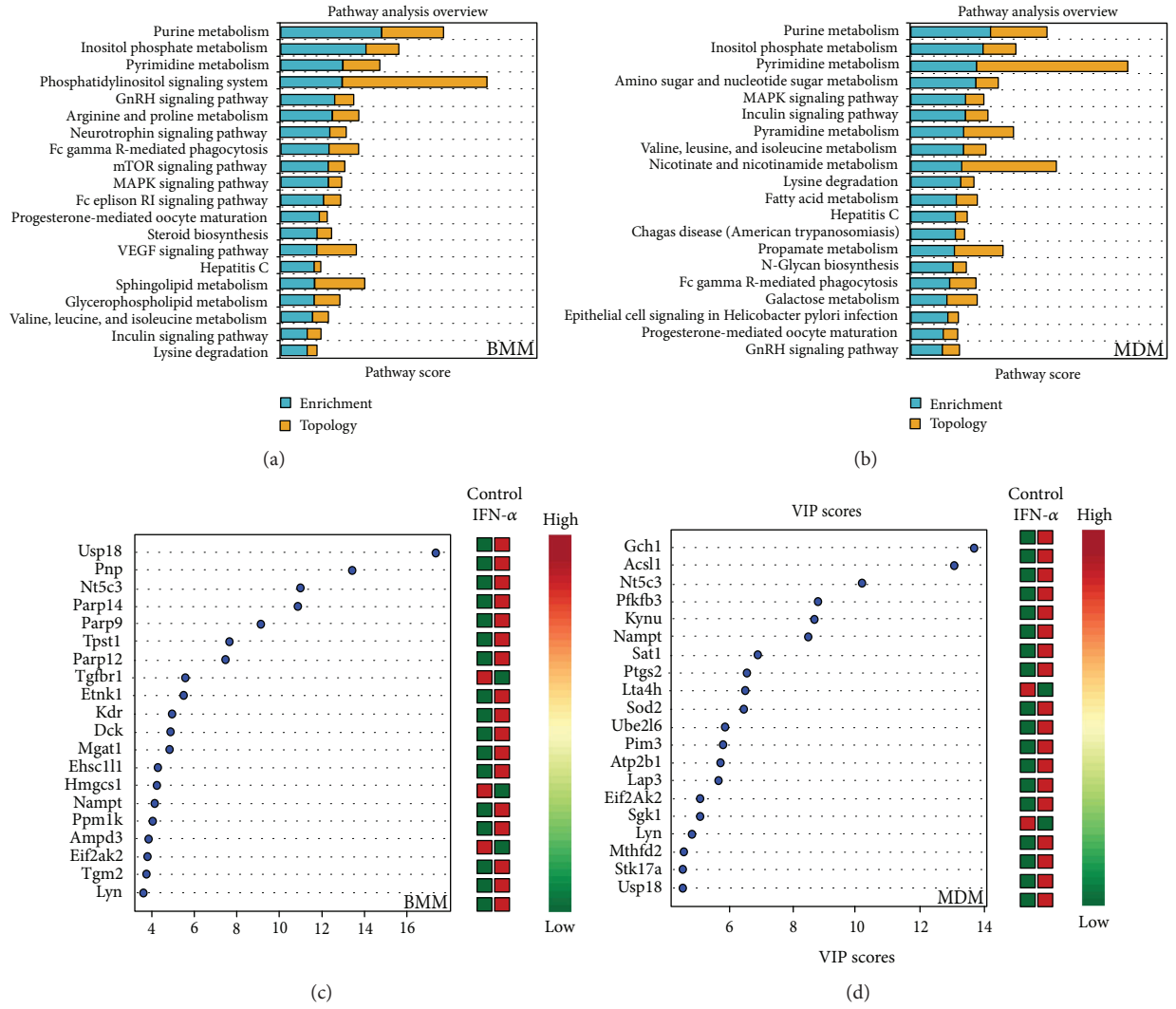

Figure 2: Metabolic genes are top classifiers of IFN-α stimulation in BMM and MDM. (a) Pathway enrichment and topology analysis of mouse BMM and human MDM following IFN-α stimulation ($p < 0.05$). Analyses were performed using all metabolic genes. The blue bars represent enrichment analysis. The yellow bars represent topology scores. (b) Top metabolic classifiers of IFN-α stimulation were identified using variable importance in projection (VIP) scores based on PLS-DA models ($p < 0.05$). Analyses were performed using all metabolic genes ($p < 0.05$). Red and green in the heat map represent upregulation and downregulation of gene expression, respectively.

pathways and networks. Consistent with the literature [20], short-term IFN-α stimulation of BMM was associated with an upregulation of glycolytic genes (*HK2*, *HK3*, *PGM2*, *PFKP*, *PFKFB3*, and *INSR*) compared to unstimulated controls (Figure 3, Supplementary Figure S3). Key genes involved in pyruvate metabolism were also altered in BMM following IFN-α stimulation. Whereas pyruvate dehydrogenase kinase 3 (*PDK3*) was upregulated, pyruvate dehydrogenase phosphatase 1 (*PDP1*) and dihydrolipoamide dehydrogenase (*DLD*) were downregulated. These alterations may affect the activity of the pyruvate dehydrogenase complex (PDH) and increase lactate production. Consistent with these findings, lactate dehydrogenase D (*LDHD*) was also upregulated in IFN-α-stimulated BMM. Interestingly, IFN-α-stimulated BMMs also upregulated levels of isocitrate dehydrogenase (*IDH3A*) and the downregulation of *DLD* and dihydrolipoamide *S*-succinyltransferase (*DLST*) expression. DLD and DLST are key components of the oxoglutarate dehydrogenase complex (OGDC) and play an important role in converting 2-oxoglutarate to succinyl-CoA. Along the succinate-fumarate-malate axis, succinate dehydrogenase complex subunit A (*SDHA*) was downregulated in stimulated compared to unstimulated BMM. SDHA is the major catalytic subunit of the succinate-ubiquinone oxidoreductase. Altered SDHA expression may also have significant effects on oxidative phosphorylation (OXPHOS).

Short-term IFN-α stimulation of MDM was not associated with significant alterations in glycolytic genes or genes linked to lactate production (Figure 3, Supplementary Figure S3). Alternatively, stimulation was associated with the downregulation of genes associated with the conversion of galactose to glucose (*GALK2*, *GALT*, and *GALE*) and glycogen breakdown (*INSR*, *PHKA1*, *PHKA2*, *PHKG2*, and *AGL*). Early responses in MDM were associated with

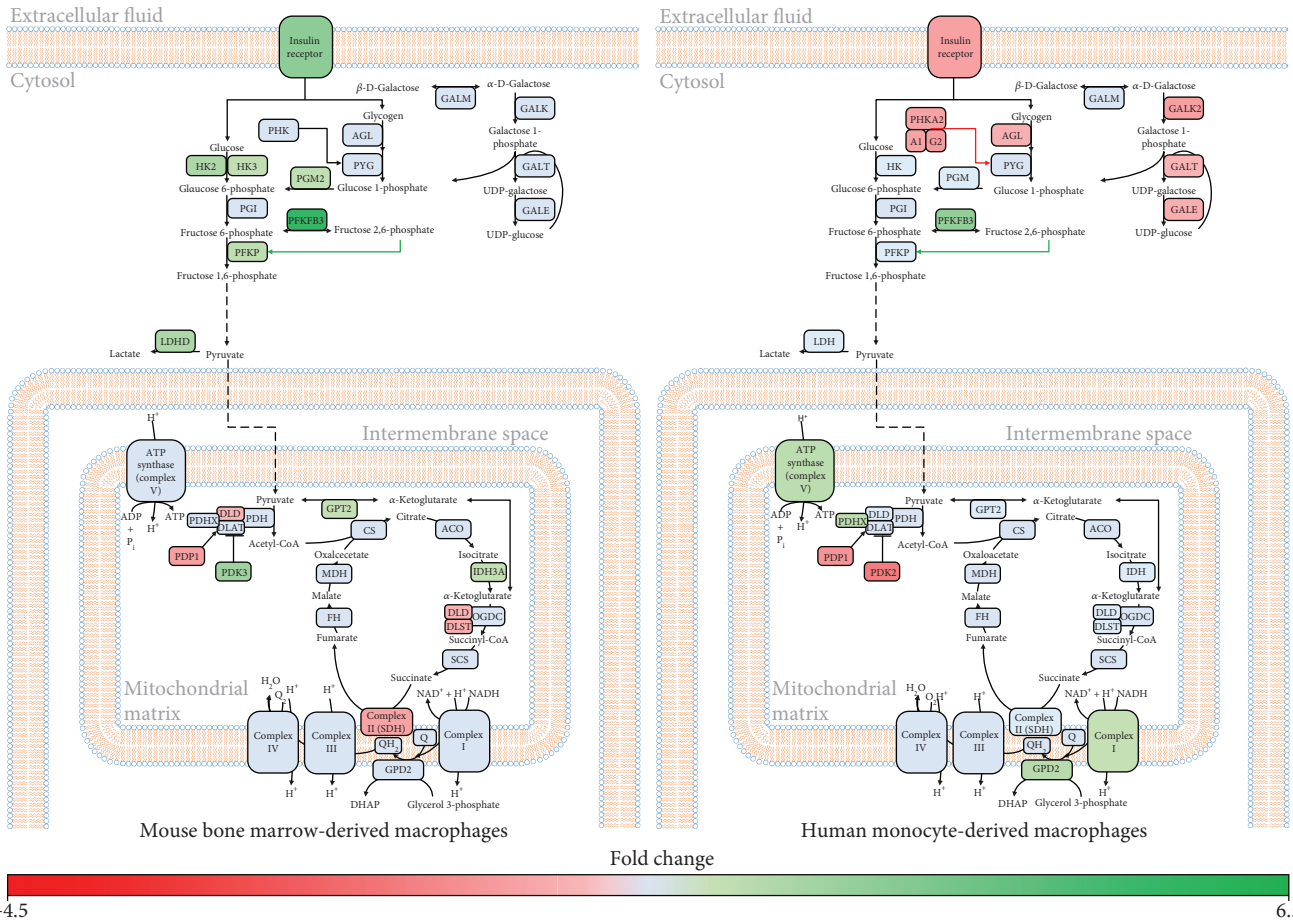

Figure 3: Genes associated with bioenergetic processes are differentially expressed in mouse BMM and human MDM following IFN-α stimulation. Significantly altered ($-1.2 \leq FC \geq 1.2$, p value ≤ 0.05, FDR ≤ 0.1) metabolic genes involved in energy production were mapped to their respective pathways using MetScape and DAVID. Green and red represent genes that have been significantly upregulated or downregulated, respectively. Blue represents genes that were not altered following IFN-α stimulation.

increased levels of phosphofructokinase (PFK) activator *PFKFB3*, which assists in the production of pyruvate from glucose and pyruvate dehydrogenase complex component X (*PDHX*), which may facilitate acetyl-CoA production from pyruvate. IFN-α was also associated with the upregulation of genes associated with OXPHOS including genes from complexes I and V of the electron transport chain (*NDUFA9*, *NDUFS4*, and *ATP5G3*) and the glycerol phosphate shuttle (glycerol 3-phosphate dehydrogenase 2 [*GPD2*]). Collectively, these results suggest that early changes in energy metabolism may play an important role in the initiation of antiviral responses in both BMM and MDM.

3.4. IFN-α-Stimulated BMM and MDM Show Signs of Alterations in Genes Associated with Redox Regulation. Given the link between energy metabolism and ROS metabolism [45–47], we next examined alterations between early IFN-α responses and genes linked to cellular redox status (oxidant and antioxidant genes). In BMM, IFN-α short-term stimulation was associated with altered expression of genes associated with the nitric oxide cycle including the upregulation of argininosuccinate synthetase 1 (*ASS1*) and nitric oxide synthase 1 (*NOS1*), and downregulation of arginase 2 (*ARG2*) expression, which may favour flux of arginine towards NO production (Figure 4, Supplementary Figure S4). Early IFN-α responses in BMM were also associated with the downregulation of genes associated with the antioxidant response (superoxide dismutase 2 (*SOD2*), glutamate-cysteine ligase, catalytic subunit (*GCLC*), NAD kinase (*NADK*), and thioredoxin reductase 1 and 3 (*TXNRD1*, *TXNRD3*)) and the upregulation of thioredoxin interacting protein (*TXNIP*), which inhibits the antioxidant activity of thioredoxin [48, 49].

Alternatively, IFN-α stimulation of MDM was associated with the upregulation of antioxidant genes including SOD2 and myeloperoxidase (*MPO*) as well as genes associated with glutathione production (glutamate-cysteine ligase, modifier subunit (*GCLM*) and NAD^+ kinase (*NADK*)) (Figure 4, Supplementary Figure S4). Short-term IFN-α was also associated with upregulation of and glutaredoxin (*GLRX*), thioredoxin 1 (*TXN1*), and thioredoxin-interacting protein (*TXNIP*). These alterations may help regulate electron linkage and subsequent ROS production associated with the

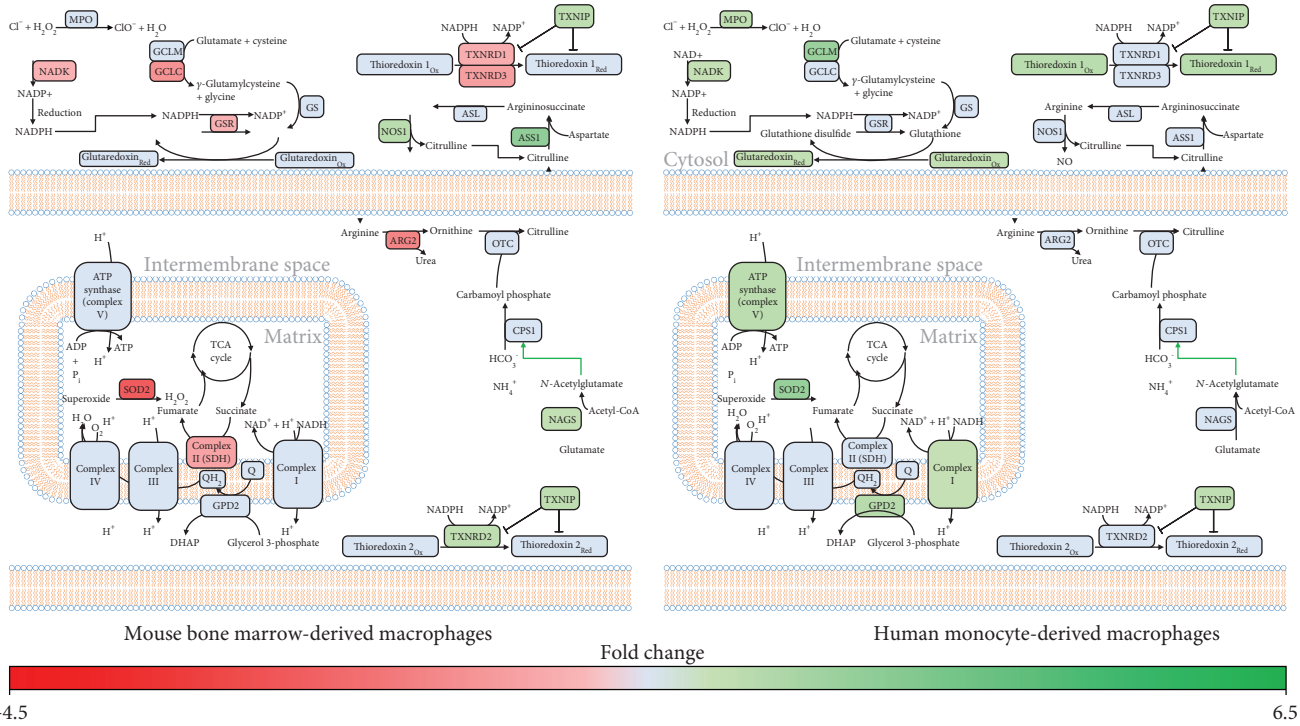

Figure 4: IFN-α stimulation of MDM is associated with increased expression of genes associated with ROS production and antioxidant responses. Differentially expressed metabolic genes ($-1.2 \leq FC \geq 1.2$, p value ≤ 0.05, FDR ≤ 0.1) were mapped to pathways associated with cellular redox status using MetScape and DAVID. Green and red represent genes that have been significantly upregulated or downregulated, respectively. Blue represents genes that were not altered following IFN-α stimulation.

upregulation of genes associated with OXPHOS in these cells (Figures 3 and 4).

3.5. Early Type I IFN Responses Are Associated with Alterations in Genes Associated with cAMP and cGMP Production. Given the enrichment of gene sets associated with nucleotide metabolism in both datasets, we examined the specific effects on short-term IFN-α stimulation on purine and pyrimidine metabolism. In BMM, short-term stimulation was associated with the downregulation of amidophosphoribosyltransferase (*PPAT*) and UMP synthetase (*UMPS*). These enzymes play a central role in ribose 5-phosphate incorporation during de novo purine and pyrimidine synthesis, which may represent an antiviral mechanism. At the level of purine degradation, IFN-α was associated with an upregulation of purine nucleoside phosphorylase (*PNP*), guanine deaminase (*GDA*), xanthine dehydrogenase (*XDH*), and ectonucleoside triphosphate diphosphohydrolase 2 and 5 (*ENTPD2*, *ENTPD5*) suggesting increased degradation. Interestingly, IFN responses were also associated with alterations in genes that regulate cyclic guanine monophosphate (cGMP)/GMP and cyclic adenosine monophosphate (cAMP)/AMP ratios (Figure 5, Supplementary Figure S5). Four phosphodiesterases (*PDE4D*, *PDE7A*, *PDE7B*, and *PDE8B*) and two adenylate cyclases (*ADCY2*, *ADCY4*) were upregulated, and adenylate kinase (*ADK*) and AMP deaminase 3 (*AMPD3*) were downregulated in stimulated versus unstimulated cells. These profiles suggest that IFN-α-activated BMM may accumulate both AMP and cAMP. IFN-α stimulation of BMM was also associated with the upregulation of guanylate kinase (*GUK*) and downregulation of phosphodiesterase 1B (*PDE1B*), suggesting these cells may favour cGMP production.

In MDM, IFN-α stimulation was not associated with significant changes in genes associated with de novo purine synthesis. However, IFN-α was associated with the downregulation of carbamoyl phosphate synthetase 2, aspartate transcarbamylase, and dihydroorotase (CAD), a protein responsible for the first three enzymatic steps of the pyrimidine biosynthesis pathway. Genes involved in nucleoside production within the purine and pyrimidine degradation pathways, such as GMP reductase (*GMPR*), *AMPD3*, 5′-nucleotidase, cytosolic II (*NT5C2*), and adenosine deaminase (*ADA*), are found to be upregulated in MDM which suggests an increase in nucleotide salvaging (Figure 5, Supplementary Figure S5). At the level of cGMP/GMP and cAMP/AMP regulation, the downregulation of *PDE6D* and adenylate cyclase 7 (*ADCY7*) as well as the upregulation of *PDE4B* and two soluble forms of guanylate cyclase (*GUCY1A3*, *GUCY1B3*) suggest a shift towards cGMP and AMP production. Varied expression of these bioactive nucleotides that function as intracellular secondary messengers may contribute to early type I IFN responses.

3.6. Short-Term IFN-α Stimulation Is Associated with Alterations in Tryptophan and Branched-Chain Amino Acid Catabolism in BMM and MDM. Consistent with the literature [50, 51], alterations in genes associated with tryptophan

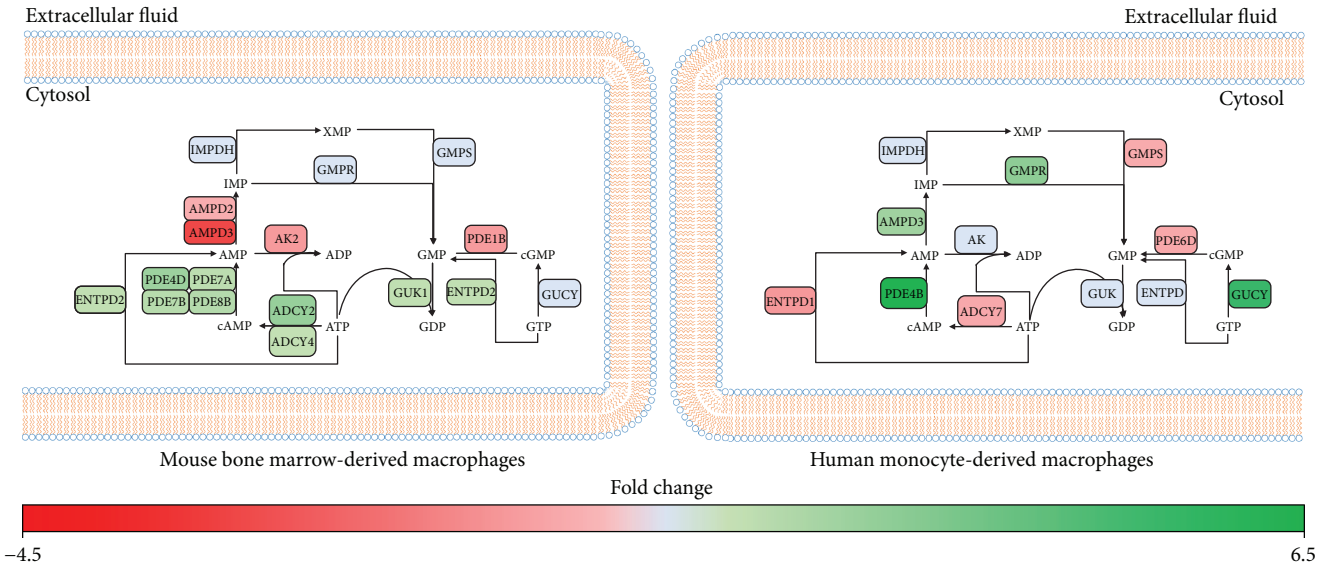

Figure 5: Type I IFN responses are associated with altered cAMP and cGMP production in BMM and MDM. Metabolic genes identified as significantly altered ($-1.2 \leq FC \geq 1.2$, p value ≤ 0.05, FDR ≤ 0.1) were mapped to pathways associated with AMP and GMP production using MetScape and DAVID. Green and red represent genes that have been significantly upregulated or downregulated, respectively. Blue represents genes that were not altered following IFN-α stimulation.

and branched-chain amino acid catabolism were pronounced in early IFN-α responses. Both BMMs and MDMs exhibited a pronounced upregulation of genes associated with tryptophan catabolism *via* the kynurenine pathway (Figure 6, Supplementary Figure S6). While IFN-α-stimulated BMM upregulated tryptophan 2,3-dioxygenase (*TDO2*) and *KMO*, stimulation of MDM was associated with the upregulation of *KMO* and kynureninase (*KYNU*). This shift in tryptophan catabolism was accompanied by the upregulation of nicotinamide phosphoribosyltransferase (*NAMPT*), suggesting an increased flux of tryptophan towards NAD^+ production.

Both IFN-α-activated BMM and MDM showed altered expression of genes associated with branched-chain amino acid (Figure 6, Supplementary Figure S6). In BMMs, IFN-α stimulation leads to the upregulation of genes associated with isoleucine (propionyl-CoA carboxylase; *PPCA*, 3-ketoacyl-CoA thiolase 1A and 2; *ACAA1A/2*) and valine (3-hydroxyisobutyrate dehydrogenase; *HIBADH*) catabolism. Upregulation of AU RNA binding/methylglutaconyl-CoA hydratase (*AUH*) and downregulation of methylcrotonoyl-CoA carboxylase 1 (*MCCC1*) and 3-hydroxymethyl-3-methylglutaryl-CoA lyase (*HMGCL*) suggest decreased leucine catabolism in BMM. However, *AUH* may be functioning in its secondary role in promoting mRNA degradation [52]. In MDM, IFN-α stimulation was associated with a downregulation of multiple genes associated with branched-chain amino acid catabolism including branched-chain aminotransferase 2 (*BCAT2*), isovaleryl-CoA dehydrogenase (*IVD*), hydroxyacyl-CoA dehydrogenase (*HADH*), and methylmalonyl-CoA epimerase (*MCEE*). Together, this indicates that alterations in branched-chain amino acid catabolism may be key to driver of early IFN-α responses in primary macrophage systems.

3.7. IFN-α Stimulation Is Associated with Altered Lipid Metabolism in BMM and MDM. Lipid metabolism has been shown to play an important role in antiviral responses in BMM and MDM [53]. Several studies have reported alterations in cholesterol metabolism during IFN and antiviral responses [21–23]. Here, we also identified alterations in genes associated with phospholipid and sphingolipid metabolism and FA biosynthesis following short-term IFN responses. Consistent with previous studies, short-term IFN-α stimulation of BMM and MDM was associated with the downregulation of genes associated with de novo cholesterol synthesis (Figure 7, Supplementary Figure S7). In BMM, IFN-α was associated with the downregulation of genes involved in mevalonate synthesis (*HMGCS1*, *HMGCR*), lanosterol synthesis (*FDFT1*, *SQLE*, and *LSS*) and cholesterol synthesis (*CYP51*, *MSMO1*, *HSD17B7*, and *SC5D*). It was also associated with the downregulation of genes associated with cholesterol ester formation and the upregulation of carboxyl ester lipase (*CEL*), cholesterol 25-hydroxylase (*CH25H*), and sterol 27-hydroxylase (*CYP27A1*). In MDM, IFN-α stimulation was associated with decreased levels of *SQLE* and sterol O-acyltransferase 1 (*SOAT1*) and increased levels of *CH25H*. SQLE catalyzes the first oxygenation step in sterol biosynthesis and is thought to be a rate-limiting enzyme of this process [54].

At the level of phospholipid and sphingolipid metabolism, IFN-α-treated BMM upregulated phospholipid phosphatase 2 (*PLPP2*) and neutral ceramidase (*ASAH2*) and downregulated sphingolipid kinases (*SPHK2*, *CERK*) suggesting a shift away from phosphorylated sphingolipids to sphingosine in acute IFN responses (Figure 7, Supplementary Figure S7). Stimulation of BMM was also associated with the upregulation of 1-acylglycerol-3-phosphate O-acyltransferase 1 (*AGPAT1*) and phosphatidate

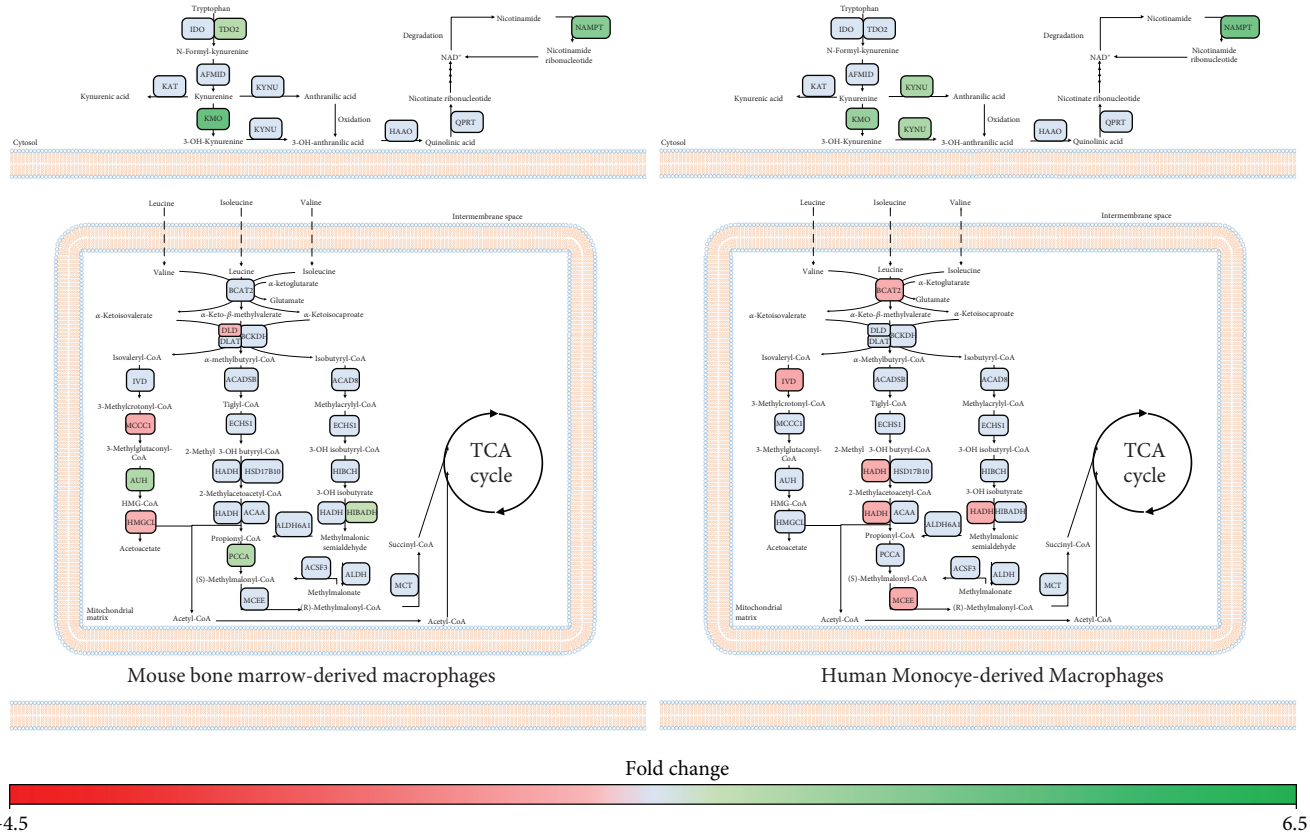

Figure 6: Tryptophan and branched-chain amino acid catabolism is altered in BMM and MDM following short-term IFN-α treatment. Metabolic genes altered in IFN-α-stimulated cells compared to controls ($-1.2 \leq FC \geq 1.2$, p value ≤ 0.05, FDR ≤ 0.1) were mapped to amino acid metabolism pathways using MetScape and DAVID. Green and red represent genes that have been significantly upregulated or downregulated, respectively. Blue represents genes that were not altered following IFN-α stimulation.

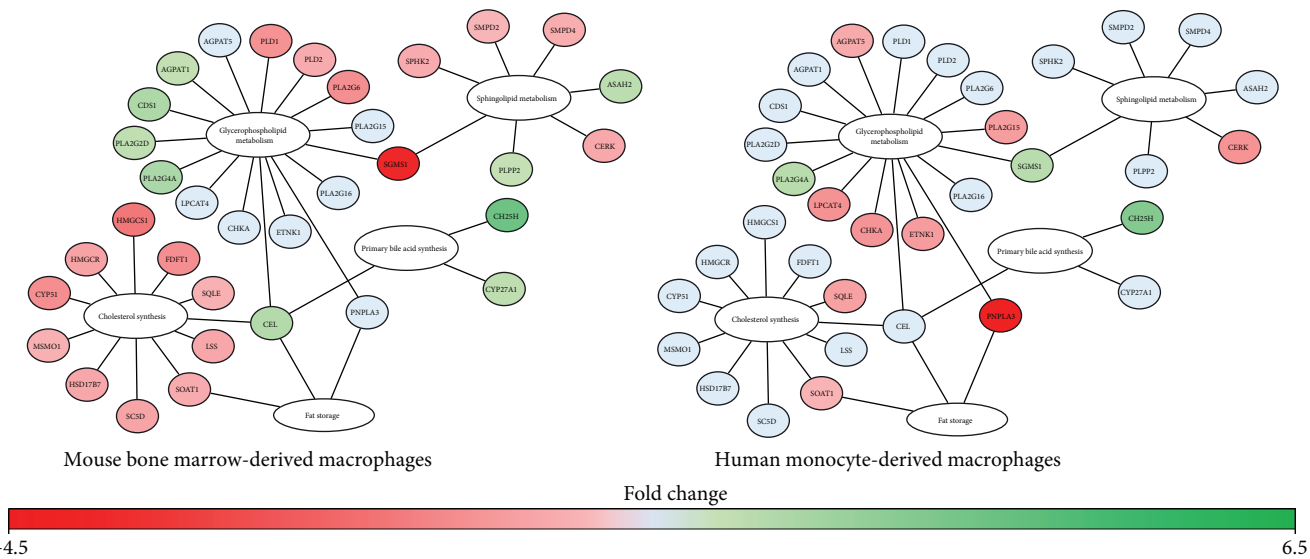

Figure 7: Expression of genes associated with lipid metabolism were differentially modulated in IFN-α-stimulated BMM compared MDM. Differentially expressed metabolic genes ($-1.2 \leq FC \geq 1.2$, p value ≤ 0.05, FDR ≤ 0.1) involved in cholesterol metabolism and phospholipid and sphingolipid synthesis were mapped using MetScape and DAVID. Green and red represent genes that have been significantly upregulated or downregulated, respectively. Blue represents genes that were not altered following IFN-α stimulation.

cytidylyltransferase 1 (*CDS1*), which may increase cytidine diphosphate- (CDP-) diacylglycerol production, a precursor for phosphatidylinositol, phosphatidylglycerol, and cardiolipin synthesis. Phosphatidylinositol is a minor component on the cytosolic side of cell membranes, and cardiolipin is an important component of the inner mitochondrial membrane [55]. Consistent with these findings, IFN-α stimulation was associated with the upregulation of three different phospholipase A2 (*PLA2G2D*, *PLA2G4A*, and *PLA2G16*) genes and the downregulation of two phospholipase D (*PLD1*, *PLD2*) genes. These genes cleave phosphatidylcholine and phosphatidylethanolamine, which represent the major phospholipids in mammalian membranes. The relative ratio of these lipids to one another within the cell membrane has significant implications on membrane integrity [55]. In MDM, *PLA2G4A* and sphingomyelin synthase 1 (*SGMS1*) were upregulated and lysophospholipid acyltransferase (*LPCAT4*) and *PLA2G15* were downregulated following IFN-α stimulation (Figure 7, Supplementary Figure S7). IFN-α stimulation was also associated with the downregulation of *AGPAT5*, choline kinase alpha (*CHKA*), and ethanolamine kinase 1 (*ETNK1*), which play an important role in the synthesis of phosphatidylglycerol, phosphatidylcholine, and phosphatidylethanolamine. Collectively, these alterations suggest IFN-α responses may alter the composition of the plasma and mitochondrial membranes of BMM and MDM as part of early type I IFN responses.

Finally, at the level of fatty acid synthesis, IFN-α stimulation of BMM was also associated with the downregulation of FA synthase (*FAS*) and FA desaturase 1 (*FADS1*) as well as the upregulation of carnitine palmitoyltransferase 1A (*CPT1A*). Alternatively, in MDM, IFN-α was associated with the upregulation of long-chain fatty acid- (LCFA-) producing aldehyde dehydrogenase 3b1 (*ALDH3B1*) and three acyl-CoA synthetase long-chain genes (*ACSL1*, *ACSL5*, and *ACSL6*) and the downregulation of carbonyl reductase 4 (*CBR4*), acetyl-CoA carboxylase-α (*ACACA*), mitochondrial 3-oxoacyl-ACP synthase (*OXSM*), trimethyllysine hydrolase ε (*TMLHE*), and hydroxyacyl-CoA dehydrogenase (*HADH*). Differences in fatty acid metabolism may indicate differential dependencies of BMM and MDM on β-oxidation for energy production.

4. Discussion

In the current study, we used publicly available transcriptional profiling datasets to develop metabolic gene signatures associated with short-term IFN-α stimulation in mouse and human macrophage models. Enrichment analysis, pathway mapping, and network construction identified alterations in central metabolic pathways in early IFN-α responses including glycolysis, oxidative phosphorylation, redox regulation, nucleotide metabolism, amino acid catabolism, and lipid metabolism. BMM had increased expression of genes associated with aerobic glycolysis, nitric oxide production, branched-chain amino acid metabolism, and fatty acid β-oxidation as well as decreased expression of genes associated with cholesterol biosynthesis. MDM had increased expression of genes associated with increased OXPHOS activity and antioxidant production and decreased expression of genes associated with branched-chain amino acid catabolism and fatty acid β-oxidation. While the current study only examines alterations in gene expression, these findings suggest that metabolic rewiring, at the level of transcription, is a key feature of early IFN-α responses. Future studies are required to validate the identified gene signatures and to validate the biological relevance of these alterations during early antiviral immune responses.

A number of studies have reported increased aerobic glycolysis and reduced oxidative phosphorylation in macrophages following activation with inflammatory stimuli [56–59]. Consistent with the literature, short-term IFN-α stimulation of BMM was associated with increased expression of genes associated with glycolysis (*HK2*, *HK3*, *PGM2*, *PFKP*, *PFKFB3*, and *INSR*) and lactate production (*LDHD*) and decreased expression of genes associated with pyruvate production (*PDK3*, *PDP1*, and *DLD*) and flux through the TCA cycle (*DLD*, *DLST*, and *SDHA*). In addition to meeting bioenergetic requirements of the cells, these alterations may increase intracellular levels of bioactive metabolites such as D-lactate, α-ketoglutarate, and succinate. Lactate accumulation in the microenvironment has been shown to suppress cytokine production and migration of human cytotoxic T cells [60, 61]. Similarly, α-ketoglutarate has been shown to quell inflammatory processes by suppressing NF-κB-mediated inflammatory pathways [62]. Succinate can also modulate inflammatory cytokine production. A recent study found that succinate stabilizes HIF-1α expression in LPS-activated macrophages [14], which facilitates HIF-1α transport into the nucleus where it induces the expression of glycolytic targets such as *LDHA*, *HK2*, and *PKM2*, as well as inflammatory genes such as *IL1B* [63, 64]. Inhibition or decreased expression of succinate dehydrogenase (SDH) has been shown to promote IL-10 expression and to repurpose the mitochondria for ROS production [19]. While functional studies are required to validate these profiles, our findings suggest bioenergetic reprogramming of BMM may represent a feedforward mechanism that may contribute to the immunomodulatory properties of type I IFNs during early antiviral immune responses.

Unlike BMM, short-term IFN-α stimulation of MDM was associated with the upregulation of a range of genes associated with the electron transport chain, which may favour OXPHOS for energy production. While OXPHOS provides more ATP per glucose molecule compared to aerobic glycolysis, energy and metabolic precursor production occurs more slowly. Further, IFN-α stimulation of MDM was associated with the downregulation of genes associated with the Leloir pathway (*GALK2*, *GALT*, and *GALE*), which is responsible for the conversion of galactose to glucose. Recent studies have shown that T cells, but not B cells, can be activated and proliferate in the presence of galactose when glucose is absent [65, 66]. However, unlike activation in glucose-rich environments, T cells in galactose are forced to rely on OXPHOS for energy production, which occurs at significantly slower rates [65]. This reliance on galactose also results in suboptimal IFN-γ and IL-2 production suggesting

galactose should only be used when no other energy substrate is available [65]. Thus, decreased expression of genes associated with the Leloir pathway in MDM may represent a means by which cells can improve the efficiency of energy production while maintaining functional immune responses.

Transcriptional profiling also identified redox regulation as a key feature of early IFN-α responses in mouse and human primary macrophage models. In BMM, IFN-α reprogramming was associated with increased expression of genes associated with nitric oxide (NO) production (*ASS1*, *NOS1*, and *NAGS*) and decreased antioxidants (*SOD2*, *GCLC*, *TXNRD1*, and *TXNRD3*). NO is a potent antimicrobial molecule that has been shown to modulate cellular metabolism [67–70] and immune function [71]. *ASS1* and *ASL* are part of the aspartate-argininosuccinate shunt, which recycles citrulline to resynthesize arginine for prolonged NO production [72, 73]. In M1 macrophages, increased expression of ASS1 and the subsequent increased flux through this shunt has been shown to replenish TCA cycle intermediates following decreased *IDH* and *SDH* gene expression [72]. Unlike BMM, IFN-α-stimulated MDM had increased expression of genes associated with OXPHOS and ROS production. ROS are also potent antimicrobial molecules, capable of killing intracellular pathogens [74]. The matched upregulation of antioxidant genes (e.g., glutathione, glutaredoxin, and thioredoxin) in conjunction with ROS likely reflects a protective mechanism to limit any associated cellular damage. Interestingly, a recent study found that the reducing nature of glutathione can prime T cell inflammatory responses by promoting mTOR-activated metabolic reprogramming [75]. It is currently unclear if similar priming occurs in macrophages. Collectively, our data suggest mouse BMM and human MDM may adopt differential metabolic strategies to mount intracellular antimicrobial responses during acute IFN responses.

Pathway mapping and network reconstruction identified IFN-α-associated alterations in nucleotide metabolism. In both BMM and MDM, IFN-α stimulation was associated with a downregulation of genes associated with de novo pyrimidine biosynthesis. A number of viruses including human cytomegalovirus and herpes simplex viruses require de novo pyrimidine synthesis for propagation and survival [76, 77]. Furthermore, inhibitors of de novo pyrimidine biosynthesis have broad antiviral effects against RNA, DNA, and retroviruses such as influenza A, hepatitis C, human adenovirus, and human immunodeficiency virus (HIV) [78, 79]. In MDM, IFN-α stimulation was also associated with increased expression of genes associated with purine and pyrimidine degradation pathways and nucleotide salvaging. The induction of nucleotide degradation pathways may act as a counterstrategy against viral-driven nucleotide biosynthesis [80]. Moreover, the activation of nucleotide salvaging pathways may allow the cell to recycle degraded bases and nucleosides and produce nucleotides to maintain cellular function. Interestingly, IFN-α responses were also associated with alterations in genes that regulate cGMP/GMP and cAMP/AMP ratios. Cyclic nucleotide second messengers, including cAMP and cGMP, are potent secondary messengers that contribute to the regulation of a variety of cellular processes including metabolism [81]. cAMP has been shown to suppress innate immune function including inflammatory cytokine production, cell adhesion, phagocytosis, and intracellular killing [82, 83]. Additionally, the cAMP axis plays an important role in antimicrobial defense as many microbes have evolved virulence-enhancing strategies that exploit this pathway [84–86]. In BMM, LPS responses are associated with low levels of cAMP and cGMP accumulation, which inhibit inflammatory cytokine production [87, 88]. Thus, alterations in the cAMP/AMP and cGMP/GMP ratio may play an important role in regulating inflammatory, antimicrobial, and metabolism responses in acute type I IFN responses.

Alterations in genes associated with tryptophan and branched-chain amino acid catabolism were pronounced in early IFN responses. Consistent with previous studies [50, 89, 90], IFN-α stimulation was associated with increased levels of genes associated with tryptophan catabolism. While we did not observe alterations in *IDO1* expression, *TDO2*, *KMO*, and *KYNU* were increased in both BMM and MDM. Many studies have shown that tryptophan catabolism (via IDO activation) represents a potent antiviral immune response [90–92]. Our study suggests downstream enzymes of the kynurenine pathway may also contribute to this phenotype. Interestingly, we also found that *NAMPT* was upregulated following acute IFN-α stimulation, suggesting tryptophan may be directed towards NAD^+ salvaging. NAMPT plays an important role in regulating glycolytic flux, phagocytic activity, and TNF-α production in LPS-stimulated macrophages and may also contribute to IFN responses [93, 94]. At the level of branched-chain amino acid metabolism, BMM had increased expression of genes associated with branched-chain amino acid catabolism. Conversely, MDM downregulated genes associated with this pathway. Catabolic products of branched-chain amino acid metabolism feed into the TCA cycle contributing to the production of succinyl-CoA and acetyl-CoA [95]. Previous studies have shown that branched-chain amino acid availability is critical for lymphocyte proliferation and M1 macrophage activation, but little is known regarding the role of these amino acids in regulating immune responses [96, 97]. Thus, upregulation of branched-chain amino acid catabolism in BMM may compensate for the loss of OXPHOS activity, which is not required in MDM.

Lipid metabolism has been shown to play an important role in antiviral responses in BMM and MDM [23, 24, 53]. Consistent with the literature, altered gene expression in BMM and MDM suggest these cells may downregulate de novo cholesterol synthesis and shunt available free cholesterol towards the production of oxysterols including 25-hydroxycholesterol and 27-hydroxycholesterol. The role of cholesterol flux in antiviral responses has been described previously [21–23]. Increased cholesterol levels help facilitate the entry of the dengue virus during the early phases of infection, which is reduced by the presence of oxysterols such as 25-hydroxycholesterol [22, 98–100]. Macrophages can also counteract this demand by switching away from de novo synthesis towards lipid import [23]. Limiting flux through the

cholesterol biosynthetic pathway induces a STING-mediated type I IFN response, which can be attenuated by exogenous free cholesterol [21, 23]. We also observed significant alterations in genes associated with phospholipid, sphingolipid, and FA metabolism. Lipid membrane composition can play a critical role in the antiviral capabilities of immune cells. Sphingolipids and phosphatidylserine have been shown to function as receptors for polyomavirus, HIV, and vesicular stomatitis virus (VSV) [101–103]. Altering the lipid composition of the plasma membrane is a vital protective strategy against viral entry by altering the potential interaction sites for viruses [104, 105]. Thus, altering the membrane lipid composition may be a critical feature of metabolic reprogramming in early antiviral responses.

Collectively, our study provides critical new insights into the molecular underpinnings of metabolic reprogramming associated with short-term IFN-α responses in mouse BMM and human MDM. This is the first study to systematically characterize changes in metabolic gene expression using transcriptional profiling in this context. However, we acknowledge certain limitations of this study. The current study only evaluates gene expression profiles via microarray. Validation and functional testing is required to understand the biological relevance of these findings. While both BMM and MDM were stimulated with short-term IFN-α, we cannot exclude the possibility that some of the reported differences may reflect the length of time in stimulant (2.5 h versus 4 h). Preliminary studies from our laboratory suggest metabolic profiles in stimulated BMM are similar within a 2–6-hour window. However, future time-course studies are required to examine how metabolic signatures change in BMM and MDM over short- and long-term IFN-α stimulation. Culture conditions and differentiation protocols may also affect metabolic profiles in BMM versus MDM. This limitation should be an important consideration across all studies examining relationships between immune and metabolic processes in vitro, whether in humans or in mice. Careful consideration of the model system may be required depending on downstream applications of the findings. Meta-analyses of transcriptional datasets may represent a powerful tool to identify metabolic signatures that are consistently altered across different studies using different models, time points, culture conditions, and so on. To minimize these effects, only studies performed in high glucose DMEM (plus glutamine and sodium pyruvate) with 10% FBS were selected for analyses. Finally, both BMM and MDM were analyzed using Affymetrix technologies' microarray chips. However, we cannot exclude the possibility that the reported differences may be affected by the microarray used. Despite these limitations, we strongly believe this comparative study provides important new insights into metabolic processes that contribute to IFN responses in mouse and human macrophages. We believe that the power of an untargeted approach such as transcriptional profiling is to systematically characterize these differences, which may have important implications on effector function depending on the local microenvironment. In the future, more targeted studies are required to evaluate the effects of these gene expression profiles on protein expression and functional metabolic and immune responses.

5. Conclusions

In summary, this study identified a variety of metabolic pathways altered following short-term IFN-α stimulation in mouse and human macrophage systems. This may have important implications for the initiation of early antiviral immune responses, including the induction of the specific antimicrobial and immunomodulatory functions of IFN-α. While functional studies are required to clearly elucidate the relationships between this metabolic reprogramming and effector function, it is clear that transcriptional regulation of metabolic processes is a key feature of early type I IFN responses. An in-depth understanding of this early reprogramming may lead to the development of targeted therapeutics that regulate and fine tune specific type I IFN effector function.

Data Availability

Gene expression data used in this study have been previously published in the GEO database under the accession numbers GSE16755 (https://www.ncbi.nlm.nih.gov/geo/query/acc.cgi?acc=GSE16755) and GSE35825 (https://www.ncbi.nlm.nih.gov/geo/query/acc.cgi?acc=GSE35825).

Conflicts of Interest

The authors declare that the research was conducted with no conflicts of interest.

Acknowledgments

Funding was provided by a research development grant provided by the Carleton University Research Office.

Supplementary Materials

Supplementary Table S1. A list of all metabolic genes identified in the BMM dataset.

Supplementary Table S2. A list of all metabolic genes identified in the MDM dataset.

Supplementary Table S3. A list of significantly altered gene sets identified by GSEA in the BMM dataset.

Supplementary Table S4. A list of significantly altered gene sets identified by GSEA in the MDM dataset.

Supplementary Figure S1. Workflow of BMM and MDM differentiation and IFN-α stimulation. Mouse bone marrow cells and human monocytes were differentiated for 7 days into BMM and MDM, respectively. Cells were then stimulated with IFN-α for less than 4 hours. RNA was extracted from total cells and prepared for microarray analysis.

Supplementary Figure S2. IFN-α is associated with differential enrichment of metabolic pathways in mouse BMM compared to human MDM. Metabolite set enrichment analysis (MSEA) was performed in MetaboAnalyst using metabolic gene datasets. Pathways shown were significantly enriched ($P < 0.05$) in either IFN-stimulated BMM, MDM, or both. Yellow and blue represent enrichment scores in BMM and MDM, respectively (error bars = sem; $n = 3$).

Supplementary Figure S3. IFN-α responses are associated with altered bioenergetic profiles in mouse and human macrophages. The bar plots show significantly altered genes associated with bioenergetics pathways (FC > 1.2, $p < 0.05$, FDR < 0.10). Light blue and dark blue represent expression levels in unstimulated (control) and IFN-α-treated macrophages, respectively (error bars = sem; $n = 3$).

Supplementary Figure S4. BMM and MDM express redox-related genes following short-term IFN-α stimulation. The bar plots show significantly altered genes associated with cellular redox pathways (FC > 1.2, $p < 0.05$, FDR < 0.10). Light blue and dark blue represent expression levels in unstimulated (control) and IFN-α-treated macrophages, respectively (error bars = sem; $n = 3$).

Supplementary Figure S5. IFN-α is associated with altered expression of genes that regulate nucleotide metabolism and cAMP/cGMP ratios. The bar plots show significantly altered genes associated with nucleotide metabolism (FC > 1.2, $p < 0.05$, FDR < 0.10). Light blue and dark blue represent expression levels in unstimulated (control) and IFN-α-treated macrophages, respectively (error bars = sem; $n = 3$).

Supplementary Figure S6. Short-term IFN-α stimulation is associated with alterations in tryptophan and branched chain amino acid catabolism. The bar plots show significantly altered genes associated with tryptophan and branched chain amino acid metabolism (FC > 1.2, $p < 0.05$, FDR < 0.10). Light blue and dark blue represent expression levels in unstimulated (control) and IFN-α-treated macrophages, respectively (error bars = sem; $n = 3$).

Supplementary Figure S7. Altered expression of genes associated with lipid metabolism is a key feature of IFN-α responses. The bar plots show significantly altered genes associated with lipid metabolism (FC > 1.2, $p < 0.05$, FDR < 0.10). Light blue and dark blue represent expression levels in unstimulated (control) and IFN-α-treated macrophages, respectively (error bars = sem; $n = 3$).

References

[1] A. Isaacs and J. Lindenmann, "Virus interference. I. The interferon," *Proceedings of the Royal Society of London - Series B: Biological Sciences*, vol. 147, no. 927, pp. 258–267, 1957.

[2] A. Isaacs, J. Lindenmann, and R. C. Valentine, "Virus interference. II. Some properties of interferon," *Proceedings of the Royal Society of London - Series B: Biological Sciences*, vol. 147, no. 927, pp. 268–273, 1957.

[3] S. Pestka, C. D. Krause, and M. R. Walter, "Interferons, interferon-like cytokines, and their receptors," *Immunological Reviews*, vol. 202, no. 1, pp. 8–32, 2004.

[4] G. Trinchieri, "Type I interferon: friend or foe?," *The Journal of Experimental Medicine*, vol. 207, no. 10, pp. 2053–2063, 2010.

[5] C. E. Samuel, "Antiviral actions of interferons," *Clinical Microbiology Reviews*, vol. 14, no. 4, pp. 778–809, 2001.

[6] G. R. Stark, I. M. Kerr, B. R. G. Williams, R. H. Silverman, and R. D. Schreiber, "How cells respond to interferons," *Annual Review of Biochemistry*, vol. 67, no. 1, pp. 227–264, 1998.

[7] L. C. Platanias, "Mechanisms of type-I- and type-II-interferon-mediated signalling," *Nature Reviews Immunology*, vol. 5, no. 5, pp. 375–386, 2005.

[8] L. B. Ivashkiv and L. T. Donlin, "Regulation of type I interferon responses," *Nature Reviews Immunology*, vol. 14, no. 1, pp. 36–49, 2014.

[9] K. I. Arimoto, S. Lochte, S. A. Stoner et al., "STAT2 is an essential adaptor in USP18-mediated suppression of type I interferon signaling," *Nature Structural & Molecular Biology*, vol. 24, no. 3, pp. 279–289, 2017.

[10] W. M. Schneider, M. D. Chevillotte, and C. M. Rice, "Interferon-stimulated genes: a complex web of host defenses," *Annual Review of Immunology*, vol. 32, no. 1, pp. 513–545, 2014.

[11] J. W. Schoggins and C. M. Rice, "Interferon-stimulated genes and their antiviral effector functions," *Current Opinion in Virology*, vol. 1, no. 6, pp. 519–525, 2011.

[12] M. E. Bianchi, "DAMPs, PAMPs and alarmins: all we need to know about danger," *Journal of Leukocyte Biology*, vol. 81, no. 1, pp. 1–5, 2007.

[13] A. Iannello, O. Debbeche, E. Martin, L. H. Attalah, S. Samarani, and A. Ahmad, "Viral strategies for evading antiviral cellular immune responses of the host," *Journal of Leukocyte Biology*, vol. 79, no. 1, pp. 16–35, 2006.

[14] G. M. Tannahill, A. M. Curtis, J. Adamik et al., "Succinate is an inflammatory signal that induces IL-1β through HIF-1α," *Nature*, vol. 496, no. 7444, pp. 238–242, 2013.

[15] A. Errea, D. Cayet, P. Marchetti et al., "Lactate inhibits the pro-inflammatory response and metabolic reprogramming in murine macrophages in a GPR81-independent manner," *PLoS One*, vol. 11, no. 11, article e0163694, 2016.

[16] V. Infantino, V. Iacobazzi, F. Palmieri, and A. Menga, "ATP-citrate lyase is essential for macrophage inflammatory response," *Biochemical and Biophysical Research Communications*, vol. 440, no. 1, pp. 105–111, 2013.

[17] P. Kesarwani, A. K. Murali, A. A. Al-Khami, and S. Mehrotra, "Redox regulation of T-cell function: from molecular mechanisms to significance in human health and disease," *Antioxidants & Redox Signaling*, vol. 18, no. 12, pp. 1497–1534, 2013.

[18] H. Wang, H. Flach, M. Onizawa, L. Wei, M. T. McManus, and A. Weiss, "Negative regulation of *Hif1a* expression and T_H17 differentiation by the hypoxia-regulated microRNA miR-210," *Nature Immunology*, vol. 15, no. 4, pp. 393–401, 2014.

[19] E. L. Mills, B. Kelly, A. Logan et al., "Succinate dehydrogenase supports metabolic repurposing of mitochondria to drive inflammatory macrophages," *Cell*, vol. 167, no. 2, pp. 457–470.e13, 2016.

[20] H. Jiang, H. Shi, M. Sun et al., "PFKFB3-driven macrophage glycolytic metabolism is a crucial component of innate antiviral defense," *Journal of Immunology*, vol. 197, no. 7, pp. 2880–2890, 2016.

[21] M. Blanc, W. Y. Hsieh, K. A. Robertson et al., "Host defense against viral infection involves interferon mediated down-regulation of sterol biosynthesis," *PLoS Biology*, vol. 9, no. 3, article e1000598, 2011.

[22] M. Blanc, W. Y. Hsieh, K. A. Robertson et al., "The transcription factor STAT-1 couples macrophage synthesis of 25-hydroxycholesterol to the interferon antiviral response," *Immunity*, vol. 38, no. 1, pp. 106–118, 2013.

[23] A. G. York, K. J. Williams, J. P. Argus et al., "Limiting cholesterol biosynthetic flux spontaneously engages type I IFN signaling," *Cell*, vol. 163, no. 7, pp. 1716–1729, 2015.

[24] M. C. S. Boshuizen, M. A. Hoeksema, A. E. Neele et al., "Interferon-β promotes macrophage foam cell formation by altering both cholesterol influx and efflux mechanisms," *Cytokine*, vol. 77, pp. 220–226, 2016.

[25] B. Maneglier, C. Rogez-Kreuz, O. Spreux-Varoquaux et al., "Comparative effects of two type I interferons, human IFN-α and ovine IFN-τ on indoleamine-2,3-dioxygenase in primary cultures of human macrophages," *Fundamental & Clinical Pharmacology*, vol. 21, no. 1, pp. 29–34, 2007.

[26] B. Acosta-Iborra, A. Elorza, I. M. Olazabal et al., "Macrophage oxygen sensing modulates antigen presentation and phagocytic functions involving IFN-γ production through the HIF-1α transcription factor," *Journal of Immunology*, vol. 182, no. 5, pp. 3155–3164, 2009.

[27] C. Peyssonnaux, V. Datta, T. Cramer et al., "HIF-1α expression regulates the bactericidal capacity of phagocytes," *The Journal of Clinical Investigation*, vol. 115, no. 7, pp. 1806–1815, 2005.

[28] C. Nagy and A. Haschemi, "Time and demand are two critical dimensions of immunometabolism: the process of macrophage activation and the pentose phosphate pathway," *Frontiers in Immunology*, vol. 6, p. 164, 2015.

[29] B. Kelly and L. A. J. O'Neill, "Metabolic reprogramming in macrophages and dendritic cells in innate immunity," *Cell Research*, vol. 25, no. 7, pp. 771–784, 2015.

[30] L. A. J. O'Neill and E. J. Pearce, "Immunometabolism governs dendritic cell and macrophage function," *The Journal of Experimental Medicine*, vol. 213, no. 1, pp. 15–23, 2016.

[31] T. Barrett, S. E. Wilhite, P. Ledoux et al., "NCBI GEO: archive for functional genomics data sets—update," *Nucleic Acids Research*, vol. 41, no. D1, pp. D991–D995, 2013.

[32] S.-Y. Liu, D. J. Sanchez, R. Aliyari, S. Lu, and G. Cheng, "Systematic identification of type I and type II interferon-induced antiviral factors," *Proceedings of the National Academy of Sciences of the United States of America*, vol. 109, no. 11, pp. 4239–4244, 2012.

[33] T. Greenwell-Wild, N. Vázquez, W. Jin, Z. Rangel, P. J. Munson, and S. M. Wahl, "Interleukin-27 inhibition of HIV-1 involves an intermediate induction of type I interferon," *Blood*, vol. 114, no. 9, pp. 1864–1874, 2009.

[34] C. Li and W. H. Wong, "Model-based analysis of oligonucleotide arrays: expression index computation and outlier detection," *Proceedings of the National Academy of Sciences of the United States of America*, vol. 98, no. 1, pp. 31–36, 2001.

[35] J. Gao, V. G. Tarcea, A. Karnovsky et al., "Metscape: a Cytoscape plug-in for visualizing and interpreting metabolomic data in the context of human metabolic networks," *Bioinformatics*, vol. 26, no. 7, pp. 971–973, 2010.

[36] A. Karnovsky, T. Weymouth, T. Hull et al., "Metscape 2 bioinformatics tool for the analysis and visualization of metabolomics and gene expression data," *Bioinformatics*, vol. 28, no. 3, pp. 373–380, 2012.

[37] M. S. Cline, M. Smoot, E. Cerami et al., "Integration of biological networks and gene expression data using Cytoscape," *Nature Protocols*, vol. 2, no. 10, pp. 2366–2382, 2007.

[38] J. Xia, I. V. Sinelnikov, B. Han, and D. S. Wishart, "MetaboAnalyst 3.0—making metabolomics more meaningful," *Nucleic Acids Research*, vol. 43, no. W1, pp. W251–W257, 2015.

[39] A. Subramanian, P. Tamayo, V. K. Mootha et al., "Gene set enrichment analysis: a knowledge-based approach for interpreting genome-wide expression profiles," *Proceedings of the National Academy of Sciences of the United States of America*, vol. 102, no. 43, pp. 15545–15550, 2005.

[40] D. W. Huang, B. T. Sherman, X. Zheng et al., "Extracting biological meaning from large gene lists with DAVID," *Current Protocols in Bioinformatics*, vol. 27, no. 1, pp. 1–13, 2009.

[41] D. W. Huang, B. T. Sherman, and R. A. Lempicki, "Systematic and integrative analysis of large gene lists using DAVID bioinformatics resources," *Nature Protocols*, vol. 4, no. 1, pp. 44–57, 2009.

[42] B. Lu, T. Nakamura, K. Inouye et al., "Novel role of PKR in inflammasome activation and HMGB1 release," *Nature*, vol. 488, no. 7413, pp. 670–674, 2012.

[43] A. Garten, S. Petzold, A. Körner, S.-i. Imai, and W. Kiess, "Nampt: linking NAD biology, metabolism and cancer," *Trends in Endocrinology & Metabolism*, vol. 20, no. 3, pp. 130–138, 2009.

[44] J. W. Schoggins, S. J. Wilson, M. Panis et al., "A diverse range of gene products are effectors of the type I interferon antiviral response," *Nature*, vol. 472, no. 7344, pp. 481–485, 2011.

[45] D. C. Liemburg-Apers, P. H. G. M. Willems, W. J. H. Koopman, and S. Grefte, "Interactions between mitochondrial reactive oxygen species and cellular glucose metabolism," *Archives of Toxicology*, vol. 89, no. 8, pp. 1209–1226, 2015.

[46] C. Quijano, M. Trujillo, L. Castro, and A. Trostchansky, "Interplay between oxidant species and energy metabolism," *Redox Biology*, vol. 8, pp. 28–42, 2016.

[47] S. W. Kang, S. Lee, and E. K. Lee, "ROS and energy metabolism in cancer cells: alliance for fast growth," *Archives of Pharmacal Research*, vol. 38, no. 3, pp. 338–345, 2015.

[48] J. Hwang, H.-W. Suh, Y. H. Jeon et al., "The structural basis for the negative regulation of thioredoxin by thioredoxin-interacting protein," *Nature Communications*, vol. 5, no. 1, p. 2958, 2014.

[49] R. Watanabe, H. Nakamura, H. Masutani, and J. Yodoi, "Anti-oxidative, anti-cancer and anti-inflammatory actions by thioredoxin 1 and thioredoxin-binding protein-2," *Pharmacology & Therapeutics*, vol. 127, no. 3, pp. 261–270, 2010.

[50] A. L. Mellor and D. H. Munn, "Tryptophan catabolism and T-cell tolerance: immunosuppression by starvation?," *Immunology Today*, vol. 20, no. 10, pp. 469–473, 1999.

[51] A. Boasso, A. W. Hardy, S. A. Anderson, M. J. Dolan, and G. M. Shearer, "HIV-induced type I interferon and tryptophan catabolism drive T cell dysfunction despite phenotypic activation," *PLoS One*, vol. 3, no. 8, article e2961, 2008.

[52] J. Nakagawa, H. Waldner, S. Meyer-Monard, J. Hofsteenge, P. Jenö, and C. Moroni, "AUH, a gene encoding an AU-specific RNA binding protein with intrinsic enoyl-CoA hydratase activity," *Proceedings of the National Academy of Sciences of the United States of America*, vol. 92, no. 6, pp. 2051–2055, 1995.

[53] F. Coulombe, J. Jaworska, M. Verway et al., "Targeted prostaglandin E_2 inhibition enhances antiviral immunity through induction of type I interferon and apoptosis in macrophages," *Immunity*, vol. 40, no. 4, pp. 554–568, 2014.

[54] A. Chugh, A. Ray, and J. B. Gupta, "Squalene epoxidase as hypocholesterolemic drug target revisited," *Progress in Lipid Research*, vol. 42, no. 1, pp. 37–50, 2003.

[55] G. van Meer, D. R. Voelker, and G. W. Feigenson, "Membrane lipids: where they are and how they behave," *Nature Reviews. Molecular Cell Biology*, vol. 9, no. 2, pp. 112–124, 2008.

[56] J. C. Rodríguez-Prados, P. G. Través, J. Cuenca et al., "Substrate fate in activated macrophages: a comparison between innate, classic, and alternative activation," *Journal of Immunology*, vol. 185, no. 1, pp. 605–614, 2010.

[57] A. Vazquez, J. Liu, Y. Zhou, and Z. N. Oltvai, "Catabolic efficiency of aerobic glycolysis: the Warburg effect revisited," *BMC Systems Biology*, vol. 4, no. 1, pp. 58-59, 2010.

[58] H. Z. Imtiyaz and M. C. Simon, "Hypoxia-inducible factors as essential regulators of inflammation," *Current Topics in Microbiology and Immunology*, vol. 345, pp. 105–120, 2010.

[59] V. Infantino, P. Convertini, L. Cucci et al., "The mitochondrial citrate carrier: a new player in inflammation," *The Biochemical Journal*, vol. 438, no. 3, pp. 433–436, 2011.

[60] K. Fischer, P. Hoffmann, S. Voelkl et al., "Inhibitory effect of tumor cell–derived lactic acid on human T cells," *Blood*, vol. 109, no. 9, pp. 3812–3819, 2007.

[61] R. Haas, J. Smith, V. Rocher-Ros et al., "Lactate regulates metabolic and pro-inflammatory circuits in control of T cell migration and effector functions," *PLoS Biology*, vol. 13, no. 7, article e1002202, 2015.

[62] L. He, H. Li, N. Huang et al., "Alpha-ketoglutarate suppresses the NF-κB-mediated inflammatory pathway and enhances the PXR-regulated detoxification pathway," *Oncotarget*, vol. 8, no. 61, pp. 102974–102988, 2017.

[63] W. Luo, H. Hu, R. Chang et al., "Pyruvate kinase M2 is a PHD3-stimulated coactivator for hypoxia-inducible factor 1," *Cell*, vol. 145, no. 5, pp. 732–744, 2011.

[64] W. Luo and G. L. Semenza, "Pyruvate kinase M2 regulates glucose metabolism by functioning as a coactivator for hypoxia-inducible factor 1 in cancer cells," *Oncotarget*, vol. 2, no. 7, pp. 551–556, 2011.

[65] C.-H. Chang, J. D. Curtis, L. B. Maggi Jr. et al., "Posttranscriptional control of T cell effector function by aerobic glycolysis," *Cell*, vol. 153, no. 6, pp. 1239–1251, 2013.

[66] S. Milasta, C. P. Dillon, O. E. Sturm et al., "Apoptosis-inducing-factor-dependent mitochondrial function is required for T cell but not B cell function," *Immunity*, vol. 44, no. 1, pp. 88–102, 2016.

[67] J. C. Drapier and J. B. Hibbs, "Differentiation of murine macrophages to express nonspecific cytotoxicity for tumor cells results in L-arginine-dependent inhibition of mitochondrial iron-sulfur enzymes in the macrophage effector cells," *Journal of Immunology*, vol. 140, pp. 2829–2838, 1988.

[68] E. Clementi, G. C. Brown, M. Feelisch, and S. Moncada, "Persistent inhibition of cell respiration by nitric oxide: crucial role of *S*-nitrosylation of mitochondrial complex I and protective action of glutathione," *Proceedings of the National Academy of Sciences of the United States of America*, vol. 95, no. 13, pp. 7631–7636, 1998.

[69] M. W. J. Cleeter, J. M. Cooper, V. M. Darley-Usmar, S. Moncada, and A. H. V. Schapira, "Reversible inhibition of cytochrome c oxidase, the terminal enzyme of the mitochondrial respiratory chain, by nitric oxide. Implications for neurodegenerative diseases," *FEBS Letters*, vol. 345, no. 1, pp. 50–54, 1994.

[70] P.-T. Doulias, M. Tenopoulou, J. L. Greene, K. Raju, and H. Ischiropoulos, "Nitric oxide regulates mitochondrial fatty acid metabolism through reversible protein *S*-nitrosylation," *Science Signaling*, vol. 6, no. 256, article rs1, 2013.

[71] S. Herbst, U. E. Schaible, and B. E. Schneider, "Interferon gamma activated macrophages kill mycobacteria by nitric oxide induced apoptosis," *PLoS One*, vol. 6, no. 5, article e19105, 2011.

[72] A. K. Jha, S. C.-C. Huang, A. Sergushichev et al., "Network integration of parallel metabolic and transcriptional data reveals metabolic modules that regulate macrophage polarization," *Immunity*, vol. 42, no. 3, pp. 419–430, 2015.

[73] K. C. El Kasmi and K. R. Stenmark, "Contribution of metabolic reprogramming to macrophage plasticity and function," *Seminars in Immunology*, vol. 27, no. 4, pp. 267–275, 2015.

[74] A. P. West, I. E. Brodsky, C. Rahner et al., "TLR signalling augments macrophage bactericidal activity through mitochondrial ROS," *Nature*, vol. 472, no. 7344, pp. 476–480, 2011.

[75] T. W. Mak, M. Grusdat, G. S. Duncan et al., "Glutathione primes T cell metabolism for inflammation," *Immunity*, vol. 46, no. 4, pp. 675–689, 2017.

[76] S. R. DeVito, E. Ortiz-Riaño, L. Martínez-Sobrido, and J. Munger, "Cytomegalovirus-mediated activation of pyrimidine biosynthesis drives UDP–sugar synthesis to support viral protein glycosylation," *Proceedings of the National Academy of Sciences of the United States of America*, vol. 111, no. 50, pp. 18019–18024, 2014.

[77] L. Vastag, E. Koyuncu, S. L. Grady, T. E. Shenk, and J. D. Rabinowitz, "Divergent effects of human cytomegalovirus and herpes simplex virus-1 on cellular metabolism," *PLoS Pathogens*, vol. 7, no. 7, article e1002124, 2011.

[78] H.-H. Hoffmann, A. Kunz, V. A. Simon, P. Palese, and M. L. Shaw, "Broad-spectrum antiviral that interferes with de novo pyrimidine biosynthesis," *Proceedings of the National Academy of Sciences of the United States of America*, vol. 108, no. 14, pp. 5777–5782, 2011.

[79] M. Lucas-Hourani, D. Dauzonne, P. Jorda et al., "Inhibition of pyrimidine biosynthesis pathway suppresses viral growth through innate immunity," *PLoS Pathogens*, vol. 9, no. 10, article e1003678, 2013.

[80] C. Gavegnano, E. M. Kennedy, B. Kim, and R. F. Schinazi, "The impact of macrophage nucleotide pools on HIV-1 reverse transcription, viral replication, and the development of novel antiviral agents," *Molecular Biology International*, vol. 2012, Article ID 625983, 8 pages, 2012.

[81] K. Taskén, B. S. Sklhegg, T. Kristin Austlid et al., "16 Structure, function, and regulation of human cAMP-dependent protein kinases," *Advances in Second Messenger and Phosphoprotein Research*, vol. 31, pp. 191–204, 1997.

[82] C. H. Serezani, M. N. Ballinger, D. M. Aronoff, and M. Peters-Golden, "Cyclic AMP: master regulator of innate immune cell function," *American Journal of Respiratory Cell and Molecular Biology*, vol. 39, no. 2, pp. 127–132, 2008.

[83] S. L. C. Jin, L. Lan, M. Zoudilova, and M. Conti, "Specific role of phosphodiesterase 4B in lipopolysaccharide-induced signaling in mouse macrophages," *Journal of Immunology*, vol. 175, no. 3, pp. 1523–1531, 2005.

[84] L. Rickman, C. Scott, D. M. Hunt et al., "A member of the cAMP receptor protein family of transcription regulators in *Mycobacterium tuberculosis* is required for virulence in mice and controls transcription of the *rpfA* gene coding for a resuscitation promoting factor," *Molecular Microbiology*, vol. 56, no. 5, pp. 1274–1286, 2005.

[85] R. S. Smith, M. C. Wolfgang, and S. Lory, "An adenylate cyclase-controlled signaling network regulates *Pseudomonas aeruginosa* virulence in a mouse model of acute pneumonia," *Infection and Immunity*, vol. 72, no. 3, pp. 1677–1684, 2004.

[86] L. Zhan, Y. Han, L. Yang et al., "The cyclic AMP receptor protein, CRP, is required for both virulence and expression of the minimal CRP regulon in *Yersinia pestis* Biovar microtus," *Infection and Immunity*, vol. 76, no. 11, pp. 5028–5037, 2008.

[87] L. Connelly, A. T. Jacobs, M. Palacios-Callender, S. Moncada, and A. J. Hobbs, "Macrophage endothelial nitric-oxide synthase autoregulates cellular activation and pro-inflammatory protein expression," *The Journal of Biological Chemistry*, vol. 278, no. 29, pp. 26480–26487, 2003.

[88] S. Endres, H. J. Fülle, B. Sinha et al., "Cyclic nucleotides differentially regulate the synthesis of tumour necrosis factor-alpha and interleukin-1 beta by human mononuclear cells," *Immunology*, vol. 72, no. 1, pp. 56–60, 1991.

[89] O. Adams, K. Besken, C. Oberdörfer, C. R. MacKenzie, O. Takikawa, and W. Däubener, "Role of Indoleamine-2,3-dioxygenase in alpha/beta and gamma interferon-mediated antiviral effects against herpes simplex virus infections," *Journal of Virology*, vol. 78, no. 5, pp. 2632–2636, 2004.

[90] M. W. Taylor and G. S. Feng, "Relationship between interferon-gamma, indoleamine 2,3-dioxygenase, and tryptophan catabolism," *The FASEB Journal*, vol. 5, no. 11, pp. 2516–2522, 1991.

[91] A. L. Mellor and D. H. Munn, "IDO expression by dendritic cells: tolerance and tryptophan catabolism," *Nature Reviews. Immunology*, vol. 4, no. 10, pp. 762–774, 2004.

[92] K. Obojes, O. Andres, K. S. Kim, W. Däubener, and J. Schneider-Schaulies, "Indoleamine 2,3-dioxygenase mediates cell type-specific anti-measles virus activity of gamma interferon," *Journal of Virology*, vol. 79, no. 12, pp. 7768–7776, 2005.

[93] G. Venter, F. T. J. J. Oerlemans, M. Willemse, M. Wijers, J. A. M. Fransen, and B. Wieringa, "NAMPT-mediated salvage synthesis of NAD^+ controls morphofunctional changes of macrophages," *PLoS One*, vol. 9, no. 5, article e97378, 2014.

[94] A. J. Al-Shabany, A. J. Moody, A. D. Foey, and R. A. Billington, "Intracellular NAD^+ levels are associated with LPS-induced TNF-α release in pro-inflammatory macrophages," *Bioscience Reports*, vol. 36, no. 1, article e00301, 2016.

[95] A. E. Harper, R. H. Miller, and K. P. Block, "Branched-chain amino acid metabolism," *Annual Review of Nutrition*, vol. 4, no. 1, pp. 409–454, 1984.

[96] S. D. Skaper, D. P. Molden, and J. E. Seegmiller, "Maple syrup urine disease: branched-chain amino acid concentrations and metabolism in cultured human lymphoblasts," *Biochemical Genetics*, vol. 14, no. 7-8, pp. 527–539, 1976.

[97] J. Meiser, L. Krämer, S. C. Sapcariu et al., "Pro-inflammatory macrophages sustain pyruvate oxidation through pyruvate dehydrogenase for the synthesis of Itaconate and to enable cytokine expression," *The Journal of Biological Chemistry*, vol. 291, no. 8, pp. 3932–3946, 2016.

[98] R. Soto-Acosta, C. Mosso, M. Cervantes-Salazar et al., "The increase in cholesterol levels at early stages after dengue virus infection correlates with an augment in LDL particle uptake and HMG-CoA reductase activity," *Virology*, vol. 442, no. 2, pp. 132–147, 2013.

[99] K. Park and A. L. Scott, "Cholesterol 25-hydroxylase production by dendritic cells and macrophages is regulated by type I interferons," *Journal of Leukocyte Biology*, vol. 88, no. 6, pp. 1081–1087, 2010.

[100] S.-Y. Liu, R. Aliyari, K. Chikere et al., "Interferon-inducible cholesterol-25-hydroxylase broadly inhibits viral entry by production of 25-hydroxycholesterol," *Immunity*, vol. 38, no. 1, pp. 92–105, 2013.

[101] S. S. Rawat, M. Viard, S. A. Gallo, R. Blumenthal, and A. Puri, "Sphingolipids, cholesterol, and HIV-1: a paradigm in viral fusion," *Glycoconjugate Journal*, vol. 23, no. 3-4, pp. 189–197, 2006.

[102] A. E. Smith, H. Lilie, and A. Helenius, "Ganglioside-dependent cell attachment and endocytosis of murine polyomavirus-like particles," *FEBS Letters*, vol. 555, no. 2, pp. 199–203, 2003.

[103] H. Ewers, W. Romer, A. E. Smith et al., "GM1 structure determines SV40-induced membrane invagination and infection," *Nature Cell Biology*, vol. 12, no. 1, pp. 11–18, 2010.

[104] T. Merino-Ramos, Á. Vázquez-Calvo, J. Casas, F. Sobrino, J.-C. Saiz, and M. A. Martín-Acebes, "Modification of the host cell lipid metabolism induced by hypolipidemic drugs targeting the acetyl coenzyme a carboxylase impairs West Nile virus replication," *Antimicrobial Agents and Chemotherapy*, vol. 60, no. 1, pp. 307–315, 2015.

[105] J. Pezacki, S. M. Sagan, A. M. Tonary et al., "Transcriptional profiling of the effects of 25-hydroxycholesterol on human hepatocyte metabolism and the antiviral state it conveys against the hepatitis C virus," *BMC Chemical Biology*, vol. 9, no. 1, p. 2, 2009.

Hindawi
Mediators of Inflammation
Volume 2018, Article ID 8261432, 18 pages
https://doi.org/10.1155/2018/8261432

Review Article

Regulation of Metabolic Disease-Associated Inflammation by Nutrient Sensors

Alex S. Yamashita,[1] Thiago Belchior,[1] Fábio S. Lira,[2] Nicolette C. Bishop,[3] Barbara Wessner,[4] José C. Rosa,[5] and William T. Festuccia[1]

[1]*Department of Physiology and Biophysics, Institute of Biomedical Sciences, University of Sao Paulo, 05508000 Sao Paulo-SP, Brazil*
[2]*Exercise and Immunometabolism Research Group, Department of Physical Education, Universidade Estadual Paulista (UNESP), 19060-900 Presidente Prudente-SP, Brazil*
[3]*School of Sports, Exercise and Health Science, Loughborough University, Loughborough, UK*
[4]*Centre for Sport Science and University Sports, Vienna, Austria*
[5]*Department of Cell Biology and Development, Institute of Biomedical Sciences, University of Sao Paulo, 05508000 Sao Paulo-SP, Brazil*

Correspondence should be addressed to William T. Festuccia; william.festuccia@gmail.com

Received 28 March 2018; Revised 21 May 2018; Accepted 14 June 2018; Published 4 July 2018

Academic Editor: Tânia Silvia Fröde

Visceral obesity is frequently associated with the development of type 2 diabetes (T2D), a highly prevalent chronic disease that features insulin resistance and pancreatic β-cell dysfunction as important hallmarks. Recent evidence indicates that the chronic, low-grade inflammation commonly associated with visceral obesity plays a major role connecting the excessive visceral fat deposition with the development of insulin resistance and pancreatic β-cell dysfunction. Herein, we review the mechanisms by which nutrients modulate obesity-associated inflammation.

1. Introduction

Visceral obesity, the excessive accumulation of fat in the adipose depots located inside the peritoneal cavity, is a major risk factor for the development of several highly prevalent, chronic diseases, namely, type 2 diabetes (T2D), cardiovascular diseases, and some types of cancer, among others [1, 2]. The increased prevalence of visceral obesity in the last decades has dramatically raised the incidence of its associated diseases. It was estimated, for example, that approximately 415 million people aged 20–79 years in the world had diabetes, such numbers that are expected to grow to 642 million in 2040 [3]. Importantly, a large portion of either overweight or obese individuals also present with T2D, supporting the strong association between both diseases [4].

T2D is a heterogeneous disease that features insulin resistance and pancreatic β-cell dysfunction as major hallmarks. Insulin resistance is defined as the inability of insulin to properly stimulate glucose uptake in skeletal muscle and adipose tissue and to inhibit hepatic glucose production. Despite of the intense research in this area, there are still some doubts about the exact sequence of events that leads to the development of obesity-associated insulin resistance as elegantly reviewed in [5]. The most traditional hypothesis suggests that either obesity or the intake of obesogenic, hypercaloric diet promotes first insulin resistance, which then results in hyperglycemia followed by hyperinsulinemia. In accordance to this hypothesis, hyperglycemia and a compensatory hyperinsulinemia are major metabolic phenotypes found in the early stages of T2D. Chronically, hyperglycemia may promote, in a more advanced stage of T2D, pancreatic islet damage and a subsequent decline in insulin secretion. Interestingly, recent studies have suggested, based on findings obtained in obese humans and rodents and patients after bariatric surgery, that hyperinsulinemia, instead of hyperglycemia, is the primary event involved in the development of insulin

resistance and T2D. In accordance with this hypothesis, either obesity or the intake of an obesogenic, hypercaloric diet enhances β-cell insulin secretion and/or reduces its degradation, promoting hyperinsulinemia, which chronically results in insulin resistance and therefore hyperglycemia. Taking into account the strong evidence supporting both of the aforementioned hypotheses, one may argue that the exact sequence of events involved in the development of obesity-associated insulin resistance and T2D may vary according to the underlying obesogenic conditions.

T2D results from a complex interaction between genetic and environmental factors. Studies evaluating familial risks indicate that T2D has a high 50% heritability, in which individuals with either one affected first-degree relative or at least two affected siblings, independently of the parental diabetes status, are at the higher risk of developing T2D [1]. Genome-wide association studies have identified so far more than 40 diabetes-associated loci, which are related to β-cell function, insulin sensitivity, and obesity and respond to approximately 10% of T2D heritability [1]. Noteworthily, the greatest majority of T2D cases are associated with two or more genetic mutations (polygenic nature), such alterations that in most cases increase the propensity, but are not sufficient to induce disease development without the contribution of environmental and/or behavioral factors. The very same rationale applies to the development of visceral obesity, a major risk factor for T2D [2].

Inflammation is at the very centre of metabolic diseases such as obesity, T2D, and metabolic syndrome, playing an important role not only in their development but also as a linking factor between them. Indeed, visceral obesity is associated with a chronic inflammatory process of low intensity, defined as metabolic inflammation or "metainflammation" that affects important metabolic tissues such as adipose tissue, liver, skeletal muscle, pancreas, intestines, and hypothalamus, among others [6]. The adipose tissue, for example, the organ that defines obesity, develops upon this condition an inflammatory process characterized by the recruitment, infiltration, and polarization of leukocytes to a proinflammatory profile [6]. Among the leukocytes recruited to adipose tissue upon obesity are neutrophils, macrophages, dendritic and mast cells from the innate immune system, and several subtypes of T and B lymphocytes from the adaptive immune system [7]. Several stimuli were suggested to mediate the induction of leukocyte recruitment to adipose tissue found upon obesity such as the following: (1) activation of adipocyte proinflammatory pathways by LPS and saturated fatty acids and secretion of chemokines such as monocyte chemoattractant protein-1 (MCP-1), (2) tissue hypoxia, (3) adipocyte death, and (4) mechanical stress between adipocytes and the extracellular matrix [6]. Importantly, after recruitment, tissue leukocytes also undergo polarization to different phenotypes. Macrophages, for example, which account for approximately 50% of the cells composing adipose tissue upon obesity, undergo during this condition a polarization to a proinflammatory M1 phenotype [8]. These proinflammatory leukocytes along with activated, hypertrophied adipocytes secrete a plethora of proinflammatory cytokines/adipokines, chemokines, and lipids, perpetuating inflammation and impairing tissue metabolism. Importantly, proinflammatory mediators have been shown to induce insulin resistance by impairing several steps in the intracellular signaling cascade of this hormone [9, 10] and adipose tissue macrophage depletion attenuates diet-induced obesity, inflammation, and insulin resistance [8].

Intake of excessive amounts of nutrients is a major underlying cause of obesity and obesity-associated complications and an important modulator of many phenotypes associated with this condition including inflammation. We review herein the mechanisms by which excessive intake of nutrients chronically modulates visceral obesity-associated inflammation with a special emphasis in the role of nutrient sensors as likely mediators of these actions.

1.1. Nutrient Sensing. Nutrients have vital functions in cells acting not only as metabolic substrates for energy production but also as building blocks for the synthesis of macromolecules and cellular components [11]. In the face of such essential roles of nutrients, organisms have evolved several mechanisms to sense levels of specific nutrients in the extra- and intracellular compartments allowing the proper coordination of rates of growth, proliferation, and function according to nutrient availability [11]. Nutrient-sensing mechanisms are found in all organisms; some of them are well conserved through evolution being found in eukaryotic organisms varying from yeast to mammals, whereas others are exclusive of prokaryotes [11]. Importantly, in multicellular organisms, some nutrient sensing mechanisms also evolved to undergo regulation by the endocrine system, allowing the coordination at whole-body level of nutrient sensing activity among different cells/tissues, which is of major importance in the maintenance of whole-body homeostasis.

Proteins that have the capacity to sense fluctuations in the concentration of a specific nutrient or a product of its metabolism within the physiological range are denominated as nutrient sensors [11]. Nutrient sensors, which can be located at different cell compartments as the plasma membrane, cytosol, organelle endomembranes, or the nucleus, respond to fluctuations in nutrient levels through diverse mechanisms varying from the activation of phosphorylation cascades, changes in gene transcription, and enzymatic activities, among others. Upon obesity, nutrient sensors are chronically challenged by excessive amounts of some nutrients, which impact their activity and regulatory role over cellular processes. More specifically, metabolomics studies have found that visceral obesity is frequently associated with increased serum concentrations of glucose, branched-chain and aromatic amino acids (BCAA and AA, resp.), and several lipids such as saturated and omega 6 fatty acids, acylcarnitines, and phospholipids, among others [12]. Chronic tissue exposure to excessive amounts of some of these nutrients has been implicated in the development of common features of obesity and T2D such as organelle dysfunction (endoplasmic reticulum and mitochondria stress) and oxidative stress, both of which being candidates as triggering factors of obesity-associated inflammation and insulin resistance. On the other hand, elevated intake of some nutrients such as

ω-3 polyunsaturated fatty acids was shown to protect from obesity-associated inflammation and insulin resistance.

1.2. Insulin Signaling and Inflammation. Insulin is a major anabolic hormone that exerts its actions by interacting with a receptor constituted of two extracellular α-chains containing the ligand-binding site and two transmembrane β-chains that possess the tyrosine kinase activity. The insulin receptor (IR) displays 50% homology to the insulin-like growth factor receptor (IGFR), and in some cells, both receptors may form IR-IGFR hybrids that recognize both insulin and IGF-1 as ligands [13, 14]. Upon interaction with insulin or IGF-1, the receptor changes its conformation and phosphorylates at tyrosine residues itself and a family of adaptor proteins known as insulin receptor substrates (IRS). Tyrosine-phosphorylated IRS then binds to the SH2 domain of the p85 regulatory subunit of the lipid kinase phosphoinositide-3-kinase (PI3K) promoting the conversion of the membrane lipid phosphatidylinositol 3,4-biphosphate (PIP2) to phosphatidylinositol 3,4,5-biphosphate (PIP3). PIP3 then binds to and recruits protein kinase B/Akt to the cell membrane promoting its phosphorylation at Ser473 and Thr308 by the mechanistic target of rapamycin complex 2 (mTORC2) and phosphoinositide dependent-kinase 1 (PDK1), respectively [15]. Upon its phosphorylation and activation, Akt promotes glucose uptake by phosphorylating Rab GAP TBC1D4 (AS160) inducing therefore the translocation of vesicle-containing glucose transporter 4 (GLUT4) to the plasma membrane [16] and inhibits hepatic gluconeogenesis by phosphorylating and inactivating the transcription factor forkhead box protein O1 (FoxO1) and the CREB-CBP-CRTC2 complex, thus suppressing the expression of gluconeogenic enzymes phosphoenolpyruvate carboxykinase (PEPCK) and glucose 6-phosphatase (G6Pase) [15, 17]. In addition to those actions that are susceptible to developing resistance upon obesity and T2D, insulin, through the sequential PI3K-Akt activation, inhibitory phosphorylation of the complex tuberous sclerosis complex 1/2 (TSC1/TSC2), and activation of Ras homolog enriched in the brain (Rheb), activates the mechanistic target of rapamycin complex 1 (mTORC1), which in turn promotes protein synthesis by phosphorylating the ribosomal protein S6K and eukaryotic translational initiation factor 4E-binding protein 1 (4E-BP), among many other processes [18]. Another important signaling pathway induced by insulin is the mitogen-activated protein kinase (MAPK), reviewed in detail elsewhere [19], which promotes cell proliferation, among other actions.

In healthy cells, intracellular insulin signaling is constantly monitored by several regulatory checkpoints that, through a complex system of negative feedback loops, keeps the level of activity of this signaling pathway within the optimal physiological range. One of these regulatory loops is exerted by mTORC1 downstream substrate S6K1 that, when phosphorylated and activated, catalyzes a negative feedback characterized by the inhibitory phosphorylation of IRS at serine residues, blocking its ability to interact and allosterically activate PI3K [20]. Another feedback loop modulating insulin signaling catalyzed by mTORC1 involves the phosphorylation and stabilization of the adaptor protein GRB10, which binds via SH2 domain to the phosphorylated tyrosine at the insulin receptor blocking the interaction with IRS [21, 22]. In addition, GRB10 may also reduce insulin signaling by promoting IRS ubiquitination via the ubiquitin ligase E2 NEDD4.2 and proteasomal degradation [23]. Importantly, dysfunction of these regulatory systems and feedback loops promotes chronic overactivation of intracellular insulin signaling and is associated with cancer incidence, whereas the opposite, that is, impaired insulin signaling (resistance), defines T2D.

The mechanisms by which cells become refractory to insulin action in obesity are not completely understood. Compelling evidence published in the early 1990s had shed light on this issue not only by establishing obesity as an inflammatory disease but also by indicating that inflammatory mediators may play a key role as linking factors between excessive fat deposition and the development of insulin resistance and other associated diseases [24]. More specifically, it was shown in these studies that the proinflammatory cytokine tumor necrosis factor- (TNF-) α is oversecreted by adipose tissue in obesity, promotes insulin resistance in rodents, and correlates with insulin resistance in obese children and adults [24–27]. Furthermore, it was later shown that deletion of TNF-α or its receptor protects mice against diet-induced obesity and insulin resistance [28], whereas TNF-α blockade by treatment with its monoclonal antibody infliximab improved glucose homeostasis in patients with rheumatic disease [29–32]. In spite of those promising findings, TNF-α blockade was not effective in treating insulin resistance in obese patients [33], such findings that were somehow expected considering that inflammation is a complex process characterized by the involvement of many protein and lipid mediators. Indeed, subsequent studies have shown that other proinflammatory mediators such as interleukin- (IL-) 1β, IL-6, interferon- (IFN-) γ, ceramides, prostaglandins, and lipopolysaccharide (LPS) from the membrane of gram-negative bacteria residing in gut microbiota, among others, are also involved in the development of obesity-associated insulin resistance [34–36]. Among those, obesity-associated elevation in the circulating levels of LPS, defined as metabolic endotoxemia, has been considered as a major triggering factor that links excessive intake of fat and the development of obesity-associated inflammation [35, 37]. Another important inflammatory mediator involved in obesity is IL-1β, a cytokine whose secretion requires its processing by caspase-1 as the result of the activation of the nucleotide-binding domain, leucine-rich-containing family, pyrin domain-containing 3 (NLRP3) inflammasome, a multimeric cytosolic protein complex activated by pathogen-associated molecular pattern (PAMP) and danger-associated molecular pattern (DAMP) molecules [38]. Indeed, blockade of IL-1β actions by treatment with a receptor antagonist (anakinra) or monoclonal antibody reduces systemic inflammation and improves glycemia and β-cell secretory function in T2D patients [34].

One common signaling event that is at the very centre of obesity-associated inflammation is the activation of nuclear factor κ-light-chain-enhancer of activated B cells (NFκB), a conserved family of transcription factors that regulate

inflammatory processes, immune function, development, and growth [39]. Importantly, chronic NFκB activation may be involved in the development of several diseases in addition to obesity such as T2D and cancer, among others. Five NFκB protein members are expressed in mammalian cells, RelA (p65), RelB, c-Rel, NFκB1 (p50/105), and NFκB2 (p52/100) [39]. In the absence of stimulus, dimers of NFκB protein members are bound to the inhibitor κB (IκB), which maintains the NFκB complex in the cytosol, inhibiting therefore its translocation to the nucleus and transcriptional activity. Proinflammatory mediators activate NFκB through a series of events that involve IκB phosphorylation by IκB kinase (IKK), followed by its ubiquitination and proteasomal degradation, which then release the p50/RelA (p65) dimer for translocation to the nucleus, where it can repress or induce gene transcription by binding to 9-10 nucleotide sequences in DNA promoter regions denominated as NFκB response elements [39].

Proinflammatory mediators through the activation of several signaling pathways such as the canonical toll-like receptor- (TLR-) IKK-NFκB, and the kinases c-Jun N-terminal kinases (JNK), Janus kinase (JAK), and mTOR, among others [10], promote insulin resistance by impairing different steps in the intracellular insulin signaling cascade, namely, by either phosphorylating IRS at inhibitory serine residues, or inhibiting Akt dual phosphorylation and activation, or reducing AS160 phosphorylation and GLUT-4 translocation [9, 10, 40]. Importantly, resistance selectively affects only few processes regulated by insulin such as glucose uptake in myocytes and adipocytes and glucose production in hepatocytes. Other insulin actions such as the activation of protein synthesis and de novo lipogenesis do not seem to be impaired in insulin-resistant conditions [40–42]. Below, we review the molecular mechanisms by which some nutrients modulate obesity-associated inflammation.

1.3. Glucose Excess (Glucotoxicity) and Inflammation. Chronic tissue exposure to hyperglycemia, due to the elevated intake of diets rich in simple carbohydrates of high glycemic index and/or impaired glucose homeostasis, is associated with the development of tissue inflammation. It has been extensively shown, for example, in rodent adipose tissue, liver, and pancreas, that high sucrose feeding promotes an inflammatory process characterized by enhanced leukocyte recruitment and polarization to a proinflammatory phenotype, as well as exacerbated cytokine production and secretion [43–47]. Similarly to rodents, acute and persistent hyperglycemia in humans is associated with elevated circulating levels of several proinflammatory cytokines and markers of endothelial and oxidative stress [48, 49]. Furthermore, human and rodent pancreatic β-cells exposed to high glucose levels displayed NLRP3 inflammasome and caspase-1 activation and enhanced IL-1β production [50]. The underlying mechanisms by which exposure to high glucose levels activates the NLRP3 inflammasome and whether this occurs in other cell types than β-cells are unknown and deserve to be investigated. Recent findings stating that mitochondrial dissociation and inhibition of the rate-limiting enzyme of glycolysis hexokinase promote

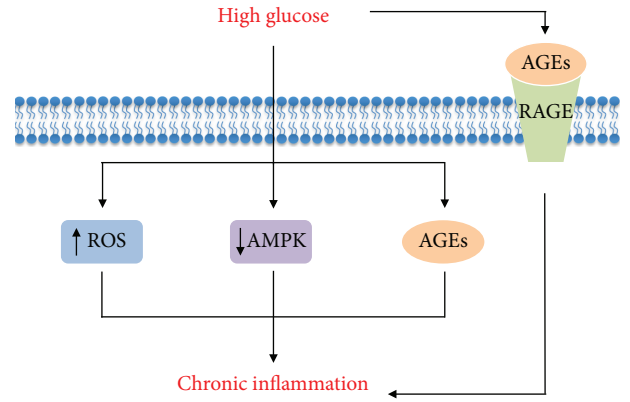

Figure 1: Main mechanisms by which glucose excess induces chronic inflammation. AGEs: advanced glycation end products; AMPK: AMP-activated protein kinase; RAGE: receptor for AGEs; ROS: reactive oxygen species.

NLRP3-inflammasome activation and IL-1β in macrophages [51] open the possibility for the involvement of this enzyme as a mediator of glucose actions towards the NLRP3 inflammasome. Indeed, high glucose levels may inhibit hexokinase by inducing cell accumulation of its allosteric inhibitor glucose 6-phosphate and/or the Krebs cycle intermediate citrate, both of which have been shown to promote inflammasome activation in macrophages [51].

In addition to pancreatic β-cells, *in vitro* exposure of endothelial cells, monocytes, macrophages, hepatocytes, adipocyte progenitor cells, or mature adipocytes to high glucose levels is associated with a proinflammatory response characterized by activation of the canonical proinflammatory NFκB signaling pathway and elevated cytokine secretion [52–56]. In terms of possible molecular mechanisms, activation of the cellular inflammatory response by high glucose levels has been attributed to the following processes: (1) enhanced production of reactive oxygen species (ROS) and oxidative stress [55], (2) activation of the MAPK pathway [54]. (3) nonenzymatic glycation and formation of advanced glycation end products (AGE) [49], (4) activation of protein kinase C (PKC) isoforms [57], (5) epigenetic and chromatin modifications [52], (6) activation of transforming growth factor- (TGF-) β-activated kinase 1 signaling [53], (7) activation of the hexosamine pathway and modification of proteins by N-acetylglucosamine (O-GlcNAc modification) [58], and (8) inhibition of AMP-activated protein kinase (AMPK) [59]. Among those processes, which have been covered before in an excellent review article [60], we will further discuss herein the mechanisms by which exposure to high glucose levels promotes inflammation by inducing oxidative stress and spontaneous glycation and by inhibiting the energy sensor AMPK (Figure 1).

Chronic cell exposure to high glucose levels is associated with an imbalance between ROS production and antioxidant buffering resulting in cellular oxidative stress. Mechanistically, high glucose levels increase ROS production and oxidative stress by enhancing glucose oxidation through the Krebs cycle, NADH/NAD and $FADH_2$/FAD ratios and electron flux in a stepwise manner through complexes I and III redox

centres, which then catalyzes the transference of some of these electrons to O_2 [49]. Oxygen radical species are highly reactive substances that when in excess promote organelle dysfunction and cellular damage by reacting with protein, lipids, carbohydrates, and DNA [49]. In oxidative stress, cells trigger an inflammatory response as a protective mechanism to repair cell damage and avoid death that includes activation of intracellular signaling through the NFκB pathway [61], as well as NLRP3 inflammasome-mediated IL-1β cleavage and secretion [62, 63].

In addition to oxidative stress, high glucose levels also promote inflammation by enhancing the spontaneous glycation of free amino groups of proteins, DNA, and other molecules, generating, through a series of reactions, AGE [49]. Importantly, glycation is concentration-dependent, does not require enzymatic activity, and, similarly to ROS, impairs the biological function of molecules, inducing organelle dysfunction, stress, and inflammation. In addition to glucose, other simple sugars such as fructose, galactose, and ribose, as well as phosphorylated intermediates of metabolism (glucose 6-phosphate, fructose 6-phosphate, ribose 5-phosphate, etc.), are also precursors for AGE formation [49]. Several circulating proteins such as albumin, insulin, hemoglobin, and the lipoproteins LDL, VLDL, and HDL have also been shown to undergo glycation in conditions of glucose excess, forming precursors of AGE denominated as Amadori products [49]. Among these, glycated albumin and LDL, for example, were shown to induce proinflammatory NFκB signaling, cytokine secretion, and inflammation through the activation of Amadori receptors in the target cells [64, 65]. Similarly to its precursors, AGE exert part of their actions through the activation of a class of ubiquitously expressed membrane receptors of AGE (RAGE). Binding and activation of RAGE by AGE promotes an oxidative stress-dependent proinflammatory cell response characterized by NFκB activation, increased cytokine secretion, activation of cyclooxygenase and prostaglandin synthesis, and enhanced recruitment and activation of both innate and adaptive immune system [49, 66–68]. Supporting this notion, RAGE activation promotes NFκB activation, IL-6 and TNF-α secretion, and polarization of bone marrow-derived macrophages to a proinflammatory M1 profile [69]. In contrast, RAGE deletion is associated with reduced leukocyte recruitment and inflammation of the peritoneal cavity in a model of thioglycollate-induced acute peritonitis [70]. Altogether, these findings indicate that modification of cellular constituents by ROS and/or glycation may be responsible, at least in part for the inflammatory response induced by hyperglycemia.

One important nutrient and energy sensor that detects variations in cell glucose availability is the heterotrimeric protein AMP-activated protein kinase (AMPK), a well-conserved, ubiquitously expressed, serine/threonine kinase whose activity is modulated by changes in ADP/ATP ratio and cell energy status. In situations of energy scarcity, AMPK is activated by an elevation in the ADP/ATP ratio, whereas the opposite, that is, a reduction in AMPK activity, occurs in situations of energy surplus and reduced ADP/ATP ratio [71]. Mechanistically, AMPK is activated by ADP and more potently by AMP through a process that involves the binding of adenine nucleotides to the AMPK γ subunit. This changes its conformation and leaves it not only prone to the phosphorylation at the α subunit Thr172 residue by liver kinase B-1 (LKB-1) but also resistant to the dephosphorylation by protein phosphatase 2A [71]. When active, AMPK promotes glucose uptake, fatty acid oxidation, mitochondrial biogenesis, and other energy-generating catabolic processes and inhibits synthetic pathways, such as fatty acid and protein syntheses [71]. In addition to its role in the regulation of metabolism, several pieces of evidence support a likely involvement of AMPK as an important modulator of obesity- and hyperglycemia-induced inflammation. Under these conditions characterized by energy surplus, AMPK Thr172 phosphorylation and activity are broadly and markedly reduced. Such a phenotype is also seen upon treatment of bone marrow-derived macrophages and dendritic cells with LPS and other proinflammatory molecules [72–75]. Indeed, *in vitro* macrophage AMPK inhibition by either RNAi or expression of AMPK dominant negative or deletion of the AMPK β1 subunit is associated with enhanced LPS-induced TNF-α, IL-6, and cyclooxygenase-2 levels, diacylglycerol accumulation and PKC activation [72, 74]. *In vivo*, genetic AMPK inhibition in macrophages exacerbates obesity-associated liver and adipose tissue inflammation by increasing macrophage recruitment and polarization to a proinflammatory M1 profile [72]. In accordance with the notion emerged from the above-mentioned loss-of-function studies suggesting that AMPK activity is anti-inflammatory in nature, both *in vitro* and *in vivo* pharmacological activation of this kinase with either AICAR (5-aminoimidazole-4-carboxamide ribonucleotide) or the antidiabetic drugs metformin and troglitazone or the glycolysis inhibitor 2-deoxyglucose is associated with marked attenuation of LPS-induced NFκB activation, as well as iNOS and TNF-α expression in myocytes, adipocytes, macrophages, neutrophils, and dendritic cells [75–77]. Furthermore, recent studies have found not only that AMPK activity is increased by the anti-inflammatory molecules IL-10, TGF-β, salicylate [74, 78], and adiponectin [79] but also that its constitutive genetic activation in macrophages resulted in impaired production of proinflammatory cytokines and enhanced cell polarization to a M2 anti-inflammatory profile [74]. Mechanistically, AMPK seems to exert its anti-inflammatory actions by impairing intracellular proinflammatory signaling through NFκB, as well as by inducing in macrophages a metabolic shift from aerobic glycolysis to oxidative pathways [74]. Altogether, these findings establish AMPK as an important pharmacological target to counteract obesity and hyperglycemia-associated inflammation.

1.4. Amino Acid Excess and Inflammation. Metabolomic characterization of the serum of fasting obese insulin-resistant patients indicates that elevated circulating levels of branched-chain (leucine, isoleucine, and valine) and aromatic (phenylalanine, tyrosine, and tryptophan) amino acids (BCAA and AA, resp.) are not only important metabolic signatures that distinguish obese patients from lean, healthy individuals [12, 80, 81] but also risk factors for the development of insulin resistance and T2D [82, 83]. Despite those

findings, it is still unknown whether BCAA have a causal role in the development of obesity-associated insulin resistance or whether elevated circulating levels of BCAA are just a metabolic consequence of this disease. In line with a possible causal contribution, supplementation of a high-fat diet with all three BCAA has deleterious effects on insulin sensitivity in rats [81, 84] and BCAA infusion to healthy man impaired insulin-stimulated glucose disposal in skeletal muscle [85]. Furthermore, treatment of myocytes and murine and human adipocytes with amino acids *in vitro* also induces insulin resistance [85, 86]. Mechanistically, this deleterious effect of BCAA on insulin sensitivity involves the activation of the nutrient and amino acid sensor mTORC1 that promotes insulin resistance by activating S6K1 and therefore the inhibitory phosphorylation of IRS-1 at serine residues. Importantly, mTORC1 is overactivated in adipose tissue, liver, and skeletal muscle of diet- and genetic-induced obese, insulin-resistant rodents [87, 88]. Another mechanism by which mTORC1 overactivation may impair IRS-1 function and induce insulin resistance is through the activation of c-JUN-N terminal kinase (JNK) as the result of exacerbated protein synthesis, endoplasmic reticulum (ER) stress, and unfolded protein response (UPR) [89, 90]. Despite this, it is still unclear whether BCAA are implicated in obesity-associated mTORC1 overactivation and whether this complex is involved in the development of obesity-linked insulin resistance.

In favor of the notion, however, that elevated serum BCAA levels are rather a consequence of obesity and insulin resistance, both inflammation and endoplasmic reticulum stress [91], major hallmarks of these diseases, were shown to increase circulating BCAA levels by reducing rates of BCAA oxidation in adipose tissue and by enhancing skeletal muscle protein degradation [83]. Furthermore, elevated intake of BCAA was associated, independently of genetics, with lower insulin resistance, inflammation, blood pressure, and adiposity-related metabolites in female twins [92]. Such beneficial BCAA actions to metabolic health were also seen in several studies in rodents, where high BCAA intake was associated with reductions in body weight, adiposity, and glucose intolerance in diet-induced obese mice [93, 94]. Along with its beneficial effects on glucose homeostasis, BCAA were shown to exert anti-inflammatory actions. Indeed, elevated intake of BCAA was associated with reductions in muscle damage and inflammation during intensive exercise training [94], in hepatic steatosis and inflammation induced by diet-induced obesity [95, 96], and in chronic white adipose tissue and liver inflammation and early-phase hepatic tumorigenesis associated with obesity [97]. Extending those findings, elevating blood BCAA levels through the deletion of the mitochondrial branched-chain aminotransferase (BCATm) in mice was shown to attenuate the catabolic and proinflammatory effects of LPS and improve survival in response to bacterial infection [98].

Although the mechanisms by which BCAA modulate inflammation are not completely defined, it may involve the activation of the amino acid sensor mTORC1, a multiprotein complex composed by the highly conserved serine-threonine kinase mTOR as its catalytic core, along with the accessory proteins regulatory-associated protein of mTOR (Raptor), mammalian lethal with Sec13 protein 8 (mLST8), DEP domain-containing mTOR-interacting protein (DEPTOR), proline-rich Akt substrate 40 (PRAS40), and Tti1/Tel2 complex proteins [18]. The BCAA leucine activates mTORC1 by inducing its translocation to the lysosomes and interaction with the GTP-bound protein Ras homolog enriched in the brain (Rheb). This requires leucine binding to sestrin 2 and activation of small GTPases denominated as Ras-related GTP-binding protein (Rags), through a process that involves the protein complexes GAP activity towards Rags (GATOR) 1 and 2 and the Ragulator [18, 99]. Importantly, mTORC1's major cellular function is to coordinate processes such as cell growth, proliferation, metabolism, autophagy, and survival according to nutrient and growth factor availability [18].

In addition to amino acids and growth factors, mTORC1 activity is also upregulated by proinflammatory mediators such as LPS via TLR-4-mediated activation of either IKKβ [100, 101] or PI3K-Akt [102, 103] and by the anti-inflammatory cytokines IL-4 and IL-13 [104], indicating that this complex may have a role in the regulation of inflammation and immune function. Indeed, pharmacological mTORC1 inhibition with the macrolide rapamycin is associated with an exacerbation of obesity-associated adipose tissue inflammation, as evidenced by the enhanced tissue recruitment and polarization of macrophages to a proinflammatory phenotype and expression of proinflammatory cytokines IL-1β and TNF-α [104, 105]. In accordance to these findings, mTORC1 inhibition with rapamycin was shown to enhance the spontaneous polarization of human monocytes *in vitro* and peripheral blood mononuclear cells *in vivo* to a proinflammatory profile [106, 107]; such a response is also seen in murine bone marrow-derived macrophages *in vitro* [104]. Importantly, Raptor deletion and therefore mTORC1 deficiency in adipocytes, but not myeloid cells [108], promoted adipose tissue inflammation, NLRP3-inflammasome activation, leukocyte recruitment, and local cytokine production [109]. Interestingly, this inflammatory response, which occurred despite of a drastic reduction in adipose tissue mass, was mediated by an increase in the local production of ceramides [109] (Figure 2).

The effects of mTORC1 constitutive activation in embryonic fibroblasts and macrophages have also been investigated reporting contrasting results. Constitutive mTORC1 activation through the inactivation of either TSC1 or TSC2 in human monocytes, murine myeloid cells, and embryonic fibroblasts was shown to (1) limit the inflammatory response by blocking LPS-induced NFκB activation and increasing IL-10 production [107], (2) induce in a cell autonomous manner granuloma formation and lung and liver infiltration of alternatively activated M2 macrophages and reduce lung iNOS [110], (3) increase the activity of the energy sensor AMPK that exerts anti-inflammatory actions [111], and (4) protect from diet-induced obesity and adipose tissue inflammation by promoting the polarization of adipose tissue-resident macrophages to a M2 phenotype (Paschoal et al., unpublished observations). Noteworthily, a recent study found that the Akt-mTORC1 pathway is an important mediator of macrophage polarization to a M2 phenotype induced

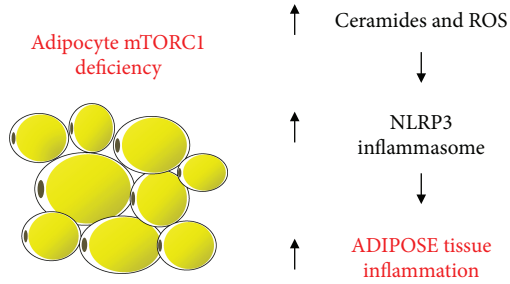

Figure 2: Mechanisms underlying adipose tissue chronic inflammation induced by mTORC1 deficiency in adipocytes. ROS: reactive oxygen species.

by IL-4, through a mechanism that involves activation of ATP-citrate lyase, histone acetylation, and transcriptional induction of a subset of M2 genes [112]. In contrast to those findings, however, *Tsc1*-deficient bone marrow-derived macrophages (BMDM) were refractory to M2 polarization induced by IL-4 and displayed enhanced M1 polarization, nitric oxide (NO) production, and cytokine secretion induced by toll-like receptor ligands [113, 114]. Surprisingly, another study found that *Tsc1*-deficient macrophages exhibited enhanced polarization to both M1 and M2 phenotypes both at steady-state condition and induced by either LPS or IL-4 [115].

In spite of the apparent contradictory findings, the scenario emerging from the aforementioned studies is that mTORC1 is an important mediator of both proinflammatory M1 and anti-inflammatory M2 macrophage responses (Figure 3). Indeed, this is in accordance with mTORC1's role in the regulation of processes such as protein, lipid and nucleotide syntheses, autophagy, and lysosome formation that are vital to macrophages independently of their phenotype. Accordingly with this notion, mTORC1 activity is increased by proinflammatory molecules (LPS, TNF-α, and IFN-γ) in M1 macrophage polarization [100, 102, 104], as well as by the M2 macrophage-promoting cytokines (IL-4 and IL-13) [104, 112]. Furthermore, mTORC1 induces metabolic processes that are important for M1 and M2 macrophage functions, namely, aerobic glycolysis and oxidative metabolism, respectively, through mechanisms that involve activation of hypoxic-inducible factor 1α (HIF-1α) in the former (M1 aerobic glycolysis) and the peroxisome proliferator-activated receptor γ (PPARγ), PPAR coativactor 1α (PGC1α), and mitochondrial biogenesis in the latter (M2 oxidative metabolism) [116]. Altogether, these findings suggest that mTORC1 is an important mediator of both classic M1 and alternative M2 macrophage polarizations, exerting its functions according to the underlying stimuli context (Figure 3). In addition to macrophages, mTORC1 seems to play an important role regulating T lymphocyte proliferation, migration, differentiation, metabolism, and activation as elegantly reviewed before [117].

Similarly to complex 1, mTORC2 is also activated by both M1 (LPS and IFN-γ) and M2 (IL-4 and IL-13) inducers playing an important role in regulation of macrophage polarization and function (Figure 4). More specifically, deletion of rapamycin-insensitive companion of mTOR (RICTOR) and therefore mTORC2 deficiency in myeloid cells was shown to enhance both polarization of bone marrow-derived macrophages to the M1 profile and the proinflammatory cytokine secretion induced by LPS and other TLR ligands and to reduce the expression of M2-related genes [103]. Furthermore, mice with mTORC2 disruption in myeloid cells had higher circulating TNF-α levels and mortality in a model of acute septic shock induced by high dose of LPS [103]. Mechanistically, this enhanced M1 polarization induced by mTORC2 deficiency was attributed to FOXO1 activation due to reduced Akt activity and therefore enhanced transcription of proinflammatory genes [118]. Subsequent studies have also shown that mTORC2 is essential for proper bone marrow-derived macrophage polarization to a M2 profile. Indeed, mTORC2-deficient M2 macrophages were shown to display impaired glucose metabolism and reduced PPARγ content, mitochondrial biogenesis, and fatty acid oxidation, effects that are mediated by Akt and, at least in part, by the transcriptional factor interferon regulatory factor 4 (IRF4) [119].

1.5. Fatty Acid Excess and Inflammation. Evidence suggests that lipids, especially fatty acids, play an important role not only in obesity development but also as a linking factor between the excessive adiposity and development of associated diseases [120]. Indeed, elevated intake of diets containing high amounts of saturated fatty acids induces obesity and its major complications including inflammation, insulin resistance, and ectopic lipid deposition, among others. Recent studies, however, have indicated that more important than quantity, diet fatty acid composition has major implications in the development of "metainflammation." High intake of diets rich in saturated fatty acids, for instance, activates the innate immune toll-like receptor 4 (TLR4) promoting chronic low-grade inflammation, insulin resistance, and cardiovascular disease [121]. In the same line, ω-6 polyunsaturated fatty acid-enriched diets were shown to be proinflammatory and deleterious to the cardiovascular function [121, 122]. In spite of the deleterious effects of saturated and ω-6 polyunsaturated fatty acids to metabolic health, other types of lipids have preventive and/or therapeutic properties that could be explored to counteract metabolic diseases. Among beneficial lipids, ω-3 polyunsaturated and short-chain fatty acids were demonstrated to have anti-inflammatory, anti-carcinogenic, hypolipidemic, and weight loss-inducing properties [123, 124]. Below, we discuss the modulation of "metainflammation" by specific types of fatty acids (Figure 5).

1.6. Saturated Fatty Acids (SFAs). Saturated fatty acids such as lauric (C12:0), miristic (C14:0), palmitic (C16:0), and stearic (C18:0) are commonly found in foods of animal source such as dairy products and meat, and some vegetables as coconut and palm oil, being therefore the most prevalent saturated fatty acids found in human diet. Many studies have associated an elevated intake of saturated fatty acids with a higher prevalence of obesity, cardiovascular disease, diabetes, and insulin resistance, diseases that share chronic low-intensity inflammation as a common feature [125].

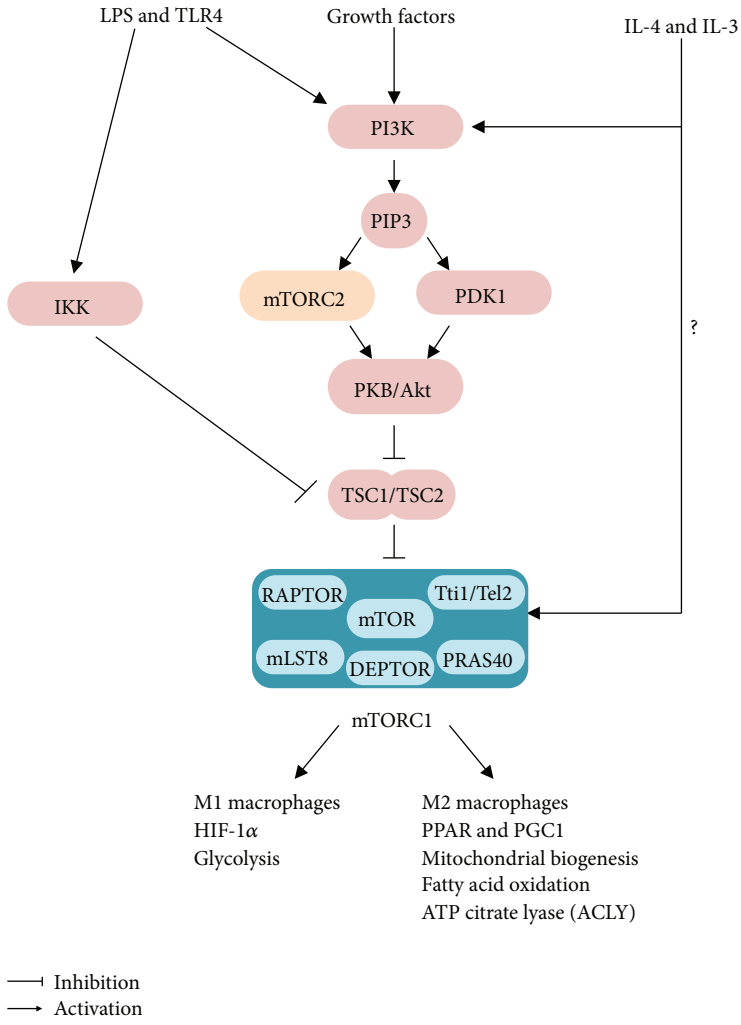

Figure 3: mTORC1 is activated in both M1 and M2 polarization and regulates important metabolic processes at both conditions. AA: amino acids; ACLY: ATP citrate lyase; HIF-1α: hypoxic inducible factor 1α; IL-4: interleukin 4; IL-13: interleukin 13; PGC1α: PPARγ coactivator 1α; PPARγ: peroxisome proliferator-activated receptor γ; TLR4: toll like receptor 4.

Therefore, since 1961, the American Heart Association recommends a reduction in the intake of foods rich in saturated fatty acids aiming to reduce the prevalence of those chronic metabolic diseases [126].

At the molecular level, saturated fatty acids promote inflammation through several mechanisms that include activation of the TLR4-IKK-NFκB signaling pathway and NLRP3 inflammasome, enhanced ROS production and oxidative stress, mitochondrial dysfunction, ER stress, accumulation of diacylglycerol and ceramides, and PKC activation, among others [63, 127–132]. Saturated fatty acids are potent activators of the pattern recognition receptor TLR4, which is also activated by LPS and others PAMPs and DAMPs and has a major role in the regulation of innate immune response [128, 133, 134]. Activation of TLR4 by saturated fatty acids elicits, through the activation of NFκB, the secretion of several proinflammatory cytokines such as TNF-α, IL-6, and MCP-1, which are involved in the development of obesity-associated inflammation and insulin resistance [128, 133, 134]. In addition, saturated fatty acids were shown to activate NLRP3 inflammasome-mediated IL-1β production in macrophages, such an effect that seems to involve AMPK inactivation, autophagy inhibition, and enhanced mitochondrial ROS production [129].

In addition to inflammatory signaling, chronic tissue exposure to high levels of saturated fatty acids may promote insulin resistance by increasing tissue content of the lipids diacylglycerol and ceramides. Diacylglycerol accumulation promotes insulin resistance by activating the PKCΘ and ε impairing IRS tyrosine phosphorylation and therefore downstream insulin signaling [135]. Ceramides, on the other hand, consist of a family of lipids structurally formed by a sphingosine base bound to a fatty acid that promote insulin resistance by two nonmutually exclusive mechanisms, involving either the allosteric activation of protein phosphatase 2A (PP2A), which dephosphorylates and inhibits Akt [136], or the activation of atypical PKC λ/ζ, which phosphorylates Akt pleckstrin domain at residue 34 impairing its translocation to the membrane and subsequent activation [137, 138]. Ceramides have been also shown to modulate inflammatory processes

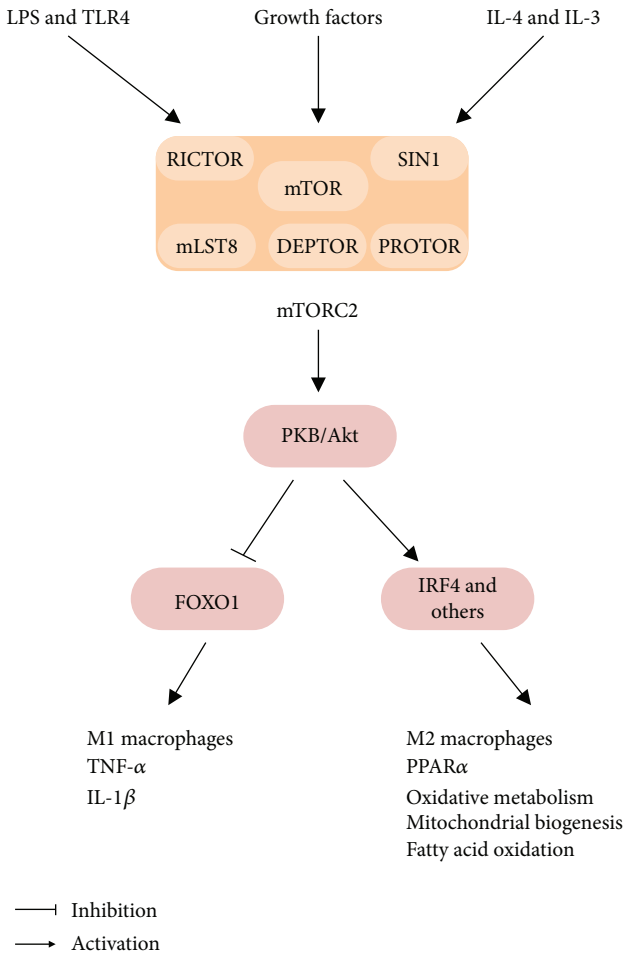

Figure 4: mTORC2 is activated in both M1 and M2 polarization and regulates important metabolic processes at both conditions. IL-1β: interleukin 1β; IL-4: interleukin 4; IL-13: interleukin 13; IRF4: interferon regulatory factor 4; LPS: lipopolysaccharide; PKB: protein kinase B; PPARγ: peroxisome proliferator-activated receptor γ; TLR4: toll-like receptor 4; TNF-α: tumor necrosis factor-α.

displaying either pro- or anti-inflammatory responses, as elegantly reviewed before [139]. Briefly, proinflammatory actions of ceramides involve activation of TLR4 signaling as a result of ceramide interaction with this receptor, formation of TLR4-lipid raft complex, and activation of NLRP3 inflammasome-mediated IL-1β and IL-18 production [139].

1.7. Monounsaturated Fatty Acids (MUFAs). In contrast to their saturated counterparts, elevated intake of monounsaturated fatty acids is associated with reduced adipocyte hypertrophy, adipose tissue infiltration of proinflammatory macrophages, and inflammation and improved insulin sensitivity [140–142]. In line with these findings, oleic acid (C18:1), the most abundant monounsaturated fatty acid found in human diet, promotes the secretion of the anti-inflammatory adipokine adiponectin and impairs the proinflammatory resistin in 3T3-L1 adipocytes [143]. Furthermore, diet supplementation with macadamia oil, a rich source of oleic acid, improves lipid metabolism and glucose homeostasis in diet-induced obese mice [144, 145]. Although oleic acid is the major fatty acid found in macadamia oil, this nut is also an important natural source of the monounsaturated fatty acid palmitoleic acid (C16:1). This fatty acid, which can be obtained either from diet or from endogenous synthesis by stearoyl-CoA desaturase- (SCD-) 1 mainly in adipose tissue and liver, was shown to enhance whole-body glucose disposal and attenuate hepatic steatosis in diet-induced obese mice [146, 147] and protect β-cell from death induced by palmitic acid [148, 149]. In line with those findings, a two-week supplementation with palmitoleic acid improved glucose homeostasis and insulin sensitivity, reduced hepatic steatosis, and increased skeletal muscle fatty acid oxidation in diet-induced obese mice [150]. In addition, palmitoleic acid also increased hepatic oxidative metabolism by activating the AMPK-fibroblast growth factor- (FGF-) 21-peroxisome proliferator-activated receptor (PPAR) α axis [151]. In addition to these beneficial metabolic actions, palmitoleic acid was recently shown to have anti-inflammatory properties. Indeed, macrophages pretreated with palmitoleic acid secrete less proinflammatory cytokines after either LPS or palmitic acid treatment [152, 153] and displayed reduced macrophage polarization to a M1 phenotype in part due to AMPK activation [154]. Altogether, these findings support a possible utilization of palmitoleic acid supplementation as a nonpharmacological strategy to reduce obesity-associated chronic low-grade inflammation [155]. Interestingly, palmitoleic acid was also shown to enhance lipolysis, glucose uptake, and GLUT-4 content in adipocytes, such effects that are mechanistically induced by PPARα and AMPK activation, respectively [156, 157]. Whether palmitoleic acid also has anti-inflammatory actions in white adipose tissue needs to be investigated.

1.8. ω-6 Polyunsaturated Fatty Acids. In addition to the high content of saturated fatty acids, another main feature defining the Western diet is the elevated ω-6 and low ω-3 polyunsaturated fatty acid contents [158]. Evidence indicates that this high ω-6/ω-3 ratio dietary pattern is one of the main causes of the rise in obesity and associated metabolic diseases seen in the last decades [159]. Linoleic acid, the most abundant ω-6 fatty acid in the Western diet, has important actions on cholesterol metabolism, as well as on inflammation. More specifically, linoleic acid was shown to lower blood cholesterol levels by increasing both hepatic clearance of low-density lipoprotein (LDL) [160] and production of bile acids and to be proinflammatory by activating NFκB in endothelial cells [161], although this does not seem to be reflected by systemic markers of inflammation [162]. Linoleic acid can be enzymatically converted to arachidonic acid, a ω-6 fatty acid that acts as the precursor for the synthesis of two classes of lipid mediators known as eicosanoids (prostaglandins, prostacyclins, thromboxane, and leukotrienes) and endocannabinoids (anandamide and 2-arachidonoylglycerol, among others). Eicosanoids are potent regulators of inflammation and immune function, being therefore implicated in the development of chronic metabolic diseases such as obesity, insulin resistance, and cancer [159]. Indeed, recent studies have shown that the eicosanoid leukotriene B4 promotes adipose tissue inflammation by inducing tissue macrophage

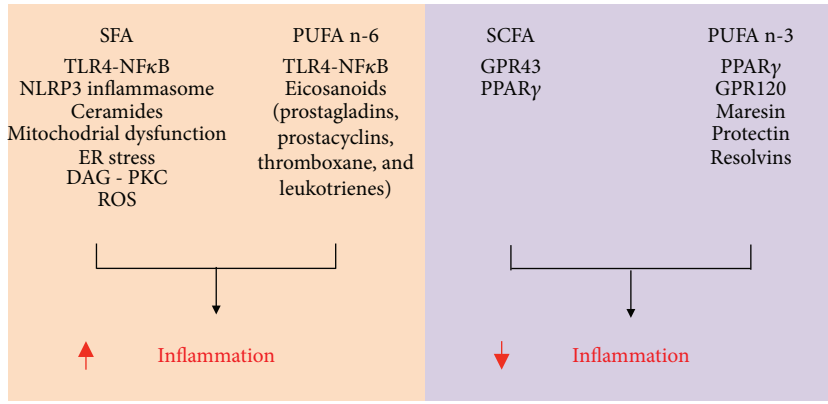

Figure 5: General overview of the mechanisms by which different fatty acids modulate inflammation. AMPK: AMP-activated protein kinase; DAG: diacylglycerol; ER: endoplasmic reticulum; GPR: G protein-coupled receptor; PKC: protein kinase C; PPAR: peroxisome proliferator-activated receptor; PUFA n-6: polyunsaturated n-6 fatty acids; PUFA n-3: polyunsaturated n-3 fatty acids; ROS: reactive oxygen species; SCFA: short-chain fatty acids; SFA: saturated fatty acids; TLR: toll-like receptor.

chemotaxis and polarization to the proinflammatory M1 profile, as well as insulin resistance in the liver and skeletal muscle [163]. Interestingly, opposite effects were seen upon treatment with the eicosanoid lipoxin A4, which reduced adipose tissue inflammation as evidenced by diminished tissue expression of proinflammatory cytokines and higher macrophage polarization to the anti-inflammatory M2 profile [164]. These findings indicate that different eicosanoids have distinct roles in the regulation of adipose tissue inflammation and therefore in the development of obesity-associated insulin resistance.

1.9. ω-3 Polyunsaturated Fatty Acids. It has been known since the 1980s that fish oil, which is rich in the ω-3 polyunsaturated fatty acids eicosapentaenoic acid (EPA) (C20:5, ω-3) and docosahexaenoic acid (DHA) (C22:6, ω-3), has many beneficial health effects. Indeed, increased whole-body ω-3 polyunsaturated fatty acid availability either genetically or through dietary supplementation is associated with hypotriglyceridemia [165], improvement in cardiovascular health by diminishing platelet aggregation and thromboxane levels [166, 167], and attenuation of systemic inflammation [168, 169]. More recently, ω-3 polyunsaturated fatty acids were also shown to protect mice from diet-induced obesity, insulin resistance, hepatic steatosis, and tumorigenesis; such effects were attributed at least in part to the anti-inflammatory properties of these fatty acids [123, 170]. Several mechanisms have been proposed to account for the anti-inflammatory actions of ω-3 polyunsaturated fatty acids including the activation of the plasma membrane G protein-coupled receptor 120 (GPR120) [171], activation of the nuclear receptor PPARγ [172], inhibition of the conversion of ω-6 fatty acids into eicosanoids [159], alterations in plasma membrane composition, fluidity and signaling [173], and induction of the synthesis of proresolution lipid mediators such as resolvins, protectins, and maresins [174]. Among these, recent studies have shown that activation of GPR120, a receptor mainly expressed in adipocytes and macrophages, may be essential to the anti-inflammatory actions of ω-3 polyunsaturated fatty acids. Indeed, both EPA and DHA were shown to impair LPS-induced JNK activation and TNF-α and IL-6 secretion by RAW 264.7 cells and 3T3-L1 adipocytes *in vitro* through the activation of GPR120 [171]. In line with those findings, mice deficient in GPR120 were resistant to the anti-inflammatory actions and the improvement in whole-body glucose homeostasis induced by the intake of diet rich in ω-3 polyunsaturated fatty acids [171]. Two recent studies, however, have challenged the notion that GPR120 activation is mandatory for those ω-3 polyunsaturated fatty acid actions. These studies have shown that intake of diet rich in ω-3 polyunsaturated fatty acids was equally effective in reducing body weight gain, improving glucose homeostasis and attenuating inflammation in a new generated mice deficient in GPR120 and wild-type controls [175, 176].

Another mechanism by which ω-3 polyunsaturated fatty acids may reduce inflammation is by enhancing the synthesis of proresolution lipid mediators, namely, protectins, resolvins, and maresins. Both EPA (e-series) and DHA (d-series) are precursors for the synthesis of these mediators [177], which have been shown to control the magnitude and duration of inflammatory processes in several rodent models of chronic diseases [174]. In line with this notion, the resolvin E1 and protectin D1 were shown to improve insulin sensitivity and reduce hepatic steatosis and adipose tissue inflammation in diet-induced obese mice [178], whereas resolvin D1 improved glucose tolerance, increased adiponectin secretion, and reduced adipose tissue macrophage recruitment and formation of crown-like structures in genetically obese *db*/*db* mice [179]. Furthermore, protectin DX improved glucose homeostasis in *db*/*db* mice by promoting IL-6 secretion from skeletal muscle without affecting white adipose tissue inflammation [180]. Further studies characterizing the biological function of already described and new metabolites from EPA and DHA are required to explore the promising usage of these lipids in the prevention and/or treatment of chronic inflammatory diseases.

1.10. Short-Chain Fatty Acids (SCFA). The short-chain fatty acids acetate (C_2), propionate (C_3), and butyrate (C_4) are produced at the intestine by anaerobic fermentation of

nondigestible dietary fibers, being readily absorbed and used as energy source by colonocytes and by other body tissues including liver and muscle [181]. In addition to their role as metabolic substrates, short-chain fatty acids regulate several aspects of inflammatory processes such as the recruitment of circulating leukocytes in the inflammatory site, production of chemokines and cytokines, expression of adhesion molecules, production of eicosanoids and reactive oxygen species, and lymphocyte proliferation and differentiation [124]. Studies evaluating the effects of short-chain fatty acids in animal models of inflammatory diseases including acute kidney injury, obesity, and T2D indicate that these molecules are potent anti-inflammatory agents [182, 183]. Indeed, sodium butyrate administration to obese and diabetic *db*/*db* mice markedly attenuated adipose tissue inflammation as evidenced by reduced tissue lymphocyte infiltration, cytokine expression and NLRP3 inflammasome activity, and improved glucose homeostasis [184]. Furthermore, propionate reduced the proinflammatory response and cytokine secretion induced by LPS in human adipose tissue explants and macrophages [185], whereas butyrate activates the anti-inflammatory Treg cells suppressing the secretion of cytokines via activation of membrane G protein-coupled receptors GPR43/FFAR2 [186]. These receptors, which are mainly expressed in adipose tissue (adipocytes), intestines, and immune cells and signals through G_q and $G_{i/o}$, ERK, MAPK, and intracellular Ca^{2+}, are important mediators of short-chain fatty acid actions [187]. Noteworthily, as recently reviewed [188], inconsistent results have been obtained in studies with GPR43 deletion in mice, which precludes a full appreciation of the role of these receptors in chronic inflammatory conditions. Finally, short-chain fatty acids were also shown to impair LPS-induced production of nitric oxide and proinflammatory cytokines in the macrophage cell line RAW264.7; such effect seems to involve inhibition of NFκB signaling [189].

In addition to inflammation, short-chain fatty acids also have important effects on energy homeostasis. Recent studies have found that diet enrichment with 5% short-chain fatty acids reduced body weight, adiposity, and hepatic steatosis in diet-induced obese mice by downregulating the activity of the nuclear receptor PPARγ [182], whereas nanoparticle-delivered acetate reduced diet-induced body weight gain, hepatic steatosis, and adiposity by enhancing hepatic mitochondrial function and inducing adipose tissue browning [190].

1.11. Newly Identified Lipids and Inflammation. The development of highly-sensitive OMICS techniques (lipidomic, metabolomic, genomic, transcriptomic, epigenomic, and proteomic) in the last decades has allowed the large-scale study of different classes of molecules in distinct compartments and conditions. Among those, metabolomic profiling and lipidomic profiling have emerged as promising methodologies to uncover new metabolites/lipids that either predict or are involved in the development of insulin resistance/T2D. Recently, a metabolomic study of the plasma of 399 nondiabetic subjects with a wide range in degree of insulin sensitivity and glucose tolerance identified a group of three metabolites (α-hydroxybutyrate, oleate, and L-glycerylphosphorylcholine) that together could predict the development of insulin resistance [191]. Furthermore, lipidomic characterization of obese, but insulin-sensitive mice, identified a class of endogenously synthesized lipids denominated as branched fatty acid esters of hydroxy fatty acids (FAHFAs) that improves glucose homeostasis and insulin sensitivity and reduces adipose tissue inflammation in diet-induced obese mice [192]. These are only two among many examples of OMICS application to the study of different aspects of obesity-associated inflammation and insulin resistance. These highly sensitive techniques will help us both to unveil the many molecules involved in the development of these diseases and provide major insights in the novel strategies to prevent and treat them.

2. Conclusions

There is an established body of literature indicating that nutrients and nutrient sensors are important players involved in the development and maintenance of obesity-associated inflammation and insulin resistance. In these studies, important advances have been made in the characterization of the mechanisms by which nutrients exert their actions, resulting in the unveiling of new therapeutic targets for the treatment of metabolic diseases. Despite this progress, we are far from having the complete understanding about the complex interaction between nutrients and obesity. Indeed, with the advances of techniques such as metabolomics and lipidomics, new nutrient-related molecules are being discovered and characterized for their potential implication in the development of obesity and insulin resistance. The characterization of nutrients and derived metabolites that present proresolution properties towards obesity-associated chronic low-grade systemic inflammation is of major importance if we are to develop novel, effective therapies to prevent metabolic and cardiovascular complications associated with this disease.

Conflicts of Interest

The authors declare no conflict of interest that would prejudice the impartiality of this scientific work.

Acknowledgments

Funding was provided by Fundação de Amparo à Pesquisa do Estado de São Paulo (FAPESP) to Alex S. Yamashita (no. 13/15825-5), Thiago Belchior (no. 15/22983-1), and William T. Festuccia (nos. 10/52191-6 and 15/19530-5). The authors thank Marina da Costa Rosa for the fruitful discussion during the development of this article.

References

[1] C. J. Nolan, P. Damm, and M. Prentki, "Type 2 diabetes across generations: from pathophysiology to prevention and management," *Lancet*, vol. 378, no. 9786, pp. 169–181, 2011.

[2] I. J. Neeland, P. Poirier, and J. P. Després, "Cardiovascular and metabolic heterogeneity of obesity: clinical challenges

and implications for management," *Circulation*, vol. 137, no. 13, pp. 1391–1406, 2018.

[3] K. Ogurtsova, J. D. da Rocha Fernandes, Y. Huang et al., "IDF diabetes atlas: global estimates for the prevalence of diabetes for 2015 and 2040," *Diabetes Research and Clinical Practice*, vol. 128, pp. 40–50, 2017.

[4] A. Guilherme, J. V. Virbasius, V. Puri, and M. P. Czech, "Adipocyte dysfunctions linking obesity to insulin resistance and type 2 diabetes," *Nature Reviews Molecular Cell Biology*, vol. 9, no. 5, pp. 367–377, 2008.

[5] M. P. Czech, "Insulin action and resistance in obesity and type 2 diabetes," *Nature Medicine*, vol. 23, no. 7, pp. 804–814, 2017.

[6] S. M. Reilly and A. R. Saltiel, "Adapting to obesity with adipose tissue inflammation," *Nature Reviews Endocrinology*, vol. 13, no. 11, pp. 633–643, 2017.

[7] J. Y. Huh, Y. J. Park, M. Ham, and J. B. Kim, "Crosstalk between adipocytes and immune cells in adipose tissue inflammation and metabolic dysregulation in obesity," *Molecules and Cells*, vol. 37, no. 5, pp. 365–371, 2014.

[8] S. P. Weisberg, D. McCann, M. Desai, M. Rosenbaum, R. L. Leibel, and A. W. Ferrante Jr, "Obesity is associated with macrophage accumulation in adipose tissue," *The Journal of Clinical Investigation*, vol. 112, no. 12, pp. 1796–1808, 2003.

[9] K. L. Hoehn, C. Hohnen-Behrens, A. Cederberg et al., "IRS1-independent defects define major nodes of insulin resistance," *Cell Metabolism*, vol. 7, no. 5, pp. 421–433, 2008.

[10] M. F. Gregor and G. S. Hotamisligil, "Inflammatory mechanisms in obesity," *Annual Review of Immunology*, vol. 29, no. 1, pp. 415–445, 2011.

[11] L. Chantranupong, R. L. Wolfson, and D. M. Sabatini, "Nutrient-sensing mechanisms across evolution," *Cell*, vol. 161, no. 1, pp. 67–83, 2015.

[12] S. Rauschert, O. Uhl, B. Koletzko, and C. Hellmuth, "Metabolomic biomarkers for obesity in humans: a short review," *Annals of Nutrition and Metabolism*, vol. 64, no. 3-4, pp. 314–324, 2014.

[13] E. M. Bailyes, B. T. Navé, M. A. Soos, S. R. Orr, A. C. Hayward, and K. Siddle, "Insulin receptor/IGF-I receptor hybrids are widely distributed in mammalian tissues: quantification of individual receptor species by selective immunoprecipitation and immunoblotting," *Biochemical Journal*, vol. 327, no. 1, pp. 209–215, 1997.

[14] M. Federici, O. Porzio, L. Zucaro et al., "Increased abundance of insulin/IGF-I hybrid receptors in adipose tissue from NIDDM patients," *Molecular and Cellular Endocrinology*, vol. 135, no. 1, pp. 41–47, 1997.

[15] R. A. Haeusler, T. E. McGraw, and D. Accili, "Biochemical and cellular properties of insulin receptor signalling," *Nature Reviews Molecular Cell Biology*, vol. 19, no. 1, pp. 31–44, 2018.

[16] F. S. Thong, C. B. Dugani, and A. Klip, "Turning signals on and off: GLUT4 traffic in the insulin-signaling highway," *Physiology*, vol. 20, pp. 271–284, 2005.

[17] L. Rui, "Energy metabolism in the liver," *Comprehensive Physiology*, vol. 4, no. 1, pp. 177–197, 2014.

[18] R. A. Saxton and D. M. Sabatini, "mTOR signaling in growth, metabolism, and disease," *Cell*, vol. 169, no. 2, pp. 361–371, 2017.

[19] H. Gehart, S. Kumpf, A. Ittner, and R. Ricci, "MAPK signalling in cellular metabolism: stress or wellness?," *EMBO Reports*, vol. 11, no. 11, pp. 834–840, 2010.

[20] F. Tremblay, S. Brûlé, S. Hee Um et al., "Identification of IRS-1 Ser-1101 as a target of S6K1 in nutrient- and obesity-induced insulin resistance," *Proceedings of the National Academy of Sciences of the United States of America*, vol. 104, no. 35, pp. 14056–14061, 2007.

[21] Y. Yu, S. O. Yoon, G. Poulogiannis et al., "Phosphoproteomic analysis identifies Grb10 as an mTORC1 substrate that negatively regulates insulin signaling," *Science*, vol. 332, no. 6035, pp. 1322–1326, 2011.

[22] P. P. Hsu, S. A. Kang, J. Rameseder et al., "The mTOR-regulated phosphoproteome reveals a mechanism of mTORC1-mediated inhibition of growth factor signaling," *Science*, vol. 332, no. 6035, pp. 1317–1322, 2011.

[23] K. J. Warren, X. Fang, N. M. Gowda, J. J. Thompson, and N. M. Heller, "The TORC1-activated proteins, p70S6K and GRB10, regulate IL-4 signaling and M2 macrophage polarization by modulating phosphorylation of insulin receptor substrate-2," *Journal of Biological Chemistry*, vol. 291, no. 48, pp. 24922–24930, 2016.

[24] G. S. Hotamisligil, N. S. Shargill, and B. M. Spiegelman, "Adipose expression of tumor necrosis factor-alpha: direct role in obesity-linked insulin resistance," *Science*, vol. 259, no. 5091, pp. 87–91, 1993.

[25] G. S. Hotamisligil and B. M. Spiegelman, "Tumor necrosis factor α: a key component of the obesity-diabetes link," *Diabetes*, vol. 43, no. 11, pp. 1271–1278, 1994.

[26] A. Festa, R. D'Agostino Jr, R. P. Tracy, S. M. Haffner, and Insulin Resistance Atherosclerosis Study, "Elevated levels of acute-phase proteins and plasminogen activator inhibitor-1 predict the development of type 2 diabetes: the insulin resistance atherosclerosis study," *Diabetes*, vol. 51, no. 4, pp. 1131–1137, 2002.

[27] J. A. Alvarez, P. B. Higgins, R. A. Oster, J. R. Fernandez, B. E. Darnell, and B. A. Gower, "Fasting and postprandial markers of inflammation in lean and overweight children," *The American Journal of Clinical Nutrition*, vol. 89, no. 4, pp. 1138–1144, 2009.

[28] K. T. Uysal, S. M. Wiesbrock, M. W. Marino, and G. S. Hotamisligil, "Protection from obesity-induced insulin resistance in mice lacking TNF-α function," *Nature*, vol. 389, no. 6651, pp. 610–614, 1997.

[29] T. L. Stanley, M. V. Zanni, S. Johnsen et al., "TNF-α antagonism with etanercept decreases glucose and increases the proportion of high molecular weight adiponectin in obese subjects with features of the metabolic syndrome," *The Journal of Clinical Endocrinology & Metabolism*, vol. 96, no. 1, pp. E146–E150, 2011.

[30] H. Dominguez, H. Storgaard, C. Rask-Madsen et al., "Metabolic and vascular effects of tumor necrosis factor-α blockade with etanercept in obese patients with type 2 diabetes," *Journal of Vascular Research*, vol. 42, no. 6, pp. 517–525, 2005.

[31] M. A. Gonzalez-Gay, J. M. De Matias, C. Gonzalez-Juanatey et al., "Anti-tumor necrosis factor-α blockade improves insulin resistance in patients with rheumatoid arthritis," *Clinical and Experimental Rheumatology*, vol. 24, no. 1, pp. 83–86, 2006.

[32] I. Ferraz-Amaro, M. Arce-Franco, J. Muñiz et al., "Systemic blockade of TNF-α does not improve insulin resistance in humans," *Hormone and Metabolic Research*, vol. 43, no. 11, pp. 801–808, 2011.

[33] T. C. Wascher, J. H. Lindeman, H. Sourij, T. Kooistra, G. Pacini, and M. Roden, "Chronic TNF-α neutralization

does not improve insulin resistance or endothelial function in "healthy" men with metabolic syndrome," *Molecular Medicine*, vol. 17, no. 3-4, pp. 189–193, 2011.

[34] C. M. Larsen, M. Faulenbach, A. Vaag et al., "Interleukin-1-receptor antagonist in type 2 diabetes mellitus," *The New England Journal of Medicine*, vol. 356, no. 15, pp. 1517–1526, 2007.

[35] P. D. Cani, J. Amar, M. A. Iglesias et al., "Metabolic endotoxemia initiates obesity and insulin resistance," *Diabetes*, vol. 56, no. 7, pp. 1761–1772, 2007.

[36] J. R. Ussher, T. R. Koves, V. J. J. Cadete et al., "Inhibition of de novo ceramide synthesis reverses diet-induced insulin resistance and enhances whole-body oxygen consumption," *Diabetes*, vol. 59, no. 10, pp. 2453–2464, 2010.

[37] P. D. Cani, R. Bibiloni, C. Knauf et al., "Changes in gut microbiota control metabolic endotoxemia-induced inflammation in high-fat diet-induced obesity and diabetes in mice," *Diabetes*, vol. 57, no. 6, pp. 1470–1481, 2008.

[38] B. Vandanmagsar, Y. H. Youm, A. Ravussin et al., "The NLRP3 inflammasome instigates obesity-induced inflammation and insulin resistance," *Nature Medicine*, vol. 17, no. 2, pp. 179–188, 2011.

[39] B. Miraghazadeh and M. C. Cook, "Nuclear factor-kappaB in autoimmunity: man and mouse," *Frontiers in Immunology*, vol. 9, p. 613, 2018.

[40] S.-X. Tan, K. H. Fisher-Wellman, D. J. Fazakerley et al., "Selective insulin resistance in adipocytes," *Journal of Biological Chemistry*, vol. 290, no. 18, pp. 11337–11348, 2015.

[41] S. Li, M. S. Brown, and J. L. Goldstein, "Bifurcation of insulin signaling pathway in rat liver: mTORC1 required for stimulation of lipogenesis, but not inhibition of gluconeogenesis," *Proceedings of the National Academy of Sciences of the United States of America*, vol. 107, no. 8, pp. 3441–3446, 2010.

[42] S. Timmers, M. Nabben, M. Bosma et al., "Augmenting muscle diacylglycerol and triacylglycerol content by blocking fatty acid oxidation does not impede insulin sensitivity," *Proceedings of the National Academy of Sciences of the United States of America*, vol. 109, no. 29, pp. 11711–11716, 2012.

[43] M. C. Oliveira, Z. Menezes-Garcia, M. C. Henriques et al., "Acute and sustained inflammation and metabolic dysfunction induced by high refined carbohydrate-containing diet in mice," *Obesity*, vol. 21, no. 9, pp. E396–E406, 2013.

[44] L. S. C. Oliveira, D. A. Santos, S. Barbosa-da-Silva, C. A. Mandarim-de-Lacerda, and M. B. Aguila, "The inflammatory profile and liver damage of a sucrose-rich diet in mice," *The Journal of Nutritional Biochemistry*, vol. 25, no. 2, pp. 193–200, 2014.

[45] Q. Hao, H. H. Lillefosse, E. Fjaere et al., "High-glycemic index carbohydrates abrogate the antiobesity effect of fish oil in mice," *American Journal of Physiology Endocrinology and Metabolism*, vol. 302, no. 9, pp. E1097–E1112, 2012.

[46] C. A. Roncal-Jimenez, M. A. Lanaspa, C. J. Rivard et al., "Sucrose induces fatty liver and pancreatic inflammation in male breeder rats independent of excess energy intake," *Metabolism*, vol. 60, no. 9, pp. 1259–1270, 2011.

[47] W. Wu, H. Tsuchida, T. Kato et al., "Fat and carbohydrate in western diet contribute differently to hepatic lipid accumulation," *Biochemical and Biophysical Research Communications*, vol. 461, no. 4, pp. 681–686, 2015.

[48] P. C. Calder, N. Ahluwalia, F. Brouns et al., "Dietary factors and low-grade inflammation in relation to overweight and obesity," *The British Journal of Nutrition*, vol. 106, Supplement 3, pp. S5–78, 2011.

[49] A. Negre-Salvayre, R. Salvayre, N. Augé, R. Pamplona, and M. Portero-Otín, "Hyperglycemia and glycation in diabetic complications," *Antioxidants & Redox Signaling*, vol. 11, no. 12, pp. 3071–3109, 2009.

[50] K. Maedler, P. Sergeev, F. Ris et al., "Glucose-induced β cell production of IL-1β contributes to glucotoxicity in human pancreatic islets," *The Journal of Clinical Investigation*, vol. 110, no. 6, pp. 851–860, 2002.

[51] A. J. Wolf, C. N. Reyes, W. Liang et al., "Hexokinase is an innate immune receptor for the detection of bacterial peptidoglycan," *Cell*, vol. 166, no. 3, pp. 624–636, 2016.

[52] T. Rønningen, A. Shah, A. H. Reiner, P. Collas, and J. Ø. Moskaug, "Epigenetic priming of inflammatory response genes by high glucose in adipose progenitor cells," *Biochemical and Biophysical Research Communications*, vol. 467, no. 4, pp. 979–986, 2015.

[53] X. Xu, X. Qi, Y. Shao et al., "High glucose induced-macrophage activation through TGF-β-activated kinase 1 signaling pathway," *Inflammation Research*, vol. 65, no. 8, pp. 655–664, 2016.

[54] N. Shanmugam, M. A. Reddy, M. Guha, and R. Natarajan, "High glucose-induced expression of proinflammatory cytokine and chemokine genes in monocytic cells," *Diabetes*, vol. 52, no. 5, pp. 1256–1264, 2003.

[55] Y. Lin, A. H. Berg, P. Iyengar et al., "The hyperglycemia-induced inflammatory response in adipocytes: the role of reactive oxygen species," *Journal of Biological Chemistry*, vol. 280, no. 6, pp. 4617–4626, 2005.

[56] Y. Li, H. Ding, X. Wang et al., "High levels of acetoacetate and glucose increase expression of cytokines in bovine hepatocytes, through activation of the NF-κB signalling pathway," *The Journal of Dairy Research*, vol. 83, no. 01, pp. 51–57, 2016.

[57] D. Koya, M. R. Jirousek, Y. W. Lin, H. Ishii, K. Kuboki, and G. L. King, "Characterization of protein kinase C beta isoform activation on the gene expression of transforming growth factor-beta, extracellular matrix components, and prostanoids in the glomeruli of diabetic rats," *The Journal of Clinical Investigation*, vol. 100, no. 1, pp. 115–126, 1997.

[58] V. Kolm-Litty, U. Sauer, A. Nerlich, R. Lehmann, and E. D. Schleicher, "High glucose-induced transforming growth factor beta1 production is mediated by the hexosamine pathway in porcine glomerular mesangial cells," *The Journal of Clinical Investigation*, vol. 101, no. 1, pp. 160–169, 1998.

[59] C. J. Green, M. Pedersen, B. K. Pedersen, and C. Scheele, "Elevated NF-κB activation is conserved in human myocytes cultured from obese type 2 diabetic patients and attenuated by AMP-activated protein kinase," *Diabetes*, vol. 60, no. 11, pp. 2810–2819, 2011.

[60] K. E. Bornfeldt and I. Tabas, "Insulin resistance, hyperglycemia, and atherosclerosis," *Cell Metabolism*, vol. 14, no. 5, pp. 575–585, 2011.

[61] A. Rimessi, M. Previati, F. Nigro, M. R. Wieckowski, and P. Pinton, "Mitochondrial reactive oxygen species and inflammation: molecular mechanisms, diseases and promising therapies," *The International Journal of Biochemistry & Cell Biology*, vol. 81, pp. 281–293, 2016.

[62] R. Zhou, A. Tardivel, B. Thorens, I. Choi, and J. Tschopp, "Thioredoxin-interacting protein links oxidative stress to

inflammasome activation," *Nature Immunology*, vol. 11, no. 2, pp. 136–140, 2010.

[63] M. Lamkanfi and V. M. Dixit, "Mechanisms and functions of inflammasomes," *Cell*, vol. 157, no. 5, pp. 1013–1022, 2014.

[64] Y. Shen, L. Lu, F. Ding et al., "Association of increased serum glycated albumin levels with low coronary collateralization in type 2 diabetic patients with stable angina and chronic total occlusion," *Cardiovascular Diabetology*, vol. 12, no. 1, p. 165, 2013.

[65] K. Isoda, E. Folco, M. R. Marwali, F. Ohsuzu, and P. Libby, "Glycated LDL increases monocyte CC chemokine receptor 2 expression and monocyte chemoattractant protein-1-mediated chemotaxis," *Atherosclerosis*, vol. 198, no. 2, pp. 307–312, 2008.

[66] S. F. Yan, R. Ramasamy, and A. M. Schmidt, "Mechanisms of disease: advanced glycation end-products and their receptor in inflammation and diabetes complications," *Nature Clinical Practice Endocrinology & Metabolism*, vol. 4, no. 5, pp. 285–293, 2008.

[67] B. Liliensiek, M. A. Weigand, A. Bierhaus et al., "Receptor for advanced glycation end products (RAGE) regulates sepsis but not the adaptive immune response," *The Journal of Clinical Investigation*, vol. 113, no. 11, pp. 1641–1650, 2004.

[68] T. Chavakis, A. Bierhaus, and P. Nawroth, "RAGE (receptor for advanced glycation end products): a central player in the inflammatory response," *Microbes and Infection*, vol. 6, no. 13, pp. 1219–1225, 2004.

[69] X. Jin, T. Yao, Z.'. Zhou et al., "Advanced glycation end products enhance macrophages polarization into M1 phenotype through activating RAGE/NF-κB pathway," *BioMed Research International*, vol. 2015, Article ID 732450, 12 pages, 2015.

[70] T. Chavakis, A. Bierhaus, N. Al-Fakhri et al., "The pattern recognition receptor (RAGE) is a counterreceptor for leukocyte integrins: a novel pathway for inflammatory cell recruitment," *The Journal of Experimental Medicine*, vol. 198, no. 10, pp. 1507–1515, 2003.

[71] S. C. Lin and D. G. Hardie, "AMPK: sensing glucose as well as cellular energy status," *Cell Metabolism*, vol. 27, no. 2, pp. 299–313, 2018.

[72] S. Galic, M. D. Fullerton, J. D. Schertzer et al., "Hematopoietic AMPK β1 reduces mouse adipose tissue macrophage inflammation and insulin resistance in obesity," *The Journal of Clinical Investigation*, vol. 121, no. 12, pp. 4903–4915, 2011.

[73] C. R. Lindholm, R. L. Ertel, J. D. Bauwens, E. G. Schmuck, J. D. Mulligan, and K. W. Saupe, "A high-fat diet decreases AMPK activity in multiple tissues in the absence of hyperglycemia or systemic inflammation in rats," *Journal of Physiology and Biochemistry*, vol. 69, no. 2, pp. 165–175, 2013.

[74] D. Sag, D. Carling, R. D. Stout, and J. Suttles, "Adenosine 5′-monophosphate-activated protein kinase promotes macrophage polarization to an anti-inflammatory functional phenotype," *Journal of Immunology*, vol. 181, no. 12, pp. 8633–8641, 2008.

[75] C. M. Krawczyk, T. Holowka, J. Sun et al., "Toll-like receptor-induced changes in glycolytic metabolism regulate dendritic cell activation," *Blood*, vol. 115, no. 23, pp. 4742–4749, 2010.

[76] G. Pilon, P. Dallaire, and A. Marette, "Inhibition of inducible nitric-oxide synthase by activators of AMP-activated protein kinase: a new mechanism of action of insulin-sensitizing drugs," *Journal of Biological Chemistry*, vol. 279, no. 20, pp. 20767–20774, 2004.

[77] X. Zhao, J. W. Zmijewski, E. Lorne et al., "Activation of AMPK attenuates neutrophil proinflammatory activity and decreases the severity of acute lung injury," *American Journal of Physiology-Lung Cellular and Molecular Physiology*, vol. 295, no. 3, pp. L497–L504, 2008.

[78] S. A. Hawley, M. D. Fullerton, F. A. Ross et al., "The ancient drug salicylate directly activates AMP-activated protein kinase," *Science*, vol. 336, no. 6083, pp. 918–922, 2012.

[79] T. Kadowaki, T. Yamauchi, N. Kubota, K. Hara, K. Ueki, and K. Tobe, "Adiponectin and adiponectin receptors in insulin resistance, diabetes, and the metabolic syndrome," *The Journal of Clinical Investigation*, vol. 116, no. 7, pp. 1784–1792, 2006.

[80] P. Felig, E. Marliss, and G. F. Cahill Jr, "Plasma amino acid levels and insulin secretion in obesity," *The New England Journal of Medicine*, vol. 281, no. 15, pp. 811–816, 1969.

[81] C. B. Newgard, J. An, J. R. Bain et al., "A branched-chain amino acid-related metabolic signature that differentiates obese and lean humans and contributes to insulin resistance," *Cell Metabolism*, vol. 9, no. 4, pp. 311–326, 2009.

[82] T. J. Wang, M. G. Larson, R. S. Vasan et al., "Metabolite profiles and the risk of developing diabetes," *Nature Medicine*, vol. 17, no. 4, pp. 448–453, 2011.

[83] C. J. Lynch and S. H. Adams, "Branched-chain amino acids in metabolic signalling and insulin resistance," *Nature Reviews Endocrinology*, vol. 10, no. 12, pp. 723–736, 2014.

[84] C. B. Newgard, "Interplay between lipids and branched-chain amino acids in development of insulin resistance," *Cell Metabolism*, vol. 15, no. 5, pp. 606–614, 2012.

[85] F. Tremblay, M. Krebs, L. Dombrowski et al., "Overactivation of S6 kinase 1 as a cause of human insulin resistance during increased amino acid availability," *Diabetes*, vol. 54, no. 9, pp. 2674–2684, 2005.

[86] F. Tremblay and A. Marette, "Amino acid and insulin signaling via the mTOR/p 70 S6 kinase pathway. A negative feedback mechanism leading to insulin resistance in skeletal muscle cells," *Journal of Biological Chemistry*, vol. 276, no. 41, pp. 38052–38060, 2001.

[87] S. H. Um, F. Frigerio, M. Watanabe et al., "Absence of S6K1 protects against age- and diet-induced obesity while enhancing insulin sensitivity," *Nature*, vol. 431, no. 7005, pp. 200–205, 2004.

[88] L. Khamzina, A. Veilleux, S. Bergeron, and A. Marette, "Increased activation of the mammalian target of rapamycin pathway in liver and skeletal muscle of obese rats: possible involvement in obesity-linked insulin resistance," *Endocrinology*, vol. 146, no. 3, pp. 1473–1481, 2005.

[89] U. Ozcan, E. Yilmaz, L. Ozcan et al., "Chemical chaperones reduce ER stress and restore glucose homeostasis in a mouse model of type 2 diabetes," *Science*, vol. 313, no. 5790, pp. 1137–1140, 2006.

[90] F. Urano, X. Wang, A. Bertolotti et al., "Coupling of stress in the ER to activation of JNK protein kinases by transmembrane protein kinase IRE1," *Science*, vol. 287, no. 5453, pp. 664–666, 2000.

[91] J. S. Burrill, E. K. Long, B. Reilly et al., "Inflammation and ER stress regulate branched-chain amino acid uptake and metabolism in adipocytes," *Molecular Endocrinology*, vol. 29, no. 3, pp. 411–420, 2015.

[92] A. Jennings, A. MacGregor, T. Pallister, T. Spector, and A. Cassidy, "Associations between branched chain amino

acid intake and biomarkers of adiposity and cardiometabolic health independent of genetic factors: a twin study," *International Journal of Cardiology*, vol. 223, pp. 992–998, 2016.

[93] Y. Zhang, K. Guo, R. E. LeBlanc, D. Loh, G. J. Schwartz, and Y. H. Yu, "Increasing dietary leucine intake reduces diet-induced obesity and improves glucose and cholesterol metabolism in mice via multimechanisms," *Diabetes*, vol. 56, no. 6, pp. 1647–1654, 2007.

[94] H. G. Shertzer, S. E. Woods, M. Krishan, M. B. Genter, and K. J. Pearson, "Dietary whey protein lowers the risk for metabolic disease in mice fed a high-fat diet," *The Journal of Nutrition*, vol. 141, no. 4, pp. 582–587, 2011.

[95] T. Li, L. Geng, X. Chen, M. Miskowiec, X. Li, and B. Dong, "Branched-chain amino acids alleviate nonalcoholic steatohepatitis in rats," *Applied Physiology, Nutrition, and Metabolism*, vol. 38, no. 8, pp. 836–843, 2013.

[96] K. Tajiri and Y. Shimizu, "Branched-chain amino acids in liver diseases," *World Journal of Gastroenterology*, vol. 19, no. 43, pp. 7620–7629, 2013.

[97] D. Terakura, M. Shimizu, J. Iwasa et al., "Preventive effects of branched-chain amino acid supplementation on the spontaneous development of hepatic preneoplastic lesions in C57BL/KsJ-*db*/*db* obese mice," *Carcinogenesis*, vol. 33, no. 12, pp. 2499–2506, 2012.

[98] C. H. Lang, C. J. Lynch, and T. C. Vary, "BCATm deficiency ameliorates endotoxin-induced decrease in muscle protein synthesis and improves survival in septic mice," *American Journal of Physiology-Regulatory, Integrative and Comparative Physiology*, vol. 299, no. 3, pp. R935–R944, 2010.

[99] R. L. Wolfson, L. Chantranupong, R. A. Saxton et al., "Sestrin 2 is a leucine sensor for the mTORC1 pathway," *Science*, vol. 351, no. 6268, pp. 43–48, 2016.

[100] D. F. Lee, H. P. Kuo, C. T. Chen et al., "IKKβ suppression of TSC1 links inflammation and tumor angiogenesis via the mTOR pathway," *Cell*, vol. 130, no. 3, pp. 440–455, 2007.

[101] D. F. Lee, H. P. Kuo, C. T. Chen et al., "IKKβ suppression of TSC1 function links the mTOR pathway with insulin resistance," *International Journal of Molecular Medicine*, vol. 22, no. 5, pp. 633–638, 2008.

[102] M. Martin, R. E. Schifferle, N. Cuesta, S. N. Vogel, J. Katz, and S. M. Michalek, "Role of the phosphatidylinositol 3 kinase-Akt pathway in the regulation of IL-10 and IL-12 by Porphyromonas gingivalis lipopolysaccharide," *Journal of Immunology*, vol. 171, no. 2, pp. 717–725, 2003.

[103] W. T. Festuccia, P. Pouliot, I. Bakan, D. M. Sabatini, and M. Laplante, "Myeloid-specific Rictor deletion induces M1 macrophage polarization and potentiates in vivo pro-inflammatory response to lipopolysaccharide," *PLoS One*, vol. 9, no. 4, article e95432, 2014.

[104] V. A. Paschoal, M. T. Amano, T. Belchior et al., "mTORC1 inhibition with rapamycin exacerbates adipose tissue inflammation in obese mice and dissociates macrophage phenotype from function," *Immunobiology*, vol. 222, no. 2, pp. 261–271, 2017.

[105] K. Makki, S. Taront, O. Molendi-Coste et al., "Beneficial metabolic effects of rapamycin are associated with enhanced regulatory cells in diet-induced obese mice," *PLoS One*, vol. 9, no. 4, article e92684, 2014.

[106] A. Mercalli, I. Calavita, E. Dugnani et al., "Rapamycin unbalances the polarization of human macrophages to M1," *Immunology*, vol. 140, no. 2, pp. 179–190, 2013.

[107] T. Weichhart, G. Costantino, M. Poglitsch et al., "The TSC-mTOR signaling pathway regulates the innate inflammatory response," *Immunity*, vol. 29, no. 4, pp. 565–577, 2008.

[108] H. Jiang, M. Westerterp, C. Wang, Y. Zhu, and D. Ai, "Macrophage mTORC1 disruption reduces inflammation and insulin resistance in obese mice," *Diabetologia*, vol. 57, no. 11, pp. 2393–2404, 2014.

[109] P. Chimin, M. L. Andrade, T. Belchior et al., "Adipocyte mTORC1 deficiency promotes adipose tissue inflammation and NLRP3 inflammasome activation via oxidative stress and de novo ceramide synthesis," *Journal of Lipid Research*, vol. 58, no. 9, pp. 1797–1807, 2017.

[110] M. Linke, H. T. T. Pham, K. Katholnig et al., "Chronic signaling via the metabolic checkpoint kinase mTORC1 induces macrophage granuloma formation and marks sarcoidosis progression," *Nature Immunology*, vol. 18, no. 3, pp. 293–302, 2017.

[111] H. Pan, X. P. Zhong, and S. Lee, "Sustained activation of mTORC1 in macrophages increases AMPKα-dependent autophagy to maintain cellular homeostasis," *BMC Biochemistry*, vol. 17, no. 1, p. 14, 2016.

[112] A. J. Covarrubias, H. I. Aksoylar, J. Yu et al., "Akt-mTORC1 signaling regulates Acly to integrate metabolic input to control of macrophage activation," *eLife*, vol. 5, article e11612, 2016.

[113] H. Pan, T. F. O'Brien, P. Zhang, and X. P. Zhong, "The role of tuberous sclerosis complex 1 in regulating innate immunity," *Journal of Immunology*, vol. 188, no. 8, pp. 3658–3666, 2012.

[114] V. Byles, A. J. Covarrubias, I. Ben-Sahra et al., "The TSC-mTOR pathway regulates macrophage polarization," *Nature Communications*, vol. 4, no. 1, p. 2834, 2013.

[115] C. Fang, J. Yu, Y. Luo et al., "Tsc 1 is a critical regulator of macrophage survival and function," *Cellular Physiology and Biochemistry*, vol. 36, no. 4, pp. 1406–1418, 2015.

[116] T. Weichhart, M. Hengstschläger, and M. Linke, "Regulation of innate immune cell function by mTOR," *Nature Reviews Immunology*, vol. 15, no. 10, pp. 599–614, 2015.

[117] J. D. Powell, K. N. Pollizzi, E. B. Heikamp, and M. R. Horton, "Regulation of immune responses by mTOR," *Annual Review of Immunology*, vol. 30, no. 1, pp. 39–68, 2012.

[118] J. Brown, H. Wang, J. Suttles, D. T. Graves, and M. Martin, "Mammalian target of rapamycin complex 2 (mTORC2) negatively regulates Toll-like receptor 4-mediated inflammatory response via FoxO1," *Journal of Biological Chemistry*, vol. 286, no. 52, pp. 44295–44305, 2011.

[119] S. C.-C. Huang, A. M. Smith, B. Everts et al., "Metabolic reprogramming mediated by the mTORC2-IRF4 signaling axis is essential for macrophage alternative activation," *Immunity*, vol. 45, no. 4, pp. 817–830, 2016.

[120] A. M. Kirwan, Y. M. Lenighan, M. E. O'Reilly, F. C. McGillicuddy, and H. M. Roche, "Nutritional modulation of metabolic inflammation," *Biochemical Society Transactions*, vol. 45, no. 4, pp. 979–985, 2017.

[121] M. B. Fessler, L. L. Rudel, and J. M. Brown, "Toll-like receptor signaling links dietary fatty acids to the metabolic syndrome," *Current Opinion in Lipidology*, vol. 20, no. 5, pp. 379–385, 2009.

[122] E. Patterson, R. Wall, G. F. Fitzgerald, R. P. Ross, and C. Stanton, "Health implications of high dietary omega-6 polyunsaturated fatty acids," *Journal of Nutrition and Metabolism*, vol. 2012, Article ID 539426, 16 pages, 2012.

[123] M. B. MacLennan, S. E. Clarke, K. Perez et al., "Mammary tumor development is directly inhibited by lifelong n-3 polyunsaturated fatty acids," *The Journal of Nutritional Biochemistry*, vol. 24, no. 1, pp. 388–395, 2013.

[124] J. Tan, C. McKenzie, M. Potamitis, A. N. Thorburn, C. R. Mackay, and L. Macia, "The role of short-chain fatty acids in health and disease," *Advances in Immunology*, vol. 121, pp. 91–119, 2014.

[125] S. Hammad, S. Pu, and P. J. Jones, "Current evidence supporting the link between dietary fatty acids and cardiovascular disease," *Lipids*, vol. 51, no. 5, pp. 507–517, 2016.

[126] Central Committee for Medical and Community Program of the American Heart Association, "Dietary fat and its relation to heart attacks and strokes," *JAMA*, vol. 175, no. 5, pp. 389–391, 1961.

[127] A. M. Murphy, C. L. Lyons, O. M. Finucane, and H. M. Roche, "Interactions between differential fatty acids and inflammatory stressors-impact on metabolic health," *Prostaglandins, Leukotrienes, and Essential Fatty Acids*, vol. 92, pp. 49–55, 2015.

[128] J. Y. Lee, K. H. Sohn, S. H. Rhee, and D. Hwang, "Saturated fatty acids, but not unsaturated fatty acids, induce the expression of cyclooxygenase-2 mediated through Toll-like receptor 4," *Journal of Biological Chemistry*, vol. 276, no. 20, pp. 16683–16689, 2001.

[129] H. Wen, D. Gris, Y. Lei et al., "Fatty acid-induced NLRP3-ASC inflammasome activation interferes with insulin signaling," *Nature Immunology*, vol. 12, no. 5, pp. 408–415, 2011.

[130] D. Wang, Y. Wei, and M. J. Pagliassotti, "Saturated fatty acids promote endoplasmic reticulum stress and liver injury in rats with hepatic steatosis," *Endocrinology*, vol. 147, no. 2, pp. 943–951, 2006.

[131] W. L. Holland, B. T. Bikman, L. P. Wang et al., "Lipid-induced insulin resistance mediated by the proinflammatory receptor TLR4 requires saturated fatty acid-induced ceramide biosynthesis in mice," *The Journal of Clinical Investigation*, vol. 121, no. 5, pp. 1858–1870, 2011.

[132] S. Crunkhorn, F. Dearie, C. Mantzoros et al., "Peroxisome proliferator activator receptor gamma coactivator-1 expression is reduced in obesity: potential pathogenic role of saturated fatty acids and p 38 mitogen-activated protein kinase activation," *Journal of Biological Chemistry*, vol. 282, no. 21, pp. 15439–15450, 2007.

[133] H. Shi, M. V. Kokoeva, K. Inouye, I. Tzameli, H. Yin, and J. S. Flier, "TLR4 links innate immunity and fatty acid-induced insulin resistance," *The Journal of Clinical Investigation*, vol. 116, no. 11, pp. 3015–3025, 2006.

[134] Y. Watanabe, Y. Nagai, and K. Takatsu, "Activation and regulation of the pattern recognition receptors in obesity-induced adipose tissue inflammation and insulin resistance," *Nutrients*, vol. 5, no. 9, pp. 3757–3778, 2013.

[135] D. M. Erion and G. I. Shulman, "Diacylglycerol-mediated insulin resistance," *Nature Medicine*, vol. 16, no. 4, pp. 400–402, 2010.

[136] C. E. Chalfant, K. Kishikawa, M. C. Mumby, C. Kamibayashi, A. Bielawska, and Y. A. Hannun, "Long chain ceramides activate protein phosphatase-1 and protein phosphatase-2A. Activation is stereospecific and regulated by phosphatidic acid," *Journal of Biological Chemistry*, vol. 274, no. 29, pp. 20313–20317, 1999.

[137] D. J. Powell, E. Hajduch, G. Kular, and H. S. Hundal, "Ceramide disables 3-phosphoinositide binding to the pleckstrin homology domain of protein kinase B (PKB)/Akt by a PKCζ-dependent mechanism," *Molecular and Cellular Biology*, vol. 23, no. 21, pp. 7794–7808, 2003.

[138] C. Lipina and H. S. Hundal, "Sphingolipids: agents provocateurs in the pathogenesis of insulin resistance," *Diabetologia*, vol. 54, no. 7, pp. 1596–1607, 2011.

[139] G. H. Norris and C. N. Blesso, "Dietary and endogenous sphingolipid metabolism in chronic inflammation," *Nutrients*, vol. 9, no. 11, 2017.

[140] O. M. Finucane, C. L. Lyons, A. M. Murphy et al., "Monounsaturated fatty acid–enriched high-fat diets impede adipose NLRP3 inflammasome–mediated IL-1β secretion and insulin resistance despite obesity," *Diabetes*, vol. 64, no. 6, pp. 2116–2128, 2015.

[141] C. L. Lyons, E. B. Kennedy, and H. M. Roche, "Metabolic inflammation-differential modulation by dietary constituents," *Nutrients*, vol. 8, no. 5, p. 247, 2016.

[142] J. Shirakawa, H. Fujii, K. Ohnuma et al., "Diet-induced adipose tissue inflammation and liver steatosis are prevented by DPP-4 inhibition in diabetic mice," *Diabetes*, vol. 60, no. 4, pp. 1246–1257, 2011.

[143] N. Granados, J. Amengual, J. Ribot, A. Palou, and M. L. Bonet, "Distinct effects of oleic acid and its trans-isomer elaidic acid on the expression of myokines and adipokines in cell models," *The British Journal of Nutrition*, vol. 105, no. 08, pp. 1226–1234, 2011.

[144] L. S. Maguire, S. M. O'Sullivan, K. Galvin, T. P. O'Connor, and N. M. O'Brien, "Fatty acid profile, tocopherol, squalene and phytosterol content of walnuts, almonds, peanuts, hazelnuts and the macadamia nut," *International Journal of Food Sciences and Nutrition*, vol. 55, no. 3, pp. 171–178, 2004.

[145] E. A. Lima, L. S. Silveira, L. N. Masi et al., "Macadamia oil supplementation attenuates inflammation and adipocyte hypertrophy in obese mice," *Mediators of Inflammation*, vol. 2014, Article ID 870634, 9 pages, 2014.

[146] H. Cao, K. Gerhold, J. R. Mayers, M. M. Wiest, S. M. Watkins, and G. S. Hotamisligil, "Identification of a lipokine, a lipid hormone linking adipose tissue to systemic metabolism," *Cell*, vol. 134, no. 6, pp. 933–944, 2008.

[147] Z. H. Yang, H. Miyahara, and A. Hatanaka, "Chronic administration of palmitoleic acid reduces insulin resistance and hepatic lipid accumulation in KK-Ay mice with genetic type 2 diabetes," *Lipids in Health and Disease*, vol. 10, no. 1, p. 120, 2011.

[148] E. Diakogiannaki, S. Dhayal, C. E. Childs, P. C. Calder, H. J. Welters, and N. G. Morgan, "Mechanisms involved in the cytotoxic and cytoprotective actions of saturated versus monounsaturated long-chain fatty acids in pancreatic β-cells," *The Journal of Endocrinology*, vol. 194, no. 2, pp. 283–291, 2007.

[149] N. G. Morgan and S. Dhayal, "Unsaturated fatty acids as cytoprotective agents in the pancreatic β-cell," *Prostaglandins, Leukotrienes, and Essential Fatty Acids*, vol. 82, no. 4-6, pp. 231–236, 2010.

[150] C. O. Souza, A. A. S. Teixeira, E. A. Lima et al., "Palmitoleic acid (n-7) attenuates the immunometabolic disturbances caused by a high-fat diet independently of PPARα," *Mediators of Inflammation*, vol. 2014, Article ID 582197, 12 pages, 2014.

[151] C. O. de Souza, A. A. S. Teixeira, L. A. Biondo, E. A. Lima Junior, H. A. P. Batatinha, and J. C. Rosa Neto, "Palmitoleic acid improves metabolic functions in fatty liver by PPARα-dependent AMPK activation," *Journal of Cellular Physiology*, vol. 232, no. 8, pp. 2168–2177, 2017.

[152] C. O. Souza, A. A. Teixeira, L. A. Biondo, L. S. Silveira, P. C. Calder, and J. C. Rosa Neto, "Palmitoleic acid reduces the inflammation in LPS-stimulated macrophages by inhibition of NFκB, independently of PPARs," *Clinical and Experimental Pharmacology & Physiology*, vol. 44, no. 5, pp. 566–575, 2017.

[153] I. Çimen, B. Kocatürk, S. Koyuncu et al., "Prevention of atherosclerosis by bioactive palmitoleate through suppression of organelle stress and inflammasome activation," *Science Translational Medicine*, vol. 8, no. 358, article 358ra126, 2016.

[154] K. L. Chan, N. J. Pillon, D. M. Sivaloganathan et al., "Palmitoleate reverses high fat-induced proinflammatory macrophage polarization via AMP-activated protein kinase (AMPK)," *Journal of Biological Chemistry*, vol. 290, no. 27, pp. 16979–16988, 2015.

[155] C. O. de Souza, G. K. Vannice, J. C. Rosa Neto, and P. C. Calder, "Is palmitoleic acid a plausible nonpharmacological strategy to prevent or control chronic metabolic and inflammatory disorders?," *Molecular Nutrition & Food Research*, vol. 62, no. 1, 2018.

[156] A. Bolsoni-Lopes, W. T. Festuccia, T. S. M. Farias et al., "Palmitoleic acid (n-7) increases white adipocyte lipolysis and lipase content in a PPARα-dependent manner," *American Journal of Physiology-Endocrinology and Metabolism*, vol. 305, no. 9, pp. E1093–E1102, 2013.

[157] A. Bolsoni-Lopes, W. T. Festuccia, P. Chimin et al., "Palmitoleic acid (n-7) increases white adipocytes GLUT4 content and glucose uptake in association with AMPK activation," *Lipids in Health and Disease*, vol. 13, no. 1, p. 199, 2014.

[158] A. P. Simopoulos, "Evolutionary aspects of diet, the omega-6/omega-3 ratio and genetic variation: nutritional implications for chronic diseases," *Biomedicine & Pharmacotherapy*, vol. 60, no. 9, pp. 502–507, 2006.

[159] A. P. Simopoulos, "An increase in the omega-6/omega-3 fatty acid ratio increases the risk for obesity," *Nutrients*, vol. 8, no. 3, p. 128, 2016.

[160] R. P. Mensink and M. B. Katan, "Effect of dietary fatty acids on serum lipids and lipoproteins. A meta- analysis of 27 trials," *Arteriosclerosis and Thrombosis*, vol. 12, no. 8, pp. 911–919, 1992.

[161] B. Hennig, M. Toborek, S. Joshi-Barve et al., "Linoleic acid activates nuclear transcription factor-κ B (NF-κ B) and induces NF-κ B-dependent transcription in cultured endothelial cells," *The American Journal of Clinical Nutrition*, vol. 63, no. 3, pp. 322–328, 1996.

[162] P. C. Calder, "Functional roles of fatty acids and their effects on human health," *JPEN Journal of Parenteral and Enteral Nutrition*, vol. 39, pp. 18S–32S, 2015.

[163] P. Li, D. Y. Oh, G. Bandyopadhyay et al., "LTB4 promotes insulin resistance in obese mice by acting on macrophages, hepatocytes and myocytes," *Nature Medicine*, vol. 21, no. 3, pp. 239–247, 2015.

[164] E. Börgeson, A. M. F. Johnson, Y. S. Lee et al., "Lipoxin A4 attenuates obesity-induced adipose inflammation and associated liver and kidney disease," *Cell Metabolism*, vol. 22, no. 1, pp. 125–137, 2015.

[165] T. A. B. Sanders, M. Vickers, and A. P. Haines, "Effect on blood lipids and haemostasis of a supplement of cod-liver oil, rich in eicosapentaenoic and docosahexaenoic acids, in healthy young men," *Clinical Science*, vol. 61, no. 3, pp. 317–324, 1981.

[166] A. A. Ahmed and B. J. Holub, "Alteration and recovery of bleeding times, platelet aggregation and fatty acid composition of individual phospholipids in platelets of human subjects receiving a supplement of cod-liver oil," *Lipids*, vol. 19, no. 8, pp. 617–624, 1984.

[167] H. R. Knapp, I. A. G. Reilly, P. Alessandrini, and G. A. FitzGerald, "In vivo indexes of platelet and vascular function during fish-oil administration in patients with atherosclerosis," *The New England Journal of Medicine*, vol. 314, no. 15, pp. 937–942, 1986.

[168] J. M. Kremer, W. Jubiz, A. Michalek et al., "Fish-oil fatty acid supplementation in active rheumatoid arthritis. A double-blinded, controlled, crossover study," *Annals of Internal Medicine*, vol. 106, no. 4, pp. 497–503, 1987.

[169] A. Bjørneboe, E. Søyland, G.-E. A. Bjørneboe, G. Rajka, and C. A. Drevon, "Effect of dietary supplementation with eicosapentaenoic acid in the treatment of atopic dermatitis," *The British Journal of Dermatology*, vol. 117, no. 4, pp. 463–469, 1987.

[170] J. Li, F. R. Li, D. Wei et al., "Endogenous ω-3 polyunsaturated fatty acid production confers resistance to obesity, dyslipidemia, and diabetes in mice," *Molecular Endocrinology*, vol. 28, no. 8, pp. 1316–1328, 2014.

[171] D. Y. Oh, S. Talukdar, E. J. Bae et al., "GPR120 is an omega-3 fatty acid receptor mediating potent anti-inflammatory and insulin-sensitizing effects," *Cell*, vol. 142, no. 5, pp. 687–698, 2010.

[172] T. Belchior, V. A. Paschoal, J. Magdalon et al., "Omega-3 fatty acids protect from diet-induced obesity, glucose intolerance, and adipose tissue inflammation through PPARγ-dependent and PPARγ-independent actions," *Molecular Nutrition & Food Research*, vol. 59, no. 5, pp. 957–967, 2015.

[173] E. A. F. Herbst, S. Paglialunga, C. Gerling et al., "Omega-3 supplementation alters mitochondrial membrane composition and respiration kinetics in human skeletal muscle," *The Journal of Physiology*, vol. 592, no. 6, pp. 1341–1352, 2014.

[174] C. N. Serhan, "Pro-resolving lipid mediators are leads for resolution physiology," *Nature*, vol. 510, no. 7503, pp. 92–101, 2014.

[175] M. Bjursell, X. Xu, T. Admyre et al., "The beneficial effects of n-3 polyunsaturated fatty acids on diet induced obesity and impaired glucose control do not require Gpr 120," *PLoS One*, vol. 9, no. 12, article e114942, 2014.

[176] S. I. Pærregaard, M. Agerholm, A. K. Serup et al., "FFAR4 (GPR120) signaling is not required for anti-inflammatory and insulin-sensitizing effects of omega-3 fatty acids," *Mediators of Inflammation*, vol. 2016, Article ID 1536047, 12 pages, 2016.

[177] C. N. Serhan, "Resolution phase of inflammation: novel endogenous anti-inflammatory and proresolving lipid mediators and pathways," *Annual Review of Immunology*, vol. 25, pp. 101–137, 2007.

[178] A. González-Périz, R. Horrillo, N. Ferré et al., "Obesity-induced insulin resistance and hepatic steatosis are alleviated by omega-3 fatty acids: a role for resolvins and protectins," *The FASEB Journal*, vol. 23, no. 6, pp. 1946–1957, 2009.

[179] J. Hellmann, Y. Tang, M. Kosuri, A. Bhatnagar, and M. Spite, "Resolvin D1 decreases adipose tissue macrophage accumulation and improves insulin sensitivity in obese-diabetic mice," *The FASEB Journal*, vol. 25, no. 7, pp. 2399–2407, 2011.

[180] P. J. White, P. St-Pierre, A. Charbonneau et al., "Protectin DX alleviates insulin resistance by activating a myokine-liver glucoregulatory axis," *Nature Medicine*, vol. 20, no. 6, pp. 664–669, 2014.

[181] N. I. McNeil, "The contribution of the large intestine to energy supplies in man," *The American Journal of Clinical Nutrition*, vol. 39, no. 2, pp. 338–342, 1984.

[182] G. den Besten, A. Bleeker, A. Gerding et al., "Short-chain fatty acids protect against high-fat diet-induced obesity via a PPARγ-dependent switch from lipogenesis to fat oxidation," *Diabetes*, vol. 64, no. 7, pp. 2398–2408, 2015.

[183] V. Andrade-Oliveira, M. T. Amano, M. Correa-Costa et al., "Gut bacteria products prevent AKI induced by ischemia–reperfusion," *JASN Journal of the American Society of Nephrology*, vol. 26, no. 8, pp. 1877–1888, 2015.

[184] X. Wang, G. He, Y. Peng, W. Zhong, Y. Wang, and B. Zhang, "Sodium butyrate alleviates adipocyte inflammation by inhibiting NLRP3 pathway," *Scientific Reports*, vol. 5, no. 1, article 12676, 2015.

[185] S.'a. al-Lahham, H. Roelofsen, F. Rezaee et al., "Propionic acid affects immune status and metabolism in adipose tissue from overweight subjects," *European Journal of Clinical Investigation*, vol. 42, no. 4, pp. 357–364, 2012.

[186] P. M. Smith, M. R. Howitt, N. Panikov et al., "The microbial metabolites, short-chain fatty acids, regulate colonic Treg cell homeostasis," *Science*, vol. 341, no. 6145, pp. 569–573, 2013.

[187] H. Ohira, W. Tsutsui, and Y. Fujioka, "Are short chain fatty acids in gut microbiota defensive players for inflammation and atherosclerosis?," *Journal of Atherosclerosis and Thrombosis*, vol. 24, no. 7, pp. 660–672, 2017.

[188] Z. Ang and J. L. Ding, "GPR41 and GPR43 in obesity and inflammation - protective or causative?," *Frontiers in Immunology*, vol. 7, p. 28, 2016.

[189] T. Liu, J. Li, Y. Liu et al., "Short-chain fatty acids suppress lipopolysaccharide-induced production of nitric oxide and proinflammatory cytokines through inhibition of NF-κB pathway in RAW264.7 cells," *Inflammation*, vol. 35, no. 5, pp. 1676–1684, 2012.

[190] M. Sahuri-Arisoylu, L. P. Brody, J. R. Parkinson et al., "Reprogramming of hepatic fat accumulation and 'browning' of adipose tissue by the short-chain fatty acid acetate," *International Journal of Obesity*, vol. 40, no. 6, pp. 955–963, 2016.

[191] W. E. Gall, K. Beebe, K. A. Lawton et al., "α-Hydroxybutyrate is an early biomarker of insulin resistance and glucose intolerance in a nondiabetic population," *PLoS One*, vol. 5, no. 5, article e10883, 2010.

[192] M. M. Yore, I. Syed, P. M. Moraes-Vieira et al., "Discovery of a class of endogenous mammalian lipids with anti-diabetic and anti-inflammatory effects," *Cell*, vol. 159, no. 2, pp. 318–332, 2014.

Hindawi
Mediators of Inflammation
Volume 2018, Article ID 1312626, 8 pages
https://doi.org/10.1155/2018/1312626

Research Article

Folic Acid Improves the Inflammatory Response in LPS-Activated THP-1 Macrophages

Mirian Samblas,[1,2] **J. Alfredo Martínez**,[1,2,3,4] **and Fermín Milagro**[1,2]

[1]*Department of Nutrition, Food Science, and Physiology, Centre for Nutrition Research, University of Navarra, Pamplona, Spain*
[2]*Centro de Investigación Biomédica en Red de la Fisiopatología de la Obesidad y Nutrición (CIBERobn), Instituto de Salud Carlos III, Madrid, Spain*
[3]*Instituto de Investigación Sanitaria de Navarra (IdiSNA), Pamplona, Spain*
[4]*IMDEA Food, Madrid, Spain*

Correspondence should be addressed to Fermín Milagro; fmilagro@unav.es

Received 16 January 2018; Revised 19 April 2018; Accepted 16 May 2018; Published 4 July 2018

Academic Editor: José C. Rosa

DNA methylation has been suggested as a regulatory mechanism behind some inflammatory processes. The physiological actions of methyl donors, such as folic acid, choline, and vitamin B_{12} on inflammation-related disease have been associated with the synthesis of the universal methyl donor S-adenosyl methionine (SAM). The aim of this study was to evaluate the effects of folic acid, choline, vitamin B_{12}, and a combination of all on preventing the lipopolysaccharide- (LPS-) induced inflammatory response in human THP-1 monocyte/macrophage cells. Folic acid and the mixture of methyl donors reduced interleukin 1 beta *(IL1B)* and tumour necrosis factor *(TNF)* expression as well as protein secretion by these cells. Folic acid and choline decreased C-C motif chemokine ligand 2 (*CCL2*) mRNA levels. In addition to this, the methyl donor mixture reduced Cluster of differentiation 40 *(CD40)* expression, but increased serpin family E member 1 *(SERPINE1)* expression. All methyl donors increased methylation levels in CpGs located in *IL1B*, *SERPINE1*, and interleukin 18 *(IL18)* genes. However, *TNF* methylation was not modified. After treatment with folic acid and the methyl donor mixture, ChIP analysis showed no change in the binding affinity of nuclear factor-κB (NF-κB) to *IL1B* and *TNF* promoter regions after the treatment with folic acid and the methyl donor mixture. The findings of this study suggest that folic acid might contribute to the control of chronic inflammation in inflammatory-related disease.

1. Introduction

Inflammation is traditionally defined as the short-term adaptive response to fight against injury, caused by pathogens or biological and chemical stimuli [1]. Although acute inflammation is a crucial component for maintaining homeostasis in the body, persistent and chronic inflammation is involved in the development of several clinical manifestations and diseases. During inflammatory disease, monocytes and macrophages produce cytokines in response to different stimuli, such as lipopolysaccharide (LPS) [2]. The proinflammatory molecules released by macrophages in the inflamed regions orchestrate the enhancement of monocyte recruitment from blood to tissue. Recruited monocytes differentiate into macrophages to continue the inflammatory response [3]. Alongside this, studies have described that epigenetic mechanisms contribute to the pathogenesis of several chronic inflammatory-related diseases by regulating important steps such as macrophage infiltration or cytokine secretion [4, 5]. For instance, inflammatory genes like interleukins (IL) *IL6*, *IL4*, *IL8*, *IL1B*, or interferon *INF-γ* have been described to be methylated differently in several chronic inflammatory diseases [4, 6].

Methionine, folate, betaine, choline, and vitamins B_2, B_6, and B_{12} are considered methyl donor precursors naturally occurring in the diet [7]. These substances participate in the methionine pathway for the synthesis of S-adenosyl methionine (SAM), which is the universal methyl donor for DNA methylation reactions [8]. The anti-inflammatory effects exerted by some of these compounds in a variety of

inflammatory diseases have been described in previous research. For example, folic acid supplementation improved disease outcomes in subjects with hypertension, diabetes, and stroke by reducing levels of inflammatory markers (CRP, VCAM-1, IL-1β, and TNF-α) [9]. In addition to this, the combined supplementation of folate and vitamin B_{12} ameliorated inflammation during pregnancy by modifying the concentration of inflammatory cytokines [10]. Lastly, vitamin B_{12} has been negatively associated with proinflammatory cytokines and low-grade systemic inflammation [11]. On the other hand, deficiencies in the abovementioned methyl donors have also been shown to lead to adverse effects [10, 12]. For example, vitamin B_{12} deficiency has been related to metabolic disturbances such as hyperhomocysteinemia, obesity, hypertension, and insulin resistance [10]. Choline deficiency has been associated with the development of fatty liver disease and demonstrated to worsen the outcome of liver fibrosis in patients with nonalcoholic steatohepatitis (NASH) [12]. Interestingly, NASH patients that were choline-deficient exhibited amelioration of steatohepatitis after choline supplementation [13]. Similarly, methyl donor supplementation prevented HFS diet-induced liver fat accumulation in rats fed an obesogenic diet [14].

The anti-inflammatory effect of methyl donors in monocytes before differentiation and LPS-induced inflammatory response in macrophages, along with the role of DNA methylation in this process, have been scarcely studied. For this reason, the aim of this study was to investigate the effects of methyl donors, both individually and together, on the attenuation of LPS-induced inflammatory response and the possible underlying epigenetic mechanisms in human THP-1 monocyte/macrophage cells. Monocytes were incubated with folic acid, choline, and vitamin B_{12} or a methyl donor mixture of folic acid, choline, and vitamin B_{12}. Monocytes were then differentiated into macrophages and an inflammatory response was induced with LPS.

2. Material and Methods

2.1. Reagents. Folic acid, vitamin B_{12}, and choline chloride were supplied from Sigma-Aldrich (MO, USA). Phorbol 12-myristate 13-acetate (TPA) (Sigma-Aldrich) was used for differentiating THP-1 monocytes into macrophage-like cells. LPS from *E. coli* K12 strain (Invitrogen, CA, USA) was applied to activate macrophages. Thiazolyl Blue Tetrazolium Bromide (MTT) (Sigma-Aldrich) was used to investigate the toxic effects of methyl donors on THP-1 cells.

2.2. Cell Culture and Treatments. Human monocyte THP-1 cells were purchased from American Type Cell Culture (ATCC® TIB-202™, VA, USA). Cells were maintained at 37°C and 5% CO_2 in RPMI-1640 medium (Gibco) modified to contain 2 mM L-glutamine, 1 mM sodium pyruvate, 4.5 g/l glucose, and 1.5 g/l sodium bicarbonate and supplemented with 10% fetal bovine serum (GIBCO), 100 U/ml penicillin, and 100 μg/ml streptomycin.

THP-1 cells were treated with 11.3 μM folic acid, dissolved in 1 M NaOH, 105 μM choline chloride, 18.5 nM vitamin B_{12}, and a mixture of methyl donors consisting of folic acid, choline chloride, and vitamin B_{12} at the concentrations previously indicated. Concentrations were determined by multiplying ten times the basal concentration present in the RPMI-1640 medium for each compound. After 24 h, cells were differentiated into macrophages by incubation with 25 ng/ml TPA for 48 h and then were activated with 100 ng/ml LPS for 24 hours. Finally, RNA and DNA were extracted and supernatants were collected for ELISA analysis.

2.3. Cell Viability Analysis. For the viability assay, THP-1 cells were pretreated with methyl donors at the selected concentrations during 24 h, as described above, in a 96-well plate. After the treatments, 20 μl MTT (5 mg/ml) was added to each well and plates were incubated for 2 h at 37°C. Formazan crystal formation was solubilised in 100 μl/well DMF-glacial acetic acid-SDS solution consisting of 40% DMF, 2% glacial acetic acid, and 16% *w*/*v* sodium SDS. Formazan production was quantified by absorbance at 570 nm using a microplate reader (Multiskan Spectrum, Thermo Electron Corporation, Finland). The results were expressed as relative cell viability (%).

2.4. Analysis of mRNA Expression by Quantitative Real-Time PCR. Total RNA was extracted from cells with TRizol® Reagent (Invitrogen). RNA quality and concentration were measured using the Nanodrop Spectrophotometer ND1000 (Thermo Fisher Scientific, MA, USA). Approximately 1 μg of total RNA was reverse-transcribed into cDNA by the MultiScribe™ Reverse Transcriptase Kit, following the manufacturer's instructions (Thermo Fisher Scientific, MA, USA). Real-time PCR was performed using ABI Prism 7900HT Sequence Detection System and Taqman Universal Master Mix (Applied Biosystems, CA, USA). Predesigned TaqMan primers and probes for *IL1B* (Hs01555410_m1), *TNF* (Hs00174128_m1), *IL18* (Hs01038788_m1), *SERPINE1* (Hs01126606_m1), *CD40* (Hs01002913_g1), *CCL2* (Hs00234140_m1), and *TLR4* (Hs00152939_m1) genes were used (Applied Biosystems). The levels of these mRNAs were normalized to the level of *GAPDH* (Hs02758991_g1) mRNA expression. Relative expression was determined by using the comparative $2^{-\Delta\Delta Ct}$ method.

2.5. Cytokine Secretion Analysis by Enzyme-Linked Immunosorbent Assay (ELISA). Culture supernatants were collected after the treatments and stored at −80°C for further cytokine analysis. Protein concentrations of IL-1β, TNF-α, PAI1, and CD40 were measured with standard ELISA kits (R&D Systems Europe, UK), according to the manufacturer's protocols. Absorbance was measured at 450 nm using a microplate reader (Multiskan Spectrum, Thermo Electron Corporation, Finland).

2.6. DNA Methylation Analysis by MALDI-TOF Mass Spectrometry. DNA was isolated using MasterPure™ DNA Purification Kit (Illumina, WI, USA), according to the manufacturer's guidelines. Genomic DNA was sodium bisulfite-converted using the EpiTect Bisulfite Kit (Qiagen, CA, USA). DNA methylation quantification was performed by MassARRAY EpiTYPER technology (Sequenom Inc., CA, USA). This method uses matrix-assisted laser desorption

ionization time-of-flight (MALDI-TOF) mass spectrometry in combination with RNA base-specific cleavage (MassCLEAVE). Four amplicons covering 32 CpG sites were selected. EpiDesigner software (Sequenom Inc.; http://www.epidesigner.com/start3.html) was used to design PCR primers for the amplicons of interest: *IL1B* (chr2: 112,837,566–112,837,895), *TNF* (chr6: 31,575,209–31,575,481), *SERPINE1* (chr7: 101,127,068–101,127,411), and *IL18* (chr11: 112,163,853–112,164,105). The designed primers are shown in Supplementary Table 1 and the complete amplicon sequences are reported in Supplementary Figure 1. The complete methodology was previously explained [15].

2.7. Chromatin Immunoprecipitation (ChIP) Assay. ChiP assay was performed with the ChIP-IT™ Express Enzymatic Kit (Active Motif, CA, USA), following the manufacturer's guidelines. THP-1 cells were cultured for 24 hours with methyl donors and were then differentiated with TPA (25 ng/μl) for 48 hours and activated with LPS (100 ng/μl) over 24 hours. The cell medium was discarded and 36.5% formaldehyde was added directly to the cell surface for 10 min. Cross-linking between proteins and DNA was stopped by the addition of glycine for 5 min at room temperature and cells were collected by scraping. Then, cells were incubated with lysis buffer for 30 min at 4°C and DNA was fragmented via enzyme-based digestion for 10 min at 37°C. Chromatin was immunoprecipitated using rabbit polyclonal antibody to nuclear factor-κB (NF-κB; ab7970, Abcam, MA, USA). After immunoprecipitation, cross-linking of protein-DNA complexes was reversed. Real-time quantitative PCR was performed using primers for *IL1B*: sense 5′-agcaacaaagctgccactta-3′ and antisense 5′-tgacgtgctgtgtgaatttg-3′, and *TNF*: sense 5′-ggagaatgtccagggctatg-3′ and antisense 5′-tcctggaggctctttcactc-3′.

2.8. Transcription Factor-Binding Site Analysis. In order to identify the putative transcription factor binding site in the CpG sites of the *IL1B* gene, a bioinformatic analysis was performed through LASAGNA-Search 2.0 using TRANSFAC matrices and aligned models, as described elsewhere [16].

2.9. Statistical Analysis. Normality was assessed by Kolmogorov-Smirnov and Shapiro-Wilk tests. For the statistical analysis of the results, a one-way ANOVA followed by Dunnett's test for multiple comparisons between groups and an unpaired Student *t*-test, for the direct comparisons between two groups, were used. Differences were considered significant at P value < 0.05. Statistics were performed using Prism 5.0 (GraphPad Software, CA, USA).

3. Results

3.1. Methyl Donors Did Not Affect Cell Viability. Cell viability was measured by MTT assay after incubation with folic acid at 11.3 μM, choline at 105 μM, vitamin B_{12} at 18.5 nM, and the methyl donor mixture. The selected concentrations were within the range proposed by previous studies [9, 17, 18]. Cell viability was not significantly affected by methyl donors at these concentrations (Supplementary Figure 2).

3.2. Effects of Methyl Donors on the Expression of Genes Associated with the Inflammatory Response in THP-1 Macrophages Activated with LPS. Treatment of THP-1 cells with the different compounds before the differentiation with TPA and activation with LPS altered the expression of most of the inflammation-related genes compared to the control treatment (Figure 1). Folic acid and the methyl donor mixture reduced *IL1B* ($P < 0.05$ for folic acid; $P < 0.01$ for the methyl donor mixture) and *TNF* ($P < 0.05$ for folic acid; $P < 0.001$ for methyl donor mixture) mRNA expression. Folic acid also reduced *TLR4* ($P < 0.05$) and *CCL2* ($P < 0.05$), but increased *SERPINE1* ($P < 0.05$) gene expression. Moreover, methyl donor mixture incubation reduced the levels of *CD40* ($P < 0.05$) but increased *SERPINE1* ($P < 0.05$). Choline decreased the expression of *CCL2* ($P < 0.05$). However, no statistically significant changes were observed after vitamin B_{12} incubation.

3.3. The Pretreatment with Folic Acid and Methyl Donor Mixture Reduced IL-1β and TNF-α Secretion of LPS-Activated Macrophages. Concerning cytokine secretion, the incubation with folic acid and the methyl donor mixture reduced the levels of IL-1β ($P < 0.01$) and TNF-α ($P < 0.01$ and $P < 0.05$, resp.), but not CD40 and PAI-1. However, no changes were observed with the other methyl donors (Figure 2).

3.4. Incubation with Methyl Donors Increased DNA Methylation in the Inflammatory Genes. The regions studied in the genes *IL1B*, *SERPINE1*, and *IL18* displayed an overall gain of methylation when LPS-activated macrophages were treated with the different methyl donors. This hypermethylation was especially significant after the incubation with folic acid. As shown in Table 1, folic acid significantly increased ($P < 0.05$) the methylation levels of CpG_1 (190%), CpG_5 (680%), and CpG_6 (200%) of *IL1B*, CpG_1 (750%), CpG_2 (88%), CpG_3.4 (136%), CpG_7 (1003%), and CpG_9 (88%) of *SERPINE1*, and CpG_4 (53%) and CpG_5 (27%) of *IL18* when compared with the methylation percentage of the nontreated LPS-activated macrophages. No changes in methylation were noted in the analyzed region of *TNF* after the treatment. Regarding choline chloride, vitamin B_{12}, and the methyl donor mixture, incubation with these compounds also significantly increased ($P < 0.05$) the methylation levels of some CpG sites concerning the studied genes (Table 1).

3.5. NF-κB Binding to IL-1β and TNF-α Was Not Affected after the Incubation with Folic Acid and the Methyl Donor Mixture. *IL1B* and *TNF* gene expression and secretion decreased after the incubation with folic acid and the methyl donor mixture (Figures 1 and 2). *IL1B* DNA methylation levels increased; *TNF* methylation levels did not. To determine the effect of DNA methylation in the sequence of proinflammatory genes on NF-κB binding to *IL1B* and *TNF* promoters, a ChIP assay was performed. The analysis showed no significant changes in NF-κB binding to *IL1B* and *TNF* promoter regions in THP-1 cells treated with folic acid and the methyl donor mixture (Figure 3).

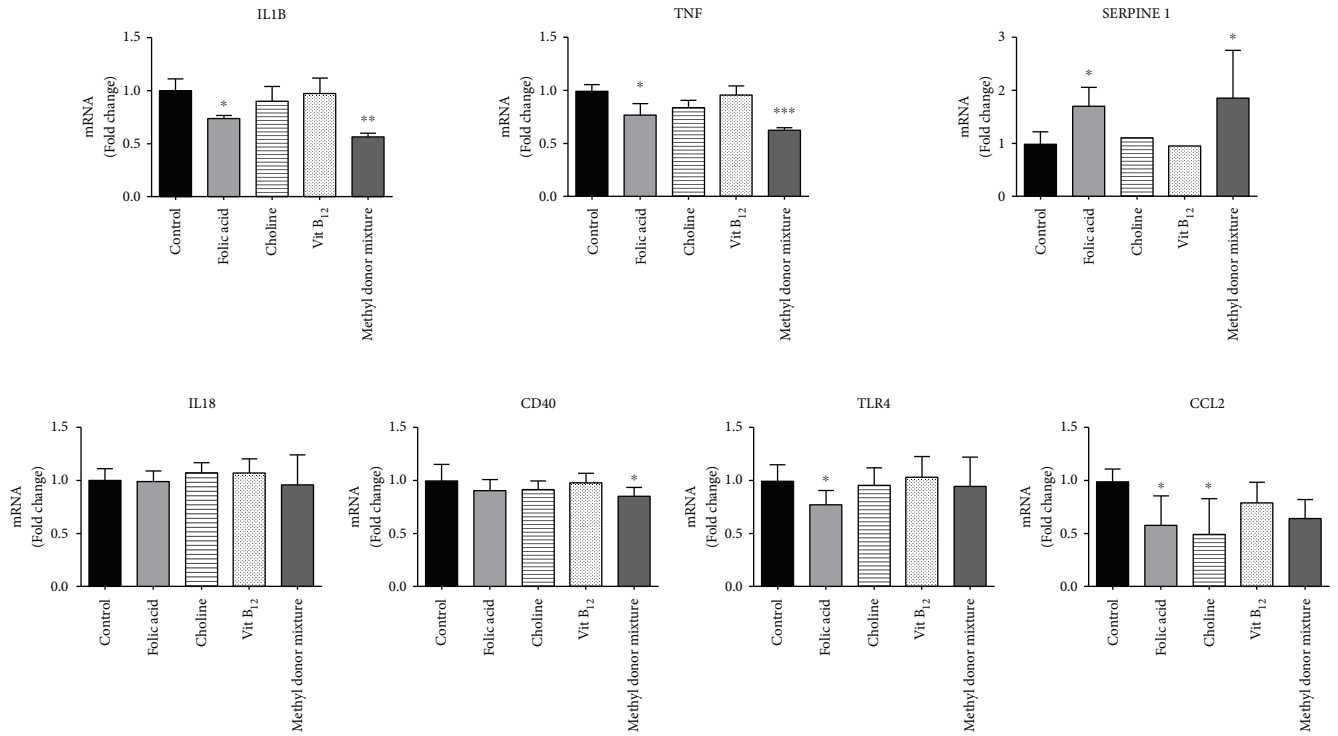

Figure 1: Effects of folic acid, choline, vitamin B_{12}, and the methyl donor mixture on the expression of inflammatory genes in THP-1 cells treated with TPA and LPS. Results are expressed as means ± SD ($n = 8$). Differences between groups were analyzed by one-way ANOVA followed by Dunnett's test. $^{*}P$ value < 0.05, $^{**}P$ value < 0.01, and $^{***}P$ value < 0.001 versus control.

4. Discussion

Previous studies in humans have analyzed the association between folic acid and inflammation. For example, a case-control study showed a reduction of cytokine levels after a 12-week treatment with folic acid [19]. In addition, folic acid supplementation in patients with a high risk of coronary artery disease was associated with a reduction in proinflammatory cytokines (e.g., monocyte chemoattractant protein 1 or MCP-1) in human monocytes [20]. In the present study, we demonstrated that folic acid and a mixture of methyl donors reduced the expression of proinflammatory genes (e.g., *TNF*, *IL1B*, *CD40*, *CCL2*, and *TLR4*) in THP-1 monocytes, when the monocytes were differentiated into macrophages and activated with LPS. In agreement with our results, the incubation of murine monocyte RAW 264.7 cells with folic acid reduced the expression of proinflammatory genes during LPS activation [17] . In contrast, folic acid deficiency in the same cell line enhanced the expression of proinflammatory genes [21].

Current data revealed that folic acid and the methyl donor mixture not only reduce proinflammatory gene expression in THP-1 monocytes, but also decrease the secretion of TNF-α and IL-1β cytokines when cells were differentiated to macrophages and activated by LPS.

During the inflammatory response, the proinflammatory mediators, specially MCP-1 (encoded by the *CCL2* gene), contribute to the migration of circulatory monocytes into the surrounding tissue [22], by specifically attracting monocytes towards the inflamed area, promoting tissue damage and disease. In this context, our results suggest that folic acid and a mixture of methyl donors could reduce the inflammatory response of the monocytes and the macrophages derived from these monocytes would decrease cytokine and chemokine secretion.

The specific mechanisms for the beneficial effects of folic acid or methyl donors on inflammation have not been clearly elucidated. One of the possible explanations is epigenetics, via DNA and histone methylation [23]. Folate, choline, and vitamin B_{12} directly participate in the formation of S-adenosyl methionine (SAM), which is the major donor of methyl groups for DNA methylation [24]. In the current trial, folic acid and the methyl donor mixture increased methylation levels of *IL1B*, *SERPINE1*, and *IL18.* However, only *IL1B* presented lower gene expression and protein secretion, which was associated with hypermethylation after folic acid supplementation. This result suggests that *IL1B* gene expression may be modulated by changes in DNA methylation induced by folic acid. However, the methylation changes of *SERPINE1* and *IL18* did not correlate with changes in gene expression. Incubation with methyl donors was for 24 hours and then the monocytes were differentiated for 48 hours and activated by LPS for a further 24 hours. A recent study of *IL18* expression in LPS-stimulated murine macrophages showed that the maximum level of expression of this interleukin was 3–6 hours after induction. No changes were found after 24 hours suggesting an earlier enzymatic activation of poly(ADP-ribose)

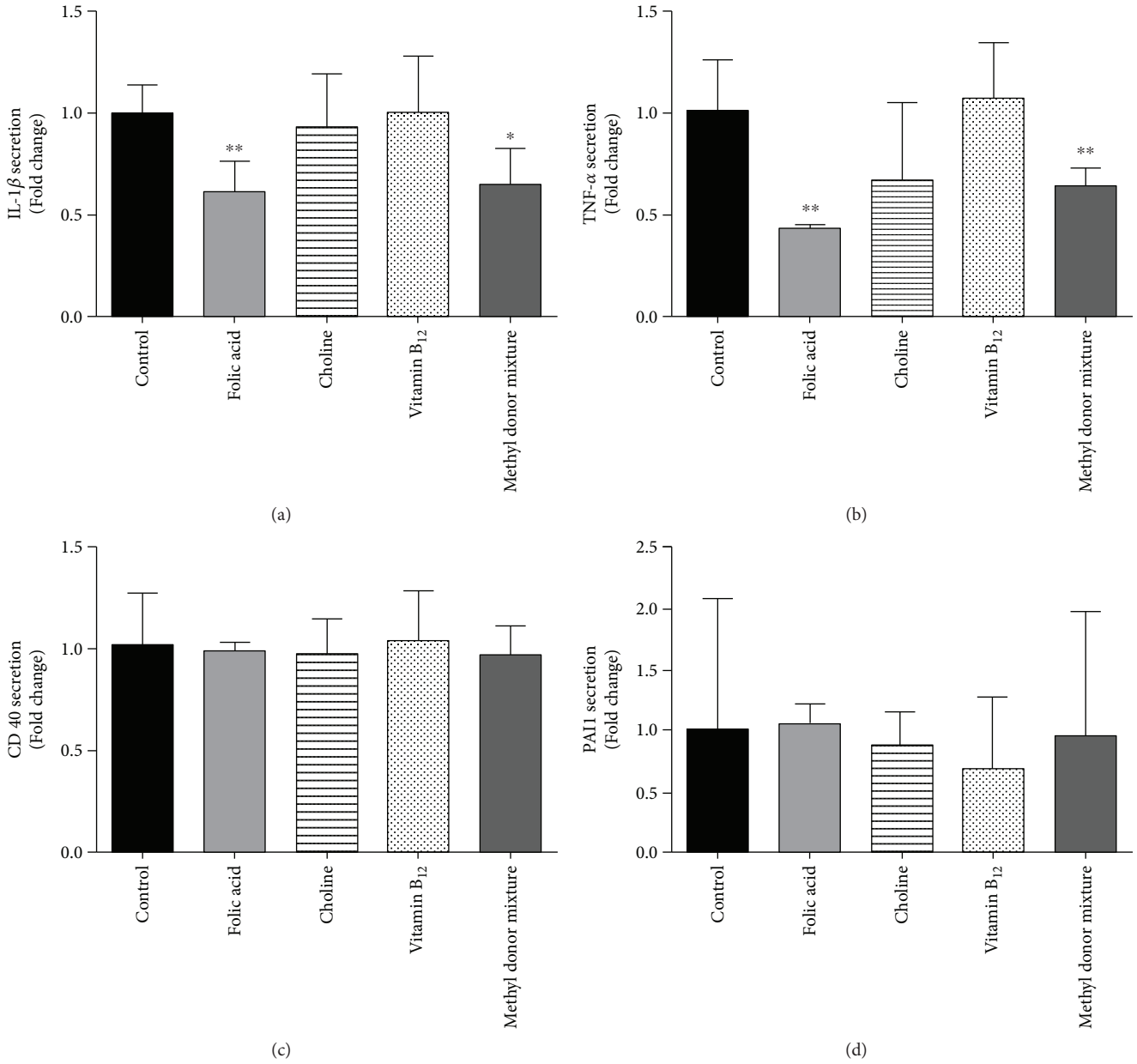

Figure 2: Effects of folic acid, choline, vitamin B_{12}, and the methyl donor mixture on the secretion of inflammatory cytokines in THP-1 cells treated with TPA and LPS. (a) IL-1β, (b) TNF-α, (c) CD40, and (d) PAI-1 secretion. Results are expressed as means ± SD ($n = 7 - 8$). Differences between groups were analyzed by one-way ANOVA followed by Dunnett's test. $^{*}P$ value < 0.05 and $^{**}P$ value < 0.01.

polymerase 1 (PARP-1) that induces *IL18* expression [24]. In this context, the time or the concentration of supplements might have been insufficient to evidence subtle changes in *IL18* and *SERPINE1* expression.

Unexpectedly, no changes in DNA methylation levels in the *TNF* gene were found after the treatment with methyl donors. In line with these results, Kolb and Petrie [21] found that although folate deficiency in murine macrophages reduced DNA methyltransferase expression, *TNF* DNA methylation did not change. In addition, in murine macrophages incubation with exogenous SAM attenuated the LPS-stimulated expression of TNF [25]. The reduction in *TNF* expression without a change in methylation could be due to folic acid causing upstream methylation. Recent studies have uncovered a new epigenetic mechanism for gene expression regulation: mRNA methylation. *In vitro* data has shown that methyladenine of mRNA influences mRNA transcription, splicing, nuclear export, translation, and mRNA stability [26, 27]. Therefore, RNA methylation may also be a regulatory mechanism altering *TNF* expression after the supplementation with the methyl donors.

Transcriptional activation of *TNF* and *IL1B* by LPS requires the stimulation of a set of pathways and transcription factors, including NF-κB, early growth response protein

Table 1: CpG methylation levels (as percentage) in *IL1B*, *TNF*, *IL18*, and *SERPINE1* genes after the incubation of THP-1 monocytes with folic acid, choline, vitamin B_{12}, and the methyl donor mixture, measured by MassARRAY. Unpaired Student's *t*-test was used to compare each CpG with the control group. $^{*}P$ value < 0.05; $^{**}P$ value < 0.01; and $^{***}P$ value < 0.001.

	Control	Folic acid	Choline	Vitamin B_{12}	Methyl donor mixture
IL1B					
CpG_1	6.88 ± 3.97	15.5 ± 6.14*	11.4 ± 1.55*	9.38 ± 0.95	14.0 ± 3.11*
CpG_2	94.9 ± 3.14	96.2 ± 1.66	94.8 ± 2.06	9.76 ± 0.85	96.9 ± 0.85
CpG_3	2.88 ± 2.09	1.75 ± 1.26	5.75 ± 1.77	3.75 ± 3.89	3.12 ± 3.75
CpG_4	2.75 ± 2.06	1.88 ± 1.79	1.25 ± 1.19	1.75 ± 0.96	3.75 ± 1.55
CpG_5	2.12 ± 2.49	6.50 ± 4.06*	1.25 ± 0.64	3.25 ± 1.55	10.0 ± 1.13
CpG_6	0.75 ± 0.50	7.12 ± 6.14*	9.50 ± 0.58***	9.25 ± 2.33***	0.88 ± 0.48
TNF					
CpG_1	98.2 ± 1.32	96.1 ± 2.78	98.0 ± 1.47	95.2 ± 2.72	95.8 ± 3.07
CpG_2	67.8 ± 3.95	64.8 ± 7.59	65.8 ± 4.48	69.9 ± 1.93	63.4 ± 6.46
CpG_3	48.1 ± 12.6	48.6 ± 8.53	51.2 ± 10.3	47.9 ± 4.71	45.0 ± 4.65
CpG_4.5.6	19.9 ± 6.76	15.2 ± 4.41	17.4 ± 3.09	19.8 ± 0.87	17.8 ± 1.79
CpG_8	33.9 ± 3.49	29.6 ± 4.37	31.8 ± 3.93	34.2 ± 2.53	34.0 ± 3.24
IL18					
CpG_1	12.5 ± 17.4	2.0 ± 0.5	2.12 ± 0.85*	1.25 ± 1.32	2.5 ± 2.0
CpG_2	6.88 ± 1.55	6.0 ± 1.22	7.38 ± 2.06*	9.50 ± 1.0	10.1 ± 2.25
CpG_3	0.67 ± 0.29	2.0 ± 0.82	0.62 ± 0.25	1.38 ± 0.75	0.88 ± 0.75
CpG_4	11.0 ± 2.04	8.38 ± 4.09*	7.75 ± 2.22	8.0 ± 1.91	7.25 ± 1.85
CpG_5	19.0 ± 3.19	13.2 ± 2.10*	15.8 ± 2.90	16.6 ± 1.11	15.0 ± 2.16
SERPINE1					
CpG_1	2.62 ± 0.63	22.0 ± 13.7**	10.8 ± 14.2	17.0 ± 16.1*	56.2 ± 5.14
CpG_2	33.5 ± 3.39	63.0 ± 12.5***	50.8 ± 7.09**	65.0 ± 5.40***	45.4 ± 8.68*
CpG_3.4	38.5 ± 9.81	91.1 ± 8.23**	79.5 ± 7.99***	85.2 ± 10.9***	62.6 ± 24.0*
CpG_6	100 ± 0.00	89.4 ± 4.09	90.9 ± 11.3	87.1 ± 10.2	96.6 ± 5.49
CpG_7	2.88 ± 1.60	32.1 ± 15.4**	13.9 ± 7.97*	28.2 ± 23.1*	15.8 ± 15.8*
CpG_8	95.1 ± 2.62	91.5 ± 6.77	92.6 ± 6.74	93.1 ± 2.66	94.9 ± 2.06
CpG_9	33.5 ± 3.39	63.0 ± 12.5**	50.8 ± 7.09**	65.0 ± 5.40***	45.4 ± 8.68
CpG_10	97.2 ± 2.59	95.0 ± 3.03	96.6 ± 1.60	88.5 ± 19.7	96.9 ± 2.46
CpG_11	97.5 ± 2.91	98.2 ± 2.36	97.1 ± 2.69	98.1 ± 0.75	98.5 ± 2.68
CpG_12	94.0 ± 7.22	95.0 ± 2.42	94.2. ± 5.52	96.0 ± 3.58	92.4 ± 6.26

1 (EGR-1), and activator protein 1 (AP-1) [28]. Available data in such research reveals that the binding levels of the NF-κB transcription factor to the *IL1B* promoter were similar to the *TNF* promoter and to macrophages without the methyl donors' supplementation. These results suggest that DNA methylation does not directly affect the binding affinity of NF-κB to *IL1B*. Similarly, Feng et al. [17] reported that folic acid decreased TNF-α and IL-1β production by inhibiting the NF-κB pathway without modifying NF-κB binding affinity. Taking into account these results, other molecular mechanisms could be affected by the tested molecules. For example, the bioinformatic analysis of the selected sequence of *IL1B* identified a putative PU.1 (Spi-1) transcription factor binding site, which could be involved in the regulation of the expression of this gene. PU.1 binds to GC-rich regions of genes to activate transcription, hence DNA methylation might impair the binding of PU.1 to the analyzed sequence and downregulate gene transcription. Interestingly, the PU.1 transcription factor is involved in macrophage differentiation and also in the transcriptional control of genes in mature macrophages [29, 30].

THP-1 is a human monocytic cell line derived from peripheral blood, which has been widely used to investigate the inflammatory response due to its ability to differentiate into macrophage-like cells. A known limitation of the use of cell lines in research is the difference to the natural environment, however previous studies have found that LPS mimics the inflammatory environment when added to THP-1 [31]. Despite this, direct extrapolation to human disease is not possible because more proinflammatory molecules and more than one cell type are involved in the response. Nevertheless, results of this investigation suggest a direct

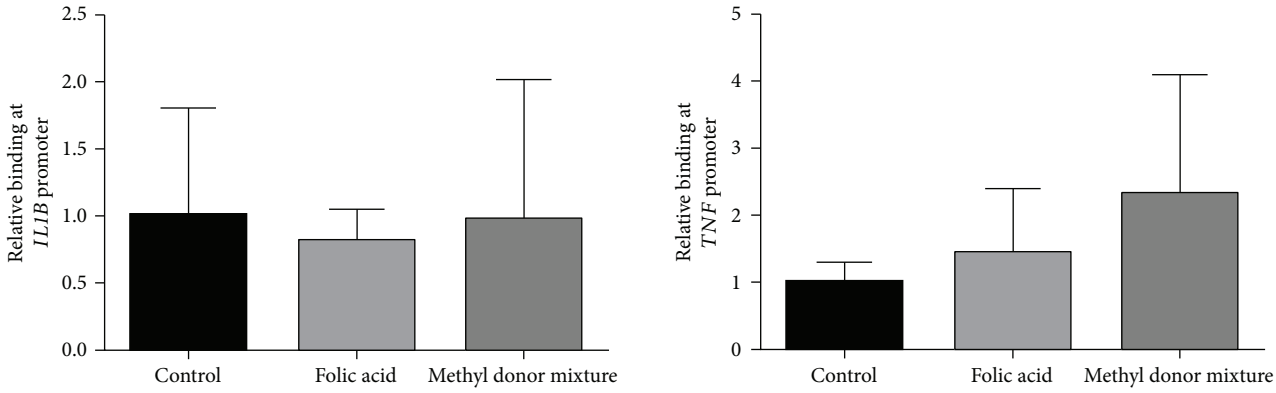

Figure 3: Relative binding of NF-κB to *IL1B* and *TNF* promoters in THP-1 cells differentiated with TPA and activated with LPS (control group) and the same cells treated with folic acid and the methyl donor mixture before differentiation. Results are expressed as means ± SD ($n = 8$). Differences between groups were tested by one-way ANOVA.

effect of methyl donors in the methylation of proinflammatory genes in LPS-activated THP-1 cells and the reduction of expression and production of proinflammatory cytokines. In addition, although methyl donor supplementation did not modify *TNF* promoter methylation, it reduced LPS-induced TNF-α production. However, the binding affinity of NF-κB to proinflammatory genes was unaffected, suggesting a minor role of this protein complex in the transcriptional regulation of these genes in response to folic acid and other methyl donors.

5. Conclusion

The findings of this study evidenced that monocyte pretreatment with specific methyl donors, particularly folic acid, reduced the inflammatory response in LPS-activated THP-1 macrophages, which could in part be mediated by increased DNA methylation in some CpG sites of important proinflammatory genes. In addition, folic acid decreased the expression of cytokines and chemokines (i.e., CCL2), suggesting a protective role through the recruitment of monocytes to the inflamed tissue.

Data Availability

Access to data will be considered by the author upon request.

Conflicts of Interest

The authors have nothing to declare concerning this issue.

Acknowledgments

The authors thank the technical assistance of Enrique Buso (UCIM, University of Valencia) for the MassARRAY® measurements. The authors are also grateful to Catherine Graham (St Mary's University, UK) for English proofreading. The authors acknowledge the financial support of MINECO (Nutrigenio Project reference AGL2013-45554-R) and Spanish Centro de Investigación Biomédica en Red de la Fisiopatología de la Obesidad y Nutrición (CIBERobn). Mirian Samblas holds a FPI grant from the MECD (BES-2014-068409).

Supplementary Materials

Supplementary Table 1: primer sequences used for MassARRAY EpiTYPER assay. Supplementary Figure 1: genomic localization and nucleotide sequences of CpG sites covered by the MassARRAY EpiTYPER probes for the study of DNA methylation levels of *IL1B*, *TNF*, *SERPINE1*, and *IL18* genes. The number on the left of each sequence represents the positions with respect to the start of the transcription or TSS. Nucleotides in the box are the sequences selected for each gene. CpGs underlined and highlighted in bold are those that were quantified by MassARRAY EpiTYPER. Transcription start site (TSS). Coding DNA sequence (CDS). Supplementary Figure 2: relative cell viability (measured by MTT assay) after THP-1 monocyte incubation with folic acid (11.3 μM), choline (105 μM), vitamin B_{12} (18.5 nM), and methyl donor mixture. Data are shown as the means ± SD ($n = 6$). Differences between groups were analyzed by one-way ANOVA. *(Supplementary Materials)*

References

[1] G. L. Larsen and P. M. Henson, "Mediators of inflammation," *Annual Review of Immunology*, vol. 1, no. 1, pp. 335–359, 1983.

[2] D. L. Laskin and K. J. Pendino, "Macrophages and inflammatory mediators in tissue injury," *Annual Review of Pharmacology and Toxicology*, vol. 35, no. 1, pp. 655–677, 1995.

[3] C. Shi and E. G. Pamer, "Monocyte recruitment during infection and inflammation," *Nature Reviews Immunology*, vol. 11, no. 11, pp. 762–774, 2011.

[4] O. Fogel, C. Richard-Miceli, and J. Tost, "Epigenetic changes in chronic inflammatory diseases," in *Advances in Protein Chemistry and Structural Biology*, pp. 139–189, Elsevier, 2017.

[5] J. L. Marques-Rocha, M. Samblas, F. I. Milagro, J. Bressan, J. A. Martínez, and A. Marti, "Noncoding RNAs, cytokines, and inflammation-related diseases," *The FASEB Journal*, vol. 29, no. 9, pp. 3595–3611, 2015.

[6] T. C. Simon and M. A. Jeffries, "The epigenomic landscape in osteoarthritis," *Current Rheumatology Reports*, vol. 19, no. 6, p. 30, 2017.

[7] K. R. Shorter, M. R. Felder, and P. B. Vrana, "Consequences of dietary methyl donor supplements: is more always better?," *Progress in Biophysics and Molecular Biology*, vol. 118, no. 1-2, pp. 14–20, 2015.

[8] N. Zhang, "Epigenetic modulation of DNA methylation by nutrition and its mechanisms in animals," *Animal Nutrition*, vol. 1, no. 3, pp. 144–151, 2015.

[9] A. Cianciulli, R. Salvatore, C. Porro, T. Trotta, and M. A. Panaro, "Folic acid is able to polarize the inflammatory response in LPS activated microglia by regulating multiple signaling pathways," *Mediators of Inflammation*, vol. 2016, Article ID 5240127, 10 pages, 2016.

[10] Z. Li, R. M. Gueant-Rodriguez, D. Quilliot et al., "Folate and vitamin B_{12} status is associated with insulin resistance and metabolic syndrome in morbid obesity," *Clinical Nutrition*, 2017.

[11] N. Al-Daghri, S. Rahman, S. Sabico et al., "Association of vitamin B_{12} with pro-inflammatory cytokines and biochemical markers related to cardiometabolic risk in Saudi subjects," *Nutrients*, vol. 8, no. 9, article 460, 2016.

[12] A. L. Guerrerio, R. M. Colvin, A. K. Schwartz et al., "Choline intake in a large cohort of patients with nonalcoholic fatty liver disease," *The American Journal of Clinical Nutrition*, vol. 95, no. 4, pp. 892–900, 2012.

[13] A. L. Buchman, M. D. Dubin, A. A. Moukarzel et al., "Choline deficiency: a cause of hepatic steatosis during parenteral nutrition that can be reversed with intravenous choline supplementation," *Hepatology*, vol. 22, no. 5, pp. 1399–1403, 1995.

[14] P. Cordero, J. Campion, F. I. Milagro, and J. A. Martinez, "Transcriptomic and epigenetic changes in early liver steatosis associated to obesity: effect of dietary methyl donor supplementation," *Molecular Genetics and Metabolism*, vol. 110, no. 3, pp. 388–395, 2013.

[15] F. I. Milagro, J. Campión, P. Cordero et al., "A dual epigenomic approach for the search of obesity biomarkers: DNA methylation in relation to diet-induced weight loss," *The FASEB Journal*, vol. 25, no. 4, pp. 1378–1389, 2011.

[16] C. Lee and C. H. Huang, "LASAGNA-Search 2.0: integrated transcription factor binding site search and visualization in a browser," *Bioinformatics*, vol. 30, no. 13, pp. 1923–1925, 2014.

[17] D. Feng, Y. Zhou, M. Xia, and J. Ma, "Folic acid inhibits lipopolysaccharide-induced inflammatory response in RAW264.7 macrophages by suppressing MAPKs and NF-κb activation," *Inflammation Research*, vol. 60, no. 9, pp. 817–822, 2011.

[18] Y. Jiang, S. Ma, H. Zhang et al., "FABP4-mediated homocysteine-induced cholesterol accumulation in THP-1 monocyte-derived macrophages and the potential epigenetic mechanism," *Molecular Medicine Reports*, vol. 14, no. 1, pp. 969–976, 2016.

[19] A. Solini, E. Santini, and E. Ferrannini, "Effect of short-term folic acid supplementation on insulin sensitivity and inflammatory markers in overweight subjects," *International Journal of Obesity*, vol. 30, no. 8, pp. 1197–1202, 2006.

[20] G. Wang, J. Dai, J. Mao, X. Zeng, X. Yang, and X. Wang, "Folic acid reverses hyper-responsiveness of LPS-induced chemokine secretion from monocytes in patients with hyperhomocysteinemia," *Atherosclerosis*, vol. 179, no. 2, pp. 395–402, 2005.

[21] A. F. Kolb and L. Petrie, "Folate deficiency enhances the inflammatory response of macrophages," *Molecular Immunology*, vol. 54, no. 2, pp. 164–172, 2013.

[22] P. C. Calder, R. Albers, J.-M. Antoine et al., "Inflammatory disease processes and interactions with nutrition," *The British Journal of Nutrition*, vol. 101, no. S1, pp. 1–45, 2009.

[23] O. S. Anderson, K. E. Sant, and D. C. Dolinoy, "Nutrition and epigenetics: an interplay of dietary methyl donors, one-carbon metabolism and DNA methylation," *The Journal of Nutritional Biochemistry*, vol. 23, no. 8, pp. 853–859, 2012.

[24] L. Liu, Y. Ke, X. Jiang et al., "Lipopolysaccharide activates ERK-PARP-1-RelA pathway and promotes nuclear factor-κb transcription in murine macrophages," *Human Immunology*, vol. 73, no. 5, pp. 439–447, 2012.

[25] A. I. Ara, M. Xia, K. Ramani, J. M. Mato, and S. C. Lu, "*S*-Adenosylmethionine inhibits lipopolysaccharide-induced gene expression via modulation of histone methylation," *Hepatology*, vol. 47, no. 5, pp. 1655–1666, 2008.

[26] H.-B. Li, J. Tong, S. Zhu et al., "m^6A mRNA methylation controls T cell homeostasis by targeting the IL-7/STAT5/SOCS pathways," *Nature*, vol. 548, no. 7667, pp. 338–342, 2017.

[27] X. Wang, B. Sun, Q. Jiang et al., "mRNA m^6A plays opposite role in regulating UCP2 and PNPLA2 protein expression in adipocytes," *International Journal of Obesity*, 2018.

[28] R. Kishore, M. R. McMullen, E. Cocuzzi, and L. E. Nagy, "Lipopolysaccharide-mediated signal transduction: stabilization of TNF-alpha mRNA contributes to increased lipopolysaccharide-stimulated TNF-alpha production by Kupffer cells after chronic ethanol feeding," *Comparative Hepatology*, vol. 3, article S31, Supplement 1, 2004.

[29] S. Ghisletti, I. Barozzi, F. Mietton et al., "Identification and characterization of enhancers controlling the inflammatory gene expression program in macrophages," *Immunity*, vol. 32, no. 3, pp. 317–328, 2010.

[30] Z. Yuan, M. A. Syed, D. Panchal, D. Rogers, M. Joo, and R. T. Sadikot, "Curcumin mediated epigenetic modulation inhibits TREM-1 expression in response to lipopolysaccharide," *The International Journal of Biochemistry & Cell Biology*, vol. 44, no. 11, pp. 2032–2043, 2012.

[31] R. Ahmad, A. Al-Roub, S. Kochumon et al., "The synergy between palmitate and TNF-α for CCL2 production is dependent on the TRIF/IRF3 pathway: implications for metabolic inflammation," *The Journal of Immunology*, vol. 200, no. 10, pp. 3599–3611, 2018.

Hindawi
Mediators of Inflammation
Volume 2018, Article ID 4934592, 12 pages
https://doi.org/10.1155/2018/4934592

Research Article

Osthole Protects against Acute Lung Injury by Suppressing NF-κB-Dependent Inflammation

Yiyi Jin,[1] Jianchang Qian,[1] Xin Ju,[2] Xiaodong Bao,[1] Li Li,[1] Suqing Zheng,[1] Xiong Chen,[1,3] Zhongxiang Xiao,[1,4] Xuemei Chen,[1] Weiwei Zhu,[1] Weixin Li,[1] Wencan Wu,[2] and Guang Liang[1]

[1]*Chemical Biology Research Center, School of Pharmaceutical Sciences, Wenzhou Medical University, Wenzhou, Zhejiang, China*
[2]*The Eye Hospital of Wenzhou Medical University, Wenzhou, Zhejiang, China*
[3]*Department of Cardiology, the First Affiliated Hospital, Wenzhou Medical University, Wenzhou, Zhejiang, China*
[4]*Department of Pharmacy, Affiliated Yueqing Hospital, Wenzhou Medical University, Wenzhou, Zhejiang, China*

Correspondence should be addressed to Wencan Wu; wuwencan118@163.com and Guang Liang; wzmcliangguang@163.com

Received 10 December 2017; Revised 13 April 2018; Accepted 29 May 2018; Published 3 July 2018

Academic Editor: Fabio S Lira

Inflammation is a key factor in the pathogenesis of ALI. Therefore, suppression of inflammatory response could be a potential strategy to treat LPS-induced lung injury. Osthole, a natural coumarin extract, has been reported to protect against acute kidney injury through an anti-inflammatory mechanism, but its effect on ALI is poorly understood. In this study, we investigated whether osthole ameliorates inflammatory sepsis-related ALI. Results from *in vitro* studies indicated that osthole treatment inhibited the LPS-induced inflammatory response in mouse peritoneal macrophages through blocking the nuclear translocation of NF-κB. Consistently, the *in vivo* studies indicated that osthole significantly prolonged the survival of septic mice which was accompanied by inflammation suppression. In the ALI mouse model, osthole effectively inhibited the development of lung tissue injury, leukocytic recruitment, and cytokine productions, which was associated with inhibition of NF-κB nuclear translocation. These findings provide evidence that osthole was a potent inhibitor of NF-κB and inflammatory injury and suggest that it could be a promising anti-inflammatory agent for therapy of septic shock and acute lung injury.

1. Introduction

Sepsis is a systemic and deleterious inflammatory response elicited by microbial infection [1–3]. The number of reported cases of sepsis continues to increase by 5 ~ 10% each year [4], making it one of the leading causes of death in intensive care facilities [5]. Among these case reports, approximately 30% of patients progress to multiorgan dysfunction syndrome (MODS) with 18% developing acute lung injury (ALI) [6–8]. ALI is a severe form of diffuse lung disease described as a clinical syndrome of acute respiratory failure with high morbidity and mortality [9]. It is characterized with persistent pulmonary inflammation [10] and increase in microvascular permeability [11]. Even with patients surviving ALI, the quality of life remains poor. Therefore, there is a great need for more effective therapeutic approaches.

Endotoxin, especially lipopolysaccharide (LPS) [12], is well recognized in the pathogenesis of ALI. LPS is a potent activator of toll-like receptor 4 (TLR4) [13–16], triggering the nuclear factor-kappa B (NF-κB) pathway, thereby producing proinflammatory molecules, such as cytokines interleukin 6 (IL-6) [17], IL-1b [18], and tumor necrosis factor α (TNF-α) [19]. Excessive inflammatory responses induced by endotoxin can lead to tissue destruction, fibrosis, and eventual organ failure [4, 18, 20]. Therefore, blocking inflammatory cascades is considered an effective strategy to attenuate lung injury. However, current effective therapeutic agents remain inadequate.

Osthole, a natural coumarin extract from the fruit of *Cnidium monnieri* (L.) [21], has several beneficial pharmacological properties, such as antiseizure [22], antiosteoporosis [23], and antitumour [24] activities. Recently, studies found

that osthole attenuates chronic kidney failure by inhibition of inflammation [25]. It also suppresses acute inflammatory responses in acute mechanical brain injury and kidney injury [26–28]. However, its potential protective effects on sepsis and ALI are not well characterized. In the present study, we evaluated the protective effects of osthole on LPS-induced ALI and its underlying mechanism. Our findings would provide important insight on potential new therapeutic approaches for inflammation-related lung injury.

2. Materials and Methods

2.1. Reagents. Osthole was purchased from Aladdin (Shanghai, China). The chemical structure is shown in Figure 1(a). Osthole was dissolved in dimethyl sulfoxide (DMSO) as 100 mM stock and diluted before use in assays. The final concentration of DMSO did not exceed 0.1%. All other reagents not mentioned were obtained from Sigma unless otherwise specified.

2.2. Cell Culture and Treatment. Mouse peritoneal macrophages (MPMs) were prepared as follows and also described in our previous paper [29]. Briefly, each ICR mice (8 weeks) was stimulated by intraperitoneal (ip) injection of 3 mL 6% thioglycollate solution (beef extract (0.3 g), tryptone (1 g), sodium chloride (0.5 g), and soluble starch (6 g)) dissolved in 100 mL water and filtrated with 0.22 μm filter. Three days later, MPMs were harvested by washing the peritoneal cavity with 8 mL PBS containing 30 mM of EDTA. The suspension was centrifuged at 4°C, 1000 rpm, resuspended in RPMI-1640 (Gibco/BRL life Technologies, Eggenstein, Germany) with 10% (*v*/*v*) FBS (HyClone, Logan, UT, USA), 100 U/mL penicillin G, and 100 mg/mL streptomycin. Cells were cultured in a 37°C, 5% CO_2 incubator, washed with medium 3 h after incubation, and used for studies after adherence firmly to culture plates.

GAPDH, P65, IκB-α, and lamin B antibodies were purchased from Santa Cruz Biotechnology (Santa Cruz, CA, USA). TNF-α and CD68 antibodies were obtained from Abcam (Abcam, USA). The secondary antibody was purchased from Santa Cruz Biotechnology.

2.3. Immunofluorescence and Immunoblotting. MPMs were plated (1×10^6) into a 6-well plate, pretreated with osthole for 1 h, and stimulated with LPS at indicated concentrations and time. After treatment, the cells were fixed with 4% paraformaldehyde and permeabilized with 100% methanol at 4°C for 5 min. The cells were washed twice with PBS containing 1% BSA and incubated with primary antibodies for anti-P65 antibody (1 : 200) overnight at 4°C, followed by a PE-conjugated secondary antibody (1 : 200). The cells were counterstained with DAPI and viewed by a Nikon fluorescence microscope (200x amplification, Nikon, Japan).

For Western blot analysis, the cells or lung tissue (30–50 mg) was prepared into homogenate samples and lysed (Boster Biological Technology, USA) and the protein concentration determined by a Bio-Rad protein assay kit (Bio-Rad, USA). Nuclear protein fractions were prepared using a kit from Beyotime (Shanghai, China) and were loaded and separated in 10% or 12% SDS-PAGE gels. The separated bands were electrotransferred to a nitrocellulose membrane and blocked in Tris-buffered saline, pH 7.6, containing 0.05% Tween 20 and 5% nonfat milk. Specific antibodies were incubated to probe for markers, and the immunoreactive bands were detected by incubating with a secondary antibody conjugated with horseradish peroxidase and visualized using enhanced chemiluminescence reagents (Bio-Rad, Hercules, CA).

2.4. Determination of TNF-α and IL-6 by ELISA. The TNF-α and IL-6 contents in culture medium or animal samples were determined by ELISA according to the manufacturer's instructions (Bioscience, San Diego, CA). The amount of TNF-α and IL-6 was normalized to protein concentration of cells, weight of animal tissues, or serum volume.

2.5. Real-Time Quantitative PCR. Total RNA was isolated from 1×10^6 cells or tissues (50–100 mg) using TRIzol (Life Technologies, Carlsbad, CA). Reverse transcription and quantitative PCR (RT-qPCR) were performed using M-MLV Platinum RT-qPCR Kit (Life Technologies). Real-time qPCR was carried out using the Eppendorf RealPlex 4 instrument (Eppendorf, Hamburg, Germany). Primers for genes (i.e., TNF-α, IL-6, and β-actin) were obtained from Life Technologies. The primer sequences used are shown in Table 1. The relative amount of each gene was normalized to β-actin.

2.6. Mouse Models. Male C57BL/6 mice weighing 18–22 g were obtained from the Animal Centre of Wenzhou Medical University (Wenzhou, China). The mice were housed at constant room temperature with a 12 : 12 h light-dark cycle, fed a standard rodent diet and water, and acclimatized to the laboratory for at least 3 days before use for studies. All animal care and experimental procedures were approved by the Wenzhou Medical College Animal Policy and Welfare Committee.

2.6.1. LPS-Induced Sepsis Model. Osthole was dissolved in 30% PEG 400 (Ludwigshafen, Germany), 1% volume of DMSO (Solarbio, Beijing, China), and 69% saline. Mice were pretreated with osthole (20 or 40 mg/kg) by ip injection, and 0.5 h later, 20 mg/kg LPS was injected through the tail vein. The mice were euthanized with chloral hydrate 6 h after LPS injection, and lung and liver tissues were excised aseptically, blotted dry, weighed, and immediately frozen in liquid nitrogen. The samples were stored at −80°C for later analyses. The body weight and mortality were recorded for 7 days.

2.6.2. LPS-Induced ALI. The mice were randomly divided into four groups as follows: control (7 mice received vehicle of 0.9% saline), LPS (7 mice received LPS alone), 20 + LPS (7 mice received 20 mg/kg/day osthole and LPS), and 40 + LPS (7 mice received 40 mg/kg/day osthole and LPS). Osthole was a pretreatment given by ip injection for one week. LPS challenge was made by intratracheal injection of 50 μL of LPS (5 mg/kg, dissolved in 0.9% saline) or 50 μL 0.9% saline as vehicle control. Mice were euthanized with chloral hydrate 6 h after LPS injection, and bronchoalveolar lavage fluid (BALF) and blood samples were collected. Lung and liver

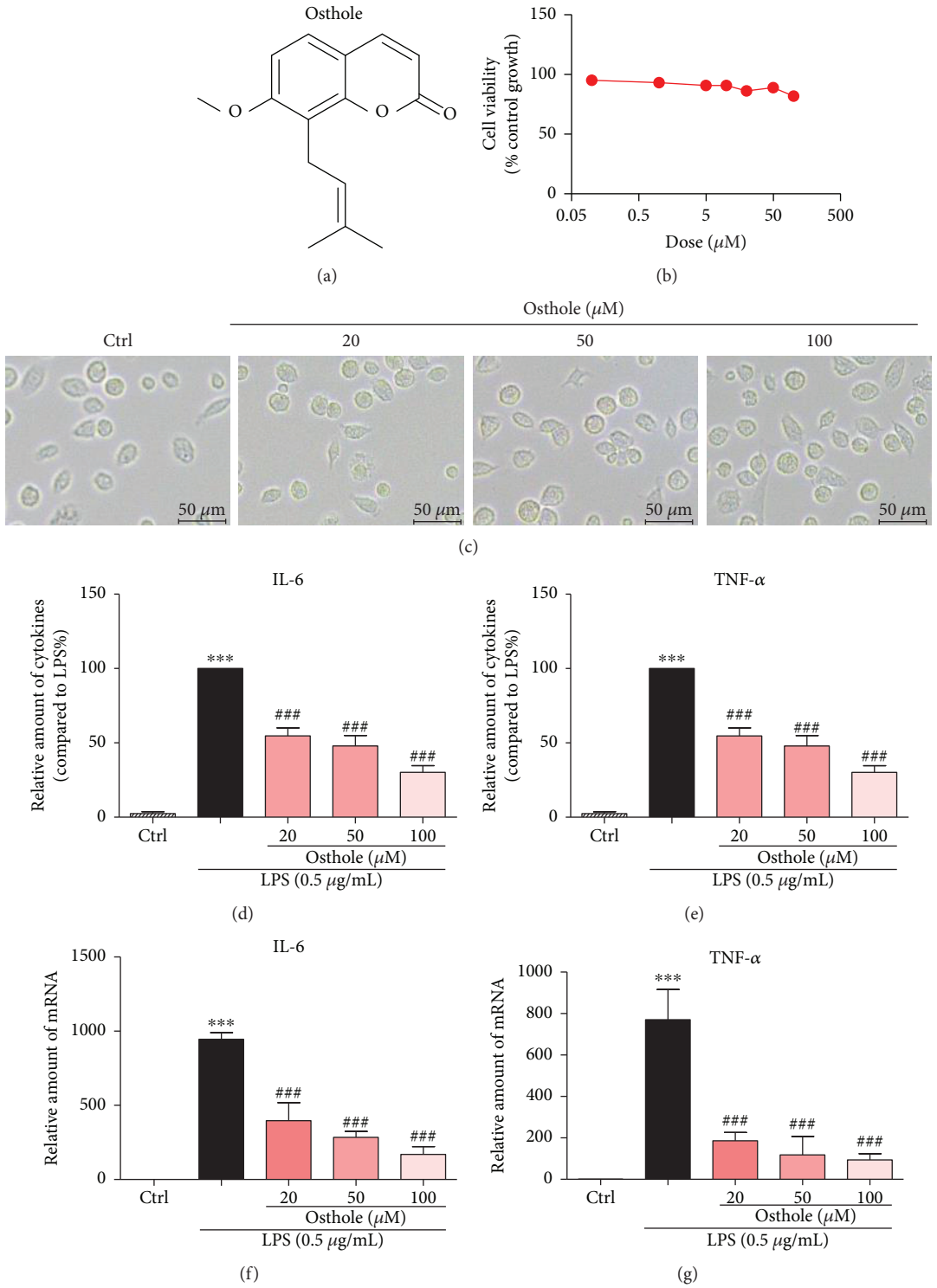

FIGURE 1: Osthole inhibits LPS-induced inflammatory cytokines in mouse peritoneal macrophages (MPMs). (a) The chemical structure of osthole. (b) MPMs were treated with various concentrations of osthole for 24 h. The viability of cells was measured by MTT assay and values reported as mean ± SEM; $n = 3$. (c) MPMs were treated with osthole (20, 50, or 100 μM) for 24 h, and light micrographs were recorded using a microscope. Representative of three evaluations, $n = 3$, micron bar = 20 μm. (d–e) MPMs were pretreated with osthole (20, 50, or 100 μM) for 0.5 h and stimulated with LPS (0.5 μg/mL) for 24 h, and secreted IL-6 (d) and TNF-α (e) were measured from conditioned media by ELISA (Materials and Methods). Values normalized to total protein of cells and reported as mean ± SEM relative to LPS alone; $n = 3$. (f–g) MPMs were pretreated with osthole (20, 50, or 100 μM) for 0.5 h and stimulated with LPS (0.5 μg/mL) for 6 h, and total RNA was extracted for real-time qPCR for IL-6 (f) and TNF-α (g). Values normalized to β-actin mRNA and reported as mean ± SEM; $n = 3$. (d–g) $^{***}p < 0.001$ versus control; $^{###}p < 0.001$ versus LPS alone.

Table 1: Primers used for real-time qPCR assay.

Gene	Species	FW (5′-3′)	RW (5′-3′)
TNF-α	Mouse	TGATCCGCGACGTGGAA	ACCGCCTGGAGTTCTGGAA
IL-6	Mouse	GAGGATACCACTCCCAACAGACC	AAGTGCATCATCGTTGTTCATACA
β-Actin	Mouse	CCGTGAAAAGATGACCCAGA	TACGACCAGAGGCATACAG

tissues were excised aseptically, frozen in liquid nitrogen, and stored at −80°C before later analyses.

2.7. BALF Analysis. The collected BALF was centrifuged at 1000 rpm for 10 min at 4°C. The supernatant was used for protein concentration and cytokine determination. The cell pellet was resuspended using 50 μL physiological saline for total cell count determination using a cell counting instrument (Count Star, Shanghai, China). The number of neutrophils in BALF was determined using Wright Giemsa staining (Nanjing Jiancheng Bioengineering Institute, Nanjing, China), and microscopic fields were counted under a Nikon fluorescence microscope (200x amplification; Nikon, Japan).

2.8. Lung Wet/Dry Ratio. For determining the ratio of wet to dry weight of lung tissue, the middle lobe of the right lung was collected and the wet weight was recorded. The tissue was heated at 65°C in a thermostatically controlled oven for 72 h and weighed. The ratio of wet/dry weight of lung tissue was reported as index of pulmonary edema.

2.9. Immunohistochemical Determination. Lung tissues were routinely fixed in 4% formalin, processed in graded alcohol and xylene, and embedded in paraffin. Paraffin blocks were sectioned into 5 μm thick sections. After rehydration, the sections were stained with hematoxylin and eosin (H&E assay kit, Beyotime, Shanghai, China).

For immunohistochemistry, paraffin was removed from the sections with xylene, rehydrated in graded alcohol series, subjected to antigen retrieval in 0.01 mol/L citrate buffer (pH 6.0) by microwaving, and then placed in 3% hydrogen peroxide in methanol for 30 min at room temperature. After blocking with 5% BSA (Sigma, USA), the sections were incubated with anti-TNF-α antibody (1 : 500, Abcam, USA) or anti-CD68 (1 : 500, Abcam, USA) overnight at 4°C, followed by the secondary antibody (1 : 200; Santa Cruz, USA). The reaction was visualized with DAB (ZSGB-Bio, Beijing, China), counterstained with hematoxylin, dehydrated, and viewed under a Nikon fluorescence microscope (200x amplification, Nikon, Japan).

2.10. Statistical Analysis. All data represent three independent experiments and are expressed as means ± SEM. Statistical analyses were performed using GraphPad Pro Prism 5.0 (GraphPad, San Diego, CA). One-way ANOVA followed by multiple comparisons test with Bonferroni correction was used to analyze the differences between sets of data.

3. Results

3.1. Osthole Inhibits LPS-Induced Production of IL-6 and TNF-α in MPMs. The MTT assay was used to investigate the effect of osthole on cell viability. For study, MPMs were treated with several doses for 24 h. The results indicated that osthole did not impair cell viability at the range of concentrations used (Figure 1(b)) or alter cell morphology (Figure 1(c)). Therefore, we selected 20–100 μM of osthole to investigate its anti-inflammatory activity. We first evaluated the effects of osthole on LPS-stimulated production of proinflammatory cytokines, IL-6 and TNF-α, in MPMs. Results indicated that LPS (0.5 μg/mL) stimulation for 24 h of MPMs robustly increased the secretion of both IL-6 and TNF-α into medium (Figures 1(d) and 1(e), resp.). Pretreatment of MPMs with osthole for 0.5 h suppressed the LPS-induced cytokine secretion in a dose-dependent manner (Figures 1(d) and 1(e)). The osthole-induced inhibition of cytokine secretion was associated with inhibition of the transcription of IL-6 and TNF-α (Figures 1(f) and 1(g)). The results indicated that osthole can inhibit LPS-induced inflammatory response in MPMs.

3.2. Osthole Blocks LPS-Induced Activation of NF-κB. The production of proinflammatory cytokines is predominantly regulated by NF-κB and/or AP-1 at the transcriptional level. MPMs were pretreated with osthole for 1 h and stimulated with LPS (0.5 μg/mL) for 1 h, and cell lysates were immunoblotted for IκB-α or the p65 subunit of NF-κB. Results indicated that LPS significantly stimulated the degradation of IκB-α, which was effectively prevented by osthole pretreatment in a dose-dependent manner (Figure 2(a)). The inhibition of the LPS-stimulated IκB-α degradation was accompanied by inhibition of nuclear translocation of the p65 subunit of NF-κB as detected by Western blot analysis of nuclear and cytoplasmic cell fractions (Figure 2(b)). Additionally, immunofluorescence staining of the p65 subunit similarly showed that osthole pretreatment prevented the LPS-induced nuclear translocation (Figure 2(c)). These data indicated that osthole suppressed LPS-induced activation of NF-κB signaling.

3.3. Osthole Ameliorates LPS-Induced Sepsis In Vivo. We used the LPS-induced sepsis mouse model to evaluate the protective effects of osthole. Mice given an iv injection of LPS died within 60 h (Figure 3(a)), as well as sharp loss of body weight (about 20%) (Figure 3(b)). However, mice pretreated with osthole, 20 or 40 mg/kg, improved survival beyond 72 h ($p < 0.05$) (Figure 3(a)), as well as body weight gain (Figure 3(b)). Uncontrollably sustained and vigorous inflammatory responses are characteristic of sepsis. In septic mice, both IL-6 and TNF-α were significantly elevated in serum and lung tissue (Figures 3(c) and 3(d)). Following osthole pretreatment, the increases in IL-6 and TNF-α content in serum and lung tissue were prevented (Figures 3(c)

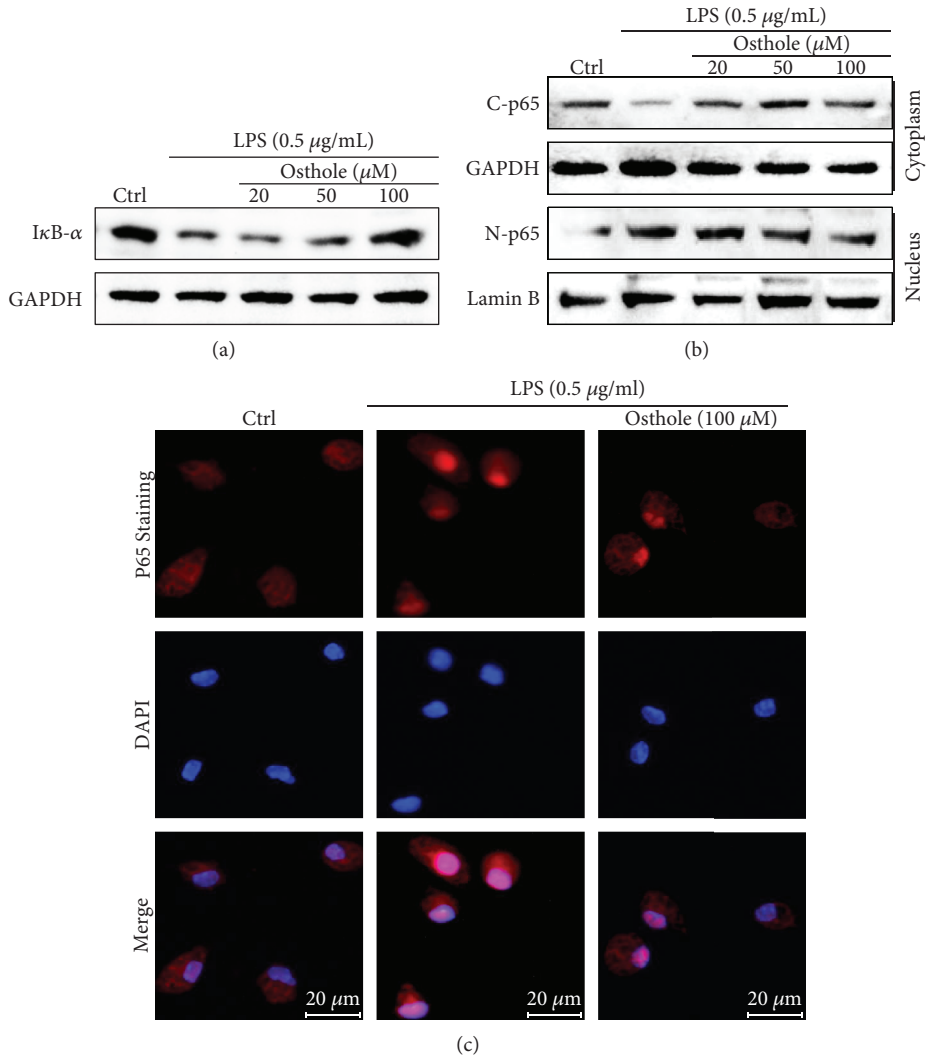

Figure 2: Osthole inhibits nuclear translocation of NF-κB. The effects of osthole on LPS-activated NF-κB were determined from MPMs pretreated with the indicated concentrations of osthole for 1 h and stimulated with LPS (0.5 μg/mL) for 0.5 h (a–b) or 1 h (c). (a) Representative Western blot analysis of cell lysates for IκB-α; GAPDH as loading control; $n = 3$. (b) Representative Western blot analysis of cytoplasmic and nuclear cell fractions for the p65 subunit of NF-κB (C-P65 and N-P65, resp.); GAPDH and lamin B are respective loading controls; $n = 3$. (c) For immunofluorescence evaluation of nuclear translocation of the p65 subunit, the osthole-pretreated MPMs were stimulated with LPS (0.5 μg/mL) for 1 h; p65 (red) and DAPI nuclear stain (blue), $n = 3$, micron bar = 20 μm.

and 3(d)). The findings indicated that osthole was a potent inhibitor of inflammatory cytokine production, which likely protected against sepsis.

3.4. Protective Effect of Osthole on LPS-Induced Acute Lung Injury (ALI). We next investigated the protective effects of osthole in the LPS ALI mouse model. Histological examination of the lung morphology stained with H&E indicated that LPS induced the expected pathologic changes, including areas of inflammatory infiltration, hemorrhage, interstitial edema, thickening of the alveolar wall, and lung tissue destruction (Figure 4(a), top panel). Moreover, LPS induced significant macrophage infiltration, as indicated by increased tissue localization of marker CD68 (Figures 4(a), middle panel and 4(b)), as well as increased tissue content of TNF-α (Figures 4(a), lower panel and 4(c)). However, osthole pretreatment effectively prevented the LPS-induced morphological derangements, as well as the induced increases in CD68 and TNF-α in lung tissue (Figures 4(a)–4(c)).

Additionally, osthole pretreatment inhibited the LPS-induced extravasation and tissue recruitment of leukocytes in ALI. Results indicated that osthole inhibited the LPS-induced increase in total cell number and neutrophils in BALF (Figures 5(a) and 5(b)). This was further corroborated by the finding that the LPS-induced increase in lung tissue MPO activity, an index of neutrophil, was significantly inhibited by osthole pretreatment (Figure 5(c)). An important characteristic of ALI is pulmonary edema, which can be assessed by the wet/dry lung weight. LPS induced ~30% increase in the wet/dry ratio, indicating the presence of pulmonary edema, which was prevented by osthole pretreatment (Figure 5(d)). Further, LPS induced increases of

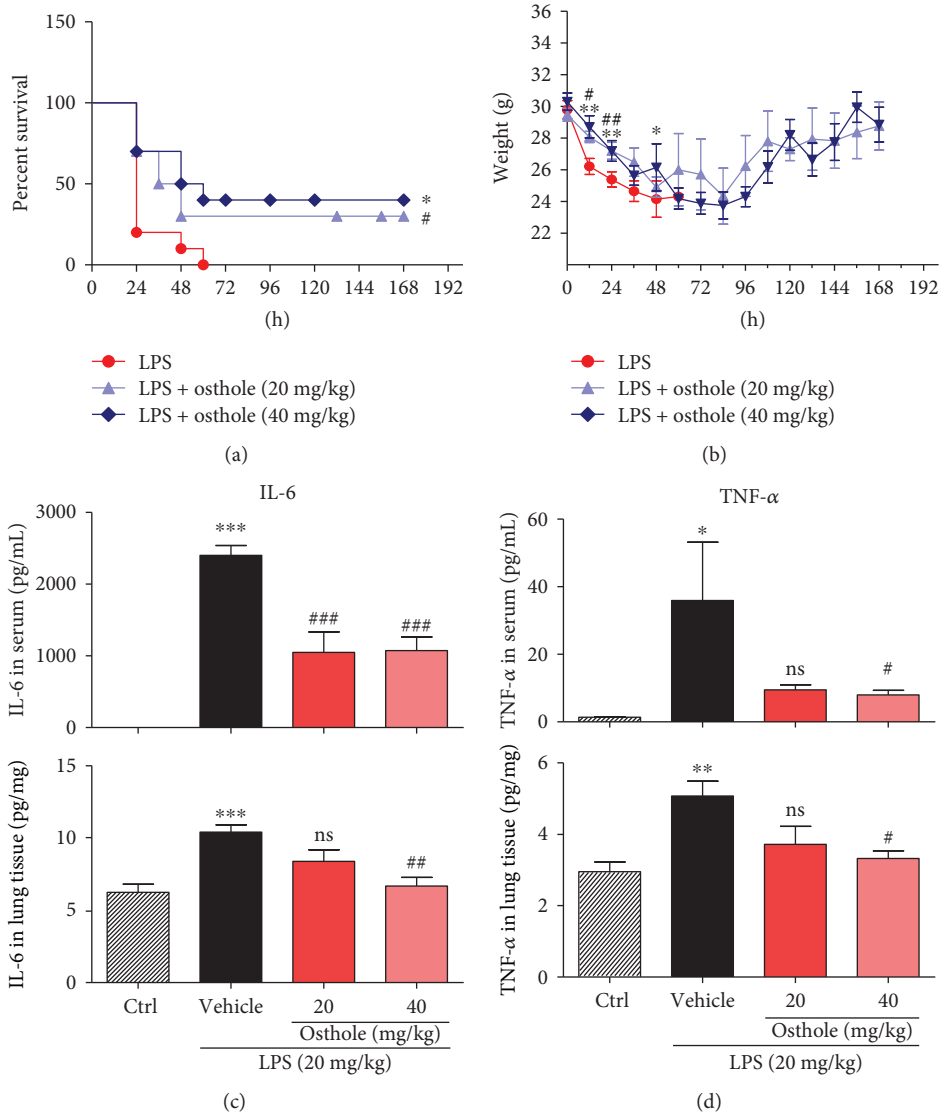

FIGURE 3: Osthole prolongs survival and inhibits inflammatory cytokines in LPS-induced septic mice. C57BL/6 mice ($n = 10$ each group) were pretreated for 0.5 h with 20 mg/kg or 40 mg/kg osthole via ip injection, followed by 20 mg/kg LPS by iv injection. (a) Percent survival for up to 168 h post-LPS injection is reported as mean ± SEM; $n = 3$; $^{*}p < 0.05$, versus control (Ctrl), and $^{\#}p < 0.05$, versus LPS. (b) Body weight change was monitored for up to 168 h post-LPS injection and reported as mean ± SEM; $n = 3$; $^{*}p < 0.05$ and $^{**}p < 0.01$, versus Ctrl; $^{\#}p < 0.05$ and $^{\#\#}p < 0.01$, versus LPS. ELISA determination of (c) IL-6 and (b) TNF-α content in serum and lung tissue from septic mice; values are normalized to serum volume (c) or tissue weights (d) and reported as mean ± SEM; ns = not significant, $^{*}p < 0.05$, $^{**}p < 0.01$, and $^{***}p < 0.001$, versus Ctrl. $^{\#}p < 0.05$, $^{\#\#}p < 0.01$, and $^{\#\#\#}p < 0.001$, versus vehicle.

proinflammatory cytokines IL-6 and TNF-α, in both BALF and serum (Figures 5(e) and 5(f)). As expected, osthole pretreatment inhibited these increases in BALF and serum (Figures 5(e) and 5(f)). These results provide strong evidence that osthole was a potent anti-inflammatory agent with therapeutic potential for treatment of ALI.

3.5. Osthole Suppresses the NF-κB Nuclear Translocation in ALI Mouse Model. We investigated the signaling mechanism by which osthole protected against inflammatory injury responses observed in our *in vivo* and *in vitro* studies. The involvement of NF-κB was first evaluated by determining IκB-α degradation in the mouse lung tissues of ALI mice. Western blot results indicated that LPS induced significant IκB-α degradation, which was effectively prevented by osthole pretreatment (Figures 6(a) and 6(b)). Moreover, LPS stimulated the nuclear translocation of the p65 subunit of NF-κB, but osthole pretreatment prevented the translocation (Figures 6(c)–6(d)). The data illustrated that osthole inhibited NF-κB signaling in lung tissue of ALI *in vivo*.

4. Discussion

ALI is characterized by persistent pulmonary inflammation [10] and increase in microvascular permeability. Enhanced inflammatory responses [30, 31], manifesting as elevated inflammatory cytokine production, and macrophage infiltration in lung are the most important pathological mechanisms [32].

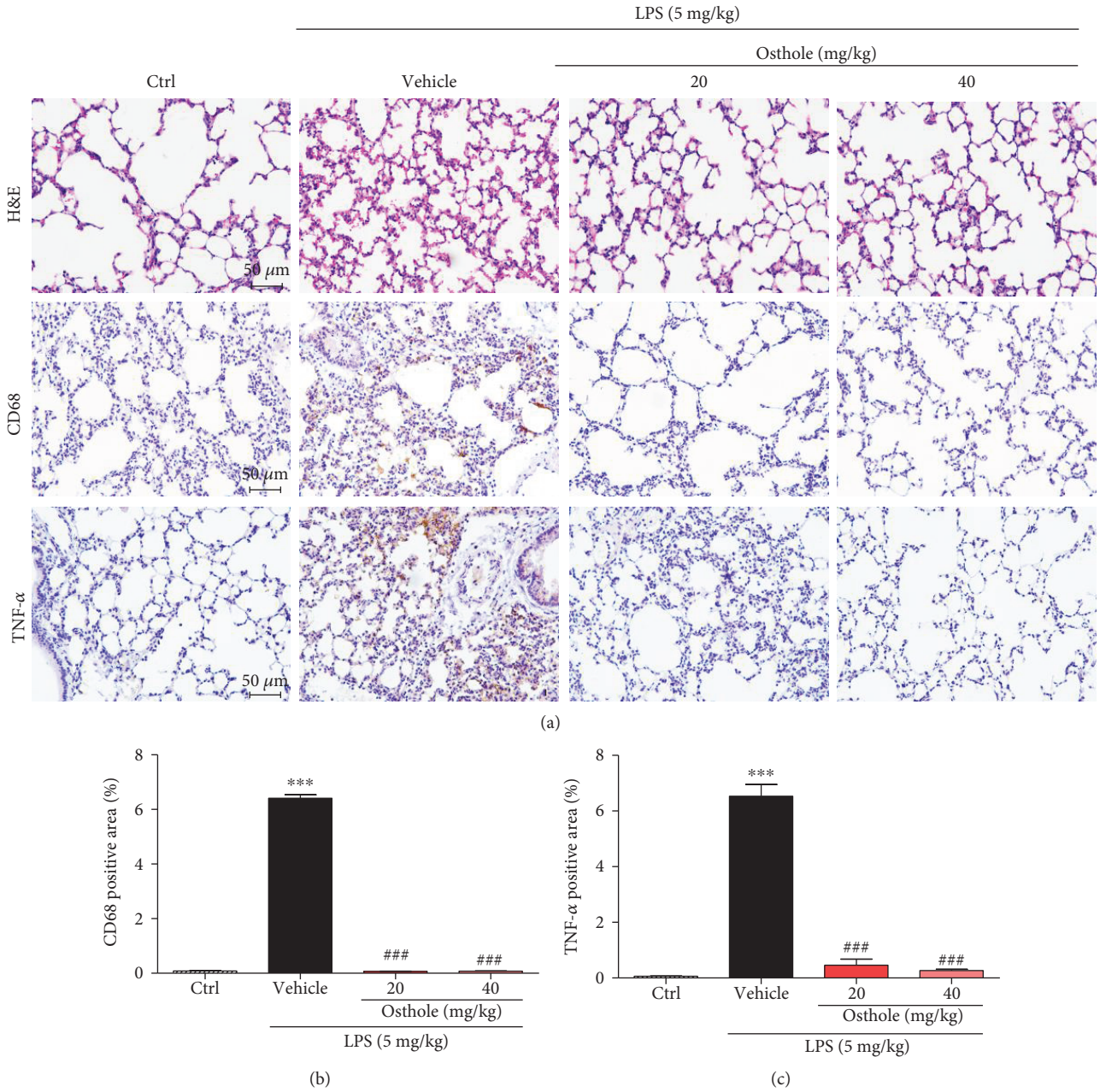

Figure 4: Osthole protects against inflammatory tissue injury in LPS-induced ALI. C57BL/6 mice were pretreated for 0.5 h with 20 mg/kg or 40 mg/kg osthole via ip injection, followed by intratracheal injection of 5 mg/kg LPS, and lungs were sampled 6 h later for analyses. (a, top panel) Representative light micrograph of lung histological changes stained with H&E, (a, middle panel) of immunolocalization of CD68, marker for macrophages (brown), and (a, bottom panel) of tissue localization of TNF-α (brown), micron bar = 50 μm. Quantification of positive lung tissue staining for (b) CD68 and (c) TNF-α in (a); values are reported as % mean ± SEM; $n = 4$. $^{***}p < 0.001$ versus control (Ctrl). $^{###}p < 0.001$ versus vehicle.

Therefore, anti-inflammatory therapy could be an attractive option to improve the quality of life in ALI patients. However, the progress in the development of novel effective therapeutic drugs for treatment of ALI is still disappointing. Discovery of active compounds from natural products would speed up the pace presently. Interestingly, several natural compounds with anti-inflammatory activities have been demonstrated to prevent inflammatory responses in experimental animal models of ALI.

Osthole has been shown to be effective in acute kidney injury via suppressing inflammatory response. However, the underlying mechanism is poorly understood. Here, we show that osthole alleviated ALI by inhibiting LPS-induced productions of IL-6 and TNF-α, likely through a mechanism in modulating NF-κB activity. It was closely related to the efficacy of osthole against ALI, such as lung tissue derangements, pulmonary edema, tissue recruitment of leukocytes, and prolonging of the survival time of septic mice. Although the dose of osthole

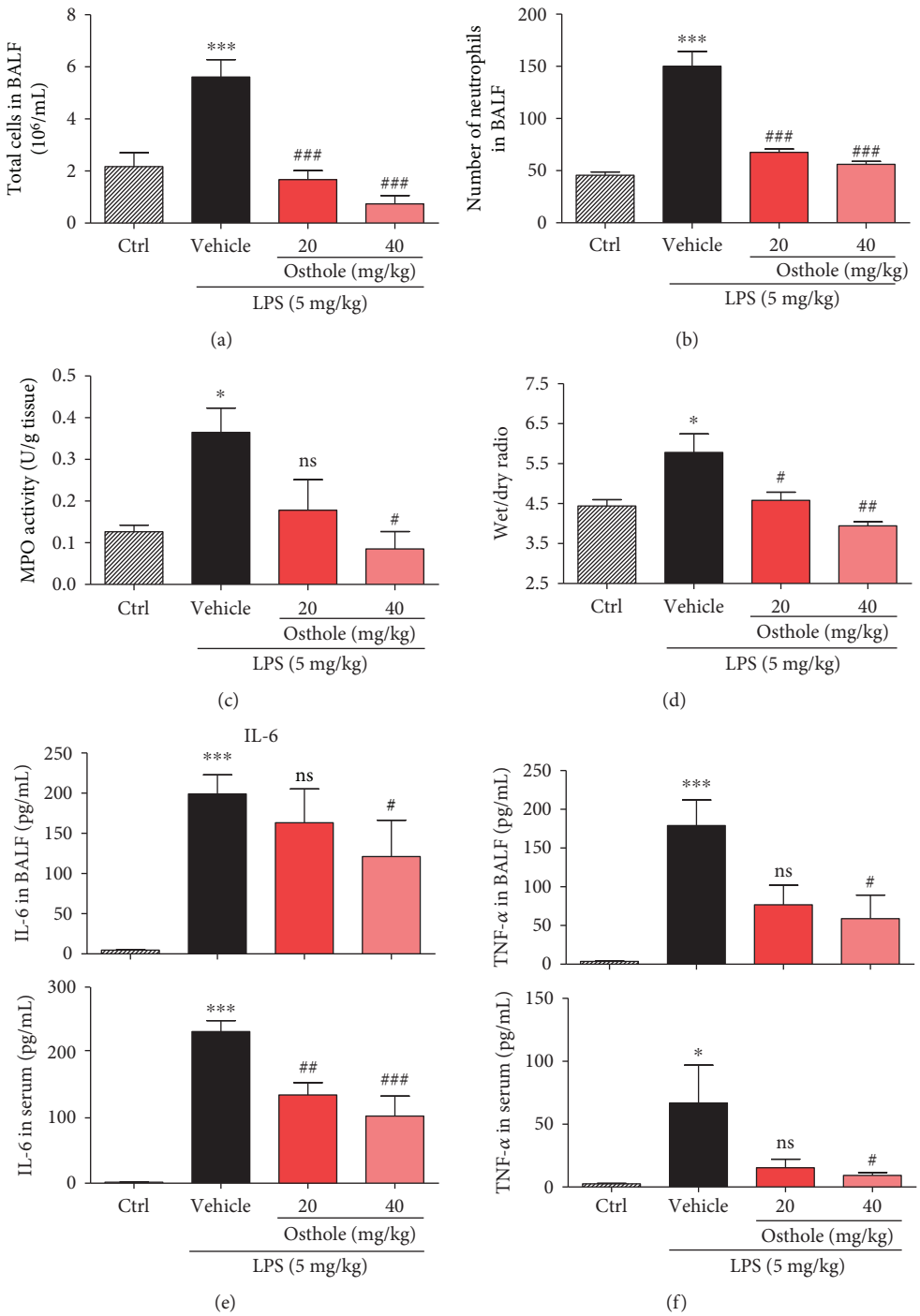

Figure 5: Osthole inhibits inflammatory cell infiltration and cytokine secretion in ALI. ALI was induced as described (Materials and Methods). Briefly, C57BL/6 mice were pretreated for 30 min with 20 mg/kg or 40 mg/kg osthole via ip injection, followed by intratracheal injection of 5 mg/kg LPS, and lungs were sampled 6 h later for analyses. (a) Number of total cells and (b) neutrophils in BALF was determined by counting microscopic fields; $n = 7$. (c) Lung tissue myeloperoxidase (MPO) activity assay was determined as an index of neutrophil activity; values are reported as mean ± SEM in U/g tissue; $n = 7$. (d) Wet and dry weights of lung tissue were measured and reported as the ratio of wet to dry as index of pulmonary edema; values are reported as mean ± SEM; $n = 7$. ELISA detection of (e) IL-6 and (f) TNF-α in BALF (upper graph) and serum (lower graph) from the experimental mice was determined, and values are reported as mean ± SEM; $n = 7$. ns = not significant; $^{*}p < 0.05$ and $^{***}p < 0.001$, versus control (Ctrl). $^{\#}p < 0.05$, $^{\#\#}p < 0.01$, and $^{\#\#\#}p < 0.001$, versus vehicle.

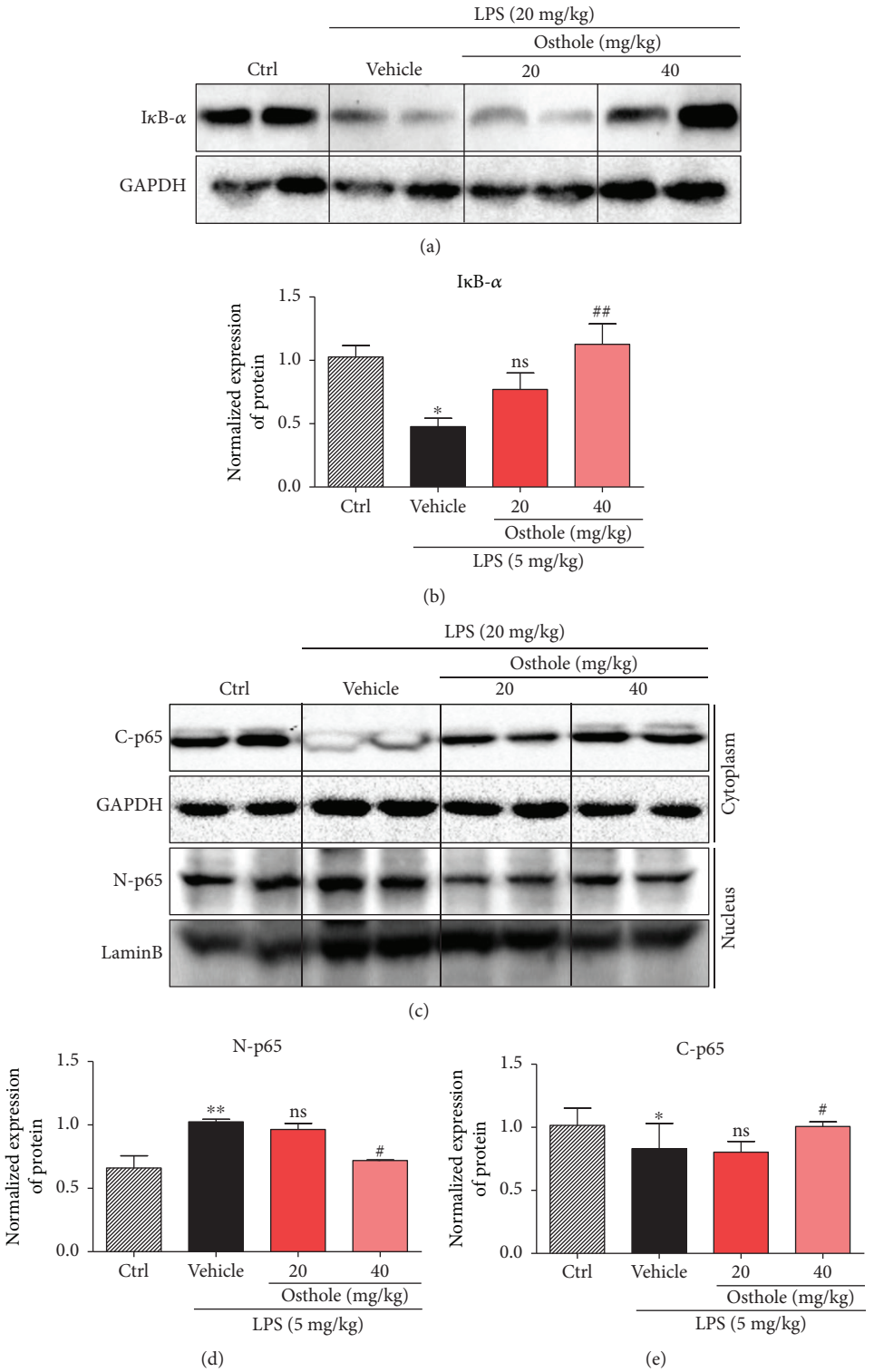

Figure 6: Osthole suppresses NF-κB signaling *in vivo*. ALI was induced as described (Materials and Methods). Briefly, C57BL/6 mice were pretreated for 30 min with 20 mg/kg or 40 mg/kg osthole via ip injection, followed by intratracheal injection of 5 mg/kg LPS, and lungs were sampled 6 h later for Western blot analyses. (a) Representative Western blot detecting for IκB-α; GAPDH as loading control. (b) Densitometric quantification of blot in (a); values are reported as mean ± SEM relative to control (Ctrl); $n = 4$. The bands were quantified by ImageJ and normalized to loading controls. (c) Representative Western blot analysis of the p65 subunit of NF-κB from cytoplasmic and nuclear cell fractions (C-p65 and N-p65, resp.); GAPDH and lamin B as respective loading controls. Densitometric quantification of (d) N-p65 and (e) C-p65 from (c); values are reported as mean ± SEM; $n = 4$. The bands were quantified by ImageJ and normalized to loading controls. ns = not significant; $^{*}p < 0.05$, $^{***}p < 0.001$ versus control (Ctrl). $^{\#}p < 0.05$, $^{\#\#}p < 0.01$ versus vehicle.

was relatively high, no toxic effects on body weight and cell proliferation were observed in our study. In addition, the effective dose of osthole we used was consistent with literatures reported previously [33, 34]. Furthermore, osthole is a natural coumarin derivative. Coumarin has been approved for some medical uses as pharmaceuticals in the treatment of lymphedema and anticoagulation via its anti-inflammatory properties. Thus, the present study would also provide a basis for expanding the indications of coumarin.

Macrophages are important participants in immune response [35–37] by providing an immediate defense against foreign agents or organisms. Besides, neutrophil infiltration into inflamed and infected tissues is a fundamental process of the innate immune response [38–41], which increased recruitment by the stimulation of LPS as the data shows. Two transcription factors, NF-κB [42–44] and AP-1 [45], are well-characterized regulators in the expression of proinflammatory cytokines [46], including TNF-α, IL-6, IL-1β, and IL-18 [47]. Our findings indicated that the inhibition of inflammatory response by osthole was through suppressing IκB-α degradation, resulting in NF-κB inhibition and thereby inhibition of its downstream cytokine gene expression. However, osthole showed no significant effect on JNK and p38 MAPK signaling pathways (data not shown). Overall, our results indicated that osthole potently inhibited LPS-activated NF-κB signaling of macrophages in the lung tissue of ALI mice, leading to significant suppression of inflammation and tissue injury. Even though nonsteroidal or steroidal anti-inflammatory drugs have potent anti-inflammation efficacy, the underlying mechanisms and side effects limit their applications in clinic. So, the present study would provide a potential strategy for treating ALI.

In summary, in this study we examined the potential pharmacological effect of osthole on sepsis and ALI and its underlying mechanism. Our work highlights osthole as a potential new candidate for treatment of injurious inflammatory responses in sepsis and ALI. However, the direct target of osthole upstream NF-κB remains unknown. The family of toll-like receptors (TLRs) are know as initiator of innate immune response. TLR4 is a typical member of TLRs which responsible for chronic and acute inflammatory disorders. Moreover, TLR4 is the primary receptor for LPS. Future studies are needed to investigate the relationship between osthole and TLR4.

Conflicts of Interest

The authors declare no competing financial interests.

Authors' Contributions

Yiyi Jin, Li Li, Zhongxiang Xiao, Xuemei Chen, and Weiwei Zhu performed the research. Guang Liang designed the research study. Suqing Zheng, Xiong Chen, and Weixin Li contributed essential reagents or tools. Guang Liang, Jianchang Qian, Yiyi Jin, Xin Ju, and Xiaodong Bao analysed the data. Guang Liang and Wencan Wu wrote the paper. Yiyi Jin and Jianchang Qian contributed equally to the work.

Acknowledgments

This work was supported by the National Natural Science Foundation of China (21502144, 81603180, 81622043, 81770825), Natural Science Funding of Zhejiang Province (LR16H310001), and National Key R&D Program of China (2017YFA0506000).

References

[1] J. Wang, H. Wu, Y. Yang et al., "Bacterial species-identifiable magnetic nanosystems for early sepsis diagnosis and extracorporeal photodynamic blood disinfection," *Nanoscale*, vol. 10, no. 1, pp. 132–141, 2018.

[2] J. Baggs, J. A. Jernigan, A. L. Halpin, L. Epstein, K. M. Hatfield, and L. C. McDonald, "Risk of subsequent sepsis within 90 days after a hospital stay by type of antibiotic exposure," *Clinical Infectious Diseases*, vol. 66, no. 7, pp. 1004–1012, 2018.

[3] M. Abbasi, Y. Greenstein, and S. Koenig, "Usefulness of ultrasound to help solve severe sepsis," *Chest*, vol. 152, no. 5, pp. e105–e108, 2017.

[4] M. J. Delano and P. A. Ward, "The immune system's role in sepsis progression, resolution, and long-term outcome," *Immunological Reviews*, vol. 274, no. 1, pp. 330–353, 2016.

[5] F. Fattahi and P. A. Ward, "Understanding immunosuppression after sepsis," *Immunity*, vol. 47, no. 1, pp. 3–5, 2017.

[6] A. Krupa, R. Fudala, J. M. Florence et al., "Bruton's tyrosine kinase mediates FcγRIIa/Toll-like receptor–4 receptor cross-talk in human neutrophils," *American Journal of Respiratory Cell and Molecular Biology*, vol. 48, no. 2, pp. 240–249, 2013.

[7] X. Sun, P. A. Singleton, E. Letsiou et al., "Sphingosine-1–phosphate receptor–3 is a novel biomarker in acute lung injury," *American Journal of Respiratory Cell and Molecular Biology*, vol. 47, no. 5, pp. 628–636, 2012.

[8] Y. Liao, H. Song, D. Xu et al., "*Gprc5a*-deficiency confers susceptibility to endotoxin-induced acute lung injury via NF-κB pathway," *Cell Cycle*, vol. 14, no. 9, pp. 1403–1412, 2015.

[9] A. J. Walkey and R. S. Wiener, "Macrolide antibiotics and survival in patients with acute lung injury," *Chest*, vol. 141, no. 5, pp. 1153–1159, 2012.

[10] L. R. Filgueiras Jr., J. O. Martins, C. H. Serezani, V. L. Capelozzi, M. B. A. Montes, and S. Jancar, "Sepsis-induced acute lung injury (ALI) is milder in diabetic rats and correlates with impaired NFkB activation," *PLoS One*, vol. 7, no. 9, article e44987, 2012.

[11] S. Thamphiwatana, P. Angsantikul, T. Escajadillo et al., "Macrophage-like nanoparticles concurrently absorbing endotoxins and proinflammatory cytokines for sepsis management," *Proceedings of the National Academy of Sciences of the United States of America*, vol. 114, no. 43, pp. 11488–11493, 2017.

[12] C. V. Rosadini and J. C. Kagan, "Early innate immune responses to bacterial LPS," *Current Opinion in Immunology*, vol. 44, pp. 14–19, 2017.

[13] B. Beutler, "Tlr4: central component of the sole mammalian LPS sensor," *Current Opinion in Immunology*, vol. 12, no. 1, pp. 20–26, 2000.

[14] J. C. Jang, J. Li, L. Gambini et al., "Human resistin protects against endotoxic shock by blocking LPS–TLR4 interaction," *Proceedings of the National Academy of Sciences of the United States of America*, vol. 114, no. 48, pp. E10399–E10408, 2017.

[15] F. Peri and M. Piazza, "Therapeutic targeting of innate immunity with Toll-like receptor 4 (TLR4) antagonists," *Biotechnology Advances*, vol. 30, no. 1, pp. 251–260, 2012.

[16] J. Yin, L. Michalick, C. Tang et al., "Role of transient receptor potential vanilloid 4 in neutrophil activation and acute lung injury," *American Journal of Respiratory Cell and Molecular Biology*, vol. 54, no. 3, pp. 370–383, 2016.

[17] H. Zhang, P. Neuhöfer, L. Song et al., "IL-6 trans-signaling promotes pancreatitis-associated lung injury and lethality," *The Journal of Clinical Investigation*, vol. 123, no. 3, pp. 1019–1031, 2013.

[18] I. Martínez-González, O. Roca, J. R. Masclans et al., "Human mesenchymal stem cells overexpressing the IL-33 antagonist soluble IL-1 receptor–like–1 attenuate endotoxin-induced acute lung injury," *American Journal of Respiratory Cell and Molecular Biology*, vol. 49, no. 4, pp. 552–562, 2013.

[19] B. V. Patel, M. R. Wilson, K. P. O'Dea, and M. Takata, "TNF-induced death signaling triggers alveolar epithelial dysfunction in acute lung injury," *Journal of Immunology*, vol. 190, no. 8, pp. 4274–4282, 2013.

[20] S. F. Ma, L. Xie, M. Pino-Yanes et al., "Type 2 deiodinase and host responses of sepsis and acute lung injury," *American Journal of Respiratory Cell and Molecular Biology*, vol. 45, no. 6, pp. 1203–1211, 2011.

[21] J. R. S. Hoult and M. Payá, "Pharmacological and biochemical actions of simple coumarins: natural products with therapeutic potential," *General Pharmacology*, vol. 27, no. 4, pp. 713–722, 1996.

[22] A. Jarząb, A. Grabarska, K. Skalicka-Woźniak, and A. Stepulak, "Pharmacological features of osthole," *Postępy Higieny i Medycyny Doświadczalnej*, vol. 71, no. 1, 2017.

[23] P. Wang, J. Ying, C. Luo et al., "Osthole promotes bone fracture healing through activation of BMP signaling in chondrocytes," *International Journal of Biological Sciences*, vol. 13, no. 8, pp. 996–1007, 2017.

[24] C. Wu, Z. Sun, B. Guo et al., "Osthole inhibits bone metastasis of breast cancer," *Oncotarget*, vol. 8, no. 35, pp. 58480–58493, 2017.

[25] H. X. Wu, Y. M. Wang, H. Xu et al., "Osthole, a coumadin analog from *Cnidium monnieri* (L.) Cusson, ameliorates nucleus pulposus-induced radicular inflammatory pain by inhibiting the activation of extracellular signal-regulated kinase in rats," *Pharmacology*, vol. 100, no. 1-2, pp. 74–82, 2017.

[26] T. Huang and Z. Dong, "Osthole protects against inflammation in a rat model of chronic kidney failure via suppression of nuclear factor-κB, transforming growth factor-β1 and activation of phosphoinositide 3-kinase/protein kinase B/nuclear factor (erythroid-derived 2)-like 2 signaling," *Molecular Medicine Reports*, vol. 16, no. 4, pp. 4915–4921, 2017.

[27] X. Zhao, F. Wang, R. Zhou, Z. Zhu, and M. Xie, "PPARα/γ antagonists reverse the ameliorative effects of osthole on hepatic lipid metabolism and inflammatory response in steatohepatitic rats," *Inflammopharmacology*, vol. 26, no. 2, pp. 425–433, 2018.

[28] W. C. Huang, P. C. Liao, C. H. Huang, S. Hu, S. C. Huang, and S. J. Wu, "Osthole attenuates lipid accumulation, regulates the expression of inflammatory mediators, and increases antioxidants in FL83B cells," *Biomedicine & Pharmacotherapy*, vol. 91, pp. 78–87, 2017.

[29] J. Wu, J. Li, Y. Cai et al., "Evaluation and discovery of novel synthetic chalcone derivatives as anti-inflammatory agents," *Journal of Medicinal Chemistry*, vol. 54, no. 23, pp. 8110–23, 2011.

[30] P. Lundbäck, J. D. Lea, A. Sowinska et al., "A novel high mobility group box 1 neutralizing chimeric antibody attenuates drug-induced liver injury and postinjury inflammation in mice," *Hepatology*, vol. 64, no. 5, pp. 1699–1710, 2016.

[31] Y. Hu, J. Lou, Y. Y. Mao et al., "Activation of MTOR in pulmonary epithelium promotes LPS-induced acute lung injury," *Autophagy*, vol. 12, no. 12, pp. 2286–2299, 2016.

[32] S. Vettorazzi, C. Bode, L. Dejager et al., "Glucocorticoids limit acute lung inflammation in concert with inflammatory stimuli by induction of SphK1," *Nature Communications*, vol. 6, no. 1, p. 7796, 2015.

[33] Y. Li, Y. Li, F. Shi, L. Wang, L. Li, and D. Yang, "Osthole attenuates right ventricular remodeling via decreased myocardial apoptosis and inflammation in monocrotaline-induced rats," *European Journal of Pharmacology*, vol. 818, pp. 525–533, 2018.

[34] C. Yu, P. Li, D. Qi et al., "Osthole protects sepsis-induced acute kidney injury via down-regulating NF-κB signal pathway," *Oncotarget*, vol. 8, no. 3, pp. 4796–4813, 2017.

[35] F. O. Martinez, L. Helming, and S. Gordon, "Alternative activation of macrophages: an immunologic functional perspective," *Annual Review of Immunology*, vol. 27, no. 1, pp. 451–483, 2009.

[36] K. Chen and J. K. Kolls, "T cell-mediated host immune defenses in the lung," *Annual Review of Immunology*, vol. 31, no. 1, pp. 605–633, 2013.

[37] M. Kopf, C. Schneider, and S. P. Nobs, "The development and function of lung-resident macrophages and dendritic cells," *Nature Immunology*, vol. 16, no. 1, pp. 36–44, 2015.

[38] K. Kienle and T. Lammermann, "Neutrophil swarming: an essential process of the neutrophil tissue response," *Immunological Reviews*, vol. 273, no. 1, pp. 76–93, 2016.

[39] B. Favier, "Regulation of neutrophil functions through inhibitory receptors: an emerging paradigm in health and disease," *Immunological Reviews*, vol. 273, no. 1, pp. 140–155, 2016.

[40] D. Hartl, N. Lehmann, F. Hoffmann et al., "Dysregulation of innate immune receptors on neutrophils in chronic granulomatous disease," *The Journal of Allergy and Clinical Immunology*, vol. 121, no. 2, pp. 375–382.e9, 2008.

[41] A. R. Martineau, S. M. Newton, K. A. Wilkinson et al., "Neutrophil-mediated innate immune resistance to mycobacteria," *The Journal of Clinical Investigation*, vol. 117, no. 7, pp. 1988–1994, 2007.

[42] M. W. Covert, T. H. Leung, J. E. Gaston, and D. Baltimore, "Achieving stability of lipopolysaccharide-induced NF-κB activation," *Science*, vol. 309, no. 5742, pp. 1854–1857, 2005.

[43] A. S. Baldwin Jr., "The NF-κB and IκB proteins: new discoveries and insights," *Annual Review of Immunology*, vol. 14, no. 1, pp. 649–681, 1996.

[44] P. Rao, M. S. Hayden, M. Long et al., "IκBβ acts to inhibit and activate gene expression during the inflammatory response," *Nature*, vol. 466, no. 7310, pp. 1115–1119, 2010.

[45] P. Wiesner, S. H. Choi, F. Almazan et al., "Low doses of lipopolysaccharide and minimally oxidized low-density lipoprotein cooperatively activate macrophages via nuclear factor κB and activator protein-1: possible mechanism for acceleration of atherosclerosis by subclinical endotoxemia," *Circulation Research*, vol. 107, no. 1, pp. 56–65, 2010.

[46] S. Jang, K. W. Kelley, and R. W. Johnson, "Luteolin reduces IL-6 production in microglia by inhibiting JNK phosphorylation and activation of AP-1," *Proceedings of the National Academy of Sciences of the United States of America*, vol. 105, no. 21, pp. 7534–7539, 2008.

[47] C. C. Li, I. Munitic, P. R. Mittelstadt, E. Castro, and J. D. Ashwell, "Suppression of dendritic cell-derived IL-12 by endogenous glucocorticoids is protective in LPS-induced sepsis," *PLoS Biology*, vol. 13, no. 10, article e1002269, 2015.

Hindawi
Mediators of Inflammation
Volume 2018, Article ID 1419352, 8 pages
https://doi.org/10.1155/2018/1419352

Research Article

New Insights into Behçet's Syndrome Metabolic Reprogramming: Citrate Pathway Dysregulation

Anna Santarsiero,[1] Pietro Leccese,[2] Paolo Convertini,[1] Angela Padula,[2] Paolo Abriola,[1] Salvatore D'Angelo,[2,3] Faustino Bisaccia,[1] and Vittoria Infantino[1]

[1]*Department of Science, University of Basilicata, Potenza, Italy*
[2]*Rheumatology Department of Lucania, Rheumatology Institute of Lucania (IReL), San Carlo Hospital of Potenza and Madonna delle Grazie Hospital of Matera, Potenza, Italy*
[3]*Basilicata Ricerca Biomedica (BRB) Foundation, Potenza, Italy*

Correspondence should be addressed to Vittoria Infantino; vittoria.infantino@unibas.it

Received 21 February 2018; Revised 10 May 2018; Accepted 4 June 2018; Published 28 June 2018

Academic Editor: Fabio S Lira

To date, a major research effort on Behçet's syndrome (BS) has been concentrated on immunological aspects. Little is known about the metabolic reprogramming in BS. Citrate is an intermediary metabolite synthesized in mitochondria, and when transported into the cytosol by the mitochondrial citrate carrier—SLC25A1-encoded protein—it is cleaved into acetyl-CoA and oxaloacetate by ATP citrate lyase (ACLY). In induced macrophages, mitochondrial citrate is necessary for the production of inflammatory mediators. The aim of our study was to evaluate SLC25A1 and ACLY expression levels in BS patients. Following a power analysis undertaken on few random samples, the number of enrolled patients was set. Thirty-nine consecutive BS patients fulfilling ISG criteria, and 21 healthy controls suitable for age and sex were recruited. BS patients were divided into two groups according to the presence (active) or absence (inactive) of clinical manifestations. Real-time PCR experiments were performed on PBMCs to quantify SLC25A1 and ACLY mRNA levels. Data processing through the Kruskal-Wallis test and Dunn's multiple comparison test as post hoc showed higher SLC25A1 and ACLY mRNA levels in BS patients compared to those in healthy controls. Therefore, SLC25A1 and ACLY upregulation suggests that metabolic reprogramming in BS involves the citrate pathway dysregulation.

1. Introduction

Behçet's syndrome (BS) is a multisystemic inflammatory disorder classified among primary vasculitis. The diagnosis is based on clinical signs due to the lack of specific tests. Typical clinical manifestations include oral and genital ulcers, uveitis, and skin lesions. The involvement of the central nervous system, vessel tree, and gastrointestinal tract even if less frequent can be life-threatening. The disease is characterized by a relapsing-remitting course with a period of substantial wellbeing between the phases [1]. BS is more common in certain geographic regions, and in nonendemic areas, the disease tends to be more frequent in female with a less severe course [2]. The pathogenesis of BS is still unknown. However, over the past years, genetic and immunological mechanisms have been investigated [3]. Little is known about metabolic signals which can be responsible for a metabolic reprogramming linked to the induction and/or control of inflammation in BS. Belguendouz et al. analyzed the arginine metabolism in BS patients. They found that nitric oxide and urea production were significantly increased in patients with active BS and NOS/arginase balance resulted depending on clinical expression [4].

Citrate is a key metabolite for energy production. Citrate is synthesized by citrate synthase from acetyl-CoA and oxaloacetate (OAA) in the mitochondrion where it usually enters the Krebs cycle and promotes oxidative phosphorylation.

Immune response of activated macrophages and dendritic cells requires a metabolic reprogramming during which citrate is diverted away from the Krebs cycle toward

the cytosol where it can be used to trigger several cellular functions [5]. Part of the mitochondrial citrate is also converted in itaconate which acts as a bactericide and negative regulator of the inflammation [6, 7].

Citrate exported to the cytosol by means of the mitochondrial citrate carrier (CIC)—SLC25A1-encoded protein—is cleaved by ATP citrate lyase (ACLY) to acetyl-coenzyme A (acetyl-CoA) and OAA [8]. Acetyl-CoA is the precursor for fatty acid and sterol biosynthesis and the universal donor for acetylation reactions. OAA is reduced to malate by cytosolic malate dehydrogenase and converted to pyruvate via malic enzyme with generation of cytosolic NADPH plus H^+ (necessary for fatty acid and sterol synthesis). We refer to CIC plus ACLY as a "citrate pathway" [8].

Recent studies have shown that the citrate pathway is activated in LPS- and cytokine-triggered macrophages [5, 9]. Indeed, an early upregulation of ACLY gene followed by an increase in SCL25A1 expression levels has been found [10–12]. Moreover, both endogenous and exogenous inducers produce an increase in cytosolic citrate levels in macrophages. Of note, acetyl-CoA- and OAA citrate-derived metabolites are essential to synthesize inflammatory mediators. Acetyl-CoA provides units for lipid elongation, including arachidonic acid, which is needed for the production of prostaglandins. OAA leads to NADPH production, necessary for NADPH oxidase and inducible NO synthase (iNOS) to generate ROS and NO, respectively. Indeed, CIC or ACLY activity inhibition by gene silencing as well as by specific inhibitors reduces the amount of ROS, NO, and proinflammatory prostaglandins [8, 10–12]. Furthermore, the addition of exogenous acetate nearly entirely prevented the inhibition of PGE_2 synthesis by citrate export pathway-specific inhibitors [11].

Thus, citrate diversion from the Krebs cycle to the citrate export pathway guarantees a strong inflammatory response and induces a Krebs cycle breaking point downstream of citrate. Isocitrate dehydrogenase (IDH) profound downregulation described in LPS-activated macrophages by Jha et al. [13] supports these metabolic changes and highlights the role of SLC25A1 and ACLY in inflammation.

Of note, increased levels of SLC25A1 and ACLY mRNAs have also been observed in activated natural killer (NK) cells [14], lymphocytes actively involved in chronic inflammatory diseases, and in obesity which is often associated to a chronic low-grade inflammation [15]. ACLY and SLC25A1 upregulation in induced NK cells is mediated by the sterol regulatory element-binding protein (SREBP) [14], according to the presence of sterol regulatory elements (SREs) in both ACLY and SLC25A1 gene promoters [16, 17]. Furthermore, Assmann et al. demonstrate that ACLY and CIC, as part of the citrate-malate shuttle, provide electron transfer from cytosolic NADH to mitochondrial NADH to sustain OXPHOS and at the same time to regenerate cytosolic NAD+ [14]. The citrate-malate shuttle activation is one of the metabolic changes ensuring an effective NK cell response during inflammation.

SLC25A1 and ACLY upregulation together with the citrate accumulation occurring in immune cells points out the importance of the breakpoint in the Krebs cycle downstream of citrate [18].

Taken together, these findings provide evidence that the citrate export pathway, via CIC and ACLY, has an essential function in metabolic reprogramming of immune cells and shed light on the relationship between energy metabolism and inflammatory diseases.

As BS displays inflammatory features and almost nothing is known about metabolic reprogramming linked to the disease, in our study, we analyzed the expression pattern of SLC25A1 and ACLY genes in BS patients and their correlation with the disease activity.

2. Materials and Methods

2.1. Study Population. Thirty-nine consecutive BS patients, fulfilling the International Study Group (ISG) classification criteria, followed at the outpatient clinic of Rheumatology Department of Lucania, and 21 matched healthy volunteers were enrolled. Healthy controls were recruited among hospital workers and were unrelated to each other or to the BS patients. All subjects signed written informed consent before participation. Research was carried out under the institutionally approved internal review board protocol and in accordance with the Declaration of Helsinki. For all subjects, the following data were collected: age, sex, erythrocyte sedimentation rate (ESR), and C-reactive protein (CRP) values. All BS patients were evaluated by the same rheumatologist, and an ocular examination was performed by an ophthalmologist. Based on the presence or not of at least one clinical manifestation, BS patients were divided in two groups: active and inactive. Disease activity was assessed by BDCAF (Behçet's Disease Current Activity Form) and BSAS (Behçet's Syndrome Activity Score) score systems. In the BS group, disease duration was calculated as the time elapsed since the onset of first clinical manifestation.

2.2. Determination of IL-1β levels in Serum. Venous blood was drawn from each subject enrolled. After clotting, serum was obtained by centrifugation at 2000 ×g for 10 minutes and stored at −80°C and thawed immediately before use. Serum samples were centrifuged at 9000 ×g for 5 minutes at 4°C and subjected to ELISA (IL-1β; ImmunoTools, Friesoythe, Germany). Each sample was tested in duplicate according to the manufacturer's procedure. In brief, microtiter ELISA plate was coated with human monoclonal antibody against IL-1β. Standards and serum samples were added to the wells and incubated for 2 hours at 37°C. After washing five times, incubation with biotinylated anti-human IL-1β antibody was performed for 2 hours at room temperature. Following a second wash, 100 μL of streptavidin-horseradish peroxidase was put into the wells and incubated for 30 minutes. Color development was ensured by using tetramethylbenzidine substrate solution. The reaction was stopped by the addition of 50 μL of 2 M of sulfuric acid. Finally, optical density at 450 nm was measured by GloMax®-Multi Detection System (Promega, Madison, WI). The standard curve was prepared on the basis of seven IL-1β dilutions. The detection range was 23–1500 pg/mL.

2.3. Isolation of PBMCs from Whole Blood. Peripheral blood mononuclear cells (PBMCs) were isolated from heparinized blood using Histopaque-1077 (Sigma-Aldrich, St Louis, MO) density centrifugation. Whole blood was mixed with HBSS (Hanks' balanced salt solution, Gibco, Grand Island, NY) at a ratio of 1 : 2 (*v*/*v*), layered on the top of Histopaque-1077 and centrifuged at 1000 ×g at room temperature for 15 minutes. The mononuclear cell layer was recovered and washed twice in HBSS for 10 minutes. Cell counting was done with the automated handheld Scepter 2.0 Cell Counter (Merck Millipore, Switzerland).

2.4. Quantitative Real-Time PCR. Total RNA was extracted from 2×10^6 PBMCs using the RNeasy Plus Mini Kit (Qiagen, Hilden, Germany) as per the manufacturer's instructions. Complementary DNA was synthesized by GeneAmp™ RNA PCR Core Kit (Thermo Fisher Scientific, Grand Island, NY) with random hexamers and murine leukemia virus reverse transcriptase (15 minutes at 42°C and 5 minutes at 99°C). Real-time PCR experiments were performed in triplicate on the 7500 Fast Real-Time PCR System (Thermo Fisher Scientific) with SLC25A1 (Hs01105608, amplicon length 75 bp, RefSeq NM_001256534.1—exon boundary 2-3), ACLY (Hs00982738, amplicon length 69 bp, RefSeq NM_001096.2—exon boundary 28-29), and β-actin (Hs01060665, amplicon length 63 bp, RefSeq NM_001101.3—exon boundary 2-3) TaqMan Gene Expression Assays (Thermo Fisher Scientific). β-Actin was used as endogenous reference gene for normalization of SLC25A1 and ACLY expression levels. To this end, the β-actin Ct value was subtracted from the target gene Ct value, generating a ΔCt value. $\Delta\Delta$Ct was calculated by subtracting the mean value of ΔCt of the control group from ΔCt of each patient. Finally, fold changes in SLC25A1 and ACLY gene expression were calculated via the comparative $2^{-\Delta\Delta Ct}$ method using the formula: $2^{-\Delta\Delta Ct} = \Delta Ct_{\text{BS patient}} - \Delta Ct_{\text{control}}$.

2.5. Statistical Analysis. After a preliminary study on 5 active and 5 inactive BS patients, a power analysis was performed to determine the sample size. The research was designed using mean values and pooled standard deviations of SLC25A1 and ACLY mRNA levels from the aforementioned few subjects to have a statistical power of 80% with an α-level of 0.05. The Shapiro-Wilk test at an α-level of 0.05 was used to assess for data normality. Statistical significance of differences of SLC25A1 and ACLY expression levels was determined by using the Kruskal-Wallis test followed by the Dunn's multiple comparison test with p values adjusted with the Benjamini-Hochberg method. Differences were considered as significant ($^*p < 0.05$), very significant ($^{**}p < 0.01$), and highly significant ($^{***}p < 0.001$). All statistical analyses were performed by using RStudio (version 1.1.423, RStudio Inc., Boston, MA).

3. Results

3.1. Sample Size Estimation. Preliminary data on 5 active and 5 inactive BS patients indicated that both SLC25A1 and ACLY were upregulated during the active phase. In particular, the differences of mean values between mRNAs from active and inactive BS patients were 3.64 for SLC25A1 and 1.00 for ACLY. The pooled standard deviations were 3.47 and 1.03 for SLC25A1 and ACLY, respectively. A power analysis by using preliminary data was performed to fix the sample size in order to obtain 80% power to detect the above reported differences at the α-level of 0.05. We achieved that active and inactive BS groups would need to consist of 16 and 18 patients for SLC25A1 and ACLY, respectively. We recruited 18 active and 21 inactive BS patients.

3.2. Demographic and Clinical Features of the Patients. Among the 39 consecutive BS patients enrolled, all received a pharmacological treatment, 18 had active disease (mean ± SD age = 41.3 ± 11.3 years) and the remaining 21 had no clinical manifestation (mean ± SD age = 42.8 ± 13.1 years). The male : female ratio in both groups was 2 : 1. The healthy controls recruited were suitable for sex and age (M : F = 14 : 7, mean ± SD age = 38.1 ± 12.1 years). The mean disease duration was 22.8 ± 9.7 years for the active group and 21.4 ± 11.4 years for the inactive BS group. ESR and CRP values were similar among the three groups (Table 1). On the contrary, increased serum levels of IL-1β were found in active BS patients (mean ± SD: 463.1 ± 85.9 pg/mL) compared to the inactive BS patients (mean ± SD: 393.8 ± 124.9 pg/mL) and healthy controls (mean ± SD = 234.4 ± 123.2 pg/mL, p value = 0.016, Kruskal-Wallis test) (Table 1). BSAS and BDCAF scores resulted 5.5 and 4.5 higher in active subjects compared to those in inactive subjects, respectively. One half of the active BS patients had only one clinical manifestation. The most frequent clinical manifestation was the posterior uveitis (38.9%) present in 13 eyes. Other clinical manifestations included oral ulcers (33.3%), skin lesions (27.8%), and peripheral arthritis (22.2%). Active central nervous system vasculitis and deep venous thrombosis were found in only one male and female, respectively. Skin lesions and articular involvement were more frequent in men than in women while oral ulcers and uveitis were equally distributed. Demographic characteristics of the patients and control group are detailed in Table 1.

3.3. SLC25A1 mRNA Quantification. To investigate a potential link between the citrate pathway and BS, we evaluated SLC25A1 gene expression in PBMCs from inactive and active BS patients and healthy controls.

SLC25A1 mRNA levels resulted higher in active BS patients (mean ± SD: 5.77 ± 4.34, median 4.42) compared to those in inactive BS patients (mean ± SD: 2.70 ± 1.83, median 2.22) and control subjects (mean ± SD: 1.00 ± 0.08) (Figure 1). The IQR (interquartile range) in active BS patients was about three-fold higher (4.81) than that in inactive BS patients (1.74). This means that 50% of active population had SLC25A1 mRNA levels from 2.7 to 7.51 while inactive patients SLC25A1 mRNA level range was from 1.6 to 3.34 (Figure 1).

To assess for normal distribution of SLC25A1 mRNA levels, we performed the Shapiro-Wilk test. While SLC25A1 expression levels were normally distributed in

Table 1: Demographic and clinical features of all subjects enrolled in the study.

Parameter	Active ($n = 18$)	Inactive ($n = 21$)	Control ($n = 21$)
Age, mean ± SD (years)	41.3 ± 11.3	42.8 ± 13.1	38.1 ± 12.1
Disease duration, mean ± SD (years)	22.8 ± 9.7	21.4 ± 11.4	
Male sex, number (%)	12 (66.7)	14 (66.7)	14 (66.7)
Female sex, number (%)	6 (33.3)	7 (33.3)	7 (33.3)
ESR (mm/1 h), mean ± SD	11.3 ± 8.2	12.9 ± 8.2	9.1 ± 6.3
CRP (mg/L), mean ± SD	1.9 ± 2.0	1.5 ± 1.9	0.8 ± 1.2
IL-1β (pg/mL), mean ± SD	463.1 ± 85.9	393.8 ± 124.9	234.4 ± 123.2
BSAS, mean ± SD	34.8 ± 14.7	6.1 ± 7.5	
BDCAF, mean ± SD	3.7 ± 1.7	0.8 ± 1.1	
One clinical manifestation, number (%)	9 (50.0)		
More than one clinical manifestation, number (%)	9 (50.0)		
Clinical manifestations, number (%)			
Posterior uveitis	7 (38.9)		
Oral ulcers	6 (33.3)		
Skin lesions	5 (27.8)		
Arthritis	4 (22.2)		
CNS involvement	1 (5.5)		
Vascular involvement	1 (5.5)		

All data are presented as mean ± standard deviation except gender and clinical manifestations listed as percentage. ESR = erythrocyte sedimentation rate; CRP = C-reactive protein; BSAS = Behçet's Syndrome Activity Score; BDCAF = Behçet's Disease Current Activity Form; CNS = central nervous system.

controls ($W = 0.91$, p value = 0.20), they did not follow normal distribution in inactive ($W = 0.86$, p value = 0.007) and active ($W = 0.87$, p value = 0.017) BS patients. Therefore, by using a nonparametric test, we observed statistically significant differences in SLC25A1 mRNA levels among controls and inactive and active BS patients ($\chi^2 = 25.92$, df = 2, p value = 2.36×10^{-6}, Kruskal-Wallis test). Since a post hoc analysis was necessary to make comparisons between each pair of groups, the Dunn's multiple comparison test was performed. Every pairwise comparison was statistically significant (Figure 1). p values adjusted with the Benjamini-Hochberg method were 3.20×10^{-3} for control versus inactive BS patients, 1.07×10^{-6} for control versus active BS patients, and 1.66×10^{-2} for inactive versus active BS patients (Figure 1). SLC25A1 expression levels did not correlate with gender or clinical manifestation (data not shown). Altogether, our results show a great increase of SLC25A1 mRNA levels in BS compared to control subjects. Of note, a further SLC25A1 upregulation is observed during the active phase of BS.

3.4. ACLY mRNA Quantification. SLC25A1 upregulation indicates a possible export of the citrate in BS. To strengthen this hypothesis, we quantified ACLY mRNA.

We found a two-fold increase of ACLY mRNA in active BS patients (mean ± SD: 1.92 ± 1.21, median 1.49) compared to controls (mean ± SD: 1.01 ± 0.14). No difference of ACLY expression levels was observed between inactive BS patients (mean ± SD: 0.81 ± 0.45, median 0.82) and the control group. It is interesting to note that ACLY mRNA levels were less than 1 for 75% of inactive patients and more than 1.14 for 75% of active patients (Figure 2). The Shapiro-Wilk test highlighted that ACLY transcript levels were normally distributed in controls ($W = 0.92$, p value = 0.40) and inactive BS patients ($W = 0.97$, p value = 0.66), instead they did not follow normal distribution in active BS patients ($W = 0.87$, p value = 0.019). Then, the Kruskal-Wallis test revealed statistically significant differences in ACLY mRNA levels among controls and inactive and active BS patients ($\chi^2 = 17.75$, df = 2, p value = 1.39×10^{-4}) (Figure 2). The Dunn's multiple comparison test clearly indicated that differences between controls and inactive BS patients were not statistically significant (p value = 0.24) (Figure 2).

Notably, p values adjusted with the Benjamini-Hochberg method were 3.58×10^{-2} for control versus active BS patients and 8.48×10^{-5} for inactive versus active BS patients (Figure 2).

ACLY expression levels did not correlate with gender or clinical manifestation (data not shown). The results of our study indicate that ACLY gene is upregulated in active BS patients than in healthy controls. Furthermore, it has been displayed a significant increment of ACLY mRNA levels in the presence of active disease when compared to inactive disease.

4. Discussion

Metabolism is essential to all living cells for generating energy, signalling molecules, and synthesizing or breaking down macromolecules. Metabolic adaptation and reprogramming are frequent links between environmental changes and cell function. A metabolic reprogramming occurs concurrently during immune cell activation. In resting dendritic cells, lymphocytes, and macrophages, catabolic pathways

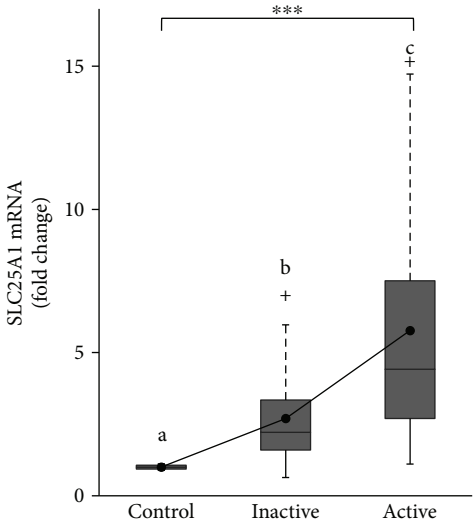

	Control ($n = 21$)	Inactive ($n = 21$)	Active ($n = 18$)
Min	0.90	0.64	1.11
Q1	0.95	1.60	2.70
Median	1.00	2.22	4.42
Q3	1.05	3.34	7.51
Max	1.12	7.00	14.88
Mean	1.00	2.70	5.77

Figure 1: Expression levels of SLC25A1 mRNA in study population. SLC25A1 mRNA levels have been quantified in PBMCs from 21 healthy adult volunteers (control) and 39 BS patients (21 with inactive disease and 18 with active disease). Results are shown as box plots, where the horizontal line within the boxes represents the median, the boxes represent the first and third quartiles, and the bars outside the boxes represent the minimum and maximum values. Where indicated, the dashed bars represent the upper ends of the farthest observed data point within 1.5 times the interquartile range and the plus signs represent outliers. Dots within the boxes indicate the mean values. Differences among the groups were highly significant (***$p < 0.001$, Kruskal-Wallis test). Pairwise comparisons were made with the post hoc Dunn's test; results are shown with letters. Distinct letters indicate that differences are significant.

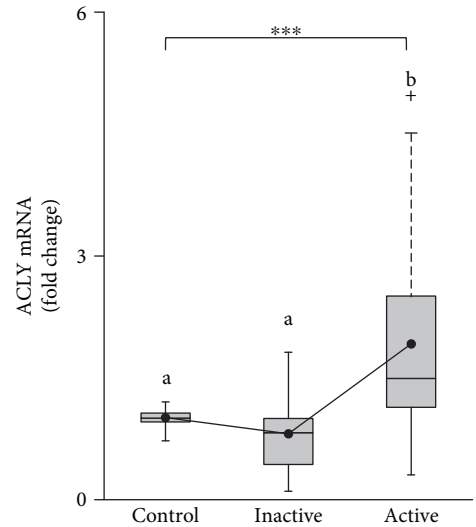

	Control ($n = 21$)	Inactive ($n = 21$)	Active ($n = 18$)
Min	0.72	0.10	0.31
Q1	0.96	0.43	1.14
Median	1.00	0.82	1.49
Q3	1.06	1.00	2.51
Max	1.20	1.81	4.98
Mean	1.01	0.81	1.92

Figure 2: Expression levels of ACLY mRNAs in study population. ACLY mRNA levels have been quantified in PBMCs from 21 healthy adult volunteers (control) and 39 BS patients (21 with inactive disease and 18 with active disease). Results are shown as box plots, where the horizontal line within the boxes represents the median, the boxes represent the first and third quartiles, and the bars outside the boxes represent the minimum and maximum values. Where indicated, the dashed bars represent the upper ends of the farthest observed data point within 1.5 times the interquartile range and the plus signs represent outliers. Dots within the boxes indicate the mean values. Differences among the groups were highly significant (***$p < 0.001$, Kruskal-Wallis test). Pairwise comparisons were made with the post hoc Dunn's test; results are shown with letters. Values sharing the same letter are not significantly different.

switch to anabolic programmes after activation by various triggers. These complex events ensure that activated cells generate energy and metabolites necessary to perform their specific function. A well-known example of metabolic shift—observed in inflammatory cells such as M1 macrophages and CD4+ T helper 17 (Th17) lymphocytes—is the enhanced glycolysis (Warburg phenotype) allowing for rapid ATP production [19]. Mitochondrial Krebs cycle enzymes are also inhibited, indicating a shift of the TCA cycle from being a purely catabolic pathway generating ATP to being, at least in part, an anabolic pathway. M1 macrophages display two breaks in the Krebs cycle downstream of citrate and succinate with a downregulation of IDH and succinate dehydrogenase, respectively [5, 20]. A so rewired Krebs cycle warrants increased levels of citrate and succinate, two key metabolites crucial for immune responses. Succinate through the hypoxia-inducible factor 1 alpha (HIF1alpha) activation induces HIF1alpha target genes including IL-1β [21]. Citrate withdrawn by the citrate export pathway activates fatty acid synthesis (which in turn participates in prostaglandin generation) and allows for reactive nitrogen species (RNS) and ROS production. Interestingly, a citrate pathway upregulation has been found in PMBCs from children affected by Down syndrome—a genetic disorder with the occurrence of many inflammatory conditions and a permanent oxidative stress [22].

In the last years, a host of studies has demonstrated that targeting different metabolic pathways is possible to regulate immune responses and treat immune-mediated pathogenesis. Thus, immunometabolism modulation might

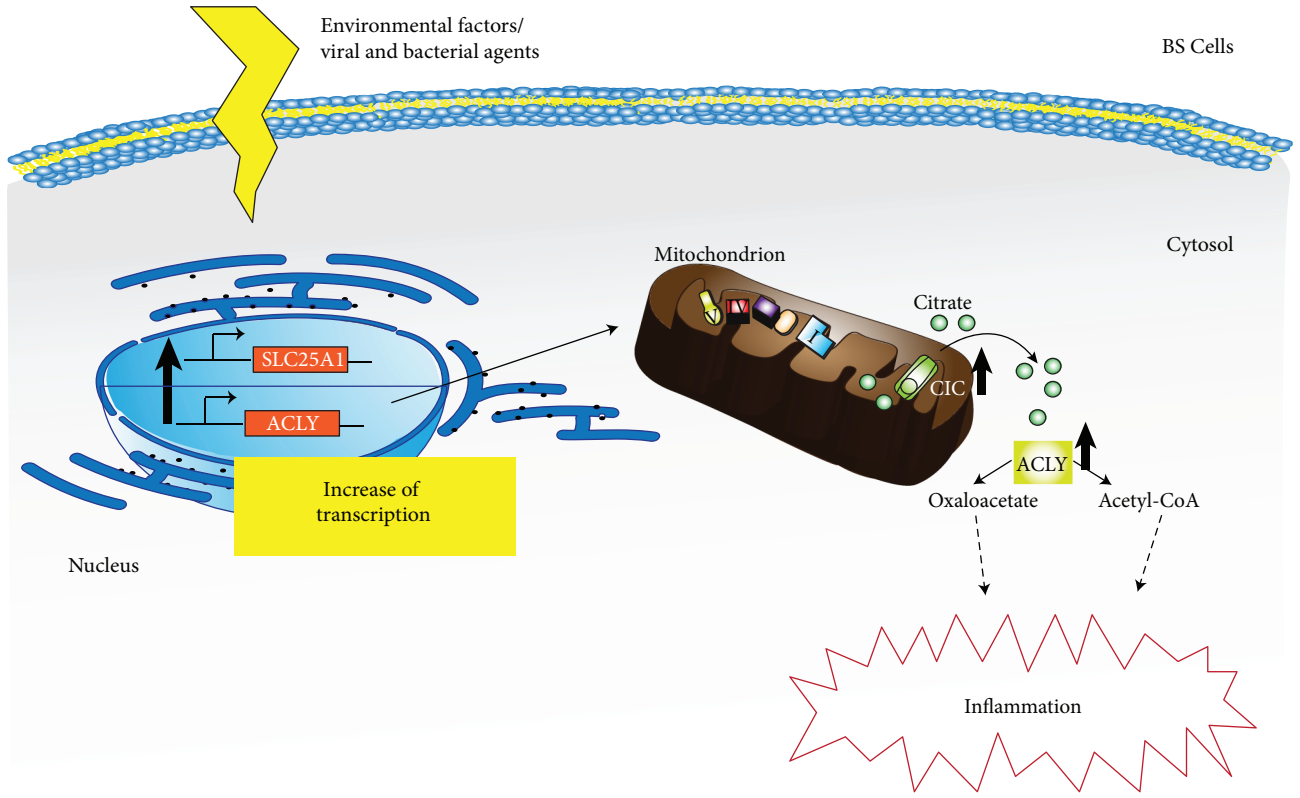

Figure 3: Role of the citrate pathway in Behçet's syndrome (BS). In BS cells, different triggers induce an increase of the SLC25A1 and ACLY transcription rate. The citrate carrier (CIC)—SLC25A1 encoded protein—exports citrate from mitochondria to the cytosol where it is cleaved by ACLY into oxaloacetate and acetyl-CoA. Both the metabolites support the production of the inflammatory mediators.

prevent a dangerous response or provide the desired response, so becoming an attractive alternative to chemotherapy or immunosuppression.

Metabolic reprogramming of immune cells is a feature deeply associated to rheumatologic diseases such as systemic lupus erythematosus, rheumatoid arthritis, and osteoarthritis and could be a novel opportunity to manipulate cellular metabolism for therapeutic purposes [23].

BS shares clinical features with well-recognised autoinflammatory disorders. There is growing evidence that environmental factors and both viral and bacterial agents may act as BS triggers in genetically predisposed subjects; genetic factors induce the immune system hyperactivity, the expression of heat shock proteins and major histocompatibility complex (MHC) class I chain-related molecules A [24, 25].

Genome-wide association studies (GWAS) showed that several susceptibility loci explaining the genetic contribution to BS onset and development correspond to genes involved in the inflammasome pathway. The human leukocyte antigen-B51 (HLA-B∗51) is the most strongly associated risk factor for BS, but it only partially explains the genetic risk of BS [26–28]. These genes involve both innate and adaptive immunities and are shared among different immune-related disorders [24, 29].

Another point to address in clarifying the inflammatory feature of BS was related to the relationship between the excessive T cell-mediated inflammatory response and the disease activity. The helper T cell (Th) homeostasis perturbation seems to be involved in this mechanism. Higher frequency of circulating Th1/Th17 cells has been reported in active BS patients compared with inactive patients, suggesting that these cells and the interleukin 17/interleukin 23 pathway can contribute to the inflammatory reaction and have a pathogenic role in BS [30, 31]. High levels of innate immunity-related cytokines such as IL-1β, IL-6, IL-12, IL-23, and TNF-α have been found in sera of BS patients compared to those of controls [32, 33]. Among proinflammatory cytokines secreted by macrophages, IL-1β could play a specific role in activation and homeostasis regulation of Th cells. Interestingly, in our study, sera from active show a significant increase of IL-1β with respect to those from inactive BS patients and healthy controls.

Proinflammatory cytokines were also secreted by hyperactivated neutrophils, so the activation of neutrophils is another key mechanism in the pathogenesis of the disease. Previous studies reported both increased proactive neutrophils and increased generation of ROS in BS patients [34–36].

However, little is known about the involvement of immunometabolism in Behçet's syndrome. Here, for the first time,

we have investigated the role of the citrate pathway in BS enrolling patients divided into two groups: patients having active disease and patients having no clinical manifestations. Interestingly, the presence of an active disease is linked to higher levels of SCL25A1 mRNA compared to those measured in inactive BS patients. Moreover, inactive BS patients show a significant rise of SCL25A1 mRNA with respect to control subjects, indicating a first step of upregulation related to the presence of BS and an additional one during the active phase. In light of our results, we have hypothesized that a metabolic trait of BS could be the diversion of the citrate from the Krebs cycle to the cytosol. Increased ACLY mRNA levels found in active BS patients compared to controls strengthen our idea. Therefore, SLC25A1 upregulation could allow a great export of the citrate from the mitochondria to the cytosol where it is cleaved by increased levels of ACLY thus producing acetyl-CoA and OAA. Since it has been reported that both the metabolites are used in immune cells to synthesize specific mediators of inflammation such as ROS, NO, and prostaglandins (Figure 3) [5], the increased citrate export pathway here described in BS patients could be responsible, at least in part, for the increased oxidative stress and inflammatory features of the disease.

Our results shed light on citrate pathway dysregulation occurring in BS. However, further investigations are needed to better understand its role in BS pathogenesis.

Data Availability

The data used to support the findings of this study are available from the corresponding author upon request.

Conflicts of Interest

The authors declare that there is no conflict of interest regarding the publication of this paper.

Acknowledgments

The authors thank Professor Ignazio Olivieri for his sincere advice, his guidance of this study, and for having taught us the enthusiasm for knowledge. This research was supported by grants from University of Basilicata to Vittoria Infantino (3010101).

References

[1] G. Hatemi, Y. Yazici, and H. Yazici, "Behcet's syndrome," *Rheumatic Diseases Clinics of North America*, vol. 39, no. 2, pp. 245–261, 2013.

[2] P. Leccese, Y. Yazici, and I. Olivieri, "Behçet's syndrome in nonendemic regions," *Current Opinion in Rheumatology*, vol. 29, no. 1, pp. 12–16, 2017.

[3] A. Gul, "Pathogenesis of Behçet's disease: autoinflammatory features and beyond," *Seminars in Immunopathology*, vol. 37, no. 4, pp. 413–418, 2015.

[4] H. Belguendouz, K. Lahmar-Belguendouz, D. Messaoudene et al., "Cytokines modulate the "immune-metabolism" interactions during Behçet disease: effect on arginine metabolism," *International Journal of Inflammation*, vol. 2015, Article ID 241738, 9 pages, 2015.

[5] V. Infantino, C. L. Pierri, and V. Iacobazzi, "Metabolic routes in inflammation: the citrate pathway and its potential as therapeutic target," *Current Medicinal Chemistry*, vol. 25, 2018.

[6] A. Michelucci, T. Cordes, J. Ghelfi et al., "Immune-responsive gene 1 protein links metabolism to immunity by catalyzing itaconic acid production," *Proceedings of the National Academy of Sciences of the United States of America*, vol. 110, no. 19, pp. 7820–7825, 2013.

[7] E. L. Mills, D. G. Ryan, H. A. Prag et al., "Itaconate is an anti-inflammatory metabolite that activates Nrf2 via alkylation of KEAP1," *Nature*, vol. 556, no. 7699, pp. 113–117, 2018.

[8] V. Iacobazzi and V. Infantino, "Citrate—new functions for an old metabolite," *Biological Chemistry*, vol. 395, no. 4, pp. 387–399, 2014.

[9] V. Iacobazzi, V. Infantino, A. Castegna et al., "Mitochondrial carriers in inflammation induced by bacterial endotoxin and cytokines," *Biological Chemistry*, vol. 398, no. 3, pp. 303–317, 2016.

[10] V. Infantino, P. Convertini, L. Cucci et al., "The mitochondrial citrate carrier: a new player in inflammation," *The Biochemical Journal*, vol. 438, no. 3, pp. 433–436, 2011.

[11] V. Infantino, V. Iacobazzi, A. Menga, M. L. Avantaggiati, and F. Palmieri, "A key role of the mitochondrial citrate carrier (*SLC25A1*) in TNFα- and IFNγ-triggered inflammation," *Biochimica et Biophysica Acta (BBA) - Gene Regulatory Mechanisms*, vol. 1839, no. 11, pp. 1217–1225, 2014.

[12] V. Infantino, V. Iacobazzi, F. Palmieri, and A. Menga, "ATP-citrate lyase is essential for macrophage inflammatory response," *Biochemical and Biophysical Research Communications*, vol. 440, no. 1, pp. 105–111, 2013.

[13] A. K. Jha, S. C. Huang, A. Sergushichev et al., "Network integration of parallel metabolic and transcriptional data reveals metabolic modules that regulate macrophage polarization," *Immunity*, vol. 42, no. 3, pp. 419–430, 2015.

[14] N. Assmann, K. L. O'Brien, R. P. Donnelly et al., "Srebp-controlled glucose metabolism is essential for NK cell functional responses," *Nature Immunology*, vol. 18, no. 11, pp. 1197–1206, 2017.

[15] N. Esser, S. Legrand-Poels, J. Piette, A. J. Scheen, and N. Paquot, "Inflammation as a link between obesity, metabolic syndrome and type 2 diabetes," *Diabetes Research and Clinical Practice*, vol. 105, no. 2, pp. 141–150, 2014.

[16] V. Infantino, V. Iacobazzi, F. De Santis, M. Mastrapasqua, and F. Palmieri, "Transcription of the mitochondrial citrate carrier gene: role of SREBP-1, upregulation by insulin and downregulation by PUFA," *Biochemical and Biophysical Research Communications*, vol. 356, no. 1, pp. 249–254, 2007.

[17] Y. A. Moon, S. W. Park, and K. S. Kim, "Characterization of cis-acting elements in the rat ATP citrate-lyase gene promoter," *Experimental & Molecular Medicine*, vol. 34, no. 1, pp. 60–68, 2002.

[18] D. G. Ryan and L. A. J. O'Neill, "Krebs cycle rewired for macrophage and dendritic cell effector functions," *FEBS Letters*, vol. 591, no. 19, pp. 2992–3006, 2017.

[19] L. A. O'Neill, "A broken Krebs cycle in macrophages," *Immunity*, vol. 42, no. 3, pp. 393-394, 2015.

[20] E. L. Mills, B. Kelly, and L. A. J. O'Neill, "Mitochondria are the powerhouses of immunity," *Nature Immunology*, vol. 18, no. 5, pp. 488–498, 2017.

[21] G. M. Tannahill, A. M. Curtis, J. Adamik et al., "Succinate is an inflammatory signal that induces IL-1β through HIF-1α," *Nature*, vol. 496, no. 7444, pp. 238–242, 2013.

[22] P. Convertini, A. Menga, G. Andria et al., "The contribution of the citrate pathway to oxidative stress in Down syndrome," *Immunology*, vol. 149, no. 4, pp. 423–431, 2016.

[23] J. P. Rhoads, A. S. Major, and J. C. Rathmell, "Fine tuning of immunometabolism for the treatment of rheumatic diseases," *Nature Reviews Rheumatology*, vol. 13, no. 5, pp. 313–320, 2017.

[24] M. Takeuchi, D. L. Kastner, and E. F. Remmers, "The immunogenetics of Behçet's disease: a comprehensive review," *Journal of Autoimmunity*, vol. 64, pp. 137–148, 2015.

[25] M. J. Zeidan, D. Saadoun, M. Garrido, D. Klatzmann, A. Six, and P. Cacoub, "Behçet's disease physiopathology: a contemporary review," *Autoimmunity Highlights*, vol. 7, no. 1, p. 4, 2016.

[26] S. Ohno, T. Asanuma, S. Sugiura, A. Wakisaka, M. Aizawa, and K. Itakura, "HLA-Bw51 and Behçet's disease," *JAMA*, vol. 240, no. 6, p. 529, 1978.

[27] M. Takeuchi, M. J. Ombrello, Y. Kirino et al., "A single endoplasmic reticulum aminopeptidase-1 protein allotype is a strong risk factor for Behçet's disease in HLA-B∗51 carriers," *Annals of the Rheumatic Diseases*, vol. 75, no. 12, pp. 2208–2211, 2016.

[28] J. M. Xavier, F. Davatchi, O. Abade et al., "Characterization of the major histocompatibility complex locus association with Behçet's disease in Iran," *Arthritis Research & Therapy*, vol. 17, no. 1, p. 81, 2015.

[29] I. Sousa, F. Shahram, D. Francisco et al., "Brief report: association of *CCR1*, *KLRC4*, *IL12A-AS1*, *STAT4*, and *ERAP1* with Behçet's disease in Iranians," *Arthritis & Rhematology*, vol. 67, no. 10, pp. 2742–2748, 2015.

[30] Y. Nanke, T. Yago, and S. Kotake, "The role of Th17 cells in the pathogenesis of Behcet's disease," *Journal of Clinical Medicine*, vol. 6, no. 7, p. 74, 2017.

[31] L. Cantarini, V. Pucino, A. Vitale et al., "Immunometabolic biomarkers of inflammation in Behçet's disease: relationship with epidemiological profile, disease activity and therapeutic regimens," *Clinical & Experimental Immunology*, vol. 184, no. 2, pp. 197–207, 2016.

[32] G. Yosipovitch, B. Shohat, J. Bshara, A. Wysenbeek, and A. Weinberger, "Elevated serum interleukin 1 receptors and interleukin 1B in patients with Behçet's disease: correlations with disease activity and severity," *Israel Journal of Medical Sciences*, vol. 31, no. 6, pp. 345–348, 1995.

[33] N. Gholijani, M. R. Ataollahi, A. Samiei, E. Aflaki, S. Shenavandeh, and E. Kamali-Sarvestani, "An elevated pro-inflammatory cytokines profile in Behcet's disease: a multiplex analysis," *Immunology Letters*, vol. 186, pp. 46–51, 2017.

[34] E. Eksioglu-Demiralp, H. Direskeneli, A. Kibaroglu, S. Yavuz, T. Ergun, and T. Akoglu, "Neutrophil activation in Behcet's disease," *Clinical and Experimental Rheumatology*, vol. 19, no. 5, Supplement 24, pp. S19–S24, 2001.

[35] A. Salmaninejad, A. Gowhari, S. Hosseini et al., "Genetics and immunodysfunction underlying Behçet's disease and immunomodulant treatment approaches," *Journal of Immunotoxicology*, vol. 14, no. 1, pp. 137–151, 2017.

[36] H. Yazici, "The lumps and bumps of Behçet's syndrome," *Autoimmunity Reviews*, vol. 3, Supplement 1, pp. S53–S54, 2004.

Hindawi
Mediators of Inflammation
Volume 2018, Article ID 9186940, 11 pages
https://doi.org/10.1155/2018/9186940

Review Article

The Role of Galectins as Modulators of Metabolism and Inflammation

Monica Fengsrud Brinchmann, Deepti Manjari Patel, and Martin Haugmo Iversen

Faculty of Biosciences and Aquaculture, Nord University, 8049 Bodø, Norway

Correspondence should be addressed to Monica Fengsrud Brinchmann; monica.f.brinchmann@nord.no

Received 23 February 2018; Revised 19 April 2018; Accepted 9 May 2018; Published 21 May 2018

Academic Editor: Nicolette C. Bishop

Galectins are β-galcotosid-binding lectins. The function of galectins varies with their tissue-specific and subcellular location, and their binding to carbohydrates makes them key players in several intra- and extracellular processes where they bind to glycosylated proteins and lipids. In humans, there are 12 identified galectins, some with tissue-specific distribution. Galectins are found inside cells and in the nucleus, cytosol, and organelles, as well as extracellularly. Galectin-1, -2, -3, -4, -7, -8, -9, and -12 can all induce T-cell apoptosis and modulate inflammation. In the context of metabolic control and loss of the same in, for example, diabetes, galectin-1, -2, -3, -9, and -12 are especially interesting. This review presents information on galectins relevant to the control of inflammation and metabolism and the potential to target galectins for therapeutic purposes.

1. Introduction

Saccharides are key energy molecules in metabolic pathways. They are also used to modify proteins and lipids to make glycolipids and glycoproteins, that are important in intracellular and extracellular processes. It is therefore not surprising that lectins that bind sugar groups are important modulators of many processes and key functional players in others. Galectins are proteins that bind β-galactosides such as N-acetyllactosamine present in N-linked and O-linked glycoproteins. They are involved in the control of, among others, pre-mRNA splicing, and in the control of apoptosis, cell cycle, cell division, metastasis, and diabetes [1–4]. They can bind to and agglutinate bacteria, and some galectins can kill bacteria directly without the activation of other factors, such as complement factors [5, 6]. In humans, genes for galectin-1, -2, -3, -4, -7, -8, -9, -10, -12, -13, -14, and -16 are found in GenBank (https://www.ncbi.nlm.nih.gov/genbank/ version 19.12.2017, 23.30.00). Even if carbohydrate binding is the classical galectin mode of action, galectins can also interact with other proteins in a carbohydrate-independent manner [7]. One or two galectin carbohydrate recognition domain(s) (CRD(s)) is/are present in the galectins. In prototype galectins (galectin-1, -2, -7, -10, -13, -14, and -16), the protein consists of the globular CRD, the galectin fold with two beta sheets. The chimera galectin-3 has a C-terminal CRD and an N-terminal tail, whilst the tandem repeat galectins (galectin-4, -8, -9, and -12) have two CRDs. Known galectin ligands are, among others, CD45, CD7, CD43, CD2, CD3, CD4, CD107, CEA, laminin and fibronectin, glycosaminoglycans, integrins, GM1 ganglioside, polypeptide HBGp82, glycoprotein 90 K/MAC-2BP, CA125 cancer antigen, and pre-B cell receptor (reviewed in [8]). Galectins can often be both negative and positive modulators of the same processes, suggesting plasticity in isoforms, posttranslational modification(s) or comolecules present, and/or differences in localization.

Processes such as inflammation and metabolism are tightly regulated and fine-tuned. Lack of control can lead to diseases such as diabetes; in fact, chronic, low-grade inflammation is seen in obesity, and this inflammation can lead to obesity-related insulin resistance and eventually type 2 diabetes mellitus [9]. In diabetes mellitus, a long-standing hyperglycemic state can give production of advanced glycation end products (AGEs) that bind to organic molecules and cause complications [10]. In obesity, inflammation is increased, and the number of activated (proinflammatory)

macrophages, associated with insulin resistance in human obesity, increases in human fat tissues [11]. This accumulation and activation of macrophages in turn change the metabolism in white adipocytes, and obesity-related insulin resistance can be looked upon as a disease promoted by chronic inflammation in adipose tissues [12].

Galectin family members are molecules increasingly focused upon as regulators of cellular processes including metabolism and inflammation. This review will focus on the roles of galectins in metabolism and inflammation to elucidate if the galectins could be key regulators involved in the linking of both processes. The reviews' metabolism control of galectin part will be centred on diabetes and obesity, two processes where inflammation and metabolism regulation are important both in the development of imbalances and in upholding them.

2. Main Text

2.1. Galectin-1. Galectin-1 is a prototype galectin with one carbohydrate recognition domain. It is, among others, released from adipose tissues [13], stromal cells in the thymus, lymph nodes, endothelial cells [14], and placenta cells [15]. Apoptosis of activated (antigen-primed) T-cells is induced by galectin-1 in a CD45-dependent manner [14], and T-cell homeostasis can be regulated by galectin-1 through inhibition of clonal expansion and induction of apoptosis. Activated T-cell apoptosis induced by galectin-1 is caspase-8- and -9-dependent [16]. Interestingly, activated T-cells themselves can produce galectin-1 through MEK1/ERK, p38 MAP kinase, and p70S6 kinase signalling pathways, suggesting that this is an autocrine suicide mechanism used to terminate an effector immune response [17]. On the other hand, resting T-cells bind galectin-1, but apoptosis is not induced [14]. Galectin-1 is anti-inflammatory, and its mRNA is upregulated in the placenta in preeclampsia; this is suggested to be a fetal response to maternal systemic infection [15]. The anti-inflammatory activity of galectin-1 can be used to reduce allergic conjunctivitis, an inflammation of the conjunctiva and other parts of the eye. In an allergic conjunctivitis model in mice, externally administered recombinantly produced galectin-1 was an inhibitor of allergic reaction. Galectin-1 reduced IgE levels; however, this was only a slowing of the IgE response as, at 24 hours, galectin-1-treated mice had higher IgE levels than nontreated (allergy control) mice had. In spite of the higher IgE levels, clinical signs were reduced in galectin-1-treated mice [18].

Therapeutic administration of galectin-1 suppresses T-cell-dependent chronic inflammation in arthritis [19], in hepatitis [20], and in colitis [21], suggesting a broad potential for therapeutic use in inflammatory diseases.

Interestingly, in type one diabetes, T-cell-mediated autoimmunity destroys insulin-producing pancreatic β-cells. This process can be inhibited by galectin-1 *in vivo* [17]. Galectin-1 is suggested to have a role in improving glucose metabolism in obese people [22], and galectin-1 levels are higher in obese children than in normal-weight children [22]. Galectin-1 has a potential to be used as an inhibitor of inflammation-related diseases such as diabetes, and also inhibiting galectin-1 led to weight loss in diet-induced obese mice, where weekly injections with a galectin-1 inhibitor attenuated adipogenesis and lipogenesis and increased expression of proteins associated with thermogenesis and energy expenditure [23]. Hence, both stimulation and inhibition of galectin-1 can be of therapeutic value. Galectin-1 levels increase in eyes of patients with diabetes after accumulation of AGEs, and vitreous aspirates from eyes of patients with diabetic macular edema and later proliferative diabetic retinopathy have increased galectin-1 levels. AGE production induces IL-1β via ERK1/2, and PI3K signalling is involved in galectin-1 induction in these patients [24]. This increase in galectin-1 level could be a protective response to the increased AGE levels, similar to that seen in kidneys where galectin-3 is involved in clearance of AGEs [25].

2.2. Galectin-2. Galectin-2 is a prototype, single-CRD galectin, primary expressed in the gastrointestinal tract which can induce T-cell apoptosis through the caspase-3- and -9-dependent intrinsic apoptotic pathway where, among others, cytochrome c leaves the mitochondria. The apoptosis activation is independent of binding to the glycoprotein CD3 or CD7 [16]. In the presence of galectin-2, activated T-cell profiles are modulated to be dominated by Th2 [16].

Interestingly, in a search for genes associated with insulin resistance, a genotype of galectin-2, LGALS2 rs7291467, was stronger associated with changed fasting plasma glucose and serum insulin than other alleles were [26], and the same genotype which has a single-nucleotide polymorphism (3279C $\rightarrow$ T) in intron 1 of LGALS2 encoding galectin-2 was previously found to be significantly associated with myocardial infarction [27]. Galectin-2 binds to the proinflammatory cytokine lymphotoxin-α to regulate inflammation [27]. Galectin-2 is present in the pancreas, but not in islets—only in exocrine cells [28]. It would be interesting to see if galectin-2 present in the pancreas could influence inflammation and the production of insulin in beta cells in the nearby islet; however, we failed to find functional galectin-2 studies on diabetes or obesity.

2.3. Galectin-3. Galectin-3 has several alternative names. Galectin-3 was early characterised in the outer membrane of macrophages and named Mac-2 antigen [29]; found to be IgE binding and named εBP [30]; named CBP35, carbohydrate-binding protein 35 from mouse 3T3 fibroblasts [31]; and named CBP30 as baby hamster kidney carbohydrate-binding protein [32].

Galectin-3 is the only chimera galectin; it has a C-terminal carbohydrate recognition domain as well as an N-terminal tail. Galectin-3 can, like galectin-1, induce T-cell apoptosis [33]; the N-terminal end and the CRD coordinate to induce signalling pathways leading to caspase-9 activation [34]. Inhibiting the *N*-terminal end with an antibody shuts down apoptosis stimulation [34]. When it comes to apoptosis, galectin-3 can be both antiapoptotic and proapoptotic. The antiapoptotic effect is dependent on phosphorylation of serine 6 in galectin-3 and the intracellular presence of galectin-3 [35]; phosphorylated, but not unphosphorylated, galectin-3 can be exported from the nucleus to the cytoplasm

to act as an inhibitor of apoptosis by interacting with mitochondria to, among others, prevent cytochrome c release and caspase-3 activation [36, 37].

The N-terminal and C-terminal ends can both be involved in dimerization or possible oligomerisation of galectin-3, thought to be important for the function of the molecule [38, 39]. The binding properties of galectin-3 to their ligands are pH-dependent [40]; this raises the possibility that pH could be a contributing factor in determining galectin function in different locations including the cellular microenvironments. This is a property exploited in cellular sorting of galectin-3 in polarized Madin-Darby canine kidney cells [41].

Regulation of galectin-3 binding to its ligands is modulated by the phosphorylation state of serine in the N-terminal of the protein, where phosphorylation decreases binding and dephosphorylation increases binding [42]. Phosphorylation of tyrosine 107 can give the cleavage of galectin-3, and the ratio of phosphorylated/dephosphorylated galectin-3 can be used for the prognosis of prostate cancer as well as be a target for potential treatment [43].

Galectin-3 can be endocytosed by macrophages. Uptake of galectin-3 in classically activated M1 macrophages is carbohydrate-independent and mediated by N-terminal end binding, whilst uptake in alternatively activated M2 macrophages, as well as nonmacrophages, is carbohydrate-dependent and involves the C-terminal CRD [44]. In T-cells, galectin-3 is present at the cell surface associated with the TCR complex; it seems to inhibit uncontrolled T-cell activation and potentiates downregulation of TCR in T-cells [45]. Galectin-3 is observed in among others fibroblasts, chondrocytes, osteoblasts, osteoclasts, keratinocytes, Schwann cells and gastric mucosa. It is also found in endothelial cells in a number of tissues, and in immune cells such as neutrophils, eosinophils, basophils, mast cells, Langerhans cells and dendritic cells (cell types reviewed in [46]). It has a role in adipocyte proliferation, and obese mice have more galectin-3 in adipocytes than lean subjects have [47].

Interestingly, whilst galectin-1 can inhibit autoimmune diseases, the research focus on galectin-3's potential therapeutic use is in large focusing on inhibiting galectin-3. This is because galectin-3 promotes cancer and metastasis [1], and inhibition would hence have a great potential for therapeutic anticancer treatment.

Galectin-3 is however beneficial in other situations. It binds AGEs, glycated proteins, and lipids formed, among others, in diabetic patients, and galectin-3 knockout mice have accelerated glomerulopathy and higher renal/glomerular AGEs levels, suggesting that galectin-3 is involved in receptor pathways needed for AGE removal in kidneys [25]. AGEs are interesting as their receptor-mediated uptake led to cytokine production [48]. Galectin-3 can also be a receptor for lipoxidation end products (ALEs) [49]. Even if galectin-3 is beneficial to the kidney as AGE and ALE binders and thus inhibits inflammation, its proinflammatory effect can contribute to inflammation-produced kidney damage [50, 51]. The proinflammatory galectin-3 property has been linked to cardiac inflammation in obese patients [52] and to cardiac lipotoxicity (lipid deposits in the heart) and subsequent mitochondrial dysfunction affecting heart metabolism [53].

2.4. Galectin-4. Galectin-4 is a tandem-repeat galectin with two CRDs joined by a linker. Its main expression is in the gastrointestinal tract of healthy individuals where it has a role in control of intestinal inflammation [54]. In the intestine, galectin-4 interacts with activated T-cells through CD3 binding and promotes calpain-mediated T-cell apoptosis [54]. Importantly, it reduces proinflammatory cytokine production in the intestine mucosa in a colitis model [54]. However, it can also promote inflammation in the intestine by stimulating $CD4^+$ T-cells to produce IL-6 [55].

Taken together, this suggests that galectin-4 could be important not only for ulcerative colitis but also for other inflammatory bowel diseases such as Crohn's disease. Galectin-4 has anticancer properties and has been shown to suppress colorectal cancer [56]; knockdown of it promotes tumorigenesis, and lower levels of galectin-4 expression were observed in inflamed precursor lesions of colorectal cancer [57]. Since T-cell response can help remove cancer cells, the fact that galectin-4 can promote mucosal T-cell apoptosis and also suppress colorectal cancer seems counterintuitive and suggests that there are mechanisms in colorectal inflammation and cancer prevention that warrant further studies. In addition, it is interesting that galectin-4 modulates inflammation, but there seem to be no studies focused on diabetes or other inflammation-dependent obesity diseases associated with galectin-4, suggesting that galectin-4 is not involved in modulation of metabolic diseases since it is mainly expressed in the intestine.

2.5. Galectin-7. Galectin-7 is a homodimeric prototype galectin with one CRD. It is mainly present in the epidermis [58] and can induce apoptosis of stimulated T-cells in a manner dependent upon caspase-1, -3, and -8, but not caspase-9 [16]. Galectin-7-deficient mice appear normal; however, when exposed to UVB irradiation, apoptosis is induced earlier and lasts longer than in wild-type mice [58]. This is surprising, since galectin-7 is proapoptotic [16]; however, the galectin-7-negative mice also show hyperproliferation of cells after UVB irradiation and after wounding [58], more in line with what one would expect when inhibiting the expression of a proapoptotic protein. Overexpression of galectin-7 in mice compromises the skin by leading to loss of cell junctions and defective skin repair [59]. Galectin-7's predominant expression in the skin suggests that it would not influence diabetes or obesity-related inflammation; however, one would suspect that it could play a role in skin diseases related to flawed control of the immune system. Hence, it is not surprising that, in the stratum corneum, galectin-7 is highly expressed in atopic dermatitis patients [60] and possible treatment of this and other skin diseases could target galectin-7.

2.6. Galectin-8. Galectin-8 is a tandem-repeat galectin with two CRDs joined by a linker [61]; it can exist in two splice variants with different linker lengths [62]. Altogether, six possible isoforms exist, three with two CRDs and three with

one CRD [63]. Galectin-8 is expressed in the liver, kidney, cardiac muscle, lung, and brain [61] as well as in a number of different tumoral cells [63]. Galectin-8 induces apoptosis in T-cells through the expression of the death factor Fas ligand and gives caspase-mediated apoptosis [64]. Dimeric galectin-8 resulted in phosphatidylserine exposure in the outer bilayer of cells, something which normally happens during apoptosis activation; however, in the case of galectin-stimulated phospholipid redistribution, this occurred independently of apoptosis [65]. Galectin-8 is secreted under basal conditions from human microvascular endothelial cells and has an autocrine function in that extracellular galectin-8 stimulates the secretion of proinflammatory molecules, CXCL1 (GRO-α), GM-CSF, IL-6, and CCL5 (RANTES), from the endothelial cells [66]. Platelets can also express galectin-8 and be activated by the lectin in an N-terminal CRD-dependent manner [62]. Hence, both endothelial cells and platelets contribute to inflammation stimulated by galectin-8. Galectin-8 can also act proinflammatory by stimulating dendritic cells that secrete proinflammatory cytokines and stimulate antigen-specific T-cells [67]. Activation of neutrophils to produce superoxide is also stimulated by galectin-8 [68]. Galectin-8 is clearly involved in regulation of the immune system; however, we failed to find involvement of galectin-8 in diabetes or other inflammation processes induced by obesity.

2.7. Galectin-9. Galectin-9 is a tandem-repeat galectin with two CRDs joined by a linker sequence. It is expressed in the liver, small intestine, and thymus and in a lesser amount in the kidney, spleen, lung, and cardiac and skeletal muscle and in a low amount in reticulocytes and brain [69].

Galectin-9 is involved in T-cell selection in the thymus where it will induce apoptosis of CD4/CD8 double-negative or double-positive thymocytes and further in promoting naïve T-cell differentiation into Treg and by inhibiting naïve T-cell differentiation into T-helper 17 cells. Finally, it is involved through interaction with TIM3 (T-cell immunoglobulin domain and mucin domain protein 3) in apoptosis induction of $CD4^+$ T-helper 1 (Th1) cells, Th17, cells and $CD8^+$ cytotoxic T-cells. TIM3-negative Th2 cells do not go into apoptosis upon exposure to galectin-9, neither do TIM3-positive Treg cells (T-cells and galectin-9 reviewed in [70]). Taken together, this points to galectin-9 as an important molecule in the regulation of the immune system; in particular, the induction of apoptosis in Th1 and Th17 cells is interesting as activation of these cells is key in regulation of inflammation in, for example, autoimmune diseases. It also suggests that there is a need for research to investigate whether differential glycosylation of the cells can explain why not all TIM3-positive cells enter apoptosis when exposed to galectin-9, whether galectin-9 can act via other receptors [70], or whether there are differences in comolecules, costimulators, or cosuppressors yet to be described. The induction of apoptosis by galectin-9 is through the calcium-calpain-caspase-1 pathway; that is, cytochrome c is released from mitochondria and caspase-activated [71].

Galectin-9 expression in intestine epithelial cells is upregulated in the intestine in patients with food allergy. Mast cells stimulate galectin-9 expression by secreting tryptase, which in turn activate the proteinase-activated receptor 2 on the epithelial cells. Secreted galectin-9 will in turn activate dendritic cells [72]. In another mucosal surface, the airways, administered galectin-9 inhibited airway hyperresponsiveness and by binding to CD44 and inhibited hyaluronan attachment; galectin-9 inhibited Th2-associated inflammation in the airways [73].

As explained above, galectin-9 binds TIM3, a marker present on many immune cells. In early preeclampsia, peripheral lymphocytes, T-cells, cytotoxic T-cells, NK cells, and $CD56^{dim}$ NK cells have reduced TIM3 levels, and an increased frequency of lymphocytic cells with positive galectin-9 expression is found. The lowered TIM3 levels could mean that the normal role of TIM3/galectin-9 in suppressing Th1 cells and secretion of IFN-γ and inducing apoptosis is compromised. One possible explanation is that galectin-9 cannot inhibit inflammation in a situation where TIM3 is downregulated [74]. In the maternal fetal interface, natural killer cells are involved in maternal tolerance of the fetus; the TIM-3/galectin-9 pathway is key to upholding the local tolerance by suppressing a unique NK cell subset's cytotoxicity toward trophoblasts [75]. These decidual NK cells are CD56-positive and CD16-negative cells that are important in immunomodulation in implantation and pregnancy [76]. The cytotoxic activity of decidual NK cells can be switched on; however, this is suppressed in normal pregnancies. Women with recurrent spontaneous abortion have an increased number of cytotoxic NK cells in the endometrium [77]. Interestingly, TIM3 inhibits degranulation of NK cells, and hence cytotoxicity toward trophoblasts, in a galectin-9-dependent way [75].

Galectin-9 is present in intestinal epithelial cells in low amount; however, the levels increase in patients with food allergy. Blocking galectin-9 in a mouse food allergy model inhibited the allergenic hypersensitivity status and Th2 polarization [72].

Galectin-9 is also expressed in adipose tissues, and in diet-induced obesity in mice, subcutaneous adipose tissue showed increased galectin-9 expression. Increased galectin-9 expression was also observed in both $CD11c^-$ and $CD11c^+$ macrophages in visceral adipose tissue compared to lean mice [13]. Galectin-9 is suggested to downregulate inflammation by modulating the interaction of macrophages with T lymphocytes via TIM3.

During obesity, fat can build up in the liver with nonalcoholic fatty liver disease as a result. The disease development is depending upon natural killer cells positive for TIM3; these cells will go into apoptosis when stimulated by galectin-9. Even if galectin-9 can also stimulate natural killer cell proliferation by increasing $TIM3^+$ Kupffer cells' secretion of IL-15, exogenous administration of galectin-9 decreases the development of nonalcoholic fatty liver disease [78]. Similar results are also found in obesity-induced diabetes where a Th1 inflammation response is involved in development of diabetes. In mice, galectin-9, upregulated by injection of plasmid encoding galectin-9, inhibits the development of diabetes. This probably takes place through binding to TIM3, and galectin-9/TIM3 interacting reduced Th1 cell numbers

in the spleen, pancreatic lymph node, and pancreas [79]. Galectin-9 could thus be a possible target for therapeutic strategies to reduce inflammation in obese atients to reduce diseases such as diabetes and fatty liver.

2.8. Galectin-10/Charcot-Leyden Crystal Protein. Galectin-10 is a prototype galectin present as dimers. When eosinophils are recruited to an inflamed site, they are observed to contain autocrystallizing Charcot-Leyden crystal protein, also named galectin-10. When eosinophils degranulate, the galectin-10 crystal deposited can stay in the tissues, in among others asthmatic patients, for extended periods of time. These crystals can induce inflammation in acute peritonitis and bronchitis [80]. Galectin-10 is present in large amounts in eosinophils and basophils, making up 7–10% of the total protein of eosinophils [81]. Galectin-10 is also expressed in $CD4^+CD25^+$ regulatory T-cells [82]; these T-cells are important in downregulation of antiself responses. Interestingly, inhibiting galectin-10 in activated $CD25^+$ Treg cells restored Treg cell proliferative capacity and also overrode their suppressive function [82]. A subpopulation of eosinophils are regulatory eosinophils that can suppress T-cells, through a mechanism that are partly dependent upon galectin-10 [83]. Extracellular recombinant galectin-10 can also suppress T-cell proliferation [83]. Galectin-10 could be a human-specific galectin as it has not been found in other mammals [84]. For galectin-10, there is a need for more information on its molecular role in immunology. A recent study showed induction of IL-1β release upon Charcot-Leyden crystals/galectin-10 uptake by primary human macrophages. The IL-1β release was dependent upon activation of the NLRP3 inflammasome [80]. This indicates a key role for galectin-10 in inflammation, and further studies in this field hold a potential for novel new treatments of inflammation-dependent diseases.

2.9. Galectin-12. Galectin-12 is a tandem galectin with two CRDs where the C-terminal CRD has less homology with classic CRDs than the N-terminal CRD has; the latter has the classical lectin fold with two beta-sheets [85]. Galectin-12 is predominantly expressed in adipose tissue [86].

Differentiation of 3T3-L1 cells into adipocytes is inhibited by downregulation of galectin-12, and upregulation of galectin-12 induces G1 cell cycle arrest and apoptosis [87]. This suggests that galectin-12 has a central role in adipocyte turnover. Allyl isothiocyanate (AITC) reduced the expression of galectin-12 and could reduce the body weight of high-fat-diet-fed mice, further reducing the accumulation of lipid droplets in the liver, and white adipocyte size [88]. On the other hand, a restriction in calories fed increased galectin-12 mRNA levels and treatment of obese animals with troglitazone, a thiazolidinedione, increased galectin-12 expression and decreased adipose tissue size [86]. Hence, both reduced and increased expressions of galectin-12 decrease adipocyte size. The adipose tissues are key in the balance between triglyceride synthesis during energy surplus and lipolysis during energy needs. Interestingly, galectin-12 has a role in upholding this balance, and ablation of galectin-12 in mice shows that galectin-12 has a profound effect on lipid turnover and its removal induces lipolysis and decreases adiposity [89]. Galectin-12 is localised to lipid droplets where it inhibits lipolysis. The binding of galectin-12 to other molecules is probably not through the classical N-terminal CRD, as lactose does not influence the binding; however, the C-terminal nonclassical CRD is postulated to have less affinity for lactose [85] and could be involved in still-to-be-characterised ligand binding. An increase in lipolysis was not found in the liver and muscle in galectin-12-negative mice. This is not surprising as the main localisation of galectin-12 is in the adipose tissues [89]. Galectin-12 is inhibiting phosphorylation-dependent recruitment of hormone-sensitive lipase to lipid droplets probably by restricting the amount of the second messenger cAMP, and galectin-12-negative mice show increased phosphorylation of hormone-sensitive lipase by protein kinase A activated by cAMP. Galectin-12-deficient obese mice also show less insulin resistance/glucose intolerance than do wild-type obese mice so the insulin sensitivity and the glucose tolerance are increased [89]. Hence, galectin-12 is a possible target for therapies to reduce obesity and diabetes mellitus (type 2). Galectin-12 in the adipose tissues is also important for the inflammation state of the tissue as galectin-12 promotes inflammation [90].

Galectin-12 is expressed in macrophages, in addition to adipose tissues [90]. Interestingly, macrophages are infiltrating adipose tissues in obesity [11]. In adipose tissues of mice with diet-induced obesity, there is an increase in macrophages observed in adipose tissues before there is a substantial increase in insulin levels characteristic for systematic insulin resistance [12]. This increase in macrophages is not observed in the muscle, liver, lung, and spleen until very late (after 26 weeks on a high-fat diet) where macrophage gene CD68 was expressed in the liver [12]. It is suggested that the abnormal fat metabolism caused by the increasing adiposity is causing the macrophage accumulation [12]. The macrophages in the adipose tissues could release cytokines that lessen macrophage insulin sensitivity, which again would stimulate recruitment of more macrophages due to the metabolic changes [12]. The macrophages in adipose tissues are heterogenic. Classical M1 macrophages are proinflammatory, and the alternatively activated, M2 macrophages are anti-inflammatory. The proinflammatory macrophages are associated with insulin resistance [11]. In the liver, activation of Kupffer cells by the alternative activation pathway via the peroxisome proliferator-activated receptor delta counteracts obesity-induced insulin resistance [91]. Galectin-$12^{-/-}$ macrophages showed lower phagocytosis of *E. coli* than did galectin-$12^{+/+}$ macrophages, and galectin-$12^{-/-}$ also promoted a M2 macrophage profile during macrophage activation [90] suggesting reduced inflammation when galectin-12 is not present. This is supported by the fact that galectin-12-negative mice fed a high-fat diet had less macrophage infiltrations into adipose tissue than control mice had, as well as lower cholesterol and triglyceride in serum [90]. Galectin-12 expression is linked to galectin-3 expression, and knockout of galectin-3 reduces adipose tissue expression of galectin-12 [92]. This suggests that galectin-3 inhibitors could not only target galectin-3 but also lead

to reduced galectin-12 levels and hence decreased adipose inflammation. However, inhibition of galectin-12 will not change galectin-3 levels [90]; hence, targeting galectin-12 will not clinically help reduce galectin-3 effects.

2.10. Galectin-13, Galectin-14, and Galectin-16. Galectin-13, -14, and -16 were suggested to have placenta-specific expression predominantly in the syncytiotrophoblast, a primary site of metabolic exchange [93], and they are suggested to be important for pregnancy tolerance development. Galectin-13 is special in that the monomers in the homodimer are covalently linked by disulphide bonds [94] whilst other galectins interact noncovalently. Low galectin-13 levels in the third trimester are strongly correlated with preeclampsia [95], and low levels of galectin-13 expression in week 11 were observed in trophoblasts from residual samples of chorionic villus in women who later developed preeclampsia [96]. Galectin-13 can, as galectin-1, -3, and -9, induce apoptosis of activated T-cells, and it is suggested that this could be important to hinder maternal immune cells in attacking the fetus [93].

The extravillous trophoblast from the cervix of early pregnancy loss patients had a reduced level of galectin-14 [97, 98]; also, downregulation of galectin-14 has been found in preterm severe preeclampsia [15].

Galectin-13, -14, and -16 can induce apoptosis of T-cells important in the placenta [93].

The placental localisation of these galectins suggests they are not important for obesity-developed inflammation problems in the adult.

2.11. Clinical Potential of Galectins. Galectins have major roles in processes as diverse as cancer, obesity, diabetes, preeclampsia, and cardiovascular disease. Human galectin-1, -2, -3, -4, -7, -8, -9, and -12 are all interesting in an immunological perspective as they can induce T-cell apoptosis and modulate inflammation. This review has focused on the role of galectins in inflammation and metabolism, and in this perspective, the current knowledge points to galectin-1, -2, -3, -9, and -12 as especially interesting. For galectin-1 and galectin-9, an increase in the levels of the proteins could protect against diabetes, whilst for galectin-12 inhibition of the protein could be protective. In the case of galectin-3, the data are not as straightforward. In the case of galectin-2, we did not find diabetes or obesity-related studies, but galectin-2 modulates inflammation and its presence in the pancreas is interesting and its role in inflammation in the pancreas could be further studied.

In principle, there is hence a potential to treat diseases and disorders by inhibiting some galectins; for others, direct administration of galectin on surfaces or by injections could be beneficial, and for both groups, targeted decrease or increase, respectively, of the expression of the proteins could be therapeutic. The fact that galectins are involved in numerous cellular and intracellular processes, and the fact that there is conserved sequence homology between the galectins, could complicate treatment strategies. However, increased knowledge on galectins' site-specific functions, posttranslational modifications, and binding partners could make it possible to construct modified recombinant galectins as well as specific inhibitors [99]. To increase inhibitor specificity, work on designing new inhibitors and studying the inhibitors' interactions with different galectins [100] is important and promising.

Proof of concept of galectin inhibition and the use of administered galectin as treatments come from animal experiments described for the individual galectins above and in this section, and in a limited amount from clinical trials.

Intraperitoneal injection of galectin-1 prevents onset of hyperglycemia and reverse pancreatic beta cell autoimmunity in the pancreas in mice [101]. In addition, healing of pathological wounds in diabetic mice was accelerated by subcutaneous injection of galectin-1 [102]. Galectin-1 is implicated in tumor development [3] and in obesity [22, 23], and the galectin-1 inhibitor thiodigalactoside reduced the body weight gain in mice [23].

We did not find clinical studies in human targeting galectin-1 by the use of inhibitors or injections of the protein. However, a study using bevacizumab (antibody against vascular endothelial growth factor) and ipilimumab (antibody against cytotoxic T-lymphocyte-associated antigen 4) on patients with metastatic melanoma found that patients with therapeutic responses made antibodies against galectin-1, whilst a group of patients with reduced survival had increased circulating galectin-1 protein levels [103]. There is a wide interest in galectin-1 as a possible therapeutic target, and inhibitors of galectin-1, modified galectin-1, antibodies against galectin-1, and strategies for targeted delivery are currently investigated, and several companies, universities, and institutes hold patents for the use of these potential treatment strategies (thoroughly reviewed in [99]). Since both administration of galectin-1 and inhibition of it can be beneficial, studies need to be holistic and body weight, diabetes, and cancer should be monitored in further work.

Galectin-3 is a complex therapeutic target as it is involved in both inhibition and stimulation of inflammation. Treatment targeting galectin-3 must also take into consideration the fact that galectin-3 promotes cancer and metastasis [1] and that there is not a causal necessity between a protein being upregulated in a disease and the possibility to treat the disease by inhibiting the protein. This is clearly shown in a transgenic fibrotic cardiomyopathy model in mice, where galectin-3 was upregulated both at mRNA and protein levels; however, neither galectin-3 inhibitors nor galectin-3 knockout were effective in reversing cardiac fibrosis or inflammation [104]. This suggests that in fibrotic cardiomyopathy, at least in this mouse model, galectin-3 increase is a symptom, not an inducer of the disease. In a heart failure model in mice, however, proposed inhibition of galectin-3 with modified citrus pectin reduced myocardial inflammation, and reversed isoproterenol induced fibrogenesis that, untreated, led to left ventricular dysfunction [105]. It should be noted that even though pectins inhibit galectin-3-induced hemagglutination and cell interaction [106], a thorough *in vitro* study of plant-derived polysaccharides, including pectin, showed low inhibition or no inhibition at all of galectin-3 [107]. Therefore, the reduced myocardial

inflammation effects of citrus pectin could be through other mechanisms than direct galectin-3 inhibition.

There are several inhibitors targeting galectin-3 (reviewed with a focus on patents in [108]). In humans, there are a few studies targeting galectin-3. The galectin-3 inhibitor GR-MD-02 (galactoarabino-rhamnogalacturonate; it also binds galectin-1 but with lower affinity) was used in a double-blinded study on subjects with nonalcoholic steatohepatitis with advanced fibrosis. The highest dose tested reduced fibrosis [109]. The same drug was used to study potential inhibition of inflammation in psoriasis subjects (only five subjects and no control group). Interestingly, patients infused with GR-MD-02 biweekly 13 times showed an average of >50% reduction in the Psoriasis Area Severity Index [110]. However, the lack of control subjects, the few subjects included, and the short time frame studied suggest that further studies must be conducted before one can conclude that the galectin-3 inhibitor has potential for treating psoriasis.

Galectin-9 promotes apoptosis of several cell types, including T-cells, in a TIM3-dependent manner [70] and hence modulates inflammation. In development of type 1 diabetes, insulin-producing beta cells in the pancreas are destroyed; this autoimmune destruction is dependent on Th1 cells. Interestingly, upregulation of galectin-9 by injection of a galectin-9 plasmid in mice significantly protected them from diabetes [79]. In another mouse study, injection of galectin-9 inhibited development of diabetes, and an antibody against TIM3 was at least as effective as galectin-9 injections in protecting against development of diabetes [111]. This strongly suggests that galectin-9 and molecules interacting with it such as TIM3 have key roles in diabetes and have a therapeutic potential. A study using prebiotic galactooligosaccharides and fructooligosaccharides in combination with *Bifidobacterium breve* M-16V increased serum and intestinal epithelial cell levels of galectin-9 in mice [112]. Infants with atopic dermatitis in a double-blind, placebo-controlled study fed a hydrolysed formula without (control) or with galactooligosaccharides and fructooligosaccharides in combination with *Bifidobacterium breve* for twelve weeks had reduced allergic symptoms [113]. This correlated with increased galectin-9 levels in serum [112]. This indicates that it is possible to increase galectin-9 by dietary administration of pre- and probiotica. However, in a human study, it was not possible to conclude whether galectin-9 levels were protective or promoting for the progression of diabetic nephropathy [114]. Hence, additional studies on galectin-9 and diabetes are needed to see if injection of galectin-9 can prevent diabetes also in human and if the side effects are acceptable.

Galectin-12 was identified in 2001 and is interesting since it is expressed in adipocytes [85, 86]. There are few galectin-12 studies, but importantly galectin-12-negative mice (*Lgals12*$^{-/-}$) [89] have increased lipolysis, adipocyte mitochondrial respiration, reduced whole body lipid content, increased insulin sensitivity compared to wild-type (*Lgals12*$^{+/+}$) mice. Targeting galectin-12 is interesting as it is fat tissue specific and therefore targeting it could help in the prevention/treatment of obesity and diabetes in a targeted manner where other processes, such as cancer, maybe are not affected.

3. Conclusions

This review shows that several galectins are key regulators of inflammation in general and that some galectins are involved in the regulation of inflammation processes in obesity leading to, among others, diabetes. Given their important regulatory roles, they are appealing targets for treatment of human diseases. However, limited human studies targeting galectins are available. It is therefore clear that more research is needed to target individual galectins with specificity, in a timely manner and in specific tissues and cells.

Conflicts of Interest

The authors declare that there is no conflict of interest regarding the publication of this paper.

References

[1] A. Fortuna-Costa, A. M. Gomes, E. O. Kozlowski, M. P. Stelling, and M. S. G. Pavão, "Extracellular galectin-3 in tumor progression and metastasis," *Frontiers in Oncology*, vol. 4, p. 138, 2014.

[2] F. T. Liu, R. J. Patterson, and J. L. Wang, "Intracellular functions of galectins," *Biochimica et Biophysica Acta (BBA) - General Subjects*, vol. 1572, no. 2-3, pp. 263–273, 2002.

[3] F. C. Chou, H. Y. Chen, C. C. Kuo, and H. K. Sytwu, "Role of galectins in tumors and in clinical immunotherapy," *International Journal of Molecular Sciences*, vol. 19, no. 2, 2018.

[4] G. Pugliese, C. Iacobini, C. Ricci, C. Blasetti Fantauzzi, and S. Menini, "Galectin-3 in diabetic patients," *Clinical Chemistry and Laboratory Medicine*, vol. 52, no. 10, pp. 1413–1423, 2014.

[5] S. R. Stowell, C. M. Arthur, M. Dias-Baruffi et al., "Innate immune lectins kill bacteria expressing blood group antigen," *Nature Medicine*, vol. 16, no. 3, pp. 295–301, 2010.

[6] S. R. Stowell, C. M. Arthur, R. McBride et al., "Microbial glycan microarrays define key features of host-microbial interactions," *Nature Chemical Biology*, vol. 10, no. 6, pp. 470–476, 2014.

[7] V. Wells and L. Mallucci, "Identification of an autocrine negative growth factor: mouse β-galactoside-binding protein is a cytostatic factor and cell growth regulator," *Cell*, vol. 64, no. 1, pp. 91–97, 1991.

[8] M. T. Elola, M. E. Chiesa, A. F. Alberti, J. Mordoh, and N. E. Fink, "Galectin-1 receptors in different cell types," *Journal of Biomedical Science*, vol. 12, no. 1, pp. 13–29, 2005.

[9] S. S. Pereira and J. I. Alvarez-Leite, "Low-grade inflammation, obesity, and diabetes," *Current Obesity Reports*, vol. 3, no. 4, pp. 422–431, 2014.

[10] P. Ulrich and A. Cerami, "Protein glycation, diabetes, and aging," *Recent Progress in Hormone Research*, vol. 56, no. 1, pp. 1–22, 2001.

[11] J. M. Wentworth, G. Naselli, W. A. Brown et al., "Pro-inflammatory CD11c$^+$CD206$^+$ adipose tissue macrophages are associated with insulin resistance in human obesity," *Diabetes*, vol. 59, no. 7, pp. 1648–1656, 2010.

[12] H. Xu, G. T. Barnes, Q. Yang et al., "Chronic inflammation in fat plays a crucial role in the development of obesity-related

insulin resistance," *The Journal of Clinical Investigation*, vol. 112, no. 12, pp. 1821–1830, 2003.

[13] D. H. Rhodes, M. Pini, K. J. Castellanos et al., "Adipose tissue-specific modulation of galectin expression in lean and obese mice: evidence for regulatory function," *Obesity*, vol. 21, no. 2, pp. 310–319, 2013.

[14] N. L. Perillo, K. E. Pace, J. J. Seilhamer, and L. G. Baum, "Apoptosis of T cells mediated by galectin-1," *Nature*, vol. 378, no. 6558, pp. 736–739, 1995.

[15] N. G. Than, O. Erez, D. E. Wildman et al., "Severe preeclampsia is characterized by increased placental expression of galectin-1," *The Journal of Maternal-Fetal & Neonatal Medicine*, vol. 21, no. 7, pp. 429–442, 2008.

[16] A. Sturm, M. Lensch, S. Andre et al., "Human galectin-2: novel inducer of T cell apoptosis with distinct profile of caspase activation," *The Journal of Immunology*, vol. 173, no. 6, pp. 3825–3837, 2004.

[17] M. B. Fuertes, L. L. Molinero, M. A. Toscano et al., "Regulated expression of galectin-1 during T-cell activation involves Lck and Fyn kinases and signaling through MEK1/Erk, p38 MAP kinase and $p70^{s6}$ kinase," *Molecular and Cellular Biochemistry*, vol. 267, no. 1/2, pp. 177–185, 2004.

[18] C. B. Mello, L. Ramos, A. D. Gimenes, T. R. . M. Andrade, S. M. Oliani, and C. D. Gil, "Immunomodulatory effects of galectin-1 on an IgE-mediated allergic conjunctivitis model," *Investigative Ophthalmology & Visual Science*, vol. 56, no. 2, pp. 693–704, 2015.

[19] G. A. Rabinovich, G. Daly, H. Dreja et al., "Recombinant galectin-1 and its genetic delivery suppress collagen-induced arthritis via T cell apoptosis," *The Journal of Experimental Medicine*, vol. 190, no. 3, pp. 385–398, 1999.

[20] L. Santucci, S. Fiorucci, F. Cammilleri, G. Servillo, B. Federici, and A. Morelli, "Galectin-1 exerts immunomodulatory and protective effects on concanavalin a–induced hepatitis in mice," *Hepatology*, vol. 31, no. 2, pp. 399–406, 2000.

[21] L. Santucci, S. Fiorucci, N. Rubinstein et al., "Galectin-1 suppresses experimental colitis in mice," *Gastroenterology*, vol. 124, no. 5, pp. 1381–1394, 2003.

[22] S. Acar, A. Paketçi, T. Küme et al., "Serum galectin-1 levels are positively correlated with body fat and negatively with fasting glucose in obese children," *Peptides*, vol. 95, pp. 51–56, 2017.

[23] R. Mukherjee, S. W. Kim, T. Park, M. S. Choi, and J. W. Yun, "Targeted inhibition of galectin 1 by thiodigalactoside dramatically reduces body weight gain in diet-induced obese rats," *International Journal of Obesity*, vol. 39, no. 9, pp. 1349–1358, 2015.

[24] A. Kanda, Y. Dong, K. Noda, W. Saito, and S. Ishida, "Advanced glycation endproducts link inflammatory cues to upregulation of galectin-1 in diabetic retinopathy," *Scientific Reports*, vol. 7, no. 1, article 16168, 2017.

[25] G. Pugliese, F. Pricci, C. Iacobini et al., "Accelerated diabetic glomerulopathy in galectin-3/AGE receptor 3 knockout mice," *The FASEB Journal*, vol. 15, no. 13, pp. 2471–2479, 2001.

[26] M. B. Christensen, D. A. Lawlor, T. R. Gaunt et al., "Genotype of galectin 2 (*LGALS2*) is associated with insulin-glucose profile in the British Women's Heart and Health Study," *Diabetologia*, vol. 49, no. 4, pp. 673–677, 2006.

[27] K. Ozaki, K. Inoue, H. Sato et al., "Functional variation in *LGALS2* confers risk of myocardial infarction and regulates lymphotoxin-α secretion in vitro," *Nature*, vol. 429, no. 6987, pp. 72–75, 2004.

[28] C. Lindskog, A. Asplund, M. Engkvist, M. Uhlen, O. Korsgren, and F. Ponten, "Antibody-based proteomics for discovery and exploration of proteins expressed in pancreatic islets," *Discovery Medicine*, vol. 9, no. 49, pp. 565–578, 2010.

[29] M. K. Ho and T. A. Springer, "Mac-2, a novel 32,000 Mr mouse macrophage subpopulation-specific antigen defined by monoclonal antibodies," *The Journal of Immunology*, vol. 128, no. 3, pp. 1221–1228, 1982.

[30] F. T. Liu, K. Albrandt, E. Mendel, A. Kulczycki, and N. K. Orida, "Identification of an IgE-binding protein by molecular cloning," *Proceedings of the National Academy of Sciences of the United States of America*, vol. 82, no. 12, pp. 4100–4104, 1985.

[31] S. Jia and J. L. Wang, "Carbohydrate binding protein 35. Complementary DNA sequence reveals homology with proteins of the heterogeneous nuclear RNP," *Journal of Biological Chemistry*, vol. 263, no. 13, pp. 6009–6011, 1988.

[32] B. Mehul, S. Bawumia, S. R. Martin, and R. C. Hughes, "Structure of baby hamster kidney carbohydrate-binding protein CBP30, an S-type animal lectin," *Journal of Biological Chemistry*, vol. 269, no. 27, pp. 18250–18258, 1994.

[33] T. Fukumori, Y. Takenaka, T. Yoshii et al., "CD29 and CD7 mediate galectin-3-induced type II T-cell apoptosis," *Cancer Research*, vol. 63, no. 23, pp. 8302–8311, 2003.

[34] H. Xue, L. Liu, Z. Zhao et al., "The N-terminal tail coordinates with carbohydrate recognition domain to mediate galectin-3 induced apoptosis in T cells," *Oncotarget*, vol. 8, no. 30, pp. 49824–49838, 2017.

[35] T. Yoshii, T. Fukumori, Y. Honjo, H. Inohara, H. R. C. Kim, and A. Raz, "Galectin-3 phosphorylation is required for its anti-apoptotic function and cell cycle arrest," *Journal of Biological Chemistry*, vol. 277, no. 9, pp. 6852–6857, 2002.

[36] Y. Takenaka, T. Fukumori, T. Yoshii et al., "Nuclear export of phosphorylated galectin-3 regulates its antiapoptotic activity in response to chemotherapeutic drugs," *Molecular and Cellular Biology*, vol. 24, no. 10, pp. 4395–4406, 2004.

[37] T. Fukumori, N. Oka, Y. Takenaka et al., "Galectin-3 regulates mitochondrial stability and antiapoptotic function in response to anticancer drug in prostate cancer," *Cancer Research*, vol. 66, no. 6, pp. 3114–3119, 2006.

[38] A. Lepur, E. Salomonsson, U. J. Nilsson, and H. Leffler, "Ligand induced galectin-3 protein self-association," *Journal of Biological Chemistry*, vol. 287, no. 26, pp. 21751–21756, 2012.

[39] S. Kuklinski and R. Probstmeier, "Homophilic binding properties of galectin-3: involvement of the carbohydrate recognition domain," *Journal of Neurochemistry*, vol. 70, no. 2, pp. 814–823, 1998.

[40] T. von Mach, M. C. Carlsson, T. Straube, U. Nilsson, H. Leffler, and R. Jacob, "Ligand binding and complex formation of galectin-3 is modulated by pH variations," *Biochemical Journal*, vol. 457, no. 1, pp. 107–115, 2014.

[41] T. Straube, T. von Mach, E. Honig, C. Greb, D. Schneider, and R. Jacob, "Ph-dependent recycling of galectin-3 at the apical membrane of epithelial cells," *Traffic*, vol. 14, no. 9, pp. 1014–1027, 2013.

[42] N. Mazurek, J. Conklin, J. C. Byrd, A. Raz, and R. S. Bresalier, "Phosphorylation of the β-galactoside-binding protein

galectin-3 modulates binding to its ligands," *Journal of Biological Chemistry*, vol. 275, no. 46, pp. 36311–36315, 2000.

[43] V. Balan, P. Nangia-Makker, D. H. Kho, Y. Wang, and A. Raz, "Tyrosine-phosphorylated galectin-3 protein is resistant to prostate-specific antigen (PSA) cleavage," *Journal of Biological Chemistry*, vol. 287, no. 8, pp. 5192–5198, 2012.

[44] A. Lepur, M. C. Carlsson, R. Novak, J. Dumic, U. J. Nilsson, and H. Leffler, "Galectin-3 endocytosis by carbohydrate independent and dependent pathways in different macrophage like cell types," *Biochimica et Biophysica Acta (BBA) - General Subjects*, vol. 1820, no. 7, pp. 804–818, 2012.

[45] H. Y. Chen, A. Fermin, S. Vardhana et al., "Galectin-3 negatively regulates TCR-mediated $CD4^+$ T-cell activation at the immunological synapse," *Proceedings of the National Academy of Sciences of the United States of America*, vol. 106, no. 34, pp. 14496–14501, 2009.

[46] J. Dumic, S. Dabelic, and M. Flögel, "Galectin-3: an open-ended story," *Biochimica et Biophysica Acta (BBA) - General Subjects*, vol. 1760, no. 4, pp. 616–635, 2006.

[47] K. Kiwaki, C. M. Novak, D. K. Hsu, F. T. Liu, and J. A. Levine, "Galectin-3 stimulates preadipocyte proliferation and is up-regulated in growing adipose tissue," *Obesity*, vol. 15, no. 1, pp. 32–39, 2007.

[48] H. Vlassara and M. R. Palace, "Diabetes and advanced glycation endproducts," *Journal of Internal Medicine*, vol. 251, no. 2, pp. 87–101, 2002.

[49] C. Iacobini, S. Menini, C. Ricci et al., "Advanced lipoxidation end-products mediate lipid-induced glomerular injury: role of receptor-mediated mechanisms," *The Journal of Pathology*, vol. 218, no. 3, pp. 360–369, 2009.

[50] Y. Kikuchi, S. Kobayashi, N. Hemmi et al., "Galectin-3-positive cell infiltration in human diabetic nephropathy," *Nephrology Dialysis Transplantation*, vol. 19, no. 3, pp. 602–607, 2004.

[51] A. P. Fernandes Bertocchi, G. Campanhole, P. H. M. Wang et al., "A role for galectin-3 in renal tissue damage triggered by ischemia and reperfusion injury," *Transplant International*, vol. 21, no. 10, pp. 999–1007, 2008.

[52] E. Martínez-Martínez, N. López-Ándres, R. Jurado-López et al., "Galectin-3 participates in cardiovascular remodeling associated with obesity," *Hypertension*, vol. 66, no. 5, pp. 961–969, 2015.

[53] G. Marín-Royo, I. Gallardo, E. Martínez-Martínez et al., "Inhibition of galectin-3 ameliorates the consequences of cardiac lipotoxicity in a rat model of diet-induced obesity," *Disease Models & Mechanisms*, vol. 11, no. 2, 2018.

[54] D. Paclik, S. Danese, U. Berndt, B. Wiedenmann, A. Dignass, and A. Sturm, "Galectin-4 controls intestinal inflammation by selective regulation of peripheral and mucosal t cell apoptosis and cell cycle," *PLoS One*, vol. 3, no. 7, article e2629, 2008.

[55] A. Hokama, E. Mizoguchi, K. Sugimoto et al., "Induced reactivity of intestinal $CD4^+$ T cells with an epithelial cell lectin, galectin-4, contributes to exacerbation of intestinal inflammation," *Immunity*, vol. 20, no. 6, pp. 681–693, 2004.

[56] A. Satelli, P. S. Rao, S. Thirumala, and U. S. Rao, "Galectin-4 functions as a tumor suppressor of human colorectal cancer," *International Journal of Cancer*, vol. 129, no. 4, pp. 799–809, 2011.

[57] S. W. Kim, K. C. Park, S. M. Jeon et al., "Abrogation of galectin-4 expression promotes tumorigenesis in colorectal cancer," *Cellular Oncology*, vol. 36, no. 2, pp. 169–178, 2013.

[58] G. Gendronneau, S. S. Sidhu, D. Delacour et al., "Galectin-7 in the control of epidermal homeostasis after injury," *Molecular Biology of the Cell*, vol. 19, no. 12, pp. 5541–5549, 2008.

[59] G. Gendronneau, S. Sanii, T. Dang et al., "Overexpression of *galectin-7* in mouse epidermis leads to loss of cell junctions and defective skin repair," *PLoS One*, vol. 10, no. 3, article e0119031, 2015.

[60] J. I. Sakabe, K. Kamiya, H. Yamaguchi et al., "Proteome analysis of stratum corneum from atopic dermatitis patients by hybrid quadrupole-orbitrap mass spectrometer," *The Journal of Allergy and Clinical Immunology*, vol. 134, no. 4, pp. 957–960.e8, 2014.

[61] Y. R. Hadari, K. Paz, R. Dekel, T. Mestrovic, D. Accili, and Y. Zick, "Galectin-8. A new rat lectin, related to galectin-4," *Journal of Biological Chemistry*, vol. 270, no. 7, pp. 3447–3453, 1995.

[62] M. A. Romaniuk, M. V. Tribulatti, V. Cattaneo et al., "Human platelets express and are activated by galectin-8," *Biochemical Journal*, vol. 432, no. 3, pp. 535–547, 2010.

[63] N. Bidon, F. Brichory, P. Bourguet, J. P. Le Pennec, and L. Dazord, "Galectin-8: a complex sub-family of galectins (review)," *International Journal of Molecular Medicine*, vol. 8, no. 3, pp. 245–250, 2001.

[64] A. Norambuena, C. Metz, L. Vicuña et al., "Galectin-8 induces apoptosis in Jurkat T cells by phosphatidic acid-mediated ERK1/2 activation supported by protein kinase A down-regulation," *Journal of Biological Chemistry*, vol. 284, no. 19, pp. 12670–12679, 2009.

[65] S. R. Stowell, C. M. Arthur, K. A. Slanina, J. R. Horton, D. F. Smith, and R. D. Cummings, "Dimeric galectin-8 induces phosphatidylserine exposure in leukocytes through polylactosamine recognition by the C-terminal domain," *Journal of Biological Chemistry*, vol. 283, no. 29, pp. 20547–20559, 2008.

[66] V. Cattaneo, M. V. Tribulatti, J. Carabelli, A. Carestia, M. Schattner, and O. Campetella, "Galectin-8 elicits pro-inflammatory activities in the endothelium," *Glycobiology*, vol. 24, no. 10, pp. 966–973, 2014.

[67] J. Carabelli, V. Quattrocchi, A. D'Antuono, P. Zamorano, M. V. Tribulatti, and O. Campetella, "Galectin-8 activates dendritic cells and stimulates antigen-specific immune response elicitation," *Journal of Leukocyte Biology*, vol. 102, no. 5, pp. 1237–1247, 2017.

[68] N. Nishi, H. Shoji, M. Seki et al., "Galectin-8 modulates neutrophil function via interaction with integrin αM," *Glycobiology*, vol. 13, no. 11, pp. 755–763, 2003.

[69] J. Wada and Y. S. Kanwar, "Identification and characterization of galectin-9, a novel β-galactoside-binding mammalian lectin," *Journal of Biological Chemistry*, vol. 272, no. 9, pp. 6078–6086, 1997.

[70] V. R. Wiersma, M. de Bruyn, W. Helfrich, and E. Bremer, "Therapeutic potential of galectin-9 in human disease," *Medicinal Research Reviews*, vol. 33, no. S1, pp. E102–E126, 2013.

[71] Y. Kashio, K. Nakamura, M. J. Abedin et al., "Galectin-9 induces apoptosis through the calcium-calpain-caspase-1 pathway," *The Journal of Immunology*, vol. 170, no. 7, pp. 3631–3636, 2003.

[72] X. Chen, C. H. Song, Z. Q. Liu et al., "Intestinal epithelial cells express galectin-9 in patients with food allergy that plays a critical role in sustaining allergic status in mouse intestine," *Allergy*, vol. 66, no. 8, pp. 1038–1046, 2011.

[73] S. Katoh, N. Ishii, A. Nobumoto et al., "Galectin-9 inhibits CD44–hyaluronan interaction and suppresses a murine model of allergic asthma," *American Journal of Respiratory and Critical Care Medicine*, vol. 176, no. 1, pp. 27–35, 2007.

[74] E. Miko, M. Meggyes, B. Bogar et al., "Involvement of Galectin-9/TIM-3 pathway in the systemic inflammatory response in early-onset preeclampsia," *PLoS One*, vol. 8, no. 8, article e71811, 2013.

[75] J. Sun, M. Yang, Y. Ban et al., "Tim-3 is upregulated in NK cells during early pregnancy and inhibits NK cytotoxicity toward trophoblast in galectin-9 dependent pathway," *PLoS One*, vol. 11, no. 1, article e0147186, 2016.

[76] L. A. Koopman, H. D. Kopcow, B. Rybalov et al., "Human decidual natural killer cells are a unique NK cell subset with immunomodulatory potential," *The Journal of Experimental Medicine*, vol. 198, no. 8, pp. 1201–1212, 2003.

[77] M. H. Lachapelle, P. Miron, R. Hemmings, and D. C. Roy, "Endometrial T, B, and NK cells in patients with recurrent spontaneous abortion. Altered profile and pregnancy outcome," *The Journal of Immunology*, vol. 156, no. 10, pp. 4027–4034, 1996.

[78] Z. H. Tang, S. Liang, J. Potter, X. Jiang, H. Q. Mao, and Z. Li, "Tim-3/galectin-9 regulate the homeostasis of hepatic NKT cells in a murine model of nonalcoholic fatty liver disease," *The Journal of Immunology*, vol. 190, no. 4, pp. 1788–1796, 2013.

[79] F. C. Chou, S. J. Shieh, and H. K. Sytwu, "Attenuation of Th1 response through galectin-9 and T-cell Ig mucin 3 interaction inhibits autoimmune diabetes in NOD mice," *European Journal of Immunology*, vol. 39, no. 9, pp. 2403–2411, 2009.

[80] J. F. Rodrigues-Alcazar, M. A. Ataide, G. Engels et al., "Charcot-Leyden crystals activate the NLRP3 inflammasome and cause IL-1β inflammation," *bioRxiv*, 2018.

[81] A. M. Dvorak, L. Letourneau, G. R. Login, P. F. Weller, and S. J. Ackerman, "Ultrastructural localization of the Charcot-Leyden crystal protein (lysophospholipase) to a distinct crystalloid-free granule population in mature human eosinophils," *Blood*, vol. 72, no. 1, pp. 150–158, 1988.

[82] J. Kubach, P. Lutter, T. Bopp et al., "Human $CD4^+CD25^+$ regulatory T cells: proteome analysis identifies galectin-10 as a novel marker essential for their anergy and suppressive function," *Blood*, vol. 110, no. 5, pp. 1550–1558, 2007.

[83] C. Lingblom, J. Andersson, K. Andersson, and C. Wenneras, "Regulatory eosinophils suppress T cells partly through galectin-10," *The Journal of Immunology*, vol. 198, no. 12, pp. 4672–4681, 2017.

[84] E. Choi, A. D. Miller, E. Devenish, M. Asakawa, M. McConkey, and J. Peters-Kennedy, "Charcot–Leyden crystals: do they exist in veterinary species? A case report and literature review," *Journal of Veterinary Diagnostic Investigation*, vol. 29, no. 6, pp. 904–909, 2017.

[85] R. Y. Yang, D. K. Hsu, L. Yu, J. Ni, and F. T. Liu, "Cell cycle regulation by galectin-12, a new member of the galectin superfamily," *Journal of Biological Chemistry*, vol. 276, no. 23, pp. 20252–20260, 2001.

[86] K. Hotta, T. Funahashi, Y. Matsukawa et al., "Galectin-12, an adipose-expressed galectin-like molecule possessing apoptosis-inducing activity," *Journal of Biological Chemistry*, vol. 276, no. 36, pp. 34089–34097, 2001.

[87] L. Wan, R.-Y. Yang, and F.-T. Liu, "Galectin-12 in cellular differentiation, apoptosis and polarization," *International Journal of Molecular Sciences*, vol. 19, no. 1, p. 176, 2018.

[88] C.-W. Lo, C. S. Chen, Y. C. Chen et al., "Allyl isothiocyanate ameliorates obesity by inhibiting galectin-12," *Molecular Nutrition & Food Research*, vol. 62, no. 6, 2018.

[89] R. Y. Yang, L. Yu, J. L. Graham et al., "Ablation of a galectin preferentially expressed in adipocytes increases lipolysis, reduces adiposity, and improves insulin sensitivity in mice," *Proceedings of the National Academy of Sciences of the United States of America*, vol. 108, no. 46, pp. 18696–18701, 2011.

[90] L. Wan, H. J. Lin, C. C. Huang et al., "Galectin-12 enhances inflammation by promoting M1 polarization of macrophages and reduces insulin sensitivity in adipocytes," *Glycobiology*, vol. 26, no. 7, pp. 732–744, 2016.

[91] J. I. Odegaard, R. R. Ricardo-Gonzalez, A. Red Eagle et al., "Alternative M2 activation of Kupffer cells by PPARδ ameliorates obesity-induced insulin resistance," *Cell Metabolism*, vol. 7, no. 6, pp. 496–507, 2008.

[92] J. Pang, D. H. Rhodes, M. Pini et al., "Increased adiposity, dysregulated glucose metabolism and systemic inflammation in galectin-3 KO mice," *PLoS One*, vol. 8, no. 2, article e57915, 2013.

[93] N. G. Than, R. Romero, M. Goodman et al., "A primate subfamily of galectins expressed at the maternal–fetal interface that promote immune cell death," *Proceedings of the National Academy of Sciences of the United States of America*, vol. 106, no. 24, pp. 9731–9736, 2009.

[94] N. G. Than, E. Pick, S. Bellyei et al., "Functional analyses of placental protein 13/galectin-13," *European Journal of Biochemistry*, vol. 271, no. 6, pp. 1065–1078, 2004.

[95] N. G. Than, O. Abdul Rahman, R. Magenheim et al., "Placental protein 13 (galectin-13) has decreased placental expression but increased shedding and maternal serum concentrations in patients presenting with preterm preeclampsia and HELLP syndrome," *Virchows Archiv*, vol. 453, no. 4, pp. 387–400, 2008.

[96] A. Sekizawa, Y. Purwosunu, S. Yoshimura et al., "PP13 mRNA expression in trophoblasts from preeclamptic placentas," *Reproductive Sciences*, vol. 16, no. 4, pp. 408–413, 2009.

[97] R. Fritz, H. R. Kohan-Ghadr, J. M. Bolnick et al., "Noninvasive detection of trophoblast protein signatures linked to early pregnancy loss using trophoblast retrieval and isolation from the cervix (TRIC)," *Fertility and Sterility*, vol. 104, no. 2, pp. 339–346.e4, 2015.

[98] J. M. Bolnick, H. R. Kohan-Ghadr, R. Fritz et al., "Altered biomarkers in trophoblast cells obtained noninvasively prior to clinical manifestation of perinatal disease," *Scientific Reports*, vol. 6, no. 1, article 32382, 2016.

[99] H. Blanchard, K. Bum-Erdene, M. H. Bohari, and X. Yu, "Galectin-1 inhibitors and their potential therapeutic applications: a patent review," *Expert Opinion on Therapeutic Patents*, vol. 26, no. 5, pp. 537–554, 2016.

[100] P. M. Collins, C. T. Öberg, H. Leffler, U. J. Nilsson, and H. Blanchard, "Taloside inhibitors of galectin-1 and galectin-3," *Chemical Biology & Drug Design*, vol. 79, no. 3, pp. 339–346, 2012.

[101] M. J. Perone, S. Bertera, W. J. Shufesky et al., "Suppression of autoimmune diabetes by soluble galectin-1," *The Journal of Immunology*, vol. 182, no. 5, pp. 2641–2653, 2009.

[102] Y.-T. Lin, J. S. Chen, M. H. Wu et al., "Galectin-1 accelerates wound healing by regulating the neuropilin-1/Smad3/NOX4 pathway and ROS production in myofibroblasts," *Journal of Investigative Dermatology*, vol. 135, no. 1, pp. 258–268, 2015.

[103] X. Wu, J. Li, E. M. Connolly et al., "Combined anti-VEGF and anti–CTLA-4 therapy elicits humoral immunity to galectin-1 which is associated with favorable clinical outcomes," *Cancer Immunology Research*, vol. 5, no. 6, pp. 446–454, 2017.

[104] M.-N. Nguyen, Y. Su, H. Kiriazis et al., "Upregulated galectin-3 is not a critical disease mediator of cardiomyopathy induced by β_2-adrenoceptor overexpression," *American Journal of Physiology-Heart and Circulatory Physiology*, 2018, In press.

[105] G. Vergaro, M. Prud'homme, L. Fazal et al., "Inhibition of galectin-3 pathway prevents isoproterenol-induced left ventricular dysfunction and fibrosis in mice," *Hypertension*, vol. 1979, no. 67, 2016.

[106] U. V. Sathisha, S. Jayaram, M. A. Harish Nayaka, and S. M. Dharmesh, "Inhibition of galectin-3 mediated cellular interactions by pectic polysaccharides from dietary sources," *Glycoconjugate Journal*, vol. 24, no. 8, pp. 497–507, 2007.

[107] J. Stegmayr, A. Lepur, B. Kahl-Knutson et al., "Low or no inhibitory potency of the canonical galectin carbohydrate-binding site by pectins and galactomannans," *Journal of Biological Chemistry*, vol. 291, no. 25, pp. 13318–13334, 2016.

[108] H. Blanchard, X. Yu, P. M. Collins, and K. Bum-Erdene, "Galectin-3 inhibitors: a patent review (2008–present)," *Expert Opinion on Therapeutic Patents*, vol. 24, no. 10, pp. 1053–1065, 2014.

[109] S. A. Harrison, S. R. Marri, N. Chalasani et al., "Randomised clinical study: GR-MD-02, a galectin-3 inhibitor, vs. placebo in patients having non-alcoholic steatohepatitis with advanced fibrosis," *Alimentary Pharmacology & Therapeutics*, vol. 44, no. 11-12, pp. 1183–1198, 2016.

[110] S. Ritchie, D. Neal, H. Shlevin, A. Allgood, and P. Traber, "A phase 2a, open-label pilot study of the galectin-3 inhibitor GR-MD-02 for the treatment of moderate-to-severe plaque psoriasis," *Journal of the American Academy of Dermatology*, vol. 77, no. 4, pp. 753–755, 2017.

[111] M. Kanzaki, J. Wada, K. Sugiyama et al., "Galectin-9 and t cell immunoglobulin mucin-3 pathway is a therapeutic target for type 1 diabetes," *Endocrinology*, vol. 153, no. 2, pp. 612–620, 2012.

[112] S. de Kivit, E. Saeland, A. D. Kraneveld et al., "Galectin-9 induced by dietary synbiotics is involved in suppression of allergic symptoms in mice and humans," *Allergy*, vol. 67, no. 3, pp. 343–352, 2012.

[113] L. B. van der Aa, H. S. Heymans, W. M. van Aalderen et al., "Effect of a new synbiotic mixture on atopic dermatitis in infants: a randomized-controlled trial," *Clinical & Experimental Allergy*, vol. 40, no. 5, pp. 795–804, 2010.

[114] Y. Kurose, J. Wada, M. Kanzaki et al., "Serum galectin-9 levels are elevated in the patients with type 2 diabetes and chronic kidney disease," *BMC Nephrology*, vol. 14, no. 1, p. 23, 2013.

Hindawi
Mediators of Inflammation
Volume 2018, Article ID 7859601, 11 pages
https://doi.org/10.1155/2018/7859601

Research Article

The Protective Mechanism of CAY10683 on Intestinal Mucosal Barrier in Acute Liver Failure through LPS/TLR4/MyD88 Pathway

Yao Wang[1], **Hui Chen**[2], **Qian Chen**[1], **Fang-Zhou Jiao**[1], **Wen-Bin Zhang**[1] and **Zuo-Jiong Gong**[1]

[1]*Department of Infectious Diseases, Renmin Hospital of Wuhan University, Wuhan, China*
[2]*Hubei Provincial Center for Disease Control and Prevention, Wuhan, China*

Correspondence should be addressed to Zuo-Jiong Gong; zjgong@163.com

Received 30 October 2017; Revised 30 December 2017; Accepted 11 January 2018; Published 13 March 2018

Academic Editor: Fabio S Lira

The purpose of this study was to investigate the protective mechanism of HDAC2 inhibitor CAY10683 on intestinal mucosal barrier in acute liver failure (ALF). In order to establish ALF-induced intestinal epithelial barrier disruption models, D-galactosamine/LPS and LPS were, respectively, used with rats and NCM460 cell and then administrated with CAY10683. Transepithelial electrical resistance (TEER) was measured to detect the permeability of cells. Real-time PCR and Western blotting were employed to detect the key mRNA and protein levels. The intestinal epithelial tissue pathology was detected. After interfering with CAY10683, the mRNA and protein levels of TLR4, MyD88, TRIF, and TRAF6 were decreased compared with model group ($P < 0.05$), whereas the levels of ZO-1 and occluding were elevated ($P < 0.05$). The permeability was elevated in CAY10683-interfered groups, when compared with model group ($P < 0.05$). And the degree of intestinal epithelial tissue pathological damage in CAY10683 group was significantly reduced. Moreover, CAY10683 significantly decreased the TLR4 staining in animal tissue. The HDAC2 inhibitor CAY10683 could promote the damage of intestinal mucosal barrier in ALF through inhibiting LPS/TLR4/MyD88 pathway.

1. Introduction

Acute liver failure (ALF), caused by a large area of hepatocyte necrosis, is a serious clinical syndrome and characterized by the rapid progress of hepatic encephalopathy and severe liver damage associated with high mortality [1]. Early monitor of gastrointestinal dysfunction is a key process to the development of ALF. Endotoxin is a lipopolysaccharide component located in gram-negative bacterial cell wall that easily passes through the damaged intestinal mucosal barrier. Under normal circumstances, the intestinal tract contains a large number of potential pathogens and endotoxin, but the intact intestinal mucosal barrier can effectively prevent intestinal bacteria and endotoxin into the body [2].

Systemic and intestinal immune system in the early stage of ALF showed the inhibited state, so the removal of bacterial capacity decreased and the displacement of bacteria could easily break through the limitations of mesenteric lymph nodes to migrate and colonize to the other body tissues and organs, which could result intestinal mucosal barrier dysfunction, increased permeability, intestinal bacterial translocation, and intestinal endotoxemia, and the result in inflammatory response can further cause systemic inflammatory response syndrome (SIRS) and multiple organ dysfunction syndrome (MODS) [3]. Intestinal *Escherichia coli* and endotoxin penetrate the intestinal epithelium into the blood circulation, activating the mononuclear macrophage system, to promote the release of a large number of cell "toxic factors," such as cytokines, inflammatory mediators, proteases, and oxygen-free radicals [4]. On the one hand, LPS could aggravate the inflammatory injury of the intestinal mucosal barrier, promote the migration of bacteria and endotoxin, and thus format a vicious cycle. On the other hand, the cytokines invading into the blood circulation could result in persistent inflammatory response and continued self-enhancement. Interaction between LPS and TLR4 leads

to formation of an LPS signaling complex consisting of surface molecules, including myeloid differentiation primary response gene 88 (MyD88), toll-interleukin-1 receptor domain-containing adaptor inducing interferon β (TRIF), TNF-α receptor association factor 6 (TRAF6), and activation of transcription factors, which then induce the activation of the inflammatory response [5]. The formation of cascade reaction constitutes a "second strike" to promote systemic inflammatory response syndrome and the occurrence of multiple organ dysfunction [6]. Therefore, the protective of intestinal mucosal barrier can effectively alleviate the ALF.

Aberrant expression of HDAC2 has been identified in chronically inflamed tissues [7]. In human cervical cancer cell lines, HDAC2 was reported to inhibit transcription of the expression of MHC class II genes, and antigen presentation through MHC class II is critical for activation of adaptive immune responses [8]. Cluster of differentiation 36 (CD36) could aggravate macrophage infiltration and hepatic inflammation by upregulating monocyte chemotactic protein-1 (MCP-1) expression of hepatocytes through upregulating HDAC2-dependent pathway [9]. Therefore, histone deacetylase inhibitor (HDACi) may be used to modify immunity through multiple hosts to improve the efficacy of anti-inflammation therapy. Santacruzamate A (CAY10683) is a potent selective HDAC inhibitor that has an IC50 of 119 pM for HDAC2 and a >3600-fold selectivity over other HDACs [10]. As a clinically approved HDAC inhibitor, CAY10683 has antiproliferative and immunomodulatory effects [11], thereby CAY10683 was used to treat cutaneous T-cell lymphoma [12] and breast cancer [13].

Our previous studies have indicated that the selective class I and II HDAC inhibitor trichostatin A could protect the small intestine in ALF liver failure by inflammatory inhibition [6]. However, it is still unknown which type of HDAC molecule inhibitor could protect the small intestine through which kind of specific molecular mechanism. In this study, we aimed to investigate the protective effect of selective HDAC2 inhibitor CAY10683 on LPS-induced damage in NCM460 cells line and in galactosamine/LPS-induced ALF rat model and to explore the mechanisms.

2. Material and Methods

2.1. Chemicals and Reagents. CAY10683 was purchased from Sellect (Houston, USA). DMEM basic and fetal bovine serum (FBS) were purchased from Gibco (NY, USA). Lipopolysaccharide (LPS, purity of 99%) and D-galactosamine (purity of 98%) were purchased from Sigma (St. Louis, USA). The cell counting kit-8 (CCK-8) was purchased from Dojindo Laboratories (Japan). Rabbit anti-rat/human HDAC2, histone 3, acetyl-histone 3 (Ac-histone 3), MyD88, TRIF, TRAF6, occluding, and β-actin were obtained from Cell Signaling Technology (CST) (Boston, USA). TLR4 and ZO-1 antibodies were purchased from Proteintech (Wuhan, China). The goat anti-rabbit fluorescent secondary antibody (IRDye800) was obtained from LI-COR Biosciences Inc. (Lincoln, USA). RNAiso Plus, PrimeScript™ RT reagent kit, and SYBR Premix Ex Taq kit were purchased from TaKaRa (Dalian, China).

2.2. Cell Culture and Chemical Treatment. DMEM medium mixed with 10% FBS was used to culture NCW460 cells in an incubator at 37°C, 5% CO_2, and saturated humidity [14]. The medium was replaced every 2-3 days. LPS was used for cellular model establishment. The intervention groups were divided into normal group, model group, and CAY 10683 group. After the cells were passed in 6-well plates (for real-time PCR and Western blot) or 96-well plates (for CCK8 experiments) for 24 h and cultured to 70% density, the supernatants were removed and LPS (1 μg/ml) was used to stimulate the cells excluding the normal group. At the last 12 hours, CAY 10683 (120 nM) was added into the wells expected for the normal group and model group. After 24 h, the cells were harvested.

2.3. Cell Viability Assays. The cell counting kit-8 (CCK-8) assay was used to examine cell proliferation. NCM460 cells were seeded in 96-well plates at a density of 1.0×10^5/ml for 24 h. After incubation, the medium was replaced with 100 μl various concentrations of CAY 10683 (10 nM, 100 nM, 1000 nM, 10^4 nM, 10^5 nM, 10^6 nM, 10^7 nM, and 10^8 nM). DMEM medium substituted with 10 μl CCK-8 solution was added 24 h later, and the cells were incubated at 37°C. After 2 h, the absorbance at 490 nm was read on microplate reader.

2.4. Transepithelial Electrical Resistance (TEER) Measurement. NCM460 cells were made into 2.5×10^5 cells/ml single cell suspension. The lower cell chambers were added with 1.5 ml DMEM complete medium, and the upper cell chambers were added with 1 ml cell suspension, incubated overnight in an incubator at 37°C, 5% CO_2, and saturated humidity. To observe whether the cell formed a tight layer, and there were no holes formed by dead cells, if the conditions were not met, the cells should be recultured. According to the experimental groups, upper and lower chambers in the model and CAY10683 groups were replaced by the complete medium and complete medium included CAY10683. After 2 hours, the CAY10683 group and LPS group at the same time were added by LPS. The normal group was added by complete medium as control. The cells were incubated for 24 h. And then the calibrated Millipore Millicell ERS-2 cell resistance meter was used to detect resistance value. The measured resistance value was multiplied by the area of the filter to obtain an absolute value of TEER, expressed as $\Omega\,cm^2$. And the TEER values were measured as follows: TEER = (measured resistance value−blank value) × single cell layer surface area (cm^2).

2.5. Animal Groups. Followed the previously published steps [2], a total of 18 rats were randomly divided into three groups with six rats in each group: normal, model, and CAY10683 group. The ALF rat models were administrated by intraperitoneal injection with 400 mg/kg D-galactosamine combined with 100 μg/kg of LPS. CAY10683 and the same amount of saline, respectively, were given to

the CAY10683 group and model group 2 h before ALF model protocol was conducted. All animals were killed in 48 h.

2.6. Biochemical Tests. The serum alanine aminotransferase (ALT), aspartate aminotransferase (AST), and total bilirubin (TBIL) levels were assayed using a fully automated Aeroset chemistry analyzer provided by Abbott Co. Ltd.

2.7. Specimen Collection and Histological Studies. The procedures of the H&E staining assays followed the previously described steps [15]. Fresh liver and small intestine specimens were fixed in 10% neutral-buffered formalin for 2 days and then processed for sectioning and staining by standard histological methods. Sections from the liver and small intestine were stained with H&E and evaluated under BX 51 light microscope (Olympus, Japan).

2.8. Quantitative Real-Time PCR to Detect mRNA Expression. Total RNA in NCM460 cells and small intestine specimens was isolated by using RNAiso Plus according to manufacturer's protocol. The cDNAs were produced with a PrimeScript RT reagent kit and incubated at 37°C for 15 min and at 85°C for 5 s. Real-time PCRs were performed using a StepOne Plus device (Applied Biosystems) at 95°C for 10 s, followed by 40 cycles at 95°C for 5 s, and at 60°C for 20 s, according to the instructions for the SYBR Premix Ex Taq kit. The data were analyzed by the $2^{-\Delta\Delta CT}$ method. All the primers were synthesized by Tsingke (Wuhan, China), and the sequences are listed in Table 1.

2.9. Western Blotting for Protein Expression Measurement. Western blots were carried out using whole cell and small intestine specimen extracts separated on SDS-PAGE gels and then transferred onto a nitrocellulose filter membrane. The membranes were blocked overnight with 5% nonfat milk in phosphate-buffered saline (PBS) and probed with the indicated antibody (Ab) before being washed three times in Tris-buffered saline with Tween 20 (TBST) and then incubated with an HRP-labeled secondary Ab. The dilutions of the primary and secondary antibodies were as follows: HDAC2, 1 : 1000; TLR4, 1 : 1000; MyD88, 1 : 1000; TRIF, 1 : 1000; TRAF6, 1 : 1000; ZO-1, 1 : 1000; occluding, 1 : 1000; histone 3, 1 : 1000; acetyl-histone 3, 1 : 1000; and β-actin, 1 : 1000. And then this was followed by incubation with a fluorescent secondary antibody at 37°C for 2 h. The blot was analyzed using the Odyssey Infrared Imaging System (LI-COR Biosciences). Membranes were also probed for β-actin and histone 3 as additional loading controls.

2.10. IHC to Detect TLR4 Expression in Liver Tissue. After dewaxing and hydrating, the small intestine specimens were cut into 5 mm sections and then incubated in 3% H_2O_2 methanol to eliminate endogenous peroxidase activity. The sections were incubated with normal goat serum for 10 min and incubated with TLR4 (1 : 200) antibody overnight at 4°C. Horseradish peroxidase- (HRP-) conjugated polyclonal to rabbit IgG was used to incubate the sections at 37°C for 30 min after being rinsed again with PBS. The samples were developed with diaminobenzidine and stained with hematoxylin. At last, Image-Pro Plus 6.0 (IPP) software was used to analyze the optical density of the images.

Table 1: The primer sequence for RT-PCR.

Gene		Primer sequence (5′→3′)
TLR4	Forward	TGACAGGAAACCCTATCCAGAGTT
(Human)	Reverse	TCTCCACAGCCACCAGATTCT
TLR4	Forward	TACAGTTCGTCATGCTTTCTC
(Rat)	Reverse	ATTAGGAAGTACCTCTATGCAG
ZO-1	Forward	GCAGCCACAACCAATTCATAG
(Human)	Reverse	GCAGACGATGTTCATAGTTTC
ZO-1	Forward	GCTCACCAGGGTCAAAATGT
(Rat)	Reverse	GGCTTAAAGCTGGCAGTGTC
Occludin	Forward	ACCCCCATCTGACTATGTGGAA
(Human)	Reverse	AGGAACCGGCGTGGATTTA
Occludin	Forward	TTACGGCTATGGAGGGTACAC
(Rat)	Reverse	GACGCTGGTAACAAAGATCAC
GAPDH	Forward	ACCACAGTCCATGCCATCAC
(Human)	Reverse	TCCACCACCCTGTTGCTGTA
GAPDH	Forward	GGCACAGTCAAGGCTGAGAATG
(Rat)	Reverse	ATGGTGGTGAAGACGCCAGTA

2.11. Intestinal Permeability. Small intestinal mucosal barrier function was assessed using an everted sac method as our previously described [6]. Segments were everted in ice-cold Krebs buffer (pH 7.4), gently distended by injecting 1.5 ml of Krebs, and then suspended in the organ bath for 30 min. The organ bath contained 500-ml Krebs with added FITC-labeled dextran 4000 (FD4, 10 mg/ml) and maintained at 37°C, continuously bubbled with a gas mixture containing 95% O_2 and 5% CO_2. Samples from the sac were centrifuged at 1000g at 4°C for 5 min. FD4 concentration was detected at an excitation wavelength of 492 nm and an emission wavelength of 515 nm with PerkinElmer LS-50 fluorescence spectrophotometer (PerkinElmer Inc., Waltham, MA). Intestinal permeability was expressed as FD4 concentration divided by the area of gut sac.

2.12. Statistical Analysis. All statistical analyses were performed with SPSS 12.0. The results were expressed as means ± SDs. Results were performed with Student's t-test and one-way analysis of variance (ANOVA). $P < 0.05$ was considered statistically significant.

3. Results

3.1. Detection of Cell Proliferation Activity by CCK-8. Cell viability (%) was calculated as follows: [A (experimental well)−A (blank well)]/[A (control well)−A (blank well)] × 100. Moreover, we assessed the viability of cells treated with different concentrations (10 nM, 100 nM, 1000 nM, 10^4 nM, 10^5 nM, 10^6 nM, 10^7 nM, and 10^8 nM) of CAY10683 on after 24 h. Based on the CCK8 assay, the concentration-effect curve was represented by the equation $y = 100/(1 + 10^{((2.499-x)*(-1.761))})$ (Figure 1(a)), and the

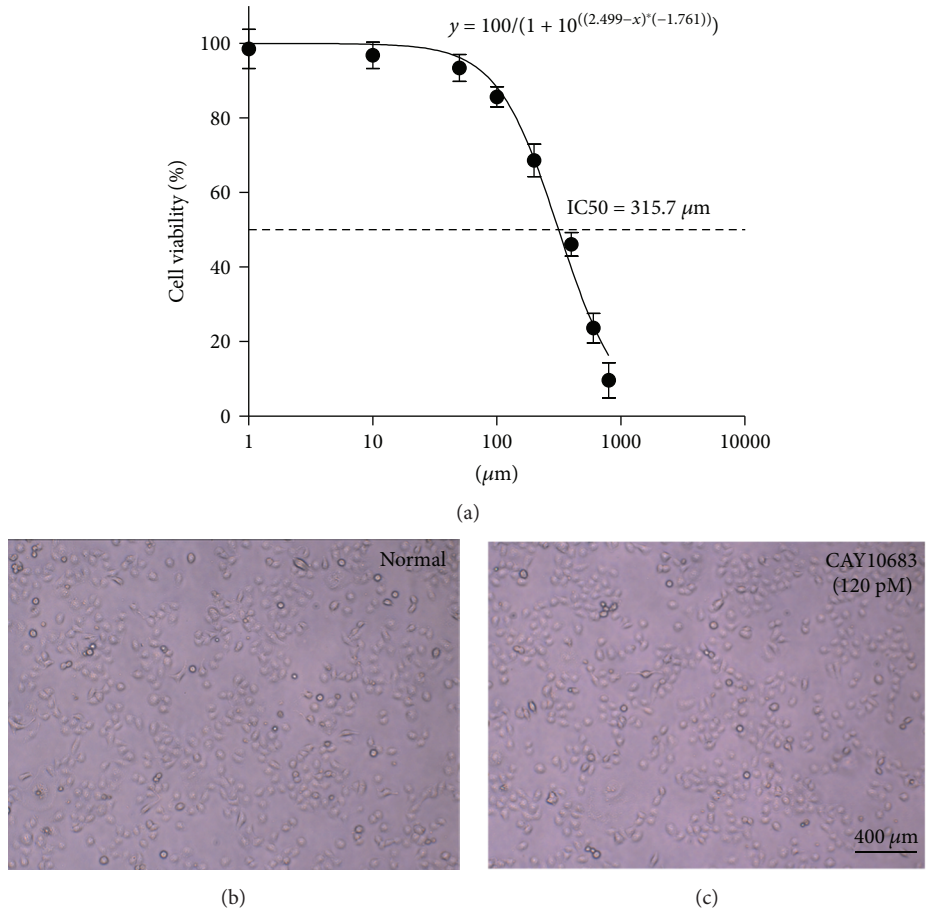

Figure 1: (a) Detection of cell proliferation activity by CCK-8. (b–c) Cell morphology was observed in normal and CAY10683-treated NCM460 cell group. Values are expressed as mean ± SD. $P < 0.05$, compared with normal group; $P < 0.05$, compared with model group.

specific parameters IC50 (315.7 nM), hillslope (−1.761), and R^2 (0.9748) were also assessed. Against HDAC2, CAY10683 showed an inhibitory concentration of 119 pM, which is over 3600-fold more potent than other HDACs [10]. For convenience, we approximated the concentration 120 pM and the viability was 99.99% for NCM460. Thus, the pretreatment concentrations of CAY10683 of unstimulated NCW460 cells were 120 pM for 24 h, none of which significantly affected cell morphology (Figures 1(b) and 1(c)). Therefore, we chose to treat cells with CAY10683 at 120 pM for 24 h in this experiment.

3.2. Effect of CAY10683 on TEER in LPS-Stimulated NCM460 Cells. As the TEER became higher, the cell permeability was lower. The small chamber film diameter, aperture, and surface area were 12 mm, 0.4 μm, and 1.13 cm^2. The background resistance of blank was deducted from each value. As shown in Figure 2(a), compared with the normal group, the TEER value in the model group was significantly decreased ($P = 0.000$, fold change (FC) = 0.28). After being treated with CAY10683, the TEER value was pronouncedly elevated ($P = 0.000$, FC = 3.31).

3.3. Effect of CAY10683 on Acetylation Regulation in LPS-Stimulated NCM460 Cells. CAY10683 is a HDACi that specifically targets the HDAC2 and consequently affects the acetylation of histone. To confirm the effects of CAY10683 on HDAC2 and histone, we firstly verify the effect of CAY10683 on HDAC2 and acetylation of histone H3. Stimulated by LPS, the expression of HDAC2 was increased in NCM460 cells ($P = 0.001$, FC = 2.94). As expected, CAY10683 showed inhibition on HDAC2 in cells (Figure 2(c), $P = 0.003$, FC = 0.577). The acetylated histone H3 was also promoted by LPS simulation ($P = 0.001$, FC = 2.27) and then enhanced by CAY10683 (Figure 2(c), $P = 0.005$, FC = 1.35).

3.4. Effect of CAY10683 on the mRNA and Protein Expression of ZO-1 and Occludin in LPS-Stimulated NCM460 Cell. As shown in Figures 2(b) and 2(d), compared with the normal group, the ZO-1 (mRNA: $P = 0.004$, FC = 0.473; protein: $P = 0.003$, FC = 0.364) and occluding (mRNA: $P = 0.005$, FC = 0.51; protein: $P = 0.001$, FC = 0.350) mRNA and protein levels in the model group were significantly decreased. After being treated with CAY10683, the expression of ZO-1(mRNA: $P = 0.013$, FC = 1.95; protein: $P = 0.001$, FC = 3.17) and occluding (mRNA: $P = 0.014$, FC = 1.82; protein: $P = 0.002$, FC = 2.23) was pronouncedly elevated.

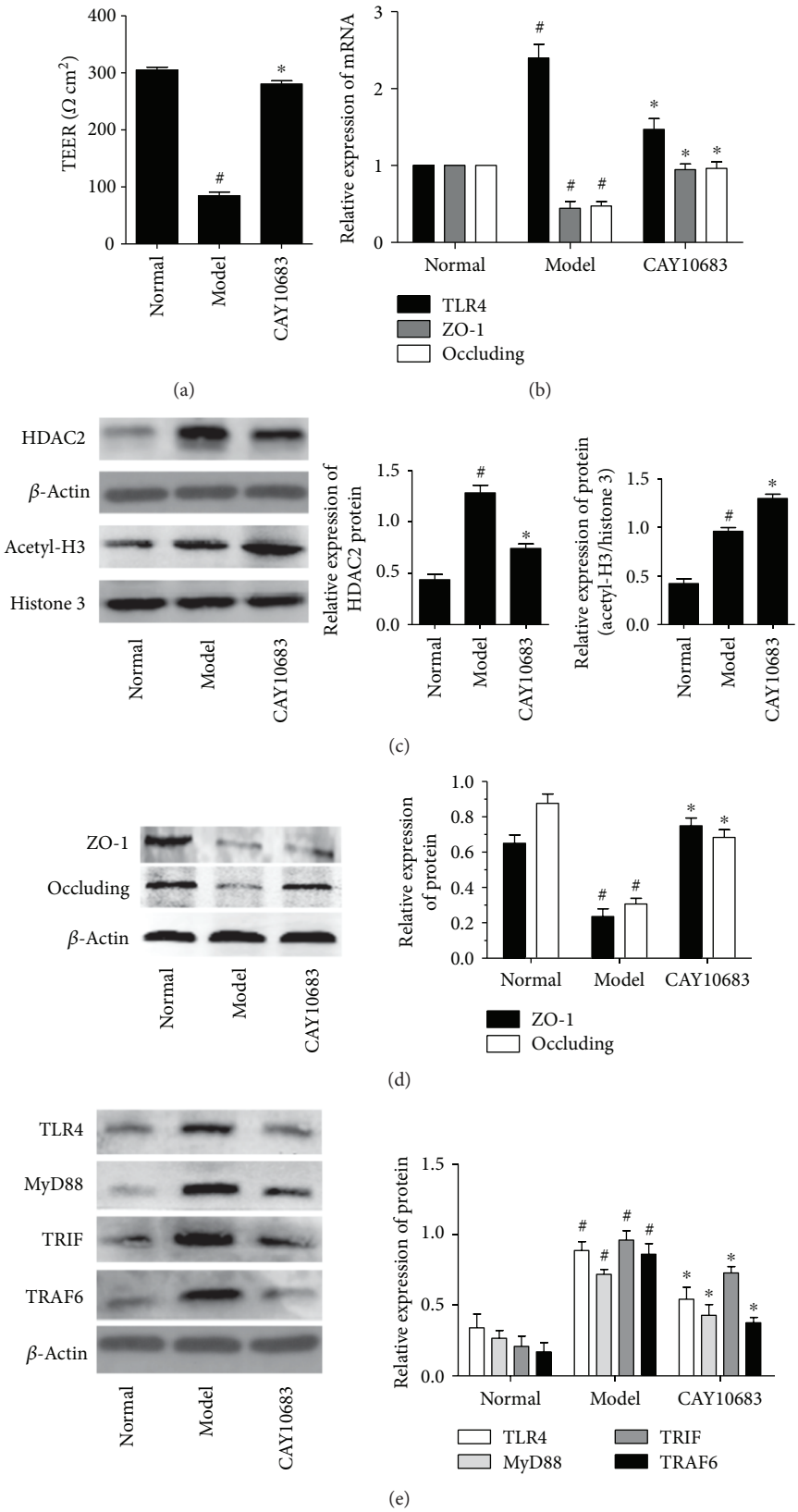

Figure 2: (a) Effect of CAY10683 on TEER in LPS-stimulated NCM460 cells. (b) Effect of CAY10683 on the mRNA expression of TLR4, ZO-1, and occludin in LPS-stimulated NCM460 cell. (c) Effect of CAY10683 on HDAC2 and acetyl-H3 in LPS-stimulated NCM460 cells. (d) Effect of CAY10683 on the protein levels of ZO-1 and occludin in LPS-stimulated NCM460 cell. (e) Effect of CAY10683 on the TLR4, MyD88, TRIF, and TRAF6 protein levels in LPS-stimulated NCM460 cells. Values are expressed as mean ± SD. $^{\#}P < 0.05$, compared with normal group; $^{*}P < 0.05$, compared with model group.

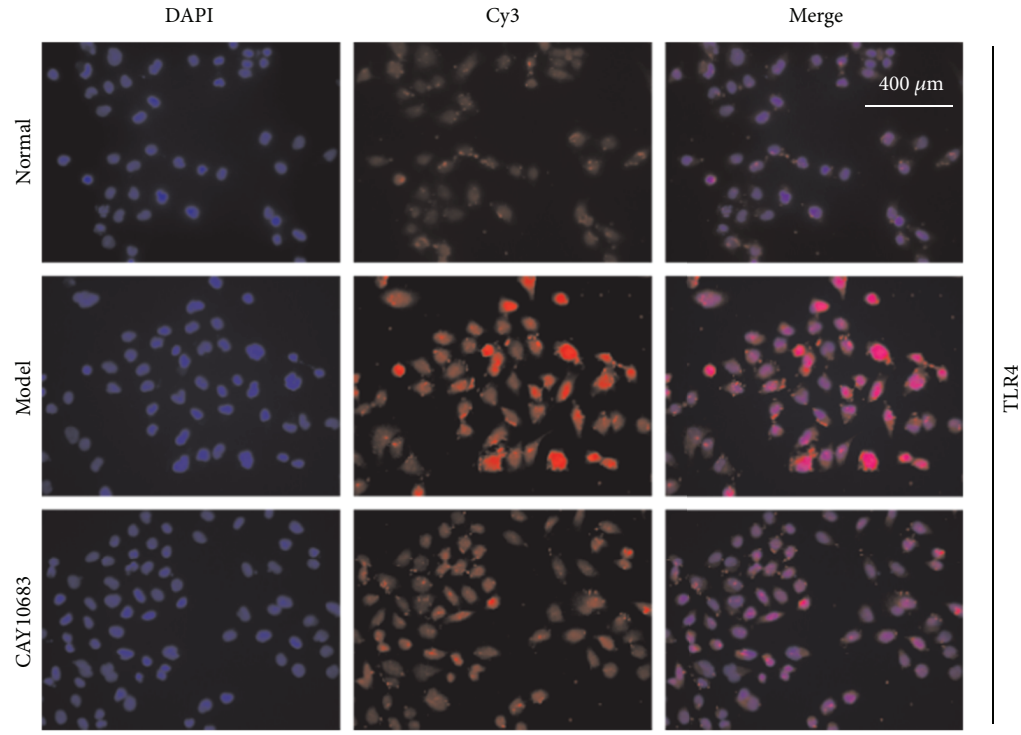

Figure 3: The IF method was used to detect the protein expressions of TLR4 in LPS-stimulated NCM460 cell.

3.5. Effect of CAY10683 on the TLR4/MyD88 Pathway in LPS-Stimulated NCM460 Cells. Next, we evaluated the effect of CAY10683 on the TLR4/MyD88 pathway in LPS-stimulated NCM460 cells. The TLR4 mRNA ($P = 0.000$, FC = 2.40) and TLR4 ($P = 0.001$, FC = 2.62), MyD88 ($P = 0.001$, FC = 2.70), TRIF ($P = 0.001$, FC = 3.19), and TRAF6 ($P = 0.001$, FC = 3.07) protein levels were dramatically increased after LPS administration. On the contrary, CAY10683 administration appeared to downregulate the TLR4 mRNA ($P = 0.002$, FC = 0.613) and TLR4 ($P = 0.005$, FC = 0.610), MyD88 ($P = 0.004$, FC = 0.597), TRIF ($P = 0.032$, FC = 0.714), and TRAF6 ($P = 0.002$, FC = 0.454) protein levels (Figures 2(b) and 2(e)). Similarly, we furtherly used immunofluorescence (IF) method to detect the protein expressions of TLR4 in LPS-stimulated NCM460 cell. The TLR4 protein level in the model group was significantly increased ($P = 0.001$, FC = 2.43), and CAY10683 could notably decrease TLR4 protein expression (Figure 3, $P = 0.002$, FC = 0.632).

3.6. Effect of CAY10683 on Hepatic Pathological Changes and Serum Biochemical Indicators in ALF Rats. Because the liver is the main target organ in ALF caused by LPS, both histology and function are certainly injured to some extent. Therefore, in vivo experiment, we primarily detect whether the ALF rats model was successfully established and then detect the effect of CAY10683 on liver pathological changes and serum biochemical indicators in ALF rats. As H&E staining shown in Figures 4(a)–4(c), the structure of liver lobules in the normal group was clear, the arrangement of liver cells was neat, and the infiltration of inflammatory cells was not observed around the liver cells. The liver lobular structure in the ALF model group was unclear, and hepatocytes were necrotic surrounded by inflammatory cell infiltration. The hepatic lobule structure in CAY10683 rat liver was clearer than that in the ALF model group, and the infiltration of inflammatory cells was also reduced. As shown in Figures 4(d)–4(f), the serum ALT ($P = 0.000$, FC = 91.3), AST ($P = 0.000$, FC = 22.3), and TBIL ($P = 0.000$, FC = 13.2) in the model group were in the higher levels. Compared with the model group, the CAY10683-treated groups showed significant decreases in the ALT ($P = 0.000$, FC = 0.156), AST ($P = 0.000$, FC = 0.138), and TBIL ($P = 0.000$, FC = 0.287) levels.

3.7. Effect of CAY10683 on Small Intestine Damages in ALF Rats. We assessed the histology and intestinal permeability changes of jejunum (5 cm away from pylorus) (Figures 5(a)–5(c)). Histologic analysis revealed mucosal damage in the model group, with elevation of the epithelial layer from the lamina propria, denuding and loss of height of the villi, and large reactive lymphoid follicles along with excess of lymphocytes in lamina propria. However, the effects of ischemia and reperfusion were markedly alleviated by CAY10683. Along with the changes in histology, the intestinal permeability significantly increased in the model group compared with the control ($P = 0.001$, FC = 2.85) and was dramatically improved by CAY10683 ($P = 0.000$, FC = 0.488, Figure 5(d)).

3.8. Effect of CAY10683 on Acetylation Regulation in ALF Rats. Compared with the normal group, the expression of HDAC2 was increased in the model group ($P = 0.001$, FC = 3.51). CAY10683 showed inhibition on HDAC2 ALF

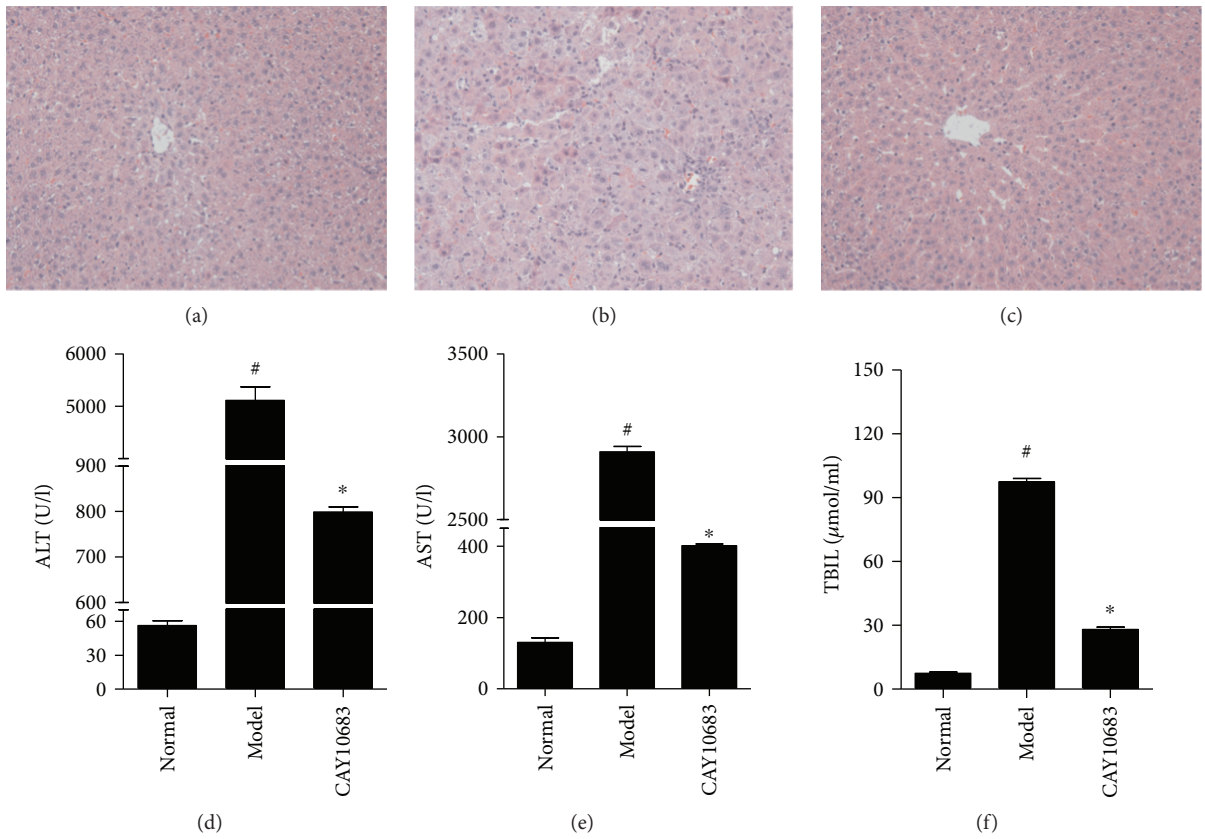

Figure 4: Effect of CAY10683 on hepatic pathological changes and serum biochemical indicators in ALF rats: (a) normal group, (b) model group, and (c) CAY10683 group. (d–f) Effect of CAY10683 on serum ALT, AST, and TBIL in ALF rats. Values are expressed as mean ± SD. $^{\#}P < 0.05$, compared with normal group; $^{*}P < 0.05$, compared with model group.

rats (Figure 5(f), $P = 0.001$, FC = 0.500). The acetylated histone H3 was also promoted in the model group ($P = 0.002$, FC = 2.26) and then enhanced by CAY10683 (Figure 5(f), $P = 0.005$, FC = 1.46).

3.9. Effect of CAY10683 on the mRNA and Protein Expression of ZO-1 and Occludin in ALF Rats. As shown in Figures 5(e) and 5(g), compared with the normal group, the ZO-1 (mRNA: $P = 0.000$, FC = 0.307; protein: $P = 0.002$, FC = 0.434) and occluding (mRNA: $P = 0.000$, FC = 0.35; protein: $P = 0.001$, FC = 0.346) mRNA and protein levels in the model group were significantly decreased. After being treated with CAY10683, the expression of ZO-1 (mRNA: $P = 0.001$, FC = 3.01; protein: $P = 0.000$, FC = 2.48) and occluding (mRNA: $P = 0.002$, FC = 2.80; protein: $P = 0.001$, FC = 2.49) were pronouncedly elevated.

3.10. Effect of CAY10683 on the TLR4/MyD88 Pathway in ALF Rats. Finally, we evaluated the effect of CAY10683 on the TLR4/MyD88 pathway in ALF rats. The TLR4 mRNA ($P = 0.000$, FC = 2.63) and TLR4 ($P = 0.000$, FC = 2.63), MyD88 ($P = 0.000$, FC = 2.41), TRIF ($P = 0.001$, FC = 3.17), and TRAF6 ($P = 0.000$, FC = 3.42) protein levels were dramatically increased after modeling. On the contrary, CAY10683 administration appeared to downregulate the TLR4 mRNA ($P = 0.003$, FC = 0.622) and TLR4 ($P = 0.002$, FC = 0.624), MyD88 ($P = 0.007$, FC = 0.642), TRIF ($P = 0.003$, FC = 0.624), and TRAF6 ($P = 0.001$, FC = 0.498) protein levels (Figures 5(e) and 5(g)). The IHC method was used to detect the protein expressions of TLR4 in liver tissues, which mainly expressed in cell membranes and cytoplasm. The TLR4 protein level in the model group was significantly increased ($P = 0.002$, FC = 10.12) and CAY10683 could notably decrease TLR4 protein expression (Figures 6(a)–6(d), $P = 0.003$, FC = 0.178).

4. Discussion

Intestinal mucosa barrier dysfunction can cause intestinal flora disturbance in ALF, and gram-negative bacilli reproduce excessively, producing a large amount of endotoxin [16]. However, the damaged liver cannot completely clear endotoxin, which not only leaded to excessive endotoxin get into the systemic circulation, but also exacerbated the endotoxin damage to the liver [17]. Endotoxin induced the production of inflammatory cytokines, destruction of intestinal mucosal barrier function, resulting in increased intestinal mucosal permeability.

Intestinal mechanical barrier is mainly composed of intestinal mucosal epithelial cells and intercellular connection [18]. And the intestinal mechanical barrier transmembrane proteins ZO-1 and occludin are important structures

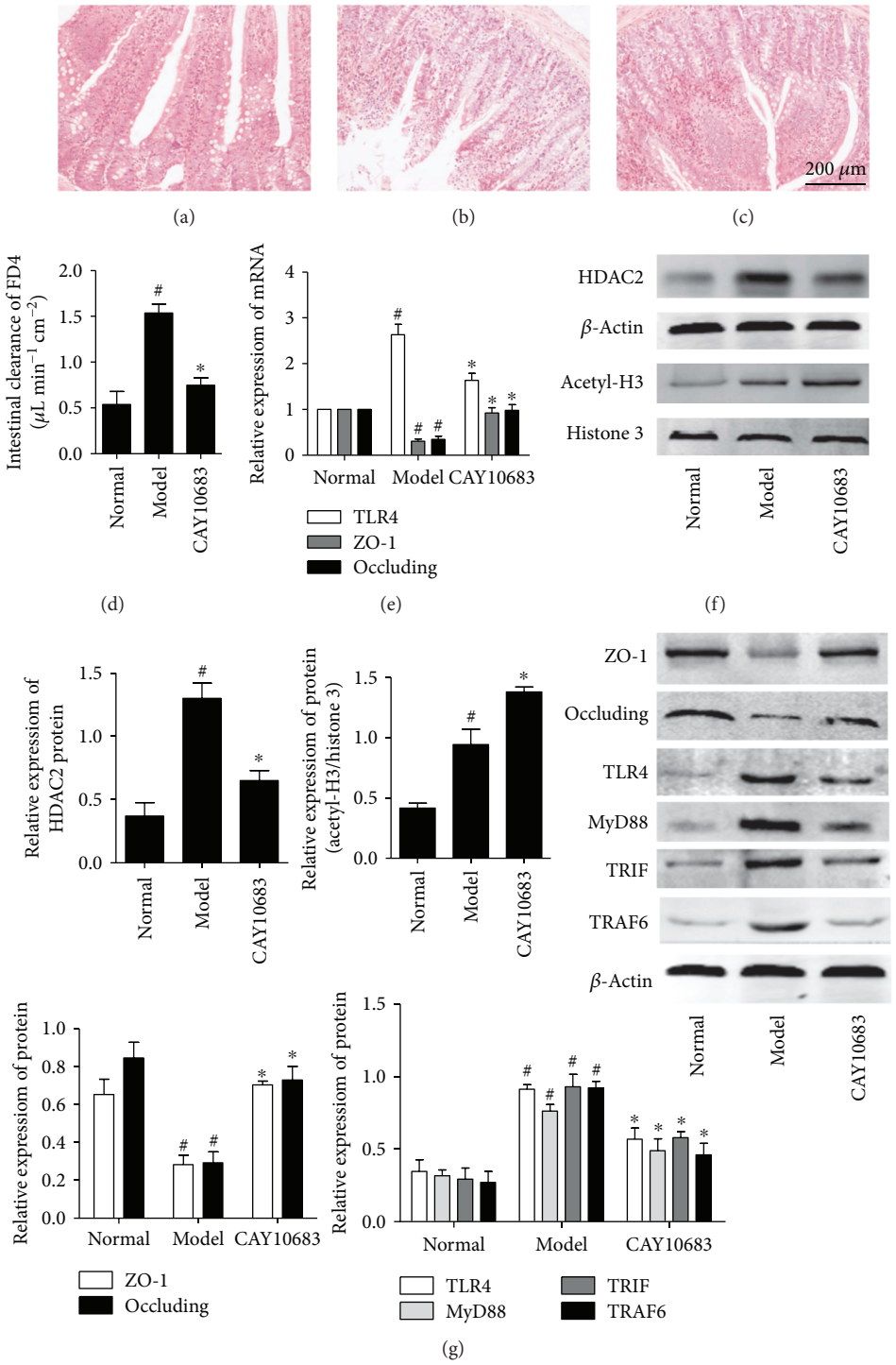

Figure 5: (a–c) Effect of CAY10683 on small intestine damages in ALF rats: (a) normal group, (b) model group, and (c) CAY10683 group. (d) Effect of CAY10683 on the intestinal permeability in ALF rats. (e) Effect of CAY10683 on the mRNA expression of TLR4, ZO-1, and occludin in ALF rats. (f) Effect of CAY10683 on HDAC2 and acetyl-H3 in ALF rats. (g) Effect of CAY10683 on the protein levels of ZO-1, occludin, TLR4, MyD88, TRIF, and TRAF6 protein levels in ALF rats. Values are expressed as mean ± SD. $^{\#}P < 0.05$, compared with normal group; $^{*}P < 0.05$, compared with model group.

that make up a tight junction, which determines the permeability of the intestinal barrier and intestinal tract [19]. Once the transmembrane proteins are reduced, missed, or mutated, the intestinal epithelial cell permeability would increase [20], and bacteria, lipopolysaccharides, and macromolecules would enter the systemic circulation through tight junctions [21, 22], resulting in local or systemic inflammatory responses that can lead to MODS, even caused death [23]. In addition, LPS can directly destroy the tight junction protein, leading to decreased resistance to intestinal

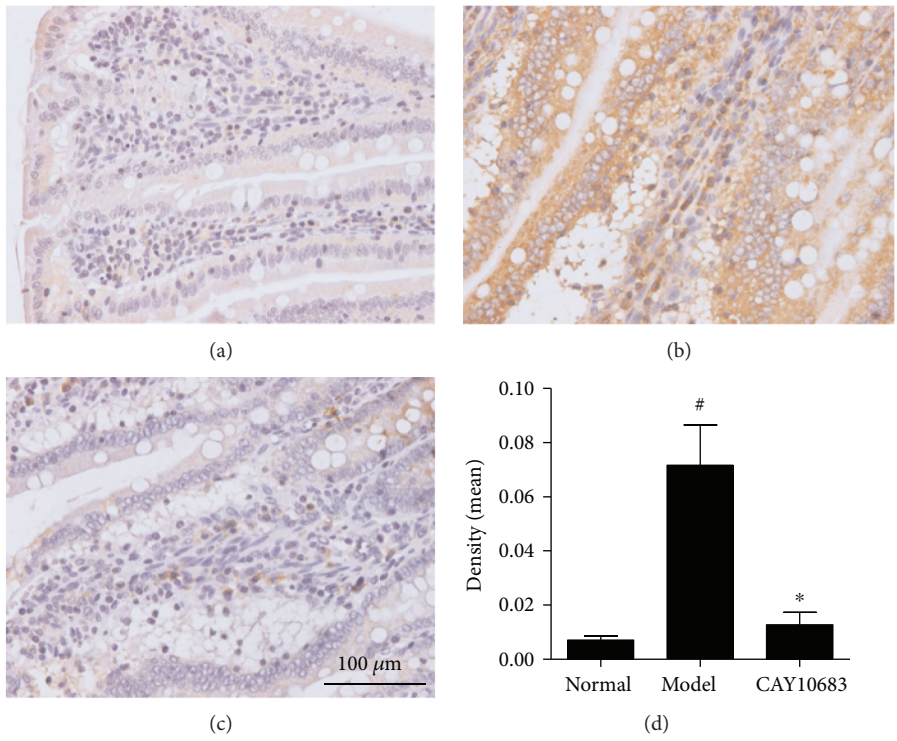

Figure 6: (a–d) Detection of TLR4 protein level in liver tissues with IHC method: (a) normal group, (b) model group, and (c) CAY10683 group. Values are expressed as mean ± SD. $^{\#}P < 0.05$, compared with normal group; $^{*}P < 0.05$, compared with model group.

epithelial [24]. At present, LPS mainly through the role of cell membrane surface receptors such as TLR4 activates the MyD88 downstream signaling pathway, thus affecting the expression of tight junction proteins [25–27]. TLR-4 recognizes pathogens, then passes the activation signals into cells, upregulates transcription factors such as MyD88, promotes the release of cytokines or inflammatory mediators, activates local or systemic inflammatory responses, causes structural changes, or decreases the expression of tight junction proteins, finally leading to intestinal mucosal barrier dysfunction, causing increased intestinal permeability [28]. Therefore, through the intestinal mucosa repair in ALF can reduce the bacteria, LPS, or macromolecules pass through the tight connection into the body circulation and decrease the release of inflammatory factors within the liver, reducing the "second strike" for the liver.

In our cell experiment, we assessed that the IC50 concentration for NCM460 was 315.7 nM, which was much higher than our selective inhibitive concentration 120 pM for HDAC2. Therefore, we chose to treat cells with CAY10683 at 120 pM for 24 h in this experiment. To confirm the effects of CAY10683 on HDAC2 and histone, we firstly verify the effect of CAY10683 on HDAC2 and acetylation of histone H3. Stimulated by LPS, the expression of HDAC2 was increased in NCM460 cells. As expected, CAY10683 showed inhibition on HDAC2 in cells. The acetylated histone H3 was also promoted by LPS simulation and then enhanced by CAY10683, whereas CAY10683 could effectively decrease the permeability in LPS-stimulated NCM460 cell. The ZO-1 and occludin mRNA and protein levels were significantly decreased in the LPS-stimulated group, which was consistent with the reported study [29] and then increased after being treated with CAY10683. Next, we evaluated the effect of CAY10683 on the TLR4/MyD88 pathway in LPS-stimulated NCM460 cells. The TLR4 mRNA and TLR4, MyD88, TRIF, and TRAF6 protein levels were dramatically decreased after CAY10683 administration for LPS-stimulated NCM460 cells. In our animal experiment, we firstly insured that the ALF rat model was successfully established by D-galactosamine/LPS and then detected alleviating effect of CAY10683 on liver pathological changes and serum biochemical indicators in ALF rats. The histology and intestinal permeability changes of jejunum could be dramatically improved by CAY10683 in ALF rat model. Compared with model rat, the expression of HDAC2 was increased by CAY10683, and CAY10683 showed inhibition on HDAC2 ALF rats. The acetylated histone H3 was also promoted in the model group and then enhanced by CAY10683. To explore the specific molecular mechanism of protecting intestinal mucosal barrier, we detected that the ZO-1 and occludin mRNA and protein levels in the CAY10683 group were significantly elevated. Finally, we verified the protective effect of CAY10683 on the TLR4/MyD88 pathway in ALF rats.

Although the broad spectrum HDAC inhibitor TSA was shown to have the protective effect on intestine in ALF [6], which specific HDAC molecule related with the protective effect and the molecular mechanism of how HDAC2 inhibitor alleviated intestinal mucosal barrier in ALF were still unknown. Being an inhibitor of HDAC2, CAY10683 reduced the high expression of HDAC2 in ALF model. In this experiment, we found that the acetylated histone H3 increased

under the stimulation by LPS. In the CAY10683 group, the acetylation of histones was further enhanced with HDAC2 reduction. The changes of HDAC2 and histone responding to CAY10683 in ALF model were similar to those in our previous studies [6, 30]. Because HDACs could not only regulate histones but also nonhistone proteins with multiple lysine residues acetylation, the gene expression or protein transcription could be upregulated or downregulated [31]. Moreover, the ubiquitinated or methylated modifications could participate in the protein regulation [32]. Therefore, the inflammatory pathway TLR4/MyD88 was suppressed, although the acetylated histone3 was increased in the CAY10683 group. The inflammatory pathway TLR4/MyD88 inhibition of CAY10683 was likely through nonhistone acetylation, and this acetylation process was through the effect of histone acetylation.

In conclusion, CAY10683 improved liver and small intestine histology, intestine permeability, and liver function in ALF rats. The inhibition of CAY10683 on inflammation is mainly via the histones acetylation. The present study not only proved that CAY10683 protected the liver in ALF rats as we previously described in ACLF rats but also further demonstrated its protection on intestine permeability. We speculated that CAY10683 could protect intestinal epithelial barrier disruption and keep the integrity of tight junction through inhabiting TLR4/MyD88 signal pathway, and CAY10683 can be considered as a therapeutic drug for protecting intestinal mucosa in ALF. This experiment not only focuses on the reliable curative effects but also provides a new avenue for clinical research and treatment and forming the foundation for future precision medicine for intestinal mucosal barrier in ALF. Further studies on the specific mechanism of CAY10683 regarding alleviating ALF may provide a potential prevention and treatment method for intestinal defense in ALF.

Conflicts of Interest

The authors declare that they have no conflicts of interests.

Acknowledgments

This work was supported by the National Natural Science Foundation of China (81371789).

References

[1] C. Bunchorntavakul and K. R. Reddy, "Acute liver failure," *Clinics in Liver Disease*, vol. 21, no. 4, pp. 769–792, 2017.

[2] L. K. Wang, L. W. Wang, X. Li, X. Q. Han, and Z. J. Gong, "Ethyl pyruvate prevents inflammatory factors release and decreases intestinal permeability in rats with D-galactosamine-induced acute liver failure," *Hepatobiliary & Pancreatic Diseases International*, vol. 12, no. 2, pp. 180–188, 2013.

[3] R. Yang, X. Zou, J. Tenhunen, and T. I. Tønnessen, "HMGB1 and extracellular histones significantly contribute to systemic inflammation and multiple organ failure in acute liver failure," *Mediators of Inflammation*, vol. 2017, Article ID 5928078, 6 pages, 2017.

[4] D. I. Sonnier, S. R. Bailey, R. M. Schuster, M. M. Gangidine, A. B. Lentsch, and T. A. Pritts, "Proinflammatory chemokines in the intestinal lumen contribute to intestinal dysfunction during endotoxemia," *Shock*, vol. 37, no. 1, pp. 63–69, 2012.

[5] I. Sukhotnik, B. Haj, Y. Pollak, T. Dorfman, J. Bejar, and I. Matter, "Effect of bowel resection on TLR signaling during intestinal adaptation in a rat model," *Surgical Endoscopy*, vol. 30, no. 10, pp. 4416–4424, 2016.

[6] Q. Zhang, F. Yang, X. Li et al., "Trichostatin A protects against intestinal injury in rats with acute liver failure," *The Journal of Surgical Research*, vol. 205, no. 1, pp. 1–10, 2016.

[7] O. H. Kramer, "HDAC2: a critical factor in health and disease," *Trends in Pharmacological Sciences*, vol. 30, no. 12, pp. 647–655, 2009.

[8] E. Zika, L. Fauquier, L. Vandel, and J. P. Y. Ting, "Interplay among coactivator-associated arginine methyltransferase 1, CBP, and CIITA in IFN-γ-inducible MHC-II gene expression," *Proceedings of the National Academy of Sciences of the United States of America*, vol. 102, no. 45, pp. 16321–16326, 2005.

[9] S. Zhong, L. Zhao, Y. Wang et al., "Cluster of differentiation 36 deficiency aggravates macrophage infiltration and hepatic inflammation by upregulating monocyte chemotactic protein-1 expression of hepatocytes through histone deacetylase 2-dependent pathway," *Antioxidants & Redox Signaling*, vol. 27, no. 4, pp. 201–214, 2017.

[10] C. M. Pavlik, C. Y. Wong, S. Ononye et al., "Santacruzamate A, a potent and selective histone deacetylase inhibitor from the Panamanian marine cyanobacterium cf. Symploca sp," *Journal of Natural Products*, vol. 76, no. 11, pp. 2026–2033, 2013.

[11] S. M. Gromek, J. A. deMayo, A. T. Maxwell et al., "Synthesis and biological evaluation of santacruzamate A analogues for anti-proliferative and immunomodulatory activity," *Bioorganic & Medicinal Chemistry*, vol. 24, no. 21, pp. 5183–5196, 2016.

[12] P. A. Marks, "Discovery and development of SAHA as an anticancer agent," *Oncogene*, vol. 26, no. 9, pp. 1351–1356, 2007.

[13] C. Damaskos, N. Garmpis, S. Valsami et al., "Histone deacetylase inhibitors: an attractive therapeutic strategy against breast cancer," *Anticancer Research*, vol. 37, no. 1, pp. 35–46, 2017.

[14] Y. Wang, F. Yang, J. Xue et al., "Antischistosomiasis liver fibrosis effects of chlorogenic acid through IL-13/miR-21/Smad7 signaling interactions *in vivo* and *in vitro*," *Antimicrobial Agents and Chemotherapy*, vol. 61, no. 2, article e01347–16, 2017.

[15] F. Yang, Y. Wang, J. Xue et al., "Effect of Corilagin on the miR-21/smad7/ERK signaling pathway in a schistosomiasis-induced hepatic fibrosis mouse model," *Parasitology International*, vol. 65, no. 4, pp. 308–315, 2016.

[16] C. Nastos, K. Kalimeris, N. Papoutsidakis et al., "Bioartificial liver attenuates intestinal mucosa injury and gut barrier dysfunction after major hepatectomy: study in a porcine model," *Surgery*, vol. 159, no. 6, pp. 1501–1510, 2016.

[17] H. L. Song, S. Lv, and P. Liu, "The roles of tumor necrosis factor-alpha in colon tight junction protein expression and intestinal mucosa structure in a mouse model of acute liver failure," *BMC Gastroenterol*, vol. 9, no. 1, p. 70, 2009.

[18] S. Koch and A. Nusrat, "Dynamic regulation of epithelial cell fate and barrier function by intercellular junctions," *Annals of the New York Academy of Sciences*, vol. 1165, no. 1, pp. 220–227, 2009.

[19] M. Deiana, S. Calfapietra, A. Incani et al., "Derangement of intestinal epithelial cell monolayer by dietary cholesterol oxidation products," *Free Radical Biology & Medicine*, vol. 113, pp. 539–550, 2017.

[20] R. Al-Sadi, K. Khatib, S. Guo, D. Ye, M. Youssef, and T. Ma, "Occludin regulates macromolecule flux across the intestinal epithelial tight junction barrier," *American Journal of Physiology. Gastrointestinal and Liver Physiology*, vol. 300, no. 6, pp. G1054–G1064, 2011.

[21] A. Parlesak, C. Schäfer, T. Schütz, J. C. Bode, and C. Bode, "Increased intestinal permeability to macromolecules and endotoxemia in patients with chronic alcohol abuse in different stages of alcohol-induced liver disease," *Journal of Hepatology*, vol. 32, no. 5, pp. 742–747, 2000.

[22] G. Kakiyama, W. M. Pandak, P. M. Gillevet et al., "Modulation of the fecal bile acid profile by gut microbiota in cirrhosis," *Journal of Hepatology*, vol. 58, no. 5, pp. 949–955, 2013.

[23] D. Ulluwishewa, R. C. Anderson, W. C. McNabb, P. J. Moughan, J. M. Wells, and N. C. Roy, "Regulation of tight junction permeability by intestinal bacteria and dietary components," *The Journal of Nutrition*, vol. 141, no. 5, pp. 769–776, 2011.

[24] S. Guo, R. Al-Sadi, H. M. Said, and T. Y. Ma, "Lipopolysaccharide causes an increase in intestinal tight junction permeability *in vitro* and *in vivo* by inducing enterocyte membrane expression and localization of TLR-4 and CD14," *The American Journal of Pathology*, vol. 182, no. 2, pp. 375–387, 2013.

[25] P. Chen, P. Stärkel, J. R. Turner, S. B. Ho, and B. Schnabl, "Dysbiosis-induced intestinal inflammation activates tumor necrosis factor receptor I and mediates alcoholic liver disease in mice," *Hepatology*, vol. 61, no. 3, pp. 883–894, 2015.

[26] S. Chen, J. Zhu, G. Chen et al., "1,25-Dihydroxyvitamin D3 preserves intestinal epithelial barrier function from TNF-α induced injury via suppression of NF-κB p65 mediated MLCK-P-MLC signaling pathway," *Biochemical and Biophysical Research Communications*, vol. 460, no. 3, pp. 873–878, 2015.

[27] M. Rawat, S. Guo, and T. Y. Ma, "Su1845 molecular mechanism of lipopolysaccharide induced increase in intestinal tight junction permeability," *Gastroenterology*, vol. 148, no. 4, Supplement 1, pp. S–532, 2015.

[28] A. Spruss, G. Kanuri, S. Wagnerberger, S. Haub, S. C. Bischoff, and I. Bergheim, "Toll-like receptor 4 is involved in the development of fructose-induced hepatic steatosis in mice," *Hepatology*, vol. 50, no. 4, pp. 1094–1104, 2009.

[29] J. Chen, R. Zhang, J. Wang et al., "Protective effects of baicalin on LPS-induced injury in intestinal epithelial cells and intercellular tight junctions," *Canadian Journal of Physiology and Pharmacology*, vol. 93, no. 4, pp. 233–237, 2015.

[30] Q. Zhang, F. Yang, X. Li et al., "Trichostatin A protects against experimental acute-on-chronic liver failure in rats through regulating the acetylation of nuclear factor-κB," *Inflammation*, vol. 38, no. 3, pp. 1364–1373, 2015.

[31] C. Choudhary, C. Kumar, F. Gnad et al., "Lysine acetylation targets protein complexes and co-regulates major cellular functions," *Science*, vol. 325, no. 5942, pp. 834–840, 2009.

[32] T. A. McKinsey and E. N. Olson, "Dual roles of histone deacetylases in the control of cardiac growth," *Novartis Foundation Symposium*, vol. 259, pp. 132–141, 2004.